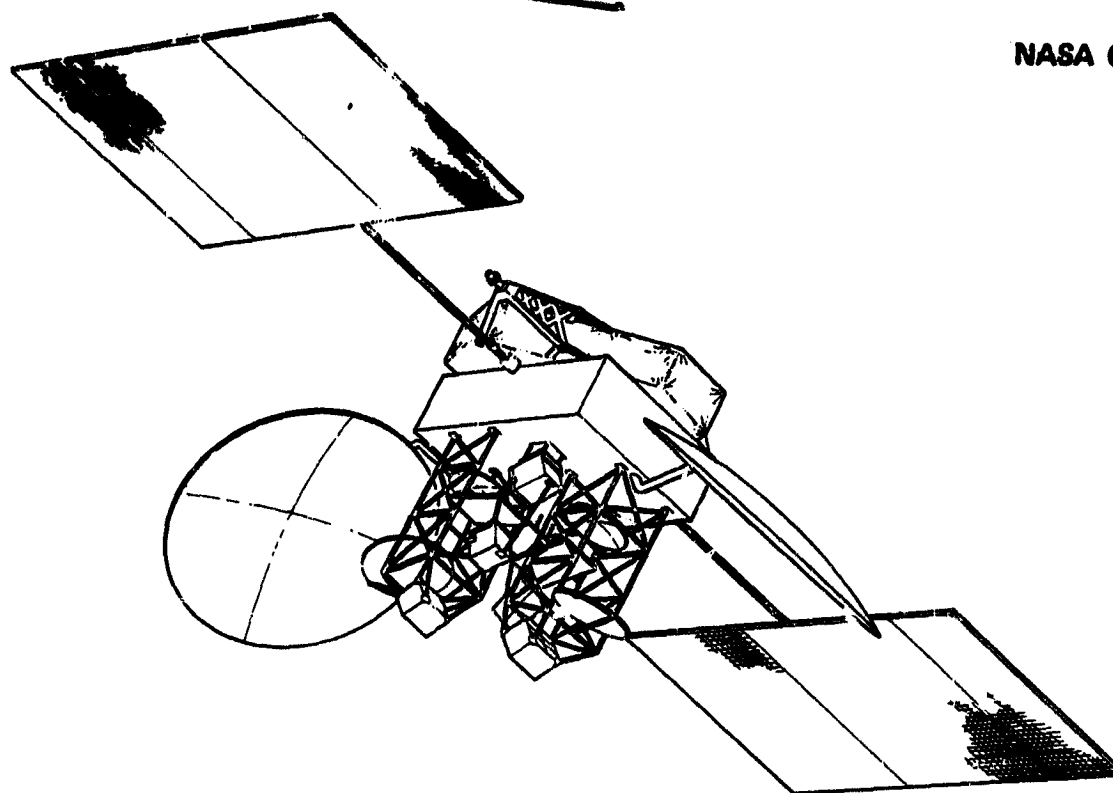


## N O T I C E

THIS DOCUMENT HAS BEEN REPRODUCED FROM  
MICROFICHE. ALTHOUGH IT IS RECOGNIZED THAT  
CERTAIN PORTIONS ARE ILLEGIBLE, IT IS BEING RELEASED  
IN THE INTEREST OF MAKING AVAILABLE AS MUCH  
INFORMATION AS POSSIBLE



# **30/20 GHz MIXED USER ARCHITECTURE DEVELOPMENT STUDY**

## **FINAL REPORT**

TRW Inc., Space Systems Division



prepared for

**NATIONAL AERONAUTICS AND SPACE ADMINISTRATION**

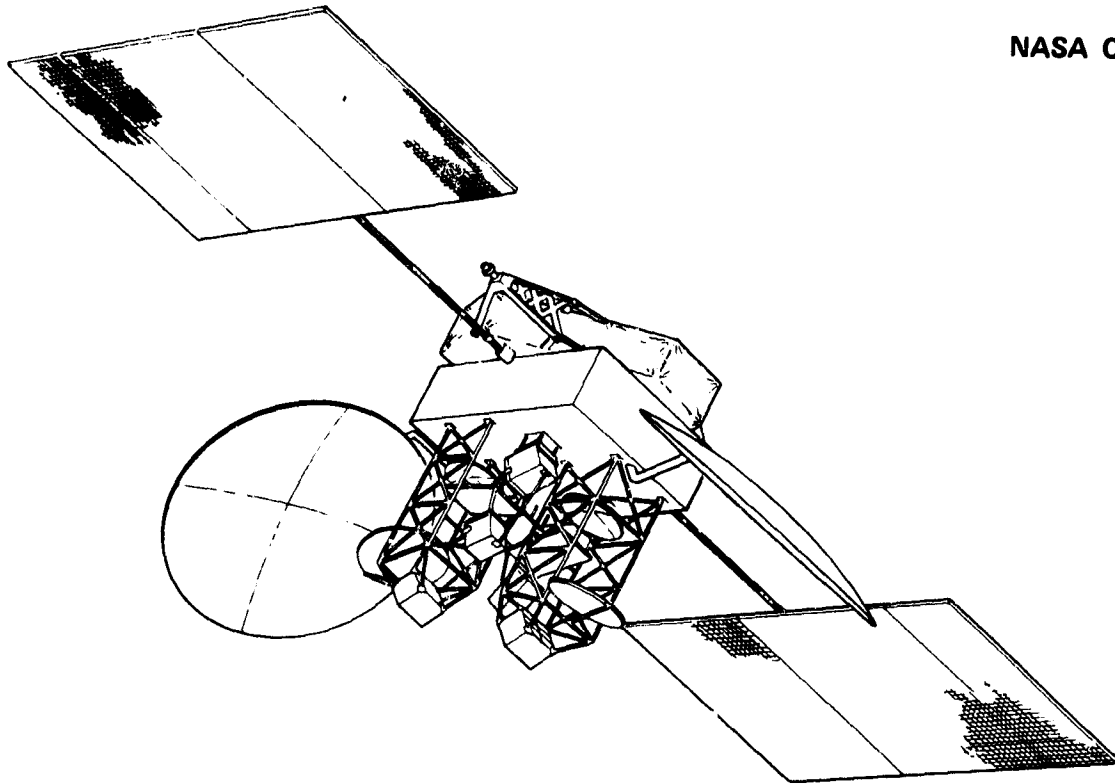
**NASA Lewis Research Center**

**Contract NAS 3- 21933**

(NASA-CR-159686) THE 30/20 GHz MIXED USER  
ARCHITECTURE DEVELOPMENT STUDY Final Report  
(TRW, Inc., Redondo Beach, Calif.) 216 p  
HC A10/MF A01 CSCL 17B

N80-10415

Unclas  
G3/32 45961



**30/20 GHz MIXED USER ARCHITECTURE  
DEVELOPMENT STUDY  
FINAL REPORT**

**TRW Inc., Space Systems Division**

**prepared for**

**NATIONAL AERONAUTICS AND SPACE ADMINISTRATION**

**NASA Lewis Research Center  
Contract NAS 3- 21933**

## CONTENTS

	Page
GLOSSARY	iii
0. SUMMARY	0-1
1. TRAFFIC DEMAND MODEL	1-1
2. TERMINAL AND SATELLITE PERFORMANCE PARAMETERS	2-1
3. SYSTEM ARCHITECTURE	3-1
4. NETWORK CONTROL	4-1
5. ANTENNA REQUIREMENTS	5-1
6. DTU TERMINAL COST CONSIDERATIONS	6-1
7. IDENTIFICATION OF CRITICAL TECHNOLOGY	7-1
8. SSTDMA ARCHITECTURE STUDIES	8-1



## GLOSSARY

baud	Signalling speed in transmitted symbols per second for digital communications. One symbol may represent one or more bits of information.
BCH	Base, Chaudhuri, and Hocquenghem (BCH) codes are a family of efficient, error-correction block codes.
bit	The smallest increment of information in a binary digital system. One bit defines a single yes-or-no information statement, often written as a "1" or "0".
bps	Bits-per-Second
CONUS	Continental United States (lower 48 states)
DPSK	Differential-phase-shift keying - a digital modulation technique which changes (shifts) the carrier phase depending on changes in the input data. This technique generally is coupled with, and implies, a noncoherent detection technique.
DS1	Bell System standard digital signal. The designation DSN refers to those common features of the digital signal at the Nth level of the network hierarchy. The data rates are:  DS1 - 1.544 Mbps DS1C - 3.152 Mbps DS2 - 6.312 Mbps DS3 - 44.736 Mbps DS4 - 274.176 Mbps
DTU	Direct-to-user
$E_b$	The energy in a single transmitted or received bit
EIRP	Effective isotropic radiated power
$E_s$	The energy in a single transmitted or received symbol
FEC	Forward-error-correction coding
FET	Field effect transistor

FSK	Frequency-shift keying - a digital modulation technique which changes (shifts) the carrier frequency depending on the input data
G/T	Antenna-gain-to-receiver-noise-temperature ratio
HPA	High power amplifier, generally a transmitter final stage
IF	Intermediate frequency
IUS	Interim upper stage
LNA	Low noise amplifier, generally a receiver first stage
LSI	Large scale integration refers to microelectronic, generally digital, technology
MBA	Multiple beam antenna
MCS	Master control station
MSK	Minimum shift keying - a variation of FSK which uses nearly minimum transmission bandwidth for a given data rate
$N_0$	Noise density in watts per Hertz
PAM/SSUS	Payload Assist Module or spinning shuttle upper stage - a family of perigee rocket motors and their associated support system designed to boost satellites from shuttle-orbiter orbits into transfer orbits to synchronous orbit.
PSK	Phase-shift-keying - a digital modulation technique which changes (shifts) the carrier phase depending on the input data
R-1/2	Rate one-half, rate in a coded system refers to the number of bits of input/output data transmitted by one symbol in a coded system. Rate one-half and rate one-third are commonly used in many systems
RAM	Random access memory
RF	Radio frequency
Rx	Receive
S/C	Spacecraft
SSTDMA	Satellite-switched time division multiple access
STS	Space Transportation System

symbol	A symbol is one of a set of possible messages or states of an information channel. It may represent any number of binary digits
T1	Bell system standard wire transmission system utilizing the DS1 signal structure
TDM	Time division multiplex
TDMA	Time division multiple access
TDRSS	Tracking and data relay satellite system
TWT	Traveling-wave tube
TWTA	Traveling-wave tube amplifier (implies integrated TWT and power supply)
Tx	Transmit

## SUMMARY

The 30/20 GHz Mixed User Architecture study has resulted in a baseline system design for cost-effective communications in the years 1990 to 2000. Generation of a useful mixed user TDMA architecture has required a broad overview of system characteristics. The 30/20 GHz baseline system consists of a synchronous orbit satellite, 18 large trunking terminals with 12-meter apertures and 10-km space diversity, 25 to 30 small, trunking terminals with 6-meter apertures and 10-km space diversity, several thousand inexpensive direct-to-user (DTU) terminals, and a master control station with at least one alternate master control station.

The DTU terminal minimum-cost design offers the greatest challenge in the 30/20 GHz communication system. Since the number of DTU terminals is very large, the DTU terminal cost is a large (perhaps the largest) element of system cost. The DTU terminal performance drives the satellite design, and hence determines the cost of a second major system element. Because the DTU system is able to avoid using terrestrial signal distribution and routing, and the charges associated with these functions, the DTU system also represents the largest economic value element of the system.

Because of these factors, the 30/20 GHz TDMA Mixed User Architecture design starts with the definition of DTU user terminal characteristics. TDMA, control, and on-board processing architectures are selected to maximize system performance with minimal DTU terminal requirements.

Trunking terminal design and the satellite trunking support components are less critical elements in determining system cost effectiveness. Trunking at 30/20 GHz provides direct cost benefits and prevents saturation of the lower frequency satellite communication bands. The greatest economic benefit of integrating both systems results from the increased utility of the DTU terminals.

DTU terminals need to integrate their communications channels with a trunking system. A large percentage, perhaps greater than half, of DTU point-to-point communication channels will terminate or originate in a trunking area. By shifting signals from the DTU system to the trunking system in the satellite, the more expensive DTU system carries less total

traffic. Signal routing is greatly simplified. Without this interconnectivity it might be necessary to provide DTU terminals at each trunking location to provide integration and avoid double-hop routing.

The baseline 30/20 GHz satellite communication system resulting from this study incorporates on-board satellite demodulation and routing of individual 64 kbps, digital voice-grade circuits. This level of routing flexibility is necessary to provide efficient communications to the very large number of DTU terminals projected. From an external point of view, the resulting system looks very much like a very large, distributed, telephone switching system. The circuit interfacing hardware is distributed among all the DTU and trunking terminals. Control and routing computers are at master control stations. The switching circuitry which provides full interconnectivity between 30 to 45 thousand circuits is in the satellite.

The satellite (Figure 0-1) must be fairly large to provide such a capability. Table 0-1 describes the satellite characteristics required to support the baseline system.

#### A. Satellite Baseline Design

The baseline system design includes a single, large, synchronous-orbit satellite. Communications design features include:

- All antenna beams provided by two 3-meter apertures
- Complete coverage of the 48 contiguous states
- Fixed-beam coverage of 18 high-density areas
- Scanning-beam coverage of all other areas
- Antenna beamwidths of 0.3 to 0.5 degree
- Dual mode 75-/7.5-watt 20-GHz downlink fixed-beam TWT transmitters
- Fixed level 35-watt downlink scanning-beam TWT transmitters
- Total radiated 20 GHz RF power of about 500 watts

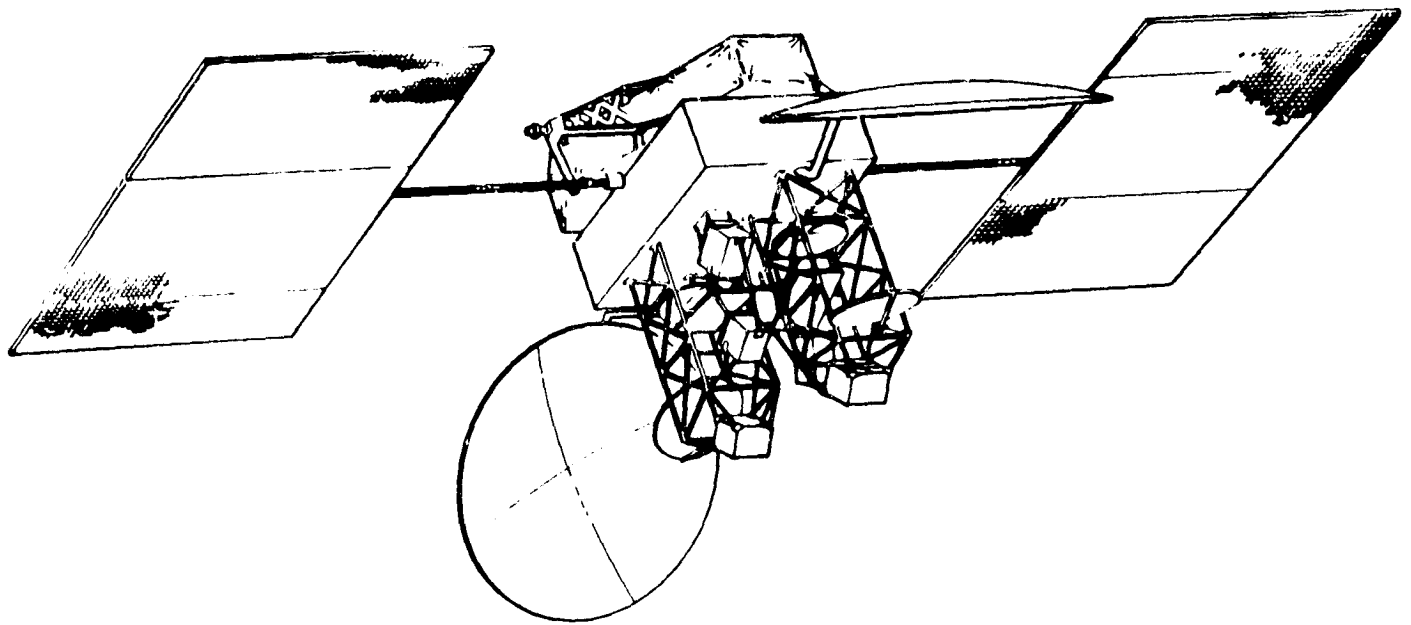


Figure 0-1. Preliminary Satellite Design

Table 0-1. Satellite Summary

- 6130 POUNDS BOL, 4360 WATTS INCLUDING ECLIPSE
- 10 YEAR STATIONKEEPING - WEIGHT IS 5160 POUNDS WITH ION PROPULSION
- 0.03 DEGREE POINTING ACCURACY RESULTS IN RF SENSING
- ABOUT 36 TWTA - 7.5/75 WATT DUAL MODE - 24 ACTIVE
- ABOUT 100 DEMODULATORS - 25, 125, 500 MBPS - 60 ACTIVE
- 10 GBPS THROUGHPUT CAPACITY - 3 GBPS PROCESSOR THROUGHPUT
- PROCESSING INCLUDES INDIVIDUAL CHANNEL ROUTING, ADAPTIVE CODING

The satellite communication subsystem block diagram is shown in Figure 0-2. It consists of a 500 Mbps per channel, spacecraft-switched, time-division multiple-access (SSTDMA) support section for trunking station and an on-board digital data processing section for small user support of small trunking terminals and DTU terminals.

The satellite provides 500 Mbps TDMA burst-rate communication between 18 large trunking users with a SSTDMA high-capacity communications system. The high-rate uplink channels are sequentially connected to different high-rate downlink channels. The connection patterns, or modes, repeat over a 1-millisecond frame period. The modes and the dwell-time in each mode may be varied by command, but are usually stable for long periods of time (hours). This interconnectivity technique allows all large trunking users communications access to all other large trunking users with an access period appropriate for the amount of data to be communicated. The large trunking user locations supported by the baseline system are shown in Figure 0-3.

The SSTDMA frame time line for the fixed-beam channels (Figure 0-4) illustrates the 500 Mbps channels being used first for communications between trunking stations and then for DTU terminal communications. Only six trunking time lines are shown for clarity, and only one of these is broken down to show DTU utilization. The Chicago uplink beam is shown being connected sequentially to New York, Los Angeles, Atlanta, and other major trunking locations. Similar sequential interconnection patterns are used on the other uplink channels.

After the Chicago trunking terminal has transmitted all outgoing traffic, the 500 Mbps channel is available for use by DTU terminals. Since they do not operate at 500 Mbps, the channel may be FDM divided to provide four 125 Mbps channels. One of these is shown to be further divided into 25 Mbps channels (31.25 MHz) to allow communication by very small DTU terminals. All DTU communications pass through the on-board processor.

Uplink and downlink SSTDMA frames are similar, but generally not identical since traffic output from an area may be different than traffic into that area. Also, DTU data rates are different for uplinks and downlinks.

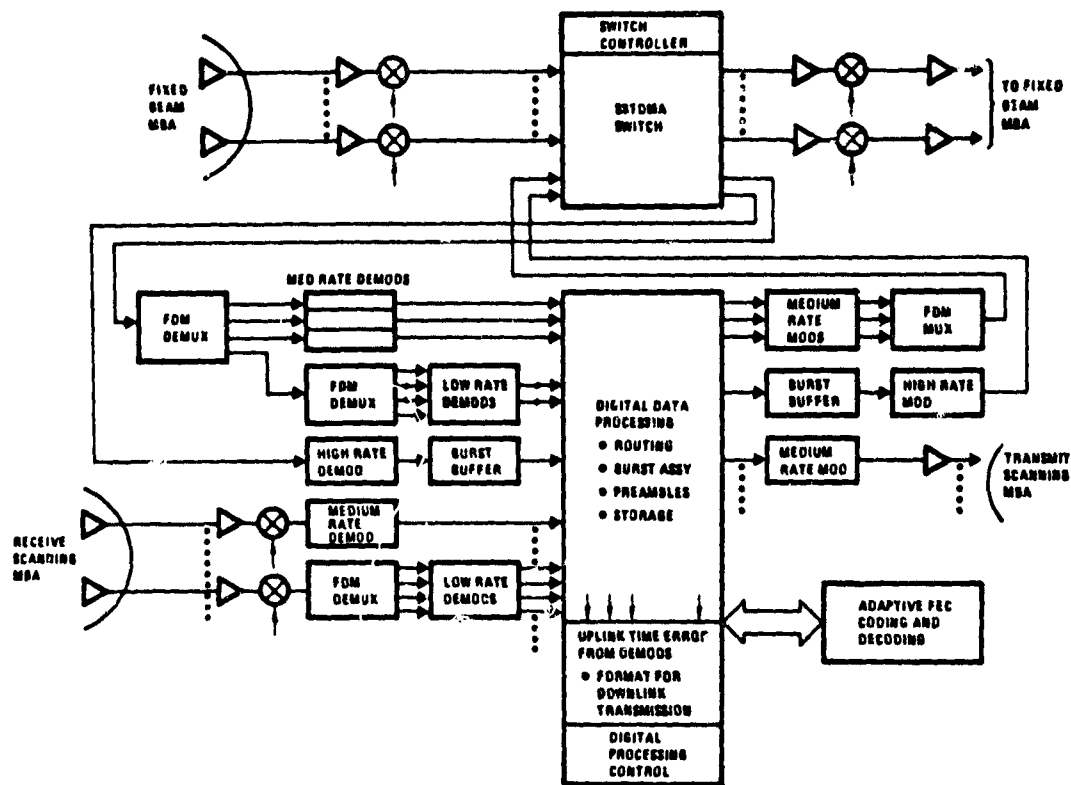


Figure 0-2. Satellite Communication Subsystem Block Diagram

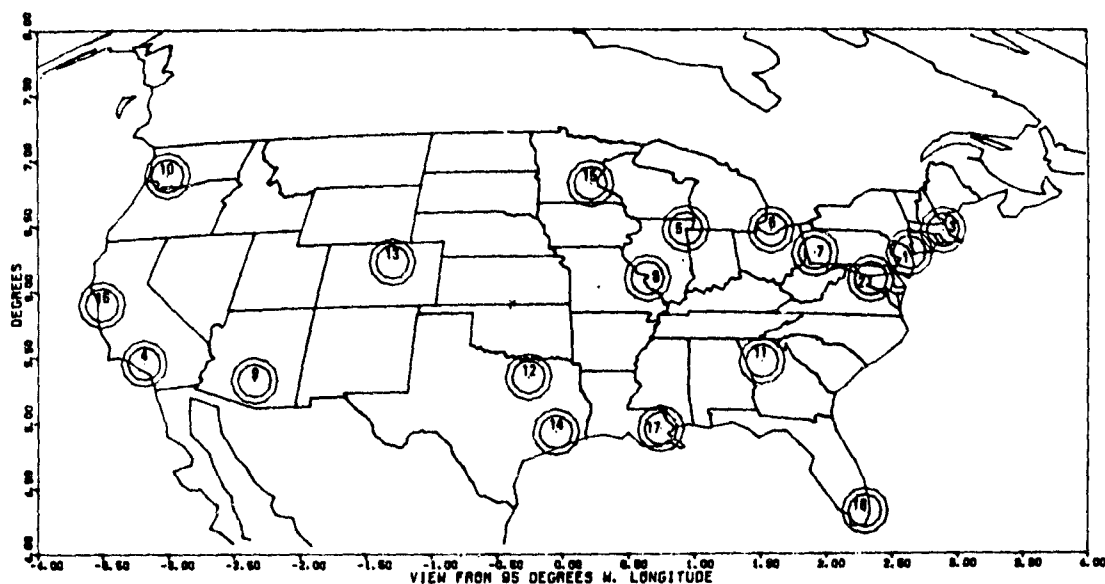


Figure 0-3. Trunking Station Plot



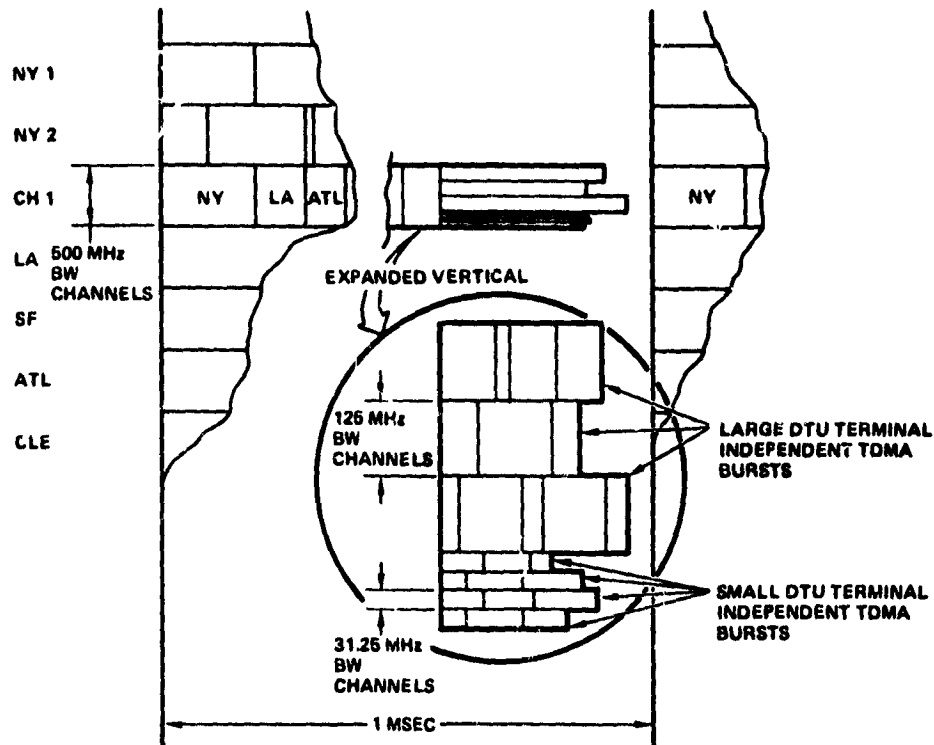


Figure 0-4. SSTDMA Frame Time Line, Fixed Beams

The satellite provides DTU communications between small terminals using 25 and 125 Mbps uplink burst rates and 250 Mbps downlink burst rates. DTU terminal average data rates vary from 64 kbps to as high as 100 Mbps. The satellite demodulates, routes, and remodulates the DTU signals and operates as a switchboard, providing the capability for one DTU terminal to talk to any combination of other DTU terminals. The satellite also provides adaptive forward error correction coding (FEC) on the uplink and downlink DTU signals to combat the effects of intense localized rain at a DTU terminal site.

There is no clear separation between DTU and trunking systems on the satellite. Those DTU terminals located in areas covered by the 18-beam, fixed-beam antenna system communicate through that antenna system in frequency-time slots not used by the high-capacity trunking terminals. Smaller trunking terminals located outside the fixed-beam areas communicate through the satellite on-board processing subsystem. Both small trunking terminals and DTU terminals communicate with large trunking terminals through buffers which interface a small portion of the 500 Mbps throughput with the on-board processor.

The entire satellite data rate capacity is about 10 Gbps. Of this, 8 Gbps is trunking and 2 Gbps is DTU traffic. About 8 Gbps of the traffic is located in the high-density areas served by the 18 beam fixed-beam antennae, and about 2 Gbps is in the scanning beam coverage area. Since all DTU traffic and all trunking in scanning-beam coverage areas must flow through the processor subsystem, the total on-board processor throughput is about 3 Gbps. About 1 Gbps of data must interface between the high capacity 500 Mbps SSTDMA and the on-board processing subsystems.

A portion of the 500 Mbps large trunking station data must be demodulated and remodulated to allow interfacing with the small trunking and DTU data. Because of the complexity of large SSTDMA IF switches, demodulation and remodulation of all high-rate data may be attractive. The complexity, size, weights, and power of demodulators may be small enough to reduce the overall system cost by this approach.

Because of the uncertainty of the development rate of the required technology, and because demodulation strips off timing information needed for system timing functions, the baseline satellite design uses IF switching SSTDMA at the 500 Mbps data rate. Complete demodulation and remodulation will be considered an option, subject to technology availability.

Spacecraft design requirements imposed by the communications mission, normal design practices, and assumed schedule are as follows:

- Ten-year design life, including 0.05- to 0.1-degree inclination control
- 0.03- to 0.05-degree antenna pointing
- Multimode 75-/7.5-watt fixed-beam transmission with ring redundancy
- Scanning beam redundancy by 50 to 60 percent transmitter operation
- Full eclipse operation
- No single-point failures for active components
- Shuttle launch
- 1985-1986 technology for a 1990 first-launch capability.

Based on these requirements a preliminary satellite design has been synthesized. The satellite is three-axis stabilized using reaction wheel control with RF sensing on the fixed-beam antennas providing two axes of sensing and either differential RF sensing or differential RF sensing and earth sensing providing the third axis. The antenna configuration consists of two 3-meter apertures, each with its associated tower housing feed networks and auxiliary reflectors. Each antenna system supplies nine of the 18 fixed spot beams, receive and transmit, as well as transmit and receive scanning beams. The antenna designs are similar to those synthesized in previous TRW in-house studies for advanced, high capacity communications satellites. The two 3-meter reflectors are stowed in approximately a north-south orientation and are deployed with a single hinge motion to assume their in-orbit east-west orientation.

The spacecraft is modular in design and includes an upper communications module plus a lower shuttle bus. The communications module houses the communications equipment, tracking telemetry and command RF equipment as well as earth and RF sensors. The communications module, shown as a box, can be augmented by north-south compartments extending alongside the antenna towers. These will house output elements such as TWTAs and output filters, providing additional thermal radiating area and shorter waveguide runs to the feeds.

The shuttle bus houses both the spacecraft service equipment as well as the apogee-perigee propulsion equipment for injection into geosynchronous orbit. The latter consists of a set of six tanks (three fuel and three oxidizer) in combination with low-thrust bipropellant motor(s), one or two, which provide the roughly 4370 meter/sec total velocity increment required to move the satellite from the shuttle orbit to synchronous orbit. The tanks are arranged in balanced pairs (fuel and oxidizer) to maintain the configuration balance, and are jettisoned in pairs as they are depleted. TRW is in the process of performing in-house engineering on this flexible, low-acceleration approach for use on a number of geosynchronous and interplanetary missions. This approach provides considerable cost savings in both upper stage and shared Shuttle launch costs, compared with the IUS. The bipropellant engine(s) are gimballed to provide control about the transverse axes. Control about the thrust axis is supplied by the hydrazine thrusters used for on-orbit attitude control.

Apogee is reached following a set of 10 to 12 perigee burns, each of 10 to 15 minutes duration. Perigee burns are programmer-controlled due to poor ground station visibility of the areas where perigee burns occur. Communication via TDRSS might be used to provide ground override but capability is not required. Perigee burn accuracy is not critical. Up to 4-degree pointing errors can be tolerated during perigee burns. Three to four apogee burns are used to circularize the orbit. The truncated triangular shape provides a convenient trunnion shuttle interface, and allows ejection from the shuttle by springs.

Power requirements and weight estimates given in Tables 0-2 and 0-3 are dominated by communications requirements. The communications system estimates are based on extrapolations of equipment technology to the 1985-1986 era for RF LSI and for digital micro-electronics, both under development at TRW. Size, weight, and power estimates have been checked against previous estimates made at TRW for advanced high-data-rate communications satellites. The fixed-beam TWTAs are assumed to be two-level devices, 75 watts and 7.5 watts, which operate only infrequently in the high power mode. The amplifier efficiency is 35-percent in the high power mode and 25 percent in the low power mode. The high power mode is supplied from the spacecraft batteries. The scanning-beam TWTAs are single-level 35-watt amplifiers. Only 60 percent of the complement of 20 tubes are operating at any one time.

Secondary power conversion is within the communications subsystem. The power requirement estimate is based on distributed power converters within each unit, fed by an unregulated bus. The power estimate in Table 0-2 is valid for either ion propulsion or heated hydrazine thrusters (HiPeht) which normally are fired only during the 270 days of noneclipse season. Hence, the charge array is sized to provide charge power, load and trickle, throughout the year to recharge sequentially two sets of two 50-Ah, nickel hydrogen batteries. These batteries, with cell bypass redundancy, are sized to provide either full communications eclipse load or full ion propulsion load. (The HiPeht requirement is less stringent.)

REPRODUCIBILITY OF THE  
ORIGINAL PAGE IS POOR

Table 0-2. Average On-Orbit Power Requirements

	Watts
Communications	3215
Receivers	425
Digital Processing and TDMA Switch	475
Transmitters (Less TWTAs)	180
Fixed Beam TWTAs (7.5 W at 25 percent)	540
Scanning Beam TWTAs (35 W at 35 percent)	1200
Scanning Beam Drive and Control	395
Attitude Determination and Control	90
Tracking Telemetry and Command	50
Thermal Control	50
Electrical Power	10
Subtotal	3415
Distribution	75
	3490
Charge Array	460
Margin (10 percent)	400
Total	4350

Table 0-3. Spacecraft Weight Summary

	HfPeht		Ion Propulsion	
	(lb)	(kg)	(lb)	(kg)
Communications	1,406	638	1,406	638
Antennas	466	211	466	211
Electrical Power and Distribution	874	396	874	396
Attitude Determination and Control	202	92	202	92
Structure/Thermal	900	408	900	408
Hydrazine Reaction Control	185	84	46	21
Ion Propulsion	--	--	303	137
RF Sensor	12	5	12	5
Tracking Telemetry and Command	110	50	110	50
	4,155	1,884	4,319	1,958
Contingency (15 percent)	625	283	648	294
	4,780	2,167	4,967	2,252
Pressurants and Residuals	1,350	613	60	27
Hydrazine Propellants, Pressurants and Residuals	--	--	137	62
Mercury Propellants, Pressurants and Residuals				
Spacecraft at Beginning of Life	6,130	2,780	5,164	2,341
Shuttle Bus Propellants	27,300	12,380	23,000	10,430
Shuttle Bus Dry Weight	2,900	1,315	2,446	1,109
Spacecraft Weight at Shuttle Separation	36,330	16,475	30,610	13,880
Spacecraft Cradle/Ancillary Equipment	1,130	512	1,090	495
STS Installed Weight	37,460	16,987	31,700	14,375

The eclipse battery requirement can be made equivalent to the ion propulsion thruster requirement. For eclipse, the approximately 5000-Wh requirement includes two fixed-beam tubes on high power mode for 1 hour. This requires four 47-Ah batteries with 28 cells at an 80 percent depth of discharge. By contrast, two 9-millinewton ion thrusters are fired for 3.85 hours at each of two nodes requiring about 2650 Wh for each node. The requirement in this case is about 50-Ah. With a recharge rate of C/10 and recharge ratio of 1.2 (put back 1.2 times the energy used) 420 watts are required for about 8 hours to recharge the two batteries. Additional technology work on nickel hydrogen batteries is required to justify the 80 percent depth of discharge for the 2000 to 2500 cycles assumed, i.e., (10 years)(90 cycles) + (5-6 years)(270 cycles).

The solar array power of 4.4 kW can be obtained by a number of different solar array techniques. Recent studies by TRW for a NORDSAT Direct Broadcast Satellite investigated lightweight foldout such as the SEPS or PEP concept under investigation by Lockheed and TRW, the rollout array typified by DORA (AEG/Telefunken) or FRUSA (Hughes) or the lightweight rigid ULP (MBB). The particular configuration shown in Figures 0-1 and 0-2 lends itself to the lightweight rigid array of MBB, the heaviest of those studied. Assuming a cell output improvement to 80 watts/m<sup>2</sup> at 10-year solstice, roughly 15 percent better than TDRSS technology, a weight of 27 kg/kW (including yoke but without drive mechanisms) is estimated.

The spacecraft weight summary is shown on Table 0-3 for the two cases of on-orbit propulsion. For the case of heated hydrazine (HiPeht), only inclination control is provided by the HiPeht thrusters. Attitude control and east-west stationkeeping is provided by conventional hydrazine one pound thrusters. In the case of ion propulsion, the results are based on a study of mercury thrusters performed by TRW for NASA Lewis. The higher thrust 9-millinewton level is used rather than the 4.5-millinewton level studied, because of the heavier spacecraft. Conventional hydrazine thrusters are also carried for apogee/perigee control, initial acquisition and other attitude control functions, but north-south and east-west stationkeeping and momentum dumping are performed using the body mounted gimballed ion thrusters.

REPRODUCIBILITY OF THE  
ORIGINAL PAGE IS POOR

The use of ion propulsion is dramatic in its weight saving (roughly 1000 pounds at beginning of life and almost 6000 pounds in STS installed weight). Since the use of Shuttle bus rather than IUS results in a relatively short STS installation, Shuttle launch charges are based on weight rather than length. The weight saving is equivalent to a \$3.3M saving per launch in 1979 dollars using the shared launch formula for commercial launches (i.e. \$18.4M compared with \$21.7M).

The weight of the communication and antenna subsystems dominate the dry weight, as would be expected. For the fixed-beam units, a ring redundancy concept has been adopted with three sets of nine-for-six redundancy for the active units. Hence, a total of 27 TWAs are provided for the 18 active beams. For the scanning beam, redundancy is achieved by the use of 50 to 60 percent of the available scan zones. The failure of equipment will necessitate reconfiguration of the scan zone geometry by ground switching. The demodulator technology is most difficult to estimate at this time. This may cause a large swing in the final weight since about 100 are being carried. For this weight estimate 1 kg is allotted to each unit.

The antenna reflector weight estimate is  $0.5 \text{ lb/ft}^2$ , similar to TDRSS and Intelsat V antennas. Advanced mesh reflectors could be lighter at the expense of greater cost and complexity.

Electrical power and distribution includes the solar array at 27 kg/kW (discussed earlier); four 50-Ah nickel hydrogen batteries at 1.3 kg/cell for 28 cells plus 15 percent packaging plus 3.7 kg/battery for cell bypass circuitry; a power control unit, a spacecraft converter and the power and signal harness. All RF cabling is estimated as part of the communications subsystem. Attitude determination and control is based on the aforementioned NORDSAT Study, on TDRSS/FLTSATCOM technology, and a three-axis control study (for Intelsat) on the use of four skewed reaction wheels. Tracking, telemetry and command assumes the use of S-band for preorbital operation and K-band for on-orbit operation. TDRSS technology and weights have been assumed. The adoption of advanced technology would undoubtedly lead to some weight saving but it would not be dramatic compared with the new communications technology savings or HiPeht versus ion propulsion savings.

Structure/thermal is estimated based on factors calculated for FLTSATCOM and TDRSS. Thermal control for the high power communications equipment would utilize heat pipe radiators especially because of the high and low power modes and the ring redundancy. If such a common baseplate approach were not used, each 7.5-/75-watt TWTAs would have to be designed for its maximum heat dissipation. The increase in radiator weight would be a prohibitive factor of 10.

A contingency factor of 15 percent is typical for such a preliminary estimate. The weight at shuttle separation is roughly six times the weight of the spacecraft at beginning of life. This is based on a number of propulsion-sizing studies recently performed at TRW. The lightweight cradle design is also extrapolated from recent TRW studies.

#### B. DTU Terminals

There are two DTU terminal classes, both corresponding to nominal terminal apertures of 3 meters. Terminal requirements are summarized in Table 0-4. There may actually be a range of DTU terminal sizes and designs. Figure 0-5 is a generalized small terminal block diagram. Certain DTU terminal parameters are allowed to vary to match site and user requirements. These parameters include antenna size, transmitter power, preamplifier noise-figure, transmitter redundancy level, and receiver redundancy level. Other terminal components will be standardized, leaving the variable parameters to accommodate individual user and site requirements.

The smallest DTU terminal class uses a 25-Mbps uplink burst rate and a 10-watt transmitter. The downlink data rate is the standard 250-Mbps burst rate, but the clear-weather margin will be low and adaptive forward error correction coding (FEC) will be needed quite often to overcome rain losses. The satellite charges for service to this class of user should be relatively large, since a disproportionate share of satellite resources are required to provide communication service. Five times as many satellite demodulators are required to provide a given throughput as compared to the large DTU terminals.



Table 0-4. Terminal Summary

<b>LARGE TRUNKING TERMINALS (18 REQUIRED)</b>
12-M ANTENNAS
DUAL TERMINAL 10 KM SEPARATION DIVERSITY (0.9999 AVAILABILITY)
500 MBPS SSTDMA
<b>LARGE DIRECT-TO-USER TERMINALS (SEVERAL THOUSAND)</b>
3-M ANTENNAS, 50 WATT TRANSMITTERS
NO DIVERSITY (0.999 AVAILABILITY)
125 MBPS UP, 250 MBPS DOWN BURST RATE
INTERFACE BASED ON DS1 1.544 MBPS SIGNAL
INDIVIDUAL 64 Kbps CHANNEL ROUTING
<b>SMALL TRUNKING TERMINAL (50 REQUIRED)</b>
TWO LARGE DTU TERMINALS WITH 10 KM DIVERSITY
0.9999 AVAILABILITY
<b>SMALL DTU TERMINAL (SEVERAL THOUSAND)</b>
25 MBPS UP, 250 MBPS DOWN
3-M ANTENNA, 5-WATT TRANSMITTER

REPRODUCIBILITY OF THE  
ORIGINAL PAGE IS POOR

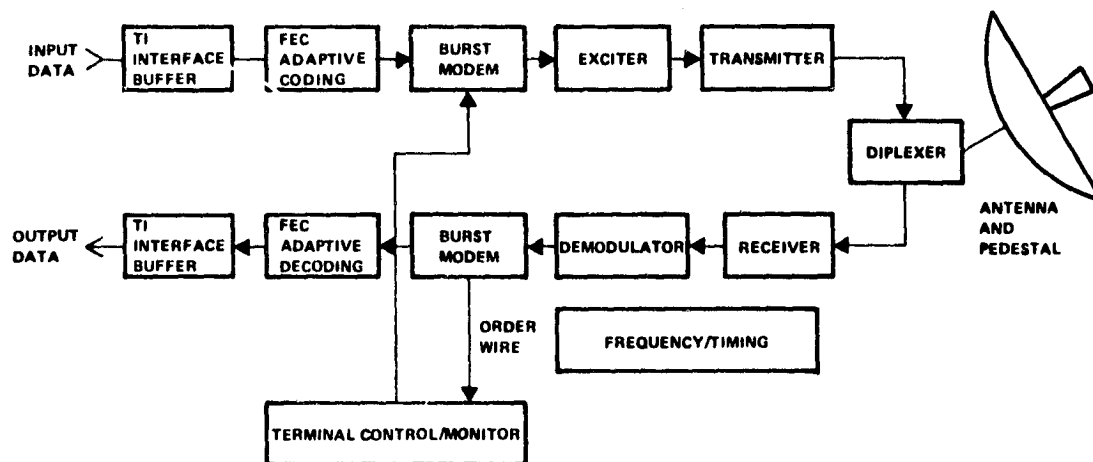


Figure 0-5. Small Earth Terminal Block Diagram

Larger DTU terminals use a 125-Mbps uplink burst rate and a 50-watt transmitter. Satellite charges should, therefore, be lower for these terminals on a per-circuit basis since less satellite hardware is required for their support. The terminal class must be selected on a location-by-location basis to minimize the total communication cost.

Within the two classes, design flexibility is provided to minimize terminal cost, also on a location-by-location basis. DTU terminals in urban areas may be mechanized with smaller apertures and more expensive transmitters and receiver preamplifiers to reduce site requirements. The advantages include smaller wind loads for roof-mounted structures, less visual impact, and less use of valuable space. In rural areas, larger apertures may allow using less expensive transmitters and receiver preamplifiers for the same overall EIRP and G/T performance. Similarly, Gulf Coast users will have to use large apertures and more expensive transmitters and receiver preamplifiers, as compared to Western users, because of the larger rain-loss effects.

DTU terminal design complexity is minimized by using a standard DS1 interface, as used in the Bell System T1 digital carrier system for up to 24-voice channels of traffic. Special video interfaces will be required for video users, other than slow-scan video users who can operate within the 1.536-Mbps-effective DS1 data rate. Using a standard interface will allow commercially available, high-volume hardware up to the terminal interface.

The entire DS1 signal will not be transmitted through the satellite system, however. Synchronization pulses will be stripped out, unassigned channel data will be detected and deleted, and only the 64 kbps per active voice channel data will be transmitted. On the receive side, 64-kbps channel data from multiple sources will be assembled into a standard DS1 output signal with locally generated synchronization pulses. Automatic demand assignment will provide new channel connections within as required, giving a DTU terminal 24 effective full-time channels for each DS1 interface. Routing is accomplished on the satellite on a per-voice channel basis, so the voice channels coming into a DTU terminal on a particular DS1 interface may be routed to any number of destinations.

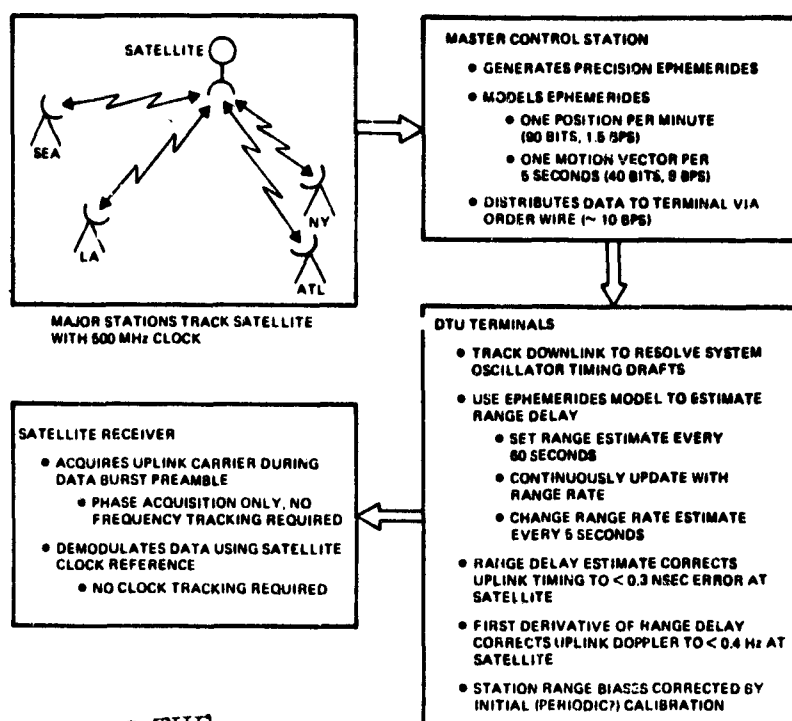
Several of the features of the DTU terminal were selected to standardize hardware designs and reduce terminal cost. DS1 signal buffering and automatic demand assignment features, described above, are examples. The DTU terminal design philosophy is to utilize command and telemetry data over a system order wire to provide the more complex functions in the system master control station. Local "intelligence" will be used in each terminal to keep each terminal's order-wire command and telemetry requirements below 1 kbps, or one bit per frame.

The DTU terminal synchronization subsystem uses calculator technology to calculate precise and accurate time advance for the terminal transmit signal (Figure 0-6). The calculation rate is very slow: 1 per 5 seconds. The calculated data drives a simple indirect synthesizer which deletes pulses from the receive time/frequency reference signal to provide the transmit time/frequency reference signal. Calculations are based on order wire "command" data, station location data, and station timing-bias calibration data. The result is a precise open-loop terminal synchronization technique that makes initial synchronization and net entry trivial. The cost should be less than burst-acquisition synchronization techniques since all circuit parameters are noncritical.

Minimization of terminal cost, primarily for the DTU terminals is a major decision factor in all design decisions. DTU terminal cost must be below \$100,000 (1979 dollars) for an economic system design. A cost goal of \$30,000 would, if met, make the system extremely competitive with terrestrial communication techniques. Table 0-5 describes a first cut at terminal costing. Further work is needed in integrating components and in assessing "learning-curve" factors in volume production.

#### C. Small Trunking Terminals

Small trunking terminals are mechanized using the same hardware as for DTU terminals, except that they require two terminal locations separated by about 10 km to provide space diversity. Trunking terminals require an availability of 99.99 percent to meet commercial trunking standards. In most parts of the country rain losses will drive availability below the "four nines" level with any reasonable degree of rain margin.



REPRODUCIBILITY OF THE  
ORIGINAL PAGE IS POOR

Figure 0-6. Terminal Timing Control

Table 0-5. DTU Terminal Cost Projections Summary

	Rack Space (inches)	Small Quantity Cost (\$)	Total (%)	Development Cost (\$)	Large Quantity Estimate (\$)	(%)
<u>Rack Mounted Modules</u>						
Power Supply	12	7K	2.4	2000 K	5K	3.9
Time and Freq Control	8	25K	8.5		15K	11.7
Encoder Decoder	3	3K	1.0		2K	1.6
Modem	12	125K	42.7		35K	27.3
Fault Iso and Test	10	30K	10.2		20K	15.6
Receiver - IF	6	16K	5.5	1000 K	10K	7.8
Exciter-up Conv	6	12K	4.1		8K	6.3
Power Amp (Solid Sta)	6	10K	3.4		5K	3.9
Other (Rack, Cables)	-	15K	5.1		5K	3.9
Subtotal	5'3"	\$243K	72.9		\$105K	72.0
<u>Pedestal Mounted</u>						
Diplexer		2.5K	0.9	200 K	1.5K	1.2
LNA		2.0K	0.7		1.5K	1.2
Antenna and Pedestal		15.5K	5.3		10.0K	7.8
Step Track		30.0K	10.2		10.0K	7.8
Subtotal		\$50K	17.1		\$23K	18.0
Total		\$293K			\$128K	

A 10-km separation between diversity sites reduces the rain-margin requirement to reasonable levels. The rain storms that cause outages are intense and small. Large rain storms do not have the rain intensity necessary to cause outages, or have small high-rain-intensity cells embedded in them. This fortunate physical characteristic results in statistical "decorrelation" of outages and makes 99.99 percent availability achievable with site diversity.

Fiber-optic communications are used to connect the two diversity sites. Microwave links may also be used where right-of-way problems are severe. However, the microwave link design must consider the same rain-loss effects that preclude single-site satellite tracking communications. Repeaterless operation of fiber-optic links over 10 km paths should be feasible in the planned operational time frame for the 30/20 GHz system.

Normal diversity operation will consist of parallel reception at both sites with transmission from a designated primary site. Data output will be from the site indicating the highest SNR or signal quality. Reduction in the received signal level at the designated primary site will cause transmission to be shifted to the designated alternate terminal. Rain attenuation effects between 20 and 30 GHz are very highly correlated, especially at intense rain rates where drop-size variations are small. As a result, downlink quality provides an excellent indicator to control uplink diversity switching.

#### D. Large Trunking Terminals

The large trunking terminals may be relatively expensive without strongly affecting system cost. This results from the small number of large trunking terminals. A very few large terminals may have very high data throughputs, up to three or four 500 Mbps channels. Most will have a single 500 Mbps burst rate TDMA channel.

The terminal receivers will use fast-acquisition demodulators to derive synchronization on each received TDMA burst if IF switching is used for 500 Mbps SSTDMA in the operational system. Transmit synchronization will use return modes in the SSTDMA switch, or transmit synchronization data may be extracted by the master control station (which will be at one of the large terminals) and distributed by system order wire.

Large terminal synchronization will be similar to DTU terminal synchronization if demodulation and remodulation with digital SSTDMA switching is used in the satellite, with some satellite received-clock-error feedback to the master control station.

In addition to data transmission, the large trunking terminals will provide the raw data used to derive the satellite position. This is done by measuring time delay on the 500-MHz high-rate data clock. The clock timing information is collected at each large terminal and transmitted to the master control station by order wire.

#### E. Master Control Station

The master control station will be located at one of the large trunking terminals. At least one alternate control station will be provided at another large trunking terminal. The master control station controls the satellite and the individual terminals. Functions controlled include:

- Satellite On-board Processing
- Scanning-Antenna Phase Shifting
- SSTDMA Modes and Dwell Times
- TWTAs Power Levels
- Satellite Attitude Control Bases
- Satellite Stationkeeping
- Satellite Redundancy
- Satellite Housekeeping, Telemetry, and Command
- Satellite Ephemerides Data Reduction
- Individual Terminal TDMA assignments
- Individual Data Channel Routing Control
- Individual Terminal Control and Maintenance Planning.

To accomplish all the required functions, the master control station will incorporate a large computing capability. The master control station cost can be significant, but overall system cost will be minimized by centralizing the system computing requirements and utilizing the inherent system communication capability to collect data and distribute results.

Since alternate master control station capability is required for reliability and availability, the optimum design may place identical master control station facilities at several large trunking terminals. Computational tasks may normally be distributed to achieve high hardware utilization. Failures requiring shifts of control capabilities can be handled by deferring low priority tasks (maintenance scheduling and parameter trend evaluation, for example), and redistributing high priority tasks.

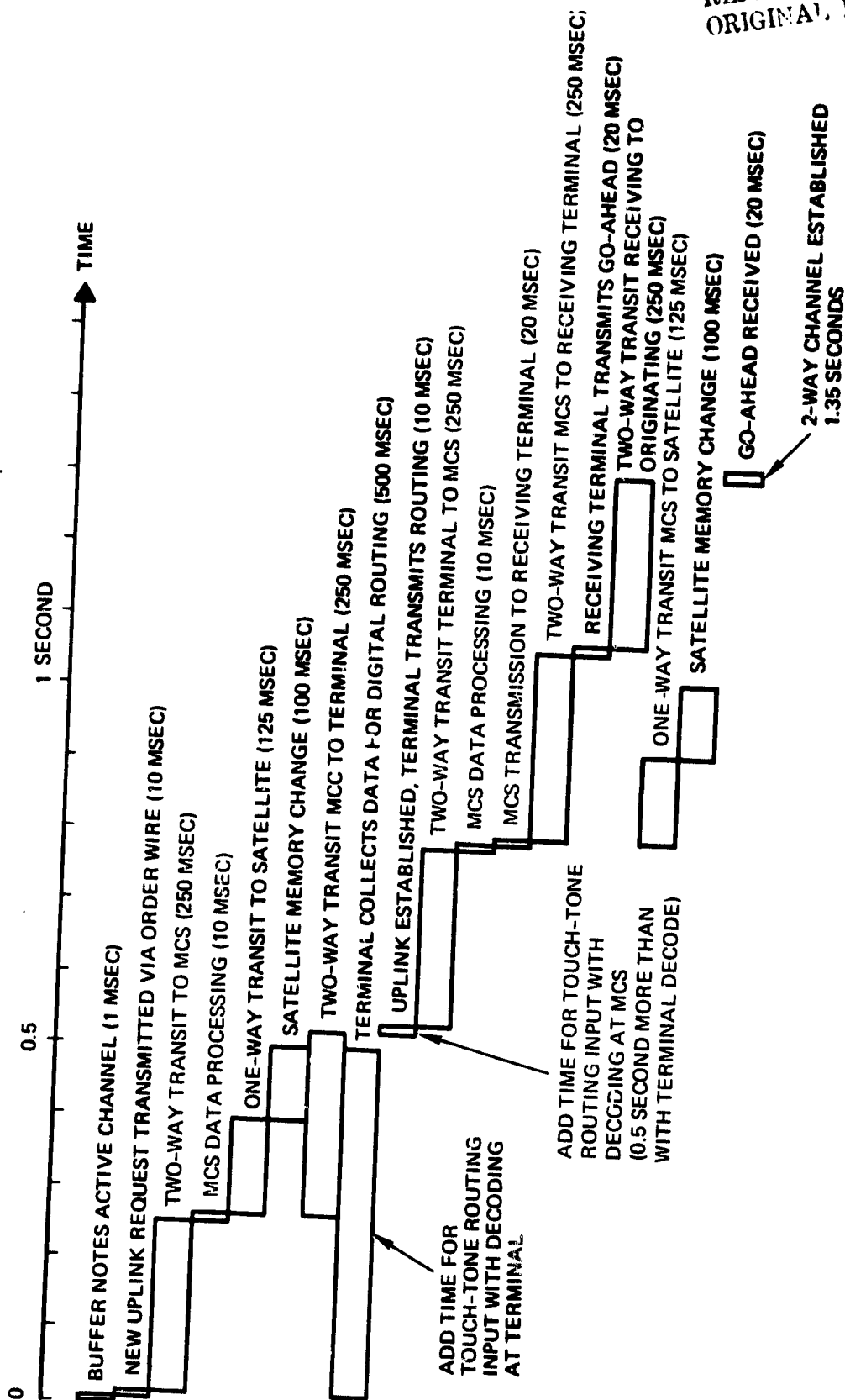
#### F. 30/20 GHz System TDMA Architecture

The baseline TDMA architecture has, for the most part, been described in the process of describing the baseline system segments; the satellite terminals, and master control station. DTU users communicate at 25- or 125-Mbps uplink burst rate and receive at 250-Mbps downlink burst rate. Small trunking users transmit 125-Mbps uplink burst rate data and receive at 250-Mbps downlink data rate. Small trunking terminals are indistinguishable from large DTU terminals in the TDMA architecture hierarchy. The only difference is site diversity which is required at most small trunking terminals to achieve 99.99 percent availability.

Large trunking users transmit and receive at 500 Mbps burst rate on both uplink and downlink. Their TDMA architecture is a straightforward SSTDMA, except for the sharing of their uplink and downlink channels by the DTU users (Figure 0-4).

The master control station philosophy provides efficient control of the instantaneous system TDMA architecture within the design limits. An example of the adaptive nature of this approach is provided by Figure 0-7, the time line for establishing a new voice.

Establishing new 64-kbps, voice-quality channels within the 1.35 seconds shown will require TDMA timing changes that could, theoretically, affect timing of all stations in the network. This level of impact will be avoided by appropriate distribution of system unused capacity throughout the areas being served. This time line illustrates the flexible behavior possible with a large disciplined system under centralized control.



FOR ONE-WAY CHANNEL, GO-AHEAD  
 ROUTING IS VIA MCS ON ORDER WIRE.  
 ADD 250 MSEC TURN AROUND AND  
 20 MSEC TRANSMISSION PROCESSING.

Figure 0-7. New Voice Channel Establishing Time Line



## 1. TRAFFIC DEMAND MODEL

A multirate SSTDMA architecture for a 30/20 GHz satellite system must be developed to satisfy a particular well-defined traffic model. This model must define the total traffic that the 30/20 GHz satellite must accommodate and the geographical distribution of that traffic. Such a model was developed, and is described in this section.

The traffic model defined for the 30/20 GHz baseline system relies heavily upon the work performed by Western Union and ITT in their NASA-sponsored 30/20 GHz market studies. This information was obtained through NASA-approved direct contacts with both companies, and from the June 1979 oral final report at LeRC. Where discrepancies existed between these two studies or where suitable information was not available, assumptions were generated based upon TRW's experience in commercial data - traffic modeling. A very brief summary of the WU and ITT work is provided below as a general indication of the scope of their results. This is followed by a description of the TRW-derived model used in baseline system design.

### 1.1 SUMMARY OF WU AND ITT STUDY RESULTS

Under the ground rules for the NASA-sponsored marketing studies, each contractor worked separately to provide independent assessments of future demand. Consequently, the results of their studies differ significantly. Not only does the total predicted demand differ, but emphasis upon the components of that demand varies. A summary and comparison of key results for the 1990 time frame is provided in Table 1-1. This table highlights primary differences between the WU and ITT efforts. WU forecasted approximately 10 times the amount of the ITT voice traffic, while ITT predicted about six times the WU video demand. The data traffic predictions of both companies were roughly the same order of magnitude (WU about 35 percent higher).

To provide a common measure of comparison among all traffic categories the entire demand was translated into the number of the satellite transponders required to transmit that particular service. In performing this translation, ITT predicted the actual demand that would be captured by

Table 1-1. Summary of WU and ITT 1990 Satellite Traffic Demand

	ITT	WU
Total Demand		
● Voice (1000 circuits)	895 (Channels)	8050 (1/2 circuits)
● Data (terabits/year)	6940	10559
● Video (channels)	1765	294
Total Satellite Demand	Captured	Net Addressable
● Total Transponders	690	829
● Total Data Rate	49680 (at 72 Mbps/ Transponder)	41,500 (at 50 Mbps/ transponder)
Total Predicted C/Ku-band Capacity		
● Transponders	648	348
● Data Rate (Mbps)	46,656 (at 72 Mbps/ transponder)	17400 (at 50 Mbps/ transponder)
30/20 GHz Satellite Demand		
● Voice (1000 circuits)	Did not provide an 18/30 GHz	215 (1/2 circuits) (2.7%)*
● Data (terabits/year)	Satellite Traffic	1732 (12.6%)
● Video (channels)	Projection	37 (16.4%)
● Total Transponders		174
● Total Data Rate		8700 (at 50 Mbps/ transponder)

\*Percentage of total traffic demand

satellite systems, while WU only identified the traffic that was operationally and economically suited to satellite transmission (the "Net Addressable Demand"). In terms of satellite transponders, the WU demand exceeded the ITT prediction by about 20 percent (820 versus 690 transponders). In terms of total data rate, however, the ITT forecast exceeded the WU traffic demand by about 20 percent. This occurred because WU assumed each satellite transponder would be limited to transmitting a maximum of 50 Mbps, and ITT used 72 Mbps for transponder capacity. The total predicted satellite data traffic demand was roughly the same.

Both companies then predicted the maximum United States domestic satellite capacity that could be achieved by satellite systems employing the allocated C-band and the Ku-band frequencies. Once again they came to somewhat different conclusions. WU expected the current frequency bands to saturate at a level of 348 transponders, while ITT viewed the situation more optimistically, predicting a maximum of 648 transponders at saturation. ITT did not provide a 30/20 GHz traffic prediction but forecast that the existing frequency band and orbital slot allocations would saturate about 1990. Western Union forecast a 30/20 GHz demand in 1990 of 174 transponders (i.e., 8.7 Gbps at 50 Mbps per transponder). As can be seen from Table 1-1, this demand was heavily weighted by the voice circuit traffic. Although a large part of the satellite traffic, this voice demand represented only 2.7 percent of the total predicted voice demand - a rather modest capture ratio. Both the video and data demand reflect similarly conservative capture ratios (less than 20 percent).

Both companies provided additional details which also served as inputs into the TRW demand model. Each company prepared its list of the 40 more important satellite trunking locations in CONUS; these locations are presented in Table 1-2. By comparing lists and combining suburban locations with principal cities, i.e., New York and Nassau/Suffolk, San Francisco and San Jose, a composite set of 45 trunking locations were identified.

The 45 trunking locations were divided into major and minor locations. Major trunking locations are to be served by fixed antenna beams. The locations of these beams are plotted in Figure 1-1 as seen from geosynchronous orbit (95°W longitude). The other trunking locations are to be served by the scanning beams and on-board processor subsystem that also serves the DTU terminals.

Table 1-2. Forty Largest Satellite Trunking Locations

Western Union	ITT
New York	Atlanta
Chicago	Chicago
Los Angeles	Dallas
San Francisco	Denver
Dallas	Houston
Minneapolis/St. Paul	Minneapolis/St. Paul
Atlanta	New York
Denver	San Francisco
Washington, DC	Washington, DC
Boston	Boston
Detroit	Buffalo
Pittsburg	Detroit
St. Louis	Miami
Miami	New Orleans
Seattle	Phoenix
New Orleans	Pittsburg
Phoenix	Portland
Portland	Seattle
Buffalo	St. Louis
Philadelphia	Albuquerque
Newark	Birmingham
Baltimore	Charlotte
Cleveland	Cincinnati
Nassau/Suffolk	Cleveland
Anaheim/Santa Ana	El Paso
Cincinnati	Indianapolis
San Jose	Jacksonville
Milwaukee	Kansas City
Kansas City	Louisville
Hartford	Memphis
Columbus	Milwaukee
San Diego	Nashville
Indianapolis	Oklahoma City
Tampa/St. Petersburg	Omaha
Memphis	San Antonio
Louisville	San Diego
Ft. Lauderdale/Hollywood	Syracuse
Oklahoma City	Tampa
Salt Lake City	Tucson

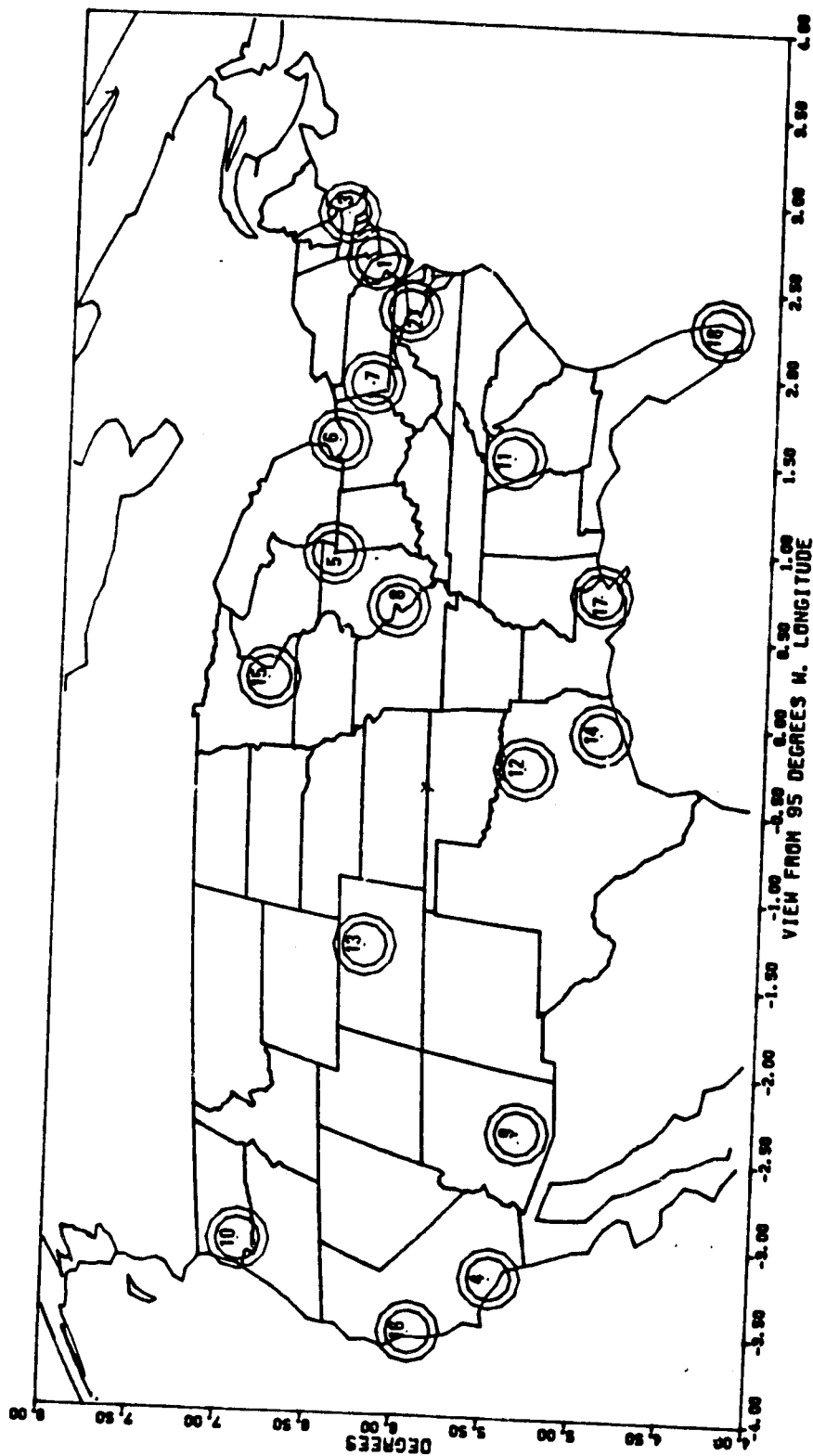


Figure 1-1. Trunking Station Plot

In addition, both ITT and WU provided important market data on the private line (or direct) user that was employed in our model. ITT distributed the 10,000 direct terminals postulated by NASA among the 158 largest metropolitan areas (SSMA) as shown in Table 1-3. The distribution ranges from a maximum of 700 terminals in the New York - New Jersey area to a minimum of 14 in Stamford, Connecticut and Killen, Texas. The direct user locations were also plotted in the same manner as the trunking statistics and the results are given in Figure 1-2.

Western Union identified three classes of private line or direct users (each with a different capacity) and provided an estimate of their distribution as shown in Table 1-4. Although the high-capacity terminal has a composite data rate of about 34 Mbps, it has a rather limited distribution. As can be seen from this table, the vast majority of the direct users have very modest information needs, i.e., less than 1 Mbps.

## 1.2 TRW OVERALL DEMAND MODEL

The WU traffic model was selected as the starting point in developing the TRW composite traffic model. These data were supplemented, where appropriate, with pertinent ITT results. TRW adopted the WU approach as our baseline for two reasons: (1) it appears reasonable that any early operation 30/20 GHz satellite system must be designed to satisfy an increased voice-trunking demand and (2) the WU prediction that a 30/20 GHz system will initially capture about 20 percent of the total net addressable satellite demand seems plausible. In addition, only Western Union provided data on the capacity requirements for direct/private line users. ITT data were used in distributing the postulated direct user traffic.

A two-step methodology was employed in developing a traffic model whose format matched the needs of the baseline system design effort. First, an overall 1990 demand was synthesized based upon the WU results supplemented by ITT data. The resultant demand was then compared against the corresponding WU 30/20 GHz forecast as a check. Second, the overall demand was distributed among CONUS locations to obtain the geographical distribution required.

Table 1-3. Distribution of 10,000 Direct-to-User Terminals  
Over the 158 Major SMSAs

Metropolitan Area	Number of Terminals
Akron, OH	48
Albany, Schenectady, Troy, NY	57
Albuquerque, NM	28
Allentown, Bethlehem, Laston, PA, NJ	45
Anaheim, Santa Ana, CA	123
Ann Arbor, MI	17
Appleton, Oshkosh, WI	20
Atlanta, GA	127
Augusta, GA, SC	20
Austin, TX	28
Bakersfield, CA	25
Baltimore, MD	155
Baton Rouge, LA	29
Beaumont, Port Arthur, Orange, TX	25
Binghamton, NY, PA	21
Birmingham, AL	56
Boston, MA	210
Bridgeport, CT	28
Buffalo, NH	95
Canton, OH	28
Charleston, North Charleston, SC	26
Charleston, WV	18
Charlotte, Gastonia, NC	42
Chattanooga, TN, GA	28
Chicago, IL	505
Cincinnati, OH, KY, IN	98
Cleveland, OH	142
Colorado Springs, CO	20
Columbia, SC	26
Columbus, GA, AL	16
Columbus, OH	76
Corpus Christi, TX	21
Dallas, Ft. Worth, TX	180
Davenport, Rock Island, Molina, IA, IL	26
Dayton, OH	60
Denver, Boulder, CO	100
Des Moines, IA	23
Detroit, MI	321
Duluth, Superior, MN, WI	19
El Paso, TX	30
Erie, PA	20
Eugene, Springfield, OR	17
Evansville, IN, KY	21

Table 1-3. Distribution of 10,000 Direct-to-User Terminals  
Over the 158 Major SMSAs (Continued)

Metropolitan Area	Number of Terminals
Fayetteville, NC	16
Flint, MI	37
Ft. Lauderdale, Hollywood, FL	61
Fort Wayne, IN	27
Fresno, CA	82
Gary, Hammond, East Chicago, IN	46
Grand Rapids, MI	40
Greensboro, Winston Salem, High Point, NC	57
Greenville, Spartanburg, SC	38
Hamilton Middletown, OH	17
Harrisburg, PA	31
Hartford, CT	52
Houston, TX	167
Huntington, Ashland, WV, VA, KY, OH	21
Huntsville, AL	20
Indianapolis, IN	81
Jackson, MS	20
Jacksonville, FL	49
Jersey City, NJ	41
Johnson City, Kingsport, Bristol, TN, VA	29
Johnstown, PA	19
Kalamazoo, Portage, MI	19
Kansas City, MO, KS	82
Killen, Temple, TX	14
Knoxville, TN	31
Lakeland, Winter Haven, FL	20
Lancaster, PA	24
Lansing, East Lansing, MI	32
Las Vegas, NV	23
Lawrence, Haverhill, MA, NH	19
Lexington, Fayette, KY	20
Lima, OH	15
Little Rock, North Little Rock, AR	25
Long Branch, Asbury Park, NH	35
Lorain, Elrya, OH	19
Los Angeles, Long Beach, CA	505
Louisville, KY, IN	63



Table 1-3. Distribution of 10,000 Direct-to-User Terminals  
Over the 158 Major SMSAs (Continued)

Metropolitan Area	Number of Terminals
Macon, GA	17
Madison, WI	21
McAllen-Pharr, Edinburg, TX	16
Melbourne, Titusville, Cocoa Beach, FL	16
Memphis, TN, AR	62
Miami, FL	103
Milwaukee, WI	100
Minneapolis, St. Paul, MN, WI	144
Mobile, AL	29
Modesto, CA	16
Montgomery, AL	19
Nashville, Davidson, TN	53
Nassau, Suffolk, NH	190
Newark, NY	143
New Brunswick, Perth Amboy, Sayreville, NH	42
New Haven, West Haven, CT	29
New London, Norwich, CT, RI	18
New Orleans, LA	78
Newport News, Hampton, VA	25
New York, NH, NJ	700
Norfolk, Virginia Beach, Portsmouth, VA, NC	55
Northeast, PA	45
Oklahoma City, OK	53
Omaha, NE, IA	41
Orlando, FL	42
Oxnard, Simi Valley, Ventura, CA	31
Paterson Clifton, Passaic, NH	32
Pensacola, FL	19
Peoria, IL	25
Philadelphia, PA, NH	137
Phoenix, AZ	87
Pittsburg, PA	169
Portland, OR, WA	77
Poughkeepsie, NH	17
Providence, Warwick, Pawtucket, RI, MA	64
Raleigh, Durham, NC	34
Reading, PA	22
Richmond, VA	42
Riverside, San Bernardino, Ontario, CA	87
Roanoke, VA	15
Rochester, NH	69
Rockford, IL	19

Table 1-3. Distribution of 10,000 Direct-to-User Terminals  
Over the 158 Major SMSAs (Continued)

Metropolitan Area	Number of Terminals
Sacramento, CA	63
Saginaw, MI	16
Salem, OR	16
Salinas, Seaside, Monterey, CA	19
Salt Lake City, UT	60
San Antonio, TX	70
San Diego, CA	113
San Francisco, Oakland, CA	228
San Jose, CA	84
Santa Barbara, Santa Maria, Lompoc, CA	20
Santa Rosa, CA	17
Seattle, Everett, WA	100
Shreveport, LA	25
South Bend, IN	20
Spokane, WA	22
Springfield, Chicopee, Holyoke, MA, CT	39
St. Louis, MO, IL	173
Stamford, CT	14
Stockton, CA	21
Syracuse, NY	46
Tacoma, WA	30
Tampa, St. Petersburg, FL	96
Toledo, OH, MI	56
Trenton, NH	23
Tucson, AZ	32
Tulsa, OK	42
Utica, Rome, NY	24
Vallejo, Fairfield, Napa, CA	20
Washington, DC, MD, VA	220
Waterbury, CT	16
West Palm Beach, Boca Raton, FL	32
Wichita, KS	27
Wilmington, DE, NH, MD	37
Worcester, MA	27
York, PA	25
Youngston, Warren, OH	39

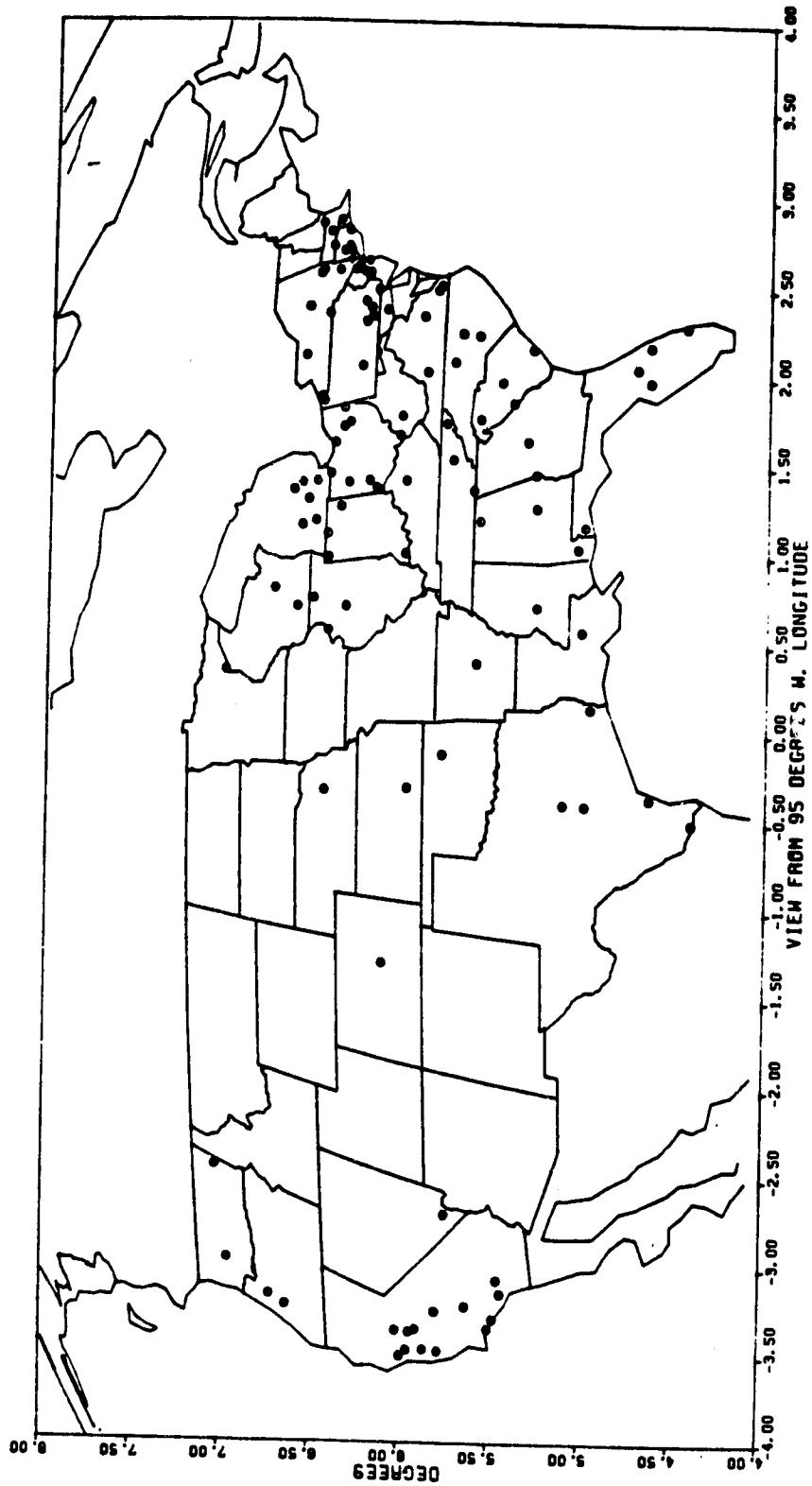


Figure 1-2. Direct/Private User Plot

Table 1-4. Direct-to-User Terminal Classes

Earth Terminal Size	Information Needs			Composite Data Rate	Distribution (percent)
	Voice*	Data	Video		
High Capacity	240	2 1.5 Mbps 20 56 kbps	1 6.3 Mbps 5 1.5 Mbps 10 56 kbps	33.84 Mbps	1.25
Medium Capacity	60	5 56 kbps	1 1.5 Mbps 2 56 kbps	5.564 Mbps	12.75
Low	12	1 56 kbps	1 56 kbps	880.0 kbps	86.00

\*One voice channel is 64 kbps.

Using data supplied by ITT, the 45 trunking locations discussed in the previous section were classified in 20 major and 25 thin-route stations. The major stations were again subdivided into four primary and 16 secondary locations. The thin-route stations were also subdivided in high-capacity and low-capacity locations. This division was based upon a detailed traffic distribution matrix provided by ITT. The information needs of each of these types of stations, with the resulting peak data rates, are presented in Table 1-5.

Of the 10,000 private-line/direct user terminals which might ultimately use the 30/20 GHz system, TRW assumed that only 2000 would be operating by 1990. It was further assumed that only 50 percent of all these terminals would be operating during the peak busy hour.

Using the above numerical values, the overall (i.e., CONUS-wide) peak busy hour traffic demand can be constructed. Assuming all the voice trunking circuits are active during the peak busy hour, the total trunking demand is 8 Gbps (see Table 1-6). By allocating the 1000 active terminals into the three classes of direct terminals contained in Table 1-4, the total peak private line (DTU) demand, as shown in Table 1-6, is 1906.08 Mbps. The traffic model peak demand is 9.9 Gbps. This result compares reasonably well with the 8700 Mbps forecast by WU. Note that

Table 1-5. Trunking Terminals Classes

Earth Terminal Size	Number of Terminals	Information Needs	Peak Data Rate (Mbps)
● Major			
- Primary	4	2 T4 Data	548.352
- Secondary	16	1 T4 Data Group	274.175
● Thin-Route			
- High Capacity	15	2 T3 Data Groups	87.472
- Low Capacity	10	2 T2 Data Groups	12.624

Table 1-6. Overall Demand Model

Terminal Description	Number of Active Terminals	Data Rate Per Terminal	Total Data Rate
<b>TRUNKING DEMAND</b>			
<u>Major Stations</u>			
● Primary	4	548.4 Mbps	2193.6 Mbps
● Secondary	16	274.2 Mbps	4387.2 Mbps
<u>Thin Route Stations</u>			
● High Capacity	15	87.5 Mbps	1312.5 Mbps
● Low Capacity	10	12.6 Mbps	126.0 Mbps
Trunking Subtotal			8019.3 Mbps
<b>PRIVATE-LINE (DTU) DEMAND</b>			
● High Capacity Stations	12	33.84 Mbps	406.08 Mbps
● Medium Capacity Stations	128	5.56 Mbps	711.68 Mbps
● Low Capacity Stations	860	880.0 Kbps	765.80 Mbps
Private-Line Subtotal	1000		1874.56 Mbps
<b>TOTAL DEMAND</b>			<b>9.894 Gbps</b>

approximately 80 percent of the total demand results from voice trunking needs, as would be expected given in our assumptions.

To define the baseline satellite architecture it is necessary to segregate the high-speed trunking traffic from the on-board processor traffic. This can be accomplished by identifying the DTU traffic generated within major concentrations, plus the trunking traffic that must be served outside the major concentrations.

Looking at the traffic within the 18 major traffic concentrations shown in Table 1-8, the total DTU traffic generated is 1.05 Gbps. This traffic is generated by only 12 of the 18 locations. The remaining six locations generate trunking traffic at the maximum rate that can be accommodated by the satellite. The DTU traffic from these 12 locations represents about 50 percent of the total system DTU traffic.

The total thin-route trunking demand within the 31 minor traffic concentrations is only 0.4 Gbps. This constitutes 19 percent of the traffic generated by these locations, but is only about 5 percent of the total trunking demand (of about 8 Gbps). While the major traffic concentrations generate a sizeable portion of the DTU traffic, the minor traffic concentrations contribute a very small part of the trunking demand.

The total small-user peak traffic (i.e., the DTU traffic plus thin-route trunking demand) is 3 Gbps. This composite rate is approximately one third of the total demand identified in Tables 1-6 and 1-8. It also appears to be a reasonable approximation of the traffic demand indicated by the WU and ITT data.

### 1.3 TRW TRAFFIC DISTRIBUTION MODEL

A highly quantized approach was used to generate the traffic distribution model. The first step was to identify representative traffic concentrations. The number of each such concentrations could then be estimated to provide CONUS-wide demand. The concentrations that were identified accumulated all traffic within a radius of 70 to 250 miles of some central hub. This range of distances corresponds roughly with the footprints provided by candidate spacecraft antennas (i.e., beamwidths of 0.3 to 0.6 degree).

Table 1-7. Typical Traffic Scenarios

	Private Line (DTU) Users										Trunking Users			
Traffic Concentration (70- to 250-mile diameter)	Total Terminals	High Capacity Terminals	Medium Capacity Terminals	Low Capacity Terminals	Total Data Rate (Mbps)	Total Terminals	Major Terminals	Thin-Route		Trunking Data Rate	Total Data Rate (Mbps)			
								High Capacity	Low Capacity					
All Private Line Users - Low Capacity	18	0	3	15	29.9	0	0	0	0	0	29.9			
All Private Line Users - High Capacity	54	1	7	46	113.3	0	0	0	0	0	113.3			
One Thin-route User Plus Private Line Users	22	1	3	18	66.4	1	0	0	1	12.6	79.0			
Two Thin-route Users Plus Private Line Users	24	1	2	9	52.9	2	0	1	1	102.1	155.0			
One Major Trunking User Plus Private Line Users	24	2	4	6	95.2	1	1	0	0	274.2	369.4			
One Major and One Thin-route Trunking Plus Private Line Users	48	1	3	20	68.1	2	1	1	0	363.7	431.8			

Table 1-8. Representative Traffic Distribution Model

Traffic Composition	Number of Locations	Location Data Rate (Mbps)	Total Data Rate (Mbps)
<u>Major Traffic Concentrations</u>			
● 1 Primary Trunking Station	4	500.0	2000.0
● 2 Secondary Trunking Stations	2	500.0	1000.0
● 1 Secondary Trunking Station plus 1 Thin-Route Station plus Private Line Users	4	431.8	1727.2
● 1 Secondary Trunking Station plus Private Line Users	8	369.4	2955.2
Subtotal			7682.4
<u>Minor Traffic Concentrations</u>			
● 2 Thin-Route Stations plus Private Line Users	3	155.0	465.0
● 1 Thin-Route Station plus Private Line Users	8	79.0	632.0
● All Private Line Users High Capacity	5	113.3	566.5
● All Private Line Users Low Capacity	15	29.9	448.5
Subtotal			2112.0
Grand Total = 9794.4 Mbps			



The baseline traffic concentrations are presented in Table 1-7. The total number of private line (DTU) terminals within each traffic concentration was derived using direct user distributions generated by ITT. Allocation of the terminals within each concentration to a particular user class employed the WU percentages given in Table 1-4. A 50 percent activity factor was assumed for the direct users. The total data rate for all active private line (DTU) users within each concentration can then be calculated. This peak rate, when added to the trunking information rate (if any), within these traffic concentrations provided the total busy hour data rate for each location. As can be seen from Table 1-7, six representative traffic concentrations were identified with total data rates varying from a low of 29.9 Mbps for a traffic location that only included a small number of private line users to a high of 431.8 Mbps for a traffic concentration that included a major trunking station, a thin-route trunking station and a group of private line users.

The final step in generating the traffic model for this study was to estimate the number of these representative scenarios that would exist within CONUS subject to constraint that the total traffic could not exceed the overall traffic developed in the previous section. A distributed traffic model was evolved by trial and error and the result is shown in Table 1-8. It should be pointed out that, in addition to other six representative traffic scenarios discussed previously, two other trunking concentrations were added in the final model which were degenerate cases of the representative concentration. The first trunking concentration was limited to a single primary trunking station with total data rate of 500 Mbps. The second trunking concentration grouped two secondary trunking stations whose combined data rate was also 500 Mbps.

Fifty-seven traffic concentrations were developed. The resultant total-system data rate of 9794.4 Mbps is within 2 percent of the total overall traffic demand developed in the previous section and within 13 percent of the forecasted WU demand of 8.7 Gbps. The traffic distribution arising from this procedure appears representative of the actual demand and is sufficiently realistic for the definition of the 30/20 GHz baseline system design requirements. The demand shown in Table 1-8 includes all major trunking stations; 18 of the 25 thin-route trunking stations and 70 to 80 percent of all the private line locations.

To gain some insight into the dispersion of the traffic contained in the postulated model, the cumulative data rate was derived as a function of the number of traffic locations. The result is displayed in Figure 1-3. Note that for a small number of locations the cumulative traffic (in terms of the total peak hour demand) increases almost linearly. A pronounced knee occurs in the region of 15 to 20 locations. The 10 largest concentrations contain more than 50 percent of the total traffic and the 20 largest contain 80 percent of the traffic. The remaining locations (31) contribute a very small part of the overall traffic. This appears to be a reasonable representation of the expected traffic distribution and further reinforces the suitability of the postulated traffic model for this study.

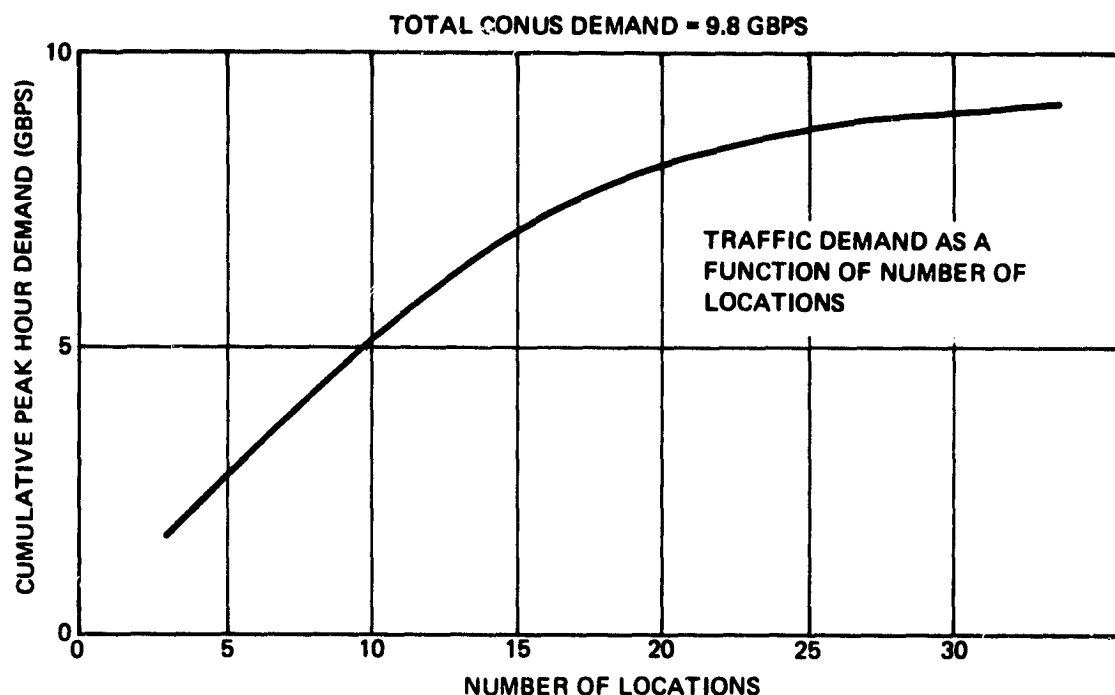


Figure 1-3. Cumulative Data Rate Versus Number of Locations Covered

## 2. TERMINAL AND SATELLITE PERFORMANCE PARAMETERS

The terminal and satellite performance parameters assumed for a 1990 operational system are summarized in Table 2-1.

### 2.1 SATELLITE PERFORMANCE PARAMETERS

#### 2.1.1 Satellite Receiver Front-Ends

The projected performance of FET low-noise receivers is superior to all other candidate satellite receivers up to approximately 30 GHz, where parametric amplifiers start to become superior on a noise-temperature basis.\* This data is based on TRW computer performance analyses for half-micron gate FETs with special impurity distributions. These results indicate that uncooled FET receivers will be superior to uncooled paramps and cooled FETs will be superior to cooled paramps.

FET low-noise receivers are greatly preferred over paramps due to their relative simplicity and reliability, even if they were not superior in performance. Considering the technical rate of progress in low-noise FET development, the demonstrated reliability of low-noise FET amplifiers, and the low size, weight, power, and cost of FET amplifiers; there is little doubt that the satellite receivers will utilize FET preamplifiers.

Receiver FET preamplifiers may also be cooled. Cooling a FET preamplifier to 77°K from room temperature reduces noise figure by a factor of three. Passive radiative cooling is attractive for spacecraft receiver cooling. The exact FET temperature is not critical as with paramps, and some variation of operating FET temperature can be tolerated.

The attractiveness of radiative cooling will depend on the complexity of the required radiators and the number of FET devices to be cooled. Cooling may be relatively easy to use for tens of devices, but will be difficult if hundreds of devices are used in a phased-array configuration.

Any degree of cooling will be helpful, and low-temperature heat pipes may provide a method for extracting heat from large arrays of FET devices.

---

\*This statement is based on unpublished work performed at TRW.

Table 2-1. Terminal and Satellite Performance Parameters (1990)

Satellite	Pessimistic	Baseline	Optimistic
<ul style="list-style-type: none"> <li>● Receiver Noise Figure (FET)</li> <li>● Transmitters                             <ul style="list-style-type: none"> <li>- FET (single device)</li> <li>- FET (8 devices)</li> <li>- TWT</li> </ul> </li> <li>● Antenna Gain (0.3° beams)                             <ul style="list-style-type: none"> <li>- Transmit</li> <li>- Receive</li> </ul> </li> </ul>	<p>3.0 dB</p> <p>1 watt (10% eff) 7.2 watts (9% eff) 20 watts (25% eff)</p> <p>52.7 dB (35% eff) 55.5 dB (30% eff)</p>	<p>2.0 dB (uncooled)</p> <p>2.0 dB</p> <p>2 watts (15% eff) 14.4 watts (13.5% eff) 50 watts (30% eff)</p> <p>54.3 dB (50% eff) 57.3 dB (45% eff)</p>	<p>0.8 dB (cooled)</p> <p>5 watts (20% eff) 36 watts (18% eff) 75 watts (35% eff)</p> <p>55.1 dB (60% eff) 58.1 dB (55% eff)</p>
<p><u>Earth Terminal</u></p> <ul style="list-style-type: none"> <li>● Antenna Gain (Tx/Rx)                             <ul style="list-style-type: none"> <li>- Trunking                                     <ul style="list-style-type: none"> <li>o Major (15 m)</li> <li>o Thin Route (10 m)</li> </ul> </li> <li>- Private Line                                     <ul style="list-style-type: none"> <li>o High-Capacity (7 m)</li> <li>o Medium-Capacity (5 m)</li> <li>o Low-Capacity (3 m)</li> </ul> </li> </ul> </li> <li>● Receiver Noise Figure (FET)</li> </ul>	<p>4 dB</p>	<p>69.4/66.8 dB (40/50% eff) 66.8/63.7 dB (50/55% eff)</p> <p>64.0/60.7 dB (53/56% eff) 61.4/58.0 dB (56/58% eff) 57.0/53.6 dB (57/60% eff)</p> <p>3 dB</p>	<p>2 dB</p>

Table 2-1. Terminal and Satellite Performance Parameters (1990) (Continued)

	Pessimistic	Baseline	Optimistic
<ul style="list-style-type: none"> <li>● HPA Capabilities <ul style="list-style-type: none"> <li>- Trunking (wideband)</li> <li>- Private Line (narrowband)</li> <li>- FET/Impatt</li> </ul> </li> </ul>	2000 watts (water-cooled) 500 watts (air-cooled) 15 watts	5000 watts (water-cooled) 800 watts (air-cooled) 25 watts	50 watts
<u>System</u> <ul style="list-style-type: none"> <li>● Rain Margins <ul style="list-style-type: none"> <li>- Trunking</li> <li>● Uplink</li> <li>● Downlink (Diversity)</li> </ul> </li> <li>- Private Line <ul style="list-style-type: none"> <li>● Uplink 0.999</li> <li>● Downlink (No Diversity)</li> </ul> </li> </ul>	Zones	1 2 3 4 5 6 9 11 13 14 20 15 3 4 4 5 7 5 1 2 3 4 5 6 13 17 24 38 50 26 4 7 8 13 19 10	7.8 dB 4.2 dB 0.999

### 2.1.2 Satellite Transmitters

Three types of satellite transmitters are of interest. Single-device FET transmitters may be used as element transmitters in a multiple-beam phased-array. Multiple-device FET transmitters compete with traveling-wave-tube-amplifiers (TWTAs) if antennas with one, or a few, transmit parts are used.

Selection of FET or TWTA transmitters is unclear at this time. The efficiency of TWTAs provides two or three times greater RF power for a given dc power input as compared to FETs. TWTAs are expensive, however, and have had reliability problems on many programs.

The state of the art in FETs is more dynamic and large performance improvements may occur. Power FET reliability is being investigated and solid-state transmitters have generally exhibited outstanding reliability. FET transmitter reliability is not yet proven, and there are some questions about voltage gradients and whisker-growth from FET chip metalization that might require basic process changes to achieve long life in the satellite environment.

### 2.1.3 Satellite Antennas

A satellite antenna diameter of 12 feet was chosen to be compatible with the Shuttle Orbiter cargo bay without folding. The performance listed is the theoretical gain, reduced by the efficiency estimated for the antenna approaches being considered. These range from 30 percent for a phased-array with RF power division from a single port, to 60 percent for a high-density fixed beam with a reflector antenna.

Considering the on-board signal processing concepts being used in this study, very different uplink and downlink mechanizations may be considered. These may include different numbers of beams, beamwidths, and data rates per beam.

## 2.2 EARTH TERMINAL

The earth terminal technology used in the system design is a very important part of the system cost. The small terminal performance drives the satellite design in terms of EIRP, G/T, and data rate. The actual cost of the terminal hardware tends to dominate system cost because of the very large number, five to ten thousand, of potential small terminal users.

Data and signal processing hardware located at the small terminal may represent the major portion of small terminal costs. However, analog condition, A/D conversion, multiplexing, and interfacing hardware do not vary as a function of the satellite communication system design. This type of hardware will be considered a fixed cost overhead item and will not be considered further in this study.

The small earth terminal, for the purpose of this study, consists of that hardware which accepts a short-term, fixed-data-rate, digital data stream from interfacing hardware, and delivers a short-term fixed-data-rate digital data stream back to interfacing hardware. The terminal block diagram is illustrated in Figure 2-1.

The variable components that affect system cost are:

- Transmitter
- Antenna and Pedestal
- Terminal Receiver
- FEC Adaptive Coding/Decoding
- Exciter/Demodulator
- Diplexer
- Frequency/Timing
- Burst Buffer
- TI Interface Buffer
- Control/Monitor

The order of importance is approximately the order of listing above.

#### 2.2.1 Terminal Transmitter

The terminal transmitter selected can change the system cost more than any other single item. Transmitters tend to be expensive. They can also cause other major terminal costs such as power, cooling, and personnel hazard protection. Too small a terminal transmitter may drive satellite costs up by increasing satellite G/T required.

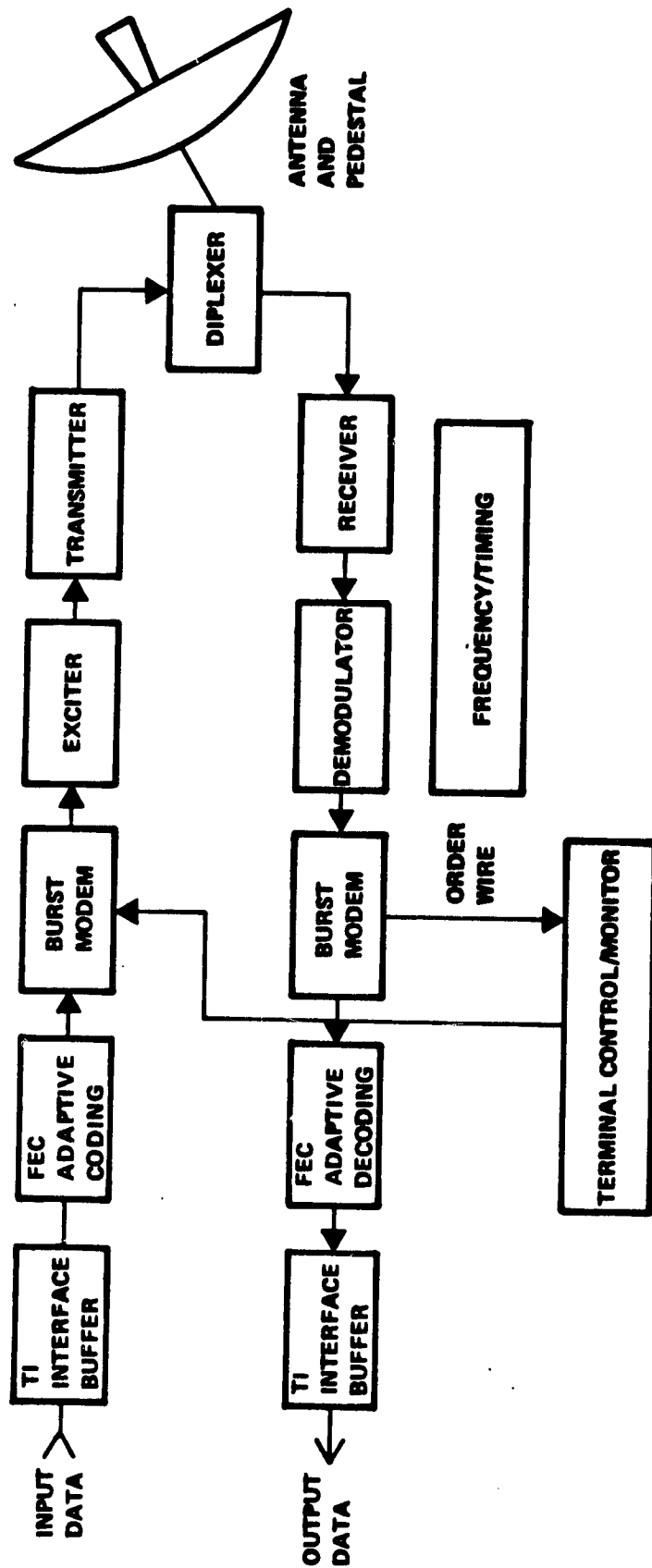


Figure 2-1. Small Earth Terminal Block Diagram



Transmitter capabilities shown in Table 2-1 are for water-cooled and air-cooled TWTAs and for FET amplifiers. FET amplifiers will be less expensive if they can provide adequate power. Other solid-state amplifiers such as impatt transmitters might also be considered.

TWTAs are more probable choices for the terminal transmitter, since they permit selection of output power over an adequate range. Air cooled TWA transmitters are preferred due to cost considerations, and are expected to have adequate power capability.

Whatever the terminal transmitter type, it will be designed for graceful degradation in all but the cheapest terminals. By simply combining the output of two power amplifiers, the output requirement of each can be 3 dB lower than without combining. Designing for a clear-weather margin of greater than 6 dB allows continued operation after one failure with increased rain-outages. Using the transmitter configuration of Figure 2-2 allows the system to operate with only a 3-dB power reduction after loss of one amplifier.

#### 2.2.2 Terminal Antennas and Pedestals

Antenna gains and antenna efficiencies are given for five antenna sites corresponding to different classes of user. The efficiencies are considered conservative, especially for the small user where the design should be carefully optimized.

Using high-performance terminal antennas is thought to be cost-effective. The antenna efficiency should depend primarily on the antenna nonrecurring or design cost. The recurring or unit cost for small antennas should be relatively independent of performance using any of several potential fabrication techniques.

Pedestal cost is a major consideration in small terminal design selection. The pedestal will be either manually adjustable or have limited range electromechanical pointing.

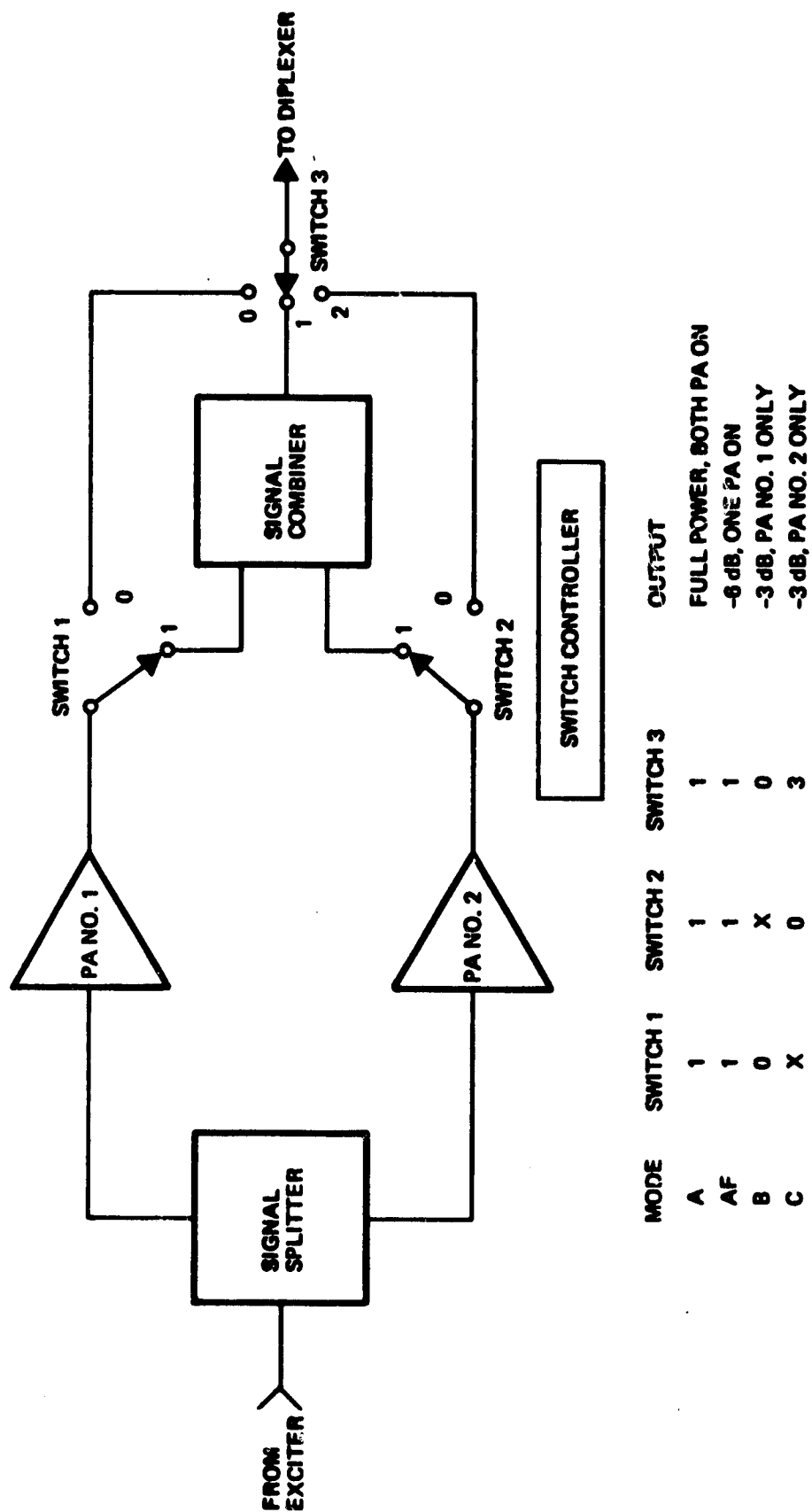


Figure 2-2. Terminal Transmitter Block Diagram

With a manually adjustable pedestal antenna pointing is set by the technician servicing the terminal. The antenna beamwidth must be wide enough to allow for pointing errors. Pointing error sources include:

- Initial alignment
- Antenna wind loading
- Building sway for roof-mounted terminals
- Satellite stationkeeping errors.

Total pointing errors, with the possible exception of roof-mounted antennas, can be held to 0.2-degree radial. This limits antenna beamwidth to about 0.4 degree or greater, and the terminal antenna size to two meters or less. By controlling the satellite station very accurately (0.03 degree) it may be possible to use 3-meter antennas without pointing capability.

Larger users may find it economically attractive to use a combination of step-track antenna pointing control, with an X-Y limited-motion pedestal. Limited motion pedestals are available for C-band small terminals. These utilize linear-motion screw actuators with inexpensive electric motor drives, and provide excellent tracking/pointing performance. The reduction in transmitter power and cost due to the increased antenna gain may make simple X-Y limited motion pedestals with larger antennas a very cost-effective approach.

### 2.2.3 Terminal Receivers

Terminal receivers will utilize FET amplifiers, unless some unexpected technology changes occur. Low cost moderate performance FET amplifiers dominate C-band small terminal design and there is no reason to expect a different result at 18 GHz.

The terminal receivers may use either cooled or uncooled FET amplifiers. With today's technology uncooled FETs are preferred at C-band. The technology of cooling devices is advancing, however, and cooling may become very cost-effective with low-cost thermoelectric coolers.

Nominal system uplink and downlink power budgets are provided in Tables 2-2 and 2-3. Table 2-2a is the uplink budget for a 125 Mbps DTU terminal. Table 2-2b is the uplink budget for a large trunking terminal.

Table 2-2a. Nominal Uplink RF Power Budget (125 Mbps DTU Terminal)

TRANSMITTER POWER (50W, PEAK)	17.0 dBw
ANTENNA GAIN (3.0m, $\eta = 0.6$ )	57.3 dB
SPACE LOSS (30 GHz, 38.7 Mm)	-213.7 dB
SATELLITE ANTENNA ( $\eta = 0.3$ )	54.5 dB
LOSSES (OHMIC, POINTING AREA)	- 9.0 dB
RECEIVED POWER (C)	- 93.9 dBw
SATELLITE NOISE TEMPERATURE (3 dB NF INCL. LOSSES)	27.6 dBK
BOLTZMANN'S K	-228.6 dBw/HzK
NOISE DENSITY	-201.0 dBw/Hz
C/N <sub>o</sub>	107.1 dB/Hz
DATA RATE (125 MBPS)	81.0 dBHz
EB/N <sub>o</sub>	26.1 dB
EB/N <sub>o</sub> REQUIRED (10 <sup>-6</sup> , 2 dB LOSS)	12.6 dB
ALLOWABLE RAIN LOSS WITHOUT CODING	13.5 dB
ALLOWABLE RAIN LOSS WITH ADAPTIVE CODING	23.5 dB

Table 2-2b. Nominal Uplink RF Power Budget Trunking Terminal

TRANSMITTER POWER (100W, PEAK)	20.0 dBw
ANTENNA GAIN (12.0m, $\eta = 0.6$ )	69.3 dB
SPACE LOSS (30 GHz, 38.7 Mm)	-213.7 dB
SATELLITE ANTENNA ( $\eta = 0.3$ )	54.5 dB
LOSSES (OHMIC, POINTING AREA)	- 9.0 dB
RECEIVED POWER (C)	- 78.9 dBw
SATELLITE NOISE TEMPERATURE (3 dB NF INCL. LOSSES)	27.6 dBK
BOLTZMANN'S K	-228.6 dBw/HzK
NOISE DENSITY	-201.0 dB-w/Hz
C/N <sub>0</sub>	122.1 dB/Hz
DATA RATE (500 MBPS)	87.0 dBHz
EB/N <sub>0</sub>	35.1 dB
WB/N <sub>0</sub> REQUIRED (10 <sup>-6</sup> , 2 dB LOSS)	12.6 dB
ALLOWABLE RAIN LOSS	22.5 dB
• ADDITIONAL RAIN LOSS CAPABILITY RESULTS FROM DUAL TERMINAL SITE DIVERSITY.	

Table 2-3a. Nominal Downlink RF Power Budget DTU Terminal

TRANSMITTER POWER (30 WATTS)	14.8 dBw
ANTENNA GAIN ( $\eta = 0.4$ )	51.0 dB
SPACE LOSS (18 GHz, 38.7 Mm)	-209.3 dB
GROUND ANTENNA (3.0m, $\eta = 0.7$ )	53.5 dB
LOSSES (OHMIC, POINTING, AREA)	- 9.0 dB
RECEIVED POWER (C)	- 99.0 dBw
TERMINAL NOISE TEMP (730°K INCL. RAIN)	28.6 dBK
BOLTZMANN'S K	-228.6 dBw/HzK
NOISE DENSITY ( $N_o$ )	-200.0 dBw/Hz
$C/N_o$	-101.0 dB/Hz
DATA RATE (250 MBPS)	84.0 dBHz
$EB/N_o$	17.0 dB
$EB/N_o$ REQUIRED ( $10^{-6}$ , 2 dB LOSS)	12.6 dB
ALLOWABLE RAIN LOSS WITHOUT CODING	4.4 dB
ALLOWABLE RAIN LOSS WITH ADAPTIVE CODING	14.4 dB

Table 2-3b. Nominal Downlink RF Power Budget Trunking Terminal

TRANSMITTER POWER (30 WATTS)	14.8 dBw
ANTENNA GAIN ( $\eta = 0.5$ )	54.3 dB
SPACE LOSS (18 GHz, 38.7 Mm)	-209.3 dB
GROUND ANTENNA (12.0m, $\eta = 0.7$ )	62.8 dB
LOSSES (OHMIC, POINTING, AREA)	- 9.0 dB
RECEIVED POWER (C)	- 89.5 dBw
TERMINAL NOISE TEMP (460°K INCL. RAIN)	26.6 dBK
BOLTZMANN'S K	-228.6 dBw/HzK
NOISE DENSITY ( $N_o$ )	-202.0 dBw/Hz
$C/N_o$	-112.5 dB/Hz
DATA RATE (500 MBPS)	87.0 dBHz
$EB/N_o$	25.5 dB
$EB/N_o$ REQUIRED ( $10^{-6}$ , 2 dB LOSS)	12.6 dB
ALLOWABLE RAIN LOSS	12.9 dB

• ADDITIONAL RAIN LOSS CAPABILITY RESULTS FROM DUAL TERMINAL SITE DIVERSITY.

Table 2-3a is the downlink budget for a DTU terminal, and Table 2-3b is the budget for a trunking terminal.

#### 2.2.4 FEC Adaptive Coding/Decoding

The boxes labeled FEC adaptive coding and decoding must include data delay buffers as well as coders and decoders. Because of the requirement to switch coding on and off, a data delay must be provided in the uncoded mode to compensate for the coding and decoding delays.

#### 2.2.5 Exciter/Demodulator

The exciter will utilize direct 30-GHz carrier modulation. The demodulator will probably operate at an IF frequency to reduce the cost of the necessary gain stages.

#### 2.2.6 Diplexer

The diplexer has no exotic requirements. Transmit power will be moderate and transmit-receive spacing is wide.

#### 2.2.7 Frequency/Timing Control

Frequency/timing control is discussed in Section 4.

#### 2.2.8 Burst Buffer

The transmit burst buffer accumulates data over a 1-millisecond frame period and transmits it at the terminal uplink burst rate, either 25 Mbps or 125 Mbps. The resulting duty factory depends on the data rate being input to the terminal. The receive burst buffer accepts data input at the downlink burst rate and outputs it at a rate compatible with the adaptive FEC decoding hardware.

#### 2.2.9 T1 Interface Buffer

The T1 interface input buffer accepts a standard T1 input at 1.544 Mbps. It searches for, and locks to, the synchronization F-pulse which occurs every 193 bits. After synchronizing, channel occupancy is determined by searching for 00011000 or 1001100 words which indicate unassigned channels. Only the data words corresponding to assigned channels are transmitted. The individual channel data words are converted from 8-bit words at the 8-kHz T1 frame rate, to 64-bit words at the 1-kHz satellite system frame rate.



The T1 interface output buffer accepts 64-bit words after they have passed through the satellite system and reverses the process. The satellite system frame timing is used to reestablish the F-pulse timing and the 64-bit individual channel words are divided and spread over eight 193-bit T1 frames at the 1.544 Mbps output rate.

#### 2.2.10 Control/Monitor

Control and monitor hardware will consist of telemetry and command hardware similar in concept to current satellite telemetry and command hardware. Telemetry and command data pass to and from the terminal over the system order wire. The master control station will collect telemetry data from all terminals. Trends will be plotted, failures will be corrected by command, and maintenance will be scheduled based on trend or failure data. The control and monitor hardware also calculates the transmit range advance parameters based on satellite ephemeris data coming in over the order wire.

### 2.3 SYSTEM PERFORMANCE PARAMETERS

The greatest single factor affecting current design and design uncertainty is rain loss. The 30/20 GHz system must provide 0.9999 availability with terminal site diversity and 0.999 availability for single sites. The rain margins described are thought to be adequate.

The rain margins correlate well with recently published Bell Laboratory data for Crawford Hill, NJ, signal transmission tests using COMSTAR beacons. It is important to realize that the variance and uncertainty in any rain margin value must be significant due to the nature of the effect. Rain statistics are not stationary on a month-to-month or year-to-year basis. Month-to-month variation is recognized, but the rain margin values deliberately ignore year-to-year variation.

The direct approach of providing large values of full-time rain margin is expensive and relatively ineffective. The approach used in this study will be to provide a moderate amount of full-time rain margin and meet

large margin requirements by a combination of adaptive coding and increased effective data bit energy by transmitting multiple symbols per bit. This approach reduces satellite and terminal cost and provides a greater available margin, which can be moved from terminal to terminal when it is needed.

### 3. SYSTEM ARCHITECTURE

The 30/20 GHz Mixed User overall system architecture is illustrated in Figure 3-1. The system network concept is shown in Figure 3-2. This section will describe the series of findings and decisions leading to this architecture and will highlight those requiring either further study or continuous reevaluation as the applicable technology evolves. Factors affecting the architecture are:

- The satellite may be very complex and expensive without excessive impact on total system cost. Conversely, the system cost is very sensitive to DTU terminal cost. Trunking terminal cost sensitivity is low.
- The bulk of the system traffic (80 percent) flows through the trunking system, but the economic value of the system may be greatest in the DTU system due to the reduction of terrestrial distribution costs.
- The system must have a large capacity to avoid early saturation and to justify its portion of the satellite orbit-frequency resource. A total requirement of 10 Gbps has been identified as the baseline capacity requirement. Of this, 8 Gbps is required by trunking users and 2 Gbps by DTU users.
- Interconnection of trunking and DTU users on-board the satellite is required to avoid introducing four-way time delays into voice communications and multiple use of the communication links and to provide DTU users direct access to common carrier transmission facilities.
- The system must provide access for a very large number of user terminals (several thousand) with a high degree of interconnectivity.
- A communication bandwidth of 2.5 GHz is allocated for 30/20 GHz communications. Frequency reuse is dictated by the EIRP and G/T requirements of the user terminals since the requirements can be met only with large satellite antennas. Large satellite antennas result in narrow beams, and coverage requirements must be met using many beams. The system is not expected to be bandwidth constrained.

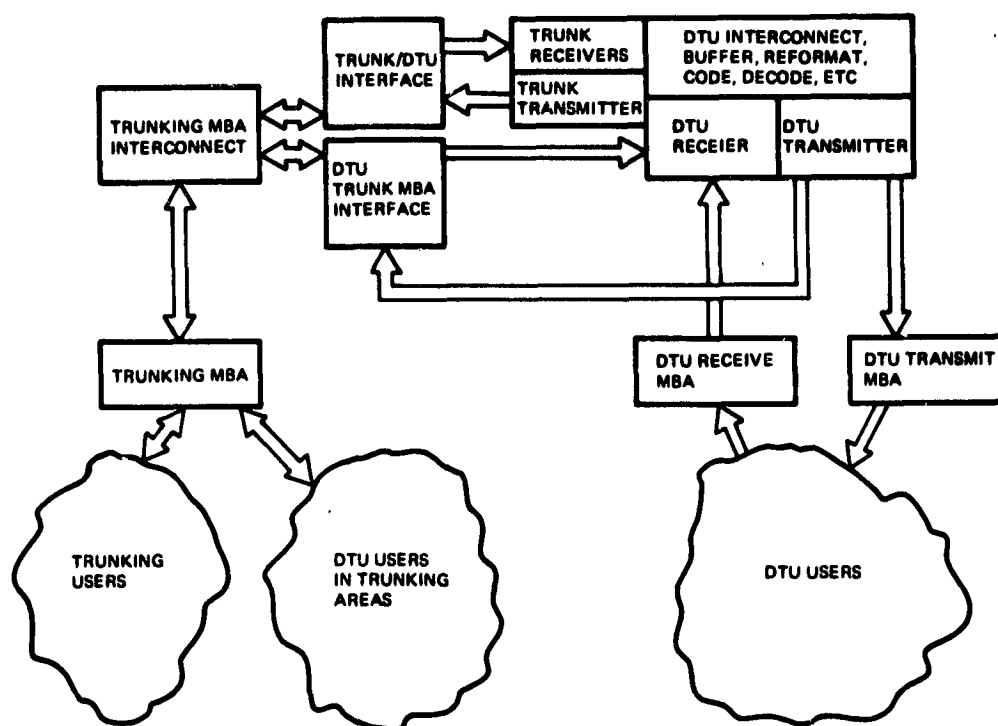


Figure 3-1. 30/20-GHz Mixed User System Architecture

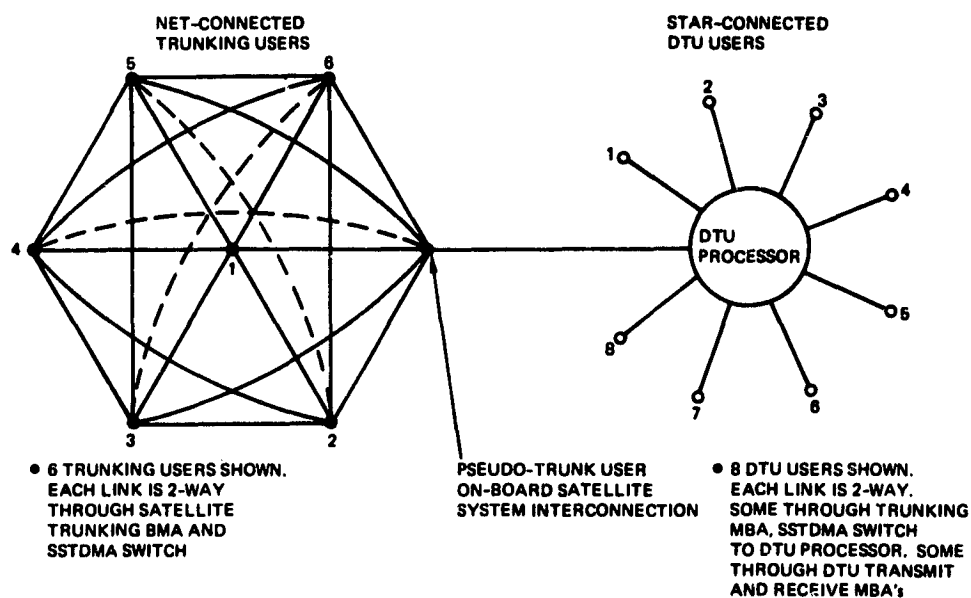


Figure 3-2. System Network Concept

- Availabilites of 0.999 for DTU and 0.9999 for trunking are minimum requirements. Most trunking users will have to employ diversity stations with 8- to 10-km geographic separation and large RF power margins to accomplish this. DTU users must have large margins, but cannot afford space diversity or large terminal EIRP or G/T. Availability requirements apply almost independently to uplinks and downlinks. Because of the greater rain loss at 30 GHz the uplinks may be more critical than the downlinks.

### 3.1 ONBOARD PROCESSING

A digital store-and-forward approach over a frame period has been selected to reduce DTU user terminal complexity and cost. The on-board processor demodulates each uplink data burst, stores the data intended for various users, and assembles a single downlink burst per frame for each DTU user.

With an IF SSTDMA mechanization, each user terminal must receive and transmit data bursts once per frame for each station communicating with it. With several thousand terminals, each communicating with tens or hundreds of others, the number of individual bursts become very large. Guard time and preambles for each burst represent TDMA "overhead." These can seriously impact system efficiency. Each terminal must use a complex fast-acquisition receiver to recover carrier and clock for each data burst as it is received.

On-board processing with data remodulation on-board the satellite allows the user terminal to operate with a single downlink carrier and data clock. This directly reduces terminal cost by making fast-acquisition receivers unnecessary. Narrowband phase-lock-loops provide adequate downlink carrier and data-clock references. With narrowband carrier and data-clock tracking loops, error-correction data coding becomes possible. The wide carrier and clock bandwidths needed in fast-acquisition systems severely degrade performance at the low SNR typical of error-correction encoded operation. The carrier and clock tracking losses are so great that error correction coding becomes impractical. Since downlink preambles are not required, TDMA overhead is greatly reduced; but more significantly on-board processing allows flexibility in selection of the DTU TDMA frame period. TDMA frame period selection may be driven by either scanning-beam speed limitations or by DTU terminal hardware considerations.

On-board data storage is required to implement on-board data processing and routing. The amount of data storage is twice the product of the process data rate and the frame period. For example, a 3-Gbps processor data rate and a 1-ms frame rate lead to a 6.0M bit storage requirement. While this sounds large, the next-generation solid-state memory standard data-storage chip being developed for computer use stores 65,000 data bits. Ninety-two chips could store the entire 6.0M bit. These chips are now available, but are not yet space qualified. By the time hardware design is started on a 1990 operational system, chips that store one-quarter million bits each may be available. On-board data storage is not thought to limit capacity or frame period selection.

### 3.1.1 Processor Routing Control

The receive and transmit routing scheme currently baselined may be described as follows. As data from a particular scanning beam arrives at the satellite receiver, it is sequentially written into a segment of the processor random-access memory (RAM). The write address is determined by a counter that repeats each address in the selected segment once each frame period. Two 3.0M bit memories are provided, and one is continuously being loaded with uplink data while the other is being read to provide the down-link. A block diagram illustrating this process is shown in Figure 3-3. The uplink data memory-loading process simply loads the memory sequentially using a counter for addressing the data to memory locations as it is received.

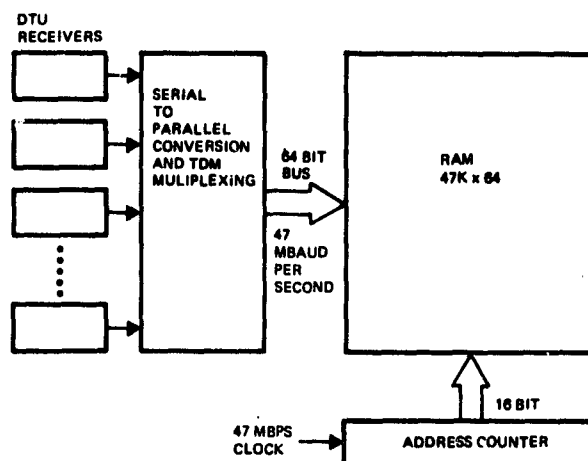


Figure 3-3. Processor Memory Loading

Downlink routing of the individual uplink data bits is provided by using a permutation of the address set used for loading the memory. For example, consider using a recirculating address register containing the individual address of each bit in the 3.0M bit RAM being read. This would clearly provide the capability to read out the data bits in any order desired, and by sequentially connecting the RAM output data stream to each downlink transmitter would provide complete routing interconnectivity. Unfortunately, the address memory would require 3.0M 21-bit words of storage, and the logic operating rate would have to be 2 Gbps to match the DTU system capacity. This is clearly unattractive, but illustrates the principle.

Various techniques exist to reduce the memory logic operating data rate. One very simple technique is to treat the data in parallel words rather than in individual data bits. For example, if we restrict data to 64-bit words, the address memory drops to forty-seven thousand 16-bit words, or about 750K bits total, and the logic operating rate is 47 Mbps. A block diagram using these parameters is shown in Figure 3-4.

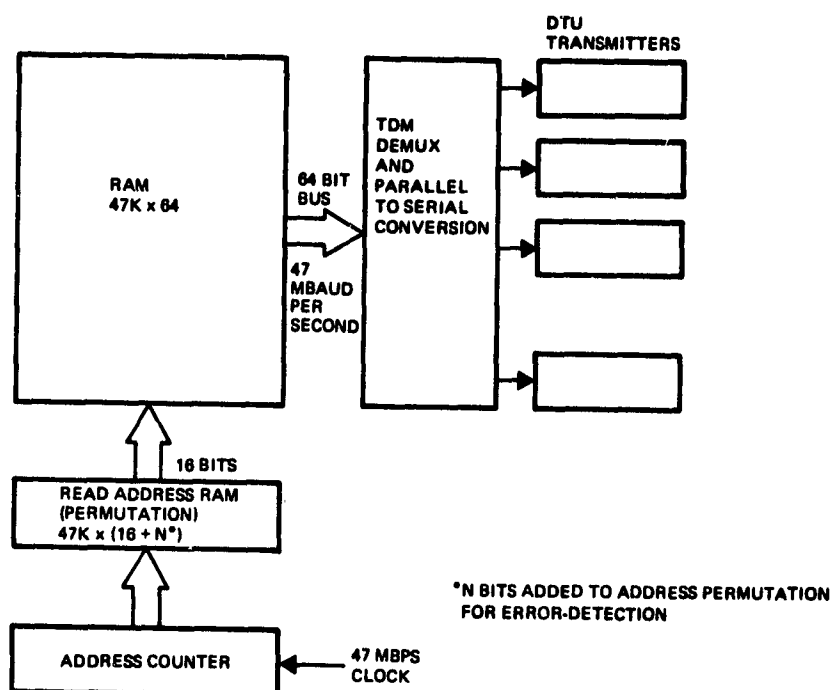


Figure 3-4. Processor Memory Output

Restricting routing to 64-bit words restricts the minimum data rate channel to 64 bits times the frame rate, or for 1-ms frames, to 64 kbps. This is not considered an excessive restriction. Forty-seven Mbps requires a 20 ns memory cycle time, and is still a high data rate for memory operation.

There are ways to segment the processing memory to reduce processing rate at the cost of some flexibility. Also, the three-way tradeoff between data packet size (and minimum data rate) against processing rate, and against frame period must be considered in detail. Considering that we are discussing technology at least two to four years in the future, and considering the rate at which technology is being driven in this particular area, the parameters used in Figures 3-3 and 3-4 are reasonable for use as a baseline this time.

The memory architecture must be segmented into several (15 to 100) modules for another reason. The fairly large memory will have a significant failure rate over a ten-year satellite operational life. Segmenting a large memory into modules and selecting the active modules by ground command is a powerful redundancy technique. This will allow adequate reliability with a total memory size increase of less than 50 percent. Meeting reliability requirements by replicating large memories is a comparatively heavy and expensive technique.

Additional storage bits are shown in the address-permutation memory of Figure 3-4. The address-permutation or routing control data is held on the spacecraft for long periods of time. Under these conditions this data may be affected by "soft" memory errors. These occur due to radiation effects in very small-geometry semiconductor memories. The additional bits in the memory provide error detection and correction for the vital data routing instructions. Error correction for soft errors is not required in the transmission data memories since the bit error rate contribution is negligible with 1-ms storage duration.

### 3.1.2 Processor Error Correction Coding/Decoding

Providing adequate rain margins to meet availability requirements is difficult on both downlinks and uplinks at 20 and 30 GHz. Rate 1/2 convolutional error correction coding provides 5.1-dB performance improvement



at significantly lower cost than equivalent system EIRP and G/T improvements. The cost of terminal coding/decoding equipment is expected to drop drastically in the next few years due to the decreasing cost-trend of digital logic.

#### 3.1.2.1 Error Correction Code Selection

The 30/20 GHz communication system being designed is not expected to be bandwidth constrained. The limitation on code rate will be set by channel signal-to-noise ratio considerations rather than bandwidth utilization. Codes with rates lower than one-third may be used, especially on downlinks where synchronization is simply due to on-board remodulation.

Soft-decision Viterbi-algorithm decoding of convolutionally encoded data is one of the most popular current coding techniques. With a TDMA system, however, the infinite-length processing of this code type requires storage of intermediate data bits for each data stream while processing the other time-interleaved data streams.

Block codes, such as the Bose, Chaudhuri, and Hocquenghem (BCH) or Reed-Solomon codes can be designed to match the data block length used in the on-board processor (such as the 32-bit words used above), and avoid storage of any intermediate values or results. Most available block decoding algorithms use hard-decision data input, however, and are thus inferior by at least 2 dB to a convolutional code with soft decisions. There are some soft-decision block-decoding algorithms in the literature, but many, if not all, utilize a multiple hypothesis correlation approach, with trial hypotheses selected by a feedback process. These tend to be complex, and have limited throughput capability with reasonable logic implementations.

Convolutional encoding will be used as the baseline downlink encoding technique. The number of intermediate data bits that must be stored between data bursts is small for convolutional encoding; perhaps as few as 7 to 12 bits per channel encoded. In the DTU terminal only a single data stream need be decoded. The decoder is simple and conventional and the soft-decision Viterbi algorithm provides excellent performance.

Selection of an uplink error correction coding technique is harder. The number of intermediate data bits that must be stored between burst is much larger for convolutional decoding, especially with soft decisions, as

compared to convolutional encoding. A coding study for TDMA channels is clearly worthwhile.

Uplink error correction coding results in a requirement for satellite hardware which either:

- a) Does time-shared convolutional decoding on up to 20 data streams (2 percent of total DTU users), with a total data rate of 40 Mbps (2 percent of total DTU data rate) and with an adaptive rain-response system control algorithm
- b) Provides soft-decision block decoding with performance similar to that of convolutional soft-decision decode, and capabilities as described above
- c) Provides full-time, high-performance, soft-decision error correction decoding for 1000 data stream with a total throughput of 2 Gbps.

Approach (a) is selected as the system baseline uplink coding technique. Approach (b) is worthy of further study. If equivalent performance can be achieved, the choice between (a) and (b) is a hardware complexity trade in the satellite design area. If equivalent performance cannot be achieved, coding technique selection must be based on a system study that trades uplink terminal EIRP against satellite complexity. Using the ground rule of minimizing terminal cost, this trade would be biased heavily towards approach "a."

In a system where a primary design goal is to reduce DTU terminal cost, adaptive uplink coding is very attractive. When the uplink channels are limited in number and must be shared by groups of users, adaptive coding can reduce the terminal EIRP requirement by a factor almost equal to the coding rate. This is a 3- to 5-dB advantage in addition to coding gain.

### 3.2 CHANNEL BURST RATES

#### 3.2.1 Trunking Channel Burst Rate

The trunking system channel burst rate, or peak data rate during TDMA bursts, has been set arbitrarily at 500 Mbps. It is important to note that in a TDMA system the channel burst rate does not need to have any particular relationship to standard terrestrial trunking data rates since all interfacing occurs through burst buffers which change data rate.

Five-hundred Mbps was selected on the basis of technology availability and a reasonable match to the largest trunking channel requirements.

The New York City area is an exception to the comment above on matching maximum trunking data rates with the 500-Mbps channel burst rate. Providing adequate capacity to this high-traffic-density area must be accomplished using several independent links. Increasing the channel burst rate to match this single area would not be a cost-effective solution since this would result in increased receiver costs and reduced performance margins for all trunking stations.

### 3.2.2 Processor Uplink Channel Burst Rates

Processor uplink channel burst rates must be minimized to reduce the DTU terminal EIRP requirement. Terminal transmitters are peak power limited, and any reduction in uplink burst rate provides a proportional reduction in the required transmitter power. Since uplink rain margin to achieve 0.999 availability is a critical system cost driver, uplink burst rate reduction at the price of increased satellite receiver complexity seems to be a valid trade.

Multiple-beam receive arrays seem to be simpler than high-efficiency multiple-beam transmit arrays. Using FET element-receivers, the number of simultaneous receive beams is limited only by the amount of beam-forming hardware in the satellite. The uplink receiving problem does not severely limit the number of uplink beams.

With an unlimited number of uplink beams and unlimited satellite complexity, the optimum solution for minimum terminal cost is to provide variable data rate reception for each terminal, with multiple terminals in a given antenna beam accessing the satellite with FDMA. This approach minimizes the EIRP requirement and/or maximizes the rain margin for each terminal. Such an ultimate performance design is not considered practical for 1990-launch satellite technology.

A compromise between satellite complexity and user terminal requirements is needed. The design process for operational system should include fairly detailed design of several levels of satellite receiving system complexity and minimization of overall system cost with satellite complexity as a parameter.

The conclusions of such a trade study will be heavily dependent on 1990 launch state-of-the-art technology, which is relatively uncertain at this time. Given this uncertainty, the benefit of a detailed study is not sufficient to justify the resources expended. The approach utilized herein will be to select a "reasonable" set of design parameters.

The typical traffic scenarios generated in the traffic study are repeated as Table 3-1. Area total data rates are below 125 Mbps and, accordingly, 125 Mbps will be selected as the maximum processor uplink channel burst rate. The uplink burst rates will be quantized to reduce satellite complexity. Lower burst rates must be provided to reduce EIRP requirements for the many users with data rates less than 1 Mbps. Very low burst rates may make the satellite too complex.

The baseline uplink design will allow processor channel burst rates at 125 and 25 Mbps. The exact burst rates and the number of burst rates available must be reevaluated for an operational system, however. The design tradeoff determining uplink data rate flexibility by balancing terminal EIRP impact against satellite complexity is a major, critical design trade, and as such should be constantly reevaluated as technology advances.

### 3.2.3 Processor Downlink Channel Burst Rates

The processor downlink channel burst-rate selection can be made independently of the uplink selection, due to the digital on-board processor's capability to change burst rates. This is fortunate since the factors affecting uplink and downlink channel burst rate selection are very different.

The desire to use high-efficiency TWTAs transmitters rather than solid-state amplifiers drives the system design towards a smaller number of higher burst-rate, downlink, simultaneous, antenna beams. Also, FDM operation, which is attractive for uplinks, is not an efficient use of a single TWTAs, because of intermodulation losses.

The FDM advantage on the processor uplinks consists of allowing more DTU terminal transmitters to operate simultaneously. Since the number of transmitters available on-board the satellite is limited, there is no similar advantage on the DTU downlink. The satellite transmitter power is

shared among the users with either FDM or TDM, and FDM suffers intermodulation losses which are not present with TDM power sharing.

By using microwave LSI techniques with batch fabrication, the cost effect of high downlink burst rates on DTU terminals should be small for burst rates as high as several hundred, perhaps even five hundred, megabits per second. Minimizing the DTU terminal G/T requirement is a much better criteria for downlink design than minimizing burst rate.

The baseline processor downlink burst rate will be selected to operate with six simultaneous downlink beams. This is thought to be the minimum number of beams providing a reasonable system design with the 2 Gbps throughput requirement. One Gbps of the total 3-Gbps processor throughput is downlinked through the fixed-beam MBA. A larger number of beams is desirable, if the input on satellite complexity is not too extreme. Since the processor downlink, or scanning-beam downlink capacity requirement is 2 Gbps, the minimum beam burst rate is 333 Mbps. Considering that 100 percent utilization efficiency will probably not be achieved and that some terminals may require more downlink utilization than their data rates would indicate, the beam burst rate must be at least 500 Mbps.

Although FDM operation with a single TWTA is not attractive, combining several TWTA outputs with an FDM multiplexer is attractive. We will assume two TWTA transmitters are used on each antenna beam. This allows reduction of the 500-Mbps beam burst-rate requirement to 250 Mbps burst rate per FDM channel, with two FDM channels in each beam. The peak logic rate in the DTU terminal is 125 Mbps using quadriphase modulation. Twelve active TWTA transmitters are used in the six-beam processor in downlink subsystem.

### 3.3 MODULATION

There are three independent modulation selections to be made. The trunking, processor uplink and processor downlink modulations may all be independently chosen.

#### 3.3.1 Trunking Modulation

The trunking system must use a modulation with reasonable bandwidth efficiency to avoid requiring exceptionally wide terminal component bandwidths. The obvious choices are quadriphase, staggered quadriphase, MSK, and some quasi-MSK formats with simplified modulators. Since the

modulation selected is not critical in terms of system efficiency, quadriphase will be assumed as the baseline trunking modulation.

### 3.3.2 Processor Uplink Modulation

Modulation types that seem worthy of study include:

- Differentially encoded biphase with noncoherent differential detection
- Biphase with coherent detection
- Quadriphase, staggered quadriphase, MSK and variants (as in the trunking system) with coherent detection.

Coherent uplink carrier operation is not possible. The only source of system carrier synchronization available to the user terminal is the down-link carrier. The phase noise of state-of-the-art frequency standards results in several cycles of phase error when attempting synchronization with approximately 0.25-second two-way transmission delay. If coherent demodulation is used, the satellite receiver must synchronize with each burst, and preamble of approximately 100-bit length must be provided. The efficiency lost due to preambles tends to offset the efficiency of coherent demodulation and the satellite receiver becomes very complex.

Noncoherent demodulation can be very efficient at high SNR but investigation of performance at the low SNRs consistent with error correction coding indicates a 2.5- to 3.0-dB degradation compared to PSK (see Figure 3-5). The efficiency loss is excessive and coherent demodulation is thought to be required even considering complexity and preamble losses.

The trade between biphase and the various quadriphase modulation types is based on both terminal and satellite complexity. Quadriphase modulations require less component bandwidth and allow a factor of two reduction in digital signaling rates. Quadriphase requires precise modulator phase and amplitude control, however, and satellite receiver carrier acquisition is more rapid with biphase.

Since uplink bandwidth is relatively unrestricted, biphase will be used as our baseline uplink modulation to allow simpler terminal and satellite hardware.

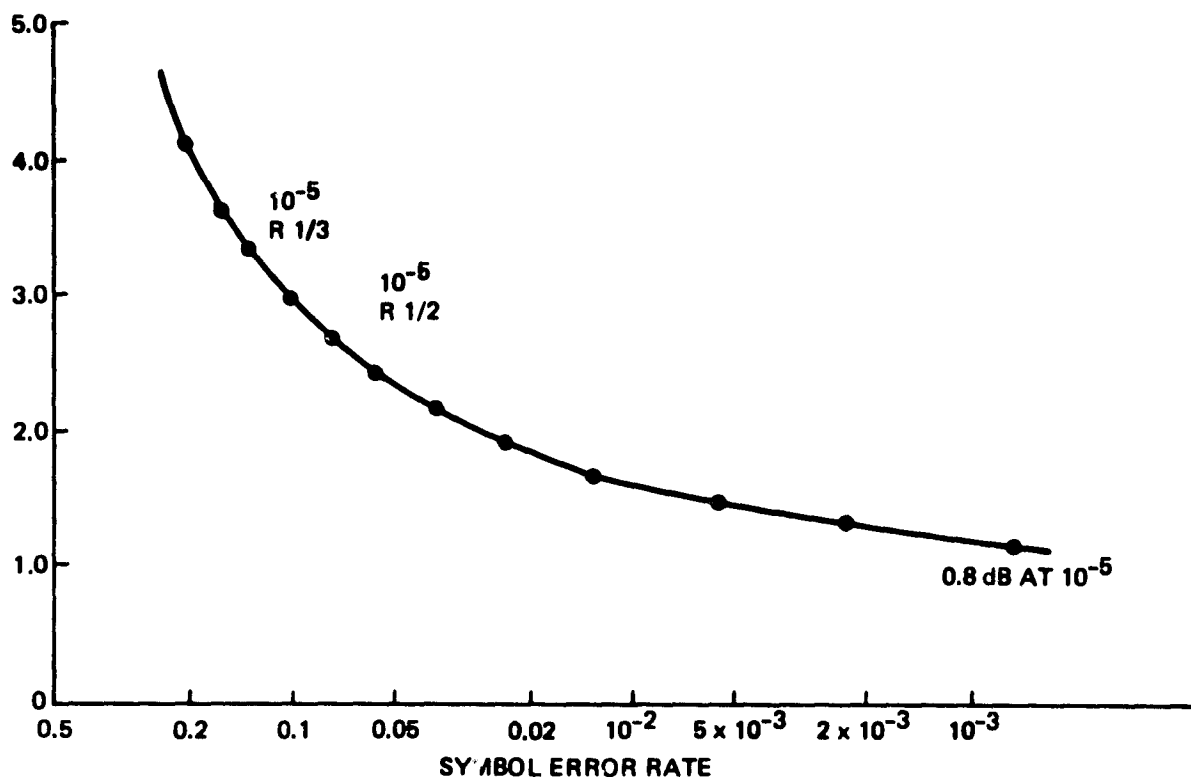


Figure 3-5. DPSK Degradation, Compared to PSK Modulation

### 3.3.3 Processor Downlink Modulation

#### 3.3.3.1 Downlink Carrier Synchronization

Since there is a single downlink carrier oscillator for the entire communication system, and there are no time-knowledge synchronization problems on the downlink; downlink demodulation will be synchronous. With frame periods of approximately 1 ms, phase errors should be:

$$360^\circ \times 20 \times 10^9 \times 10^{-11} \times 10^{-3} = 0.072^\circ$$

from frame to frame with a  $10^{-11}$  oscillator stability. Oscillators are readily available with millisecond-period, short-term stability of  $7.5 \times 10^{-13}$  (HP 105 A/B); so the terminals may use either a low bandwidth ( $< 100$  Hz) or switched-time-constant, carrier-reference, phase-locked loop.

Each active DTU small trunking terminal receives one data burst from the satellite per frame. Terminals may demodulate all data transmitted to their beam-location to improve their carrier reference and utilize only that intended for them. Because of the low tracking loop bandwidth, a minimum data rate terminal located in an area which receives no other downlink signals will have adequate tracking-loop SNR, even at error correction coding threshold with channel SNR less than 0 dB.

The approach described above avoids the complication and low-SNR degradation of rapid-acquisition receivers, and avoids the need for a separate satellite beacon and terminal beacon receiver. A satellite beacon signal was considered to provide carrier and timing synchronization. Use of a beacon was rejected, since the cost of both the satellite and the terminals would be increased and no functions would be provided that are not available with the normal processor signaling structure.

#### 3.3.3.2 Modulation Selection

Since an inexpensive approach is available for continuous downlink carrier synchronization, noncoherent detection approaches need not be considered. The processor downlink modulation will be either biphase or quadriphase (or one of the quadriphase variations: MSK, SQPSK, etc., as discussed above).

Biphase is significantly easier to demodulate. Quadriphase receivers can provide almost equivalent performance, but are more expensive due to the need for phase balances between the two orthogonal-phase detectors. The receiver channel bandwidth and the data detector operating rate both reduced by a factor of two in a quadriphase system, however, and this may offset the greater cost of a quadriphase receiver.

Selection of biphase or quadriphase as the processor downlink modulation will be based entirely on terminal cost minimization. Receiver bandwidth is not a problem, but the lower logic speed required with two parallel output data streams rather than one is thought to be significant.



Pending further study, the processor downlink modulation baseline selection is quadriphase. Selection of an exact quadriphase format need not be made at this time.

#### 3.3.4 Frame Rate Selection

The baseline frame rate has been set at 1 kHz for a 1-ms frame period. This, with the restriction of user data bursts to a 64-bit quantization, quantizes the user data rate to 64 kbps steps. This is compatible with the DS1 interface (as in the T1 digital carrier system) where each of the 24 channels in a fully-loaded DS1 signal is 64 kbps.

Factors selecting satellite system frame period selection are:

- Satellite and Terminal Buffer Size
- Satellite Scanning Antenna Scan Rate
- Compatibility of Satellite and Terrestrial Systems
- Data Transmission Delay.

Compatibility with terrestrial systems may be achieved using a synchronous transmission techniques. Transmission at a slightly higher rate with pulse-stuffing for rate equilization and rebuffering to a constant rate allows compatibility but requires more data-handling hardware.

The DS1 signal of the terrestrial T1 system has enough flexibility to accommodate the effects of satellite motion and allow entirely synchronous operation with simple terminal hardware. To achieve compatibility the frame period of the satellite system should be a multiple, preferably a binary multiple, of the DS1 frame period. Satellite frame periods of 0.125 (DS1), 0.25, 0.5, 1.0, 2.0, 4.0, 8.0, 16, or 32 ms would meet this criterion.

Frame periods should be short with respect to the satellite transmission delay period of about 250 ms. Since the additional frame processing delay should be negligible, and since as many as four frame periods are added by buffering, a frame period of 4 ms or less is desirable.

A frame period within the range of 0.125 to 4.0 ms must be selected based on system hardware complexity. During a frame period, the scanning antenna must scan all of the occupied beam locations. About 270 beam locations are required to cover the 48 contiguous states. Twenty locations are covered by the fixed-beam system. About half of the remainder, or 125 locations, are expected to be occupied at full system loading.

If 10 percent of the frame period is allocated to scan setting or switching time, the antenna beam switching time must be 1/1250 times the frame period for a single scanning beam. No more than 10 percent of the frame period should be allocated to beam switching since the switching time is a direct loss in system efficiency. The required minimum frame period may then be defined in terms of the antenna switching (settling) period;

<u>Minimum Frame Period (ms)</u>	<u>Single Beam Antenna Settling Time (<math>\mu</math>s)</u>
4.0	3.2
2.0	1.6
1.0	0.8
0.5	0.4
0.25	0.2
0.125	0.1

Utilizing multiple independent scanning beams multiplies the allowable beam-switching time by the number of independent beams. If the scanning beam has multiple beams which are not independently scanned, as in some of the space-fed array concepts, the beam coverage efficiency must be taken into account.

While antenna beam settling effects on system efficiency compel longer frame periods, satellite and buffer terminal sizes encourage shorter frame periods. The satellite buffer must provide a data storage capacity

fired by the satellite processor throughput times the frame period, in each of two memories. The total satellite buffer memory size for a 3-Gbps throughput is:

<u>Frame Period (milliseconds)</u>	<u>Satellite Buffer Memory (bits)</u>	<u>Number of 65.5 K bit Chips</u>
4.0	24 M	367
2.0	12 M	184
1.0	6 M	92
0.5	3 M	46
0.25	1.5 M	23
0.125	750 K	12

Similarly the buffer size in a DTU terminal for interfacing a 1.544 Mbps DS1 signal is:

<u>Frame Period (milliseconds)</u>	<u>DS1 Buffer (bits)</u>
4.0	6176
2.0	3088
1.0	1544
0.5	772
0.25	386
0.125	193

Considering all the factors above, a baseline frame rate of 1.0 ms has been selected for the processing subsystem. This must be considered an interim selection since final selection will be dominated by scanning beam switching time.

#### 3.4 30/20 GHz MIXED USER SYSTEM ANTENNAS

In developing system architecture some consideration of MBA characteristics is necessary to achieve system compatibility. This section will describe baseline MBA design requirements. Antenna mechanizations will be described in a later section.

Separate trunking, processor uplink, and processor downlink MBA baselines will be described. These MBAs may, and perhaps should, be integrated. It also may be attractive to split the trunking MBA into separate uplink and downlink apertures to reduce feed crowding. The three MBA requirement sets that will be described are quite dissimilar. Trunking uplink and trunking downlink MBA requirements are similar and detailed design factors will govern the selection of integrated or separate apertures.

An MBA beamwidth of 0.3 degree was assumed as an initial baseline for all beams. This beamwidth is compatible with a fixed antenna aperture capable of fitting inside the shuttle cargo bay. About 270 elemental beams are required to provide coverage of the contiguous 48 states. There are clear reasons why different beamwidths might be attractive for different categories of service. With on-board processing there is no constraint requiring the uplink and downlink beams to have similar characteristics.

Processor uplink and downlink MBAs should have variable beam size and shape capability if possible. Varying the beam size allows the downlink energy to be spread less densely over areas where less margin is needed and makes a greater portion of the satellite power-time product available to areas having greater rain-loss problems. Beam size could be varied in a fixed manner to distribute the average system margin, or could be varied adaptively to meet current requirements and conditions. Because the system described already has many adaptive capabilities, adaptive beam size control will not be considered further at this time. Similarly, the baseline design will assume fixed beam size, deferring variable beam size system effects to a separate study.

#### 3.4.1 Trunking MBA

The trunking MBA provides eighteen fixed beams, uplink and downlink, to eighteen areas containing very high data rate trunking users and heavy concentrations of DTU users. A reflector antenna with multiple feeds is used as the baseline trunking MBA. Feed crowding is reduced by using two linear polarizations and a polarization grid to generate two separate focal planes. An offset design may be attractive to reduce blockage.

The fixed-beam MBA may cause difficulty in achieving satellite capability to operate over a wide orbital arc. Currently the FCC requires a

reasonably wide orbital arc capability in all domestic COMSATS. This allows flexibility to reoptimize satellite position assignments. This policy may not apply to 30/20 GHz systems, but if it does, the trunking MBA can provide a variable beam geometry either by electrical means or simply by moving the individual feeds with linear actuators.

The trunking MBA antenna could be used for downlinks only if the processor uplink MBA is used for fixed-beam uplinks, as described below.

#### 3.4.2 Processor Uplink MBA

The baseline processor uplink MBA is a large-element phased array or a small-element phased array in a reflector or lens antenna system. Each element provides relatively constant gain over the contiguous 48 states, perhaps biased towards higher gain in the Southeast. Received signals are amplified by FETS, downconverted to a convenient IF frequency, and split to provide inputs to several beam-forming networks.

Beam-forming networks receive signals from each element, phase shift as required, and add the element signals to achieve the required MBA G/T in the direction of the formed beam. Both fixed and variable beam-forming networks can be used. An array of fixed beams could cover high density areas, perhaps including the trunking uplink areas, with variable beam forming networks providing several simultaneous scanning beams.

The antenna described above is attractive in terms of capacity and reliability. A relatively large number of simultaneous beams provides outstanding capacity. Graceful degradation of array performance with element front-end failures, combined with the ability to avoid any active devices between element front-ends and fixed beam receivers plus the capability of substituting a variable beam for a fixed beam should a critical fixed-beam receiver fail, all add up to a design capability of very high reliability with redundancy complexity factors much less than the usual satellite communication system design.

#### 3.4.3 Processor Downlink MBA

The processor downlink MBA design is severely constrained by the desire to use single carrier TWTA transmitters with RF power generation efficiencies of 30 to 35 percent rather than multiple-carrier FET transmitters with efficiencies from 5 to 10 percent. A phased-array

mechanization with individual element transmitters would make multiple-carrier FET transmissions almost mandatory. The alternate solution of several hundred TWAs as element transmitters is unattractive in terms of cost, complexity, reliability and weight.

A fixed-beam, contiguous-coverage MBA with a scanning switch was considered but it is difficult to achieve either the low loss or high reliability required at the high power and high frequencies required.

The baseline processor downlink MBA design selected is a space-fed phased array with a multiple-beam feed subarray. The concept is shown in Figures 3-6. A control address is distributed from the timing unit to all of the phased element units. In each element the address accesses a RAM which directly sets the element phase for each preprogrammed beam position.

The space-fed concept is thought to provide both rapid beam scan capacity and high RF efficiency. Multiple beam capability is achieved by placing several feeds in a cluster in the array focal plane. This does not provide independent beam pointing, and a computer program will be required to optimize the beam scan pattern and provide the most efficient match of downlink energy distribution to user downlink traffic. Some efficiency will be lost in scanning low-density regions since adjacent beams will not be utilized. In some cases the energy in all but one downlink beam may be wasted while serving isolated users.

The processor downlink MBA may be either a large element phased-array or a small-element array in a reflector or lens antenna system. Furthermore, the solid-state active element transmitter array concept must be carried as a very viable alternate to the TWA-driver space-fed array should FET transmitter efficiencies improve more rapidly than is now being predicted.

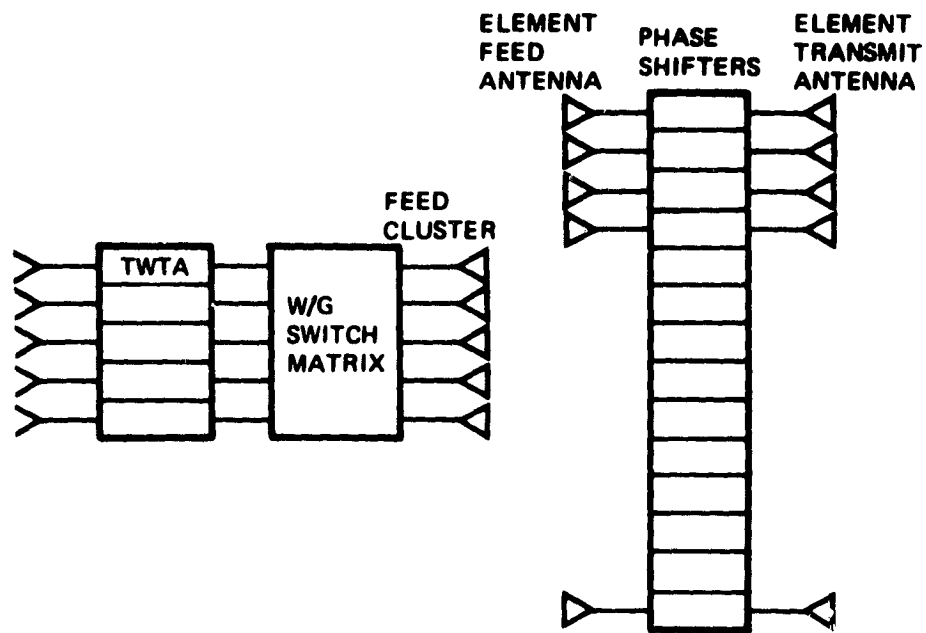
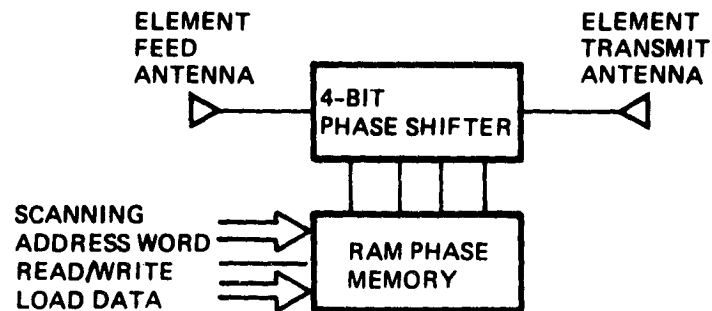


Figure 3-6a. Multiple-Beam Space-Fed Phase Array



- RAM PHASE MEMORY RETAINS ALL PHASES REQUIRED DURING FRAME PERIOD
- ADDRESS IS DISTRIBUTED TO ALL ELEMENTS IN PARALLEL FOR TIMING/CONTROL

Figure 3-6b. Space-Fed Array

### 3.5 SIGNAL POLARIZATION

Uplink and downlink polarization are not critical parameters in a communication system that is not bandwidth constrained and hence does not need polarization separation. Even with 2.5 GHz of bandwidth available, polarization separation may be attractive, however. The Northeastern United States, and in particular the New York City area, contains a very high concentration of high data rate users. Polarization separation will allow very high capacity coverage of this extremely critical area.

According to recently published Bell Laboratory data taken at Crawford Hill, N. J.\* polarization separation levels of about 15 dB are available in this area for the attenuation levels required in both the processor and trunking systems.

Fifteen dB cross-polarization interference causes less than 0.2-dB degradation in a processor channel which uses rate 1/3 coding for an  $E_s/N_0$  requirement of 1.2 dB. The  $E_s/N_0$  requirement is based on:

$E_b/N_0$ uncoded for $10^{-5}$ BER	+9.6 dB
Coding Gain for R 1/2 code	-5.6 dB
$E_s/E_b$ for rate 1/3 code	-4.8 dB
Allowance for permod. degradation	+2.0 dB
Required $E_s/N_0$	1.2 dB

$E_s$  - Signaling Element Energy  
 $E_b$  - Bit energy  
 $N_0$  - Noise density

An uncoded trunking system may suffer about 1.5-dB degradation since it operates at higher  $E_s/N_0$  in the region as 11.6-dB with uncoded data. Since tracking stations will generally have high margins such a loss is acceptable.

---

\*H. W. Arnold, D. C. Cox, H. Y. Hoffman, and R. P. Leck, "Characteristics of Rain and Ice Depolarization for a 19 and 28 GHz Propagation Path From a COMSTAR Satellite," ITC Proceedings, Paper 40.5, June 1979.



The polarization results reported are significantly better than expected. Prior to this data becoming available polarization separation had been considered infeasible. The data presented does indicate that vertical and horizontal polarization at the terminal provides the best separation. Since we will consider polarization reuse only in the congested New York City area, this result indicates that the polarization vector for a 100°W longitude synchronous-orbit satellite should be rotated about 26 degrees clockwise (looking towards the earth). The rotation will remove the geometric distortion effects, and restore vertical/horizontal polarization in the New York City area.

This rotation, plus the geometric distortion effects, result in a 51-degree total rotation on the U.S. West Coast. Since polarization reuse is not being planned on the West Coast this is of no consequence. Even if polarization reuse were being contemplated across the country, such a rotation should be used to provide maximum polarization separation in the Eastern U.S. where rain effects are greatest.

With or without polarization reuse, linear polarization is recommended. Linear polarization allows use of polarization-separation grids in antenna-feed structures. A polarization grid effectively provides two independent focal planes. This reduces the feed-crowding problem and allows two transmitters to radiate in a single area through one antenna aperture.

Polarization frequency reuse for increasing the data rate capability in the New York area will result in a requirement for uplink power control in that area. If polarization frequency reuse is utilized from a single terminal, uplink power control is automatic since rain will affect both signals. If two stations in different locations share a time-frequency slot, their uplink power levels must be controlled to provide equal power densities at the satellite; otherwise, the crosspolarization isolation may be degraded excessively.

#### 4. NETWORK CONTROL

Synchronization is a major concern in the design of any TDMA communication system. TDMA burst synchronization is necessary to prevent collisions, or multiple bursts arriving at the satellite simultaneously. When collisions occur the data in both colliding bursts are usually lost. Precise synchronization also aids in identifying data segments to be routed to different destinations. The synchronization problem is solved in most current satellite TDMA communication systems by incorporating a master control station. This station transmits timing signals and makes assignments of nonoverlapping burst periods to each user terminal.

The master control station concept is highly efficient and, with provision of one or more alternate stations, highly reliable. For a system which demodulates, processes, and remodulates data, the functions of the master control station must be modified. All of the routing, assignment, and synchronization functions that are performed may be described as network control.

##### 4.1 SATELLITE PROCESSOR CONTROL

The satellite processor accepts input data from a large number of uplink receivers, processes this data, and outputs data to the downlink transmitters. Tasks performed include forward-error correction (FEC) decoding, routing, and FEC encoding.

Only a small portion of the throughput data is FEC decoded or encoded. Selection of the appropriate portion of the data throughput is part of the routing task. Routing also includes interfacing high rate, medium rate, and low rate users. Control of the satellite processor is almost entirely concerned with routing control.

As described in Section 3, complete routing flexibility is achieved by establishing a permutation of the input addresses, and reading out the processor memory in a carefully defined order. This order will be defined by an algorithm located at the master control station. The routing control data established by that algorithm will be transmitted to the satellite and loaded into the processor control memory by the satellite digital command channel.

Routing control will be accomplished at the master control station to simplify the satellite. The only penalty for this implementation is the additional 0.25-second transmission time delay resulting from transmitting data from the satellite to the ground station and transmitting command data back to the satellite. The advantages are much more processing capability available to handle more complex algorithms, lower satellite cost, increased satellite reliability, and the ability to modify the readily assessable algorithms in the master control station computer. The situation is different for military communication systems which must operate with massive destruction of ground elements, but for a commercial communication environment the cost, reliability, and flexibility advantages of terrestrial control are overwhelming.

#### 4.2 SATELLITE SCANNING BEAM CONTROL

The satellite scanning beams will be controlled by the master control station also. An algorithm in the master control station will define the scan patterns to maximize system efficiency in coordination with the TDMA burst assignment algorithm. The scan pattern algorithm will probably operate on the requirement data first, and the scan algorithm output will be an input to the TDMA burst assignment algorithm.

The scan patterns thus defined will be operated on by another algorithm to convert scan data to the form most easily utilized by the scanning antenna. This may consist of a complete definition of the phase setting of each phase-shifter for each beam scan position. The scan control data thus generated is transmitted to the satellite via digital command channel and stored in a memory which reads out the data sequentially and periodically, as required, until a new data set is generated.

If a phase-shifter controlled scanning array is used, the satellite scanning beam control process will include periodic calibration of each element in the array. Techniques for on-line array calibration have been developed during the TDRSS multiple-access phased array development at TRW. An array may be completely calibrated without interrupting its normal utilization. Calibration data would be combined with the array control data to generate the phase-shift commands to each array element.

### 4.3 SYSTEM TIMING CONTROL

With the advent of SSTDMA, the system timing problem for communication networks takes on a new dimension. There is now a satellite-borne oscillator which must be considered in the control of TDMA timing. Two approaches are commonly considered. The satellite oscillator may be allowed to free-run and may actually define TDMA system time. Alternatively, the satellite oscillator may be controlled by the master control station.

#### 4.3.1 Satellite Timing

##### 4.3.1.1 Free-Running Satellite Timing

With a free-running satellite oscillator controlling the satellite SSTDMA switch timing, communication burst timing must track any drift in the satellite oscillator to assure that bursts arrive at the satellite while the satellite switch is in the proper configuration. With demod/remod on-board the satellite, the on-board oscillator must also be used as the reference for carrier and data clock frequency.

The advantages of using a free-running oscillator on the satellite for timing are simplicity of the satellite circuits, and the improvement in reliability resulting from that simplicity. The disadvantage is that the entire system must be designed to operate over a relatively broad range of frequency errors to accommodate aging of the satellite crystal oscillator.

##### 4.3.1.2 Controlled Oscillator Satellite Timing

The satellite timing oscillator may be controlled by the master control station. Two techniques are available: pilot-tone control, and digital oscillator frequency control. With a pilot-tone control system, the master control station transmits a continuous low-level pilot-tone to the satellite. On board the satellite, this tone is used to phase lock the satellite time-frequency standard oscillator. The pilot-tone may be derived from a very accurate standard in the master control station, and this reference may, in turn, be periodically calibrated against the national frequency standards at either NBS or Naval Observatory.

The system is significantly simplified by having stable time and frequencies. If the pilot-tone is disrupted, however, system operation may be disrupted. Pilot-tone outages may be prevented by automatic loss detection and replacement by auxiliary stations.

Another approach is to use a disciplined time-frequency standard aboard the spacecraft. A disciplined time-frequency standard is nothing more than a voltage-controlled crystal oscillator (VCXO) with the frequency-controlling input voltage set by an A/D converter. With this approach the master control station monitors the time frequency of the satellite standard, as revealed by the downlink timing and frequency, corrected for doppler effects. The master control station then sends frequency correction commands which bring the satellite time-frequency standard (VCXO) into conformance with the national standards.

The disciplined time-frequency spacecraft-standard approach has all the advantages of the pilot-tone-locked standard approach, with the additional advantage that loss of the uplink from the master control station does not degrade timing performance unless the uplink is lost for a very long time (days).

The recommended approach to establishing system timing is to use a disciplined time-frequency standard on the satellite, and control the standard to conformance with the national frequency and time standards by a digital command uplink from a master control station.

#### 4.3.1.3 Terminal TDMA Burst Assignment

The master control station will assign TDMA burst times to each terminal utilizing the 30/20 GHz communication satellite system. The algorithm used in making burst assignments must be quite complex. Complexity results from the requirement to be compatible with beam scanning and on-board routing in addition to coordination of all the traffic requirements of all the terminals. The algorithm must also operate rapidly if, as assumed elsewhere, it provides response to terminal rain conditions by switching adaptive error correction coding on links affected by excessive rain loss.

Adaptive error correction coding modifies burst assignments to provide additional burst duration on affected terminals. Rate 1/3 coding, the baseline code selection, requires a burst duration of three times normal. When the burst duration changes for one terminal, the adjacent terminal bursts must be moved. The resulting time shift could ripple through the entire TDMA system. Proper selection of normal burst assignments will distribute any unused system capacity throughout the frame period and can reduce this ripple effect.

The burst-assignment algorithm must also respond rapidly to provide demand assignment of new channels when requested. The "New Voice Channel Establishment Time Line" described elsewhere allows 10 ms for master control station data processing. This processing includes interpretation of the request, planning the burst-assignment changes necessary to accommodate the new channel request, formatting the control memory changes required in the satellite processor, and transmitting the control message to the satellite processor. While the 10-ms allocation can be relaxed, if necessary, it is clear that the algorithm must operate rapidly since very little time is available.

The solution to the algorithm response requirement may result in two types of assignment algorithms. A "local" algorithm may provide rapid response within a small portion of the system, while a less-rapid, optimization algorithm modifies the allocation of system capacity to each of the "local" algorithms.

#### 4.3.2 Terminal Timing and Frequency Control

Control of terminal time and frequency is a major concern in the design of a TDMA system with many inexpensive terminals. Careful system design can lead to inexpensive synchronization hardware that, by providing accurate synchronization, increases system efficiency and decreases system cost. This statement is based on some concepts that are not generally accepted at this time, however, and must be explained and defended in some detail.

Accurate synchronization allows operation without TDMA burst preambles. TDMA burst preambles are used in most TDMA systems to reestablish channel carrier, data clock, and data epoch timing independently for each data burst. These preambles must be on the order of 100 bits long to

accomplish their function. In a system with 2000 active users and a 1-ms frame rate, preambles add a 200 Mbps overhead data load with on-board routing. Without on-board routing, each user will have to transmit several bursts per frame, and the preamble overhead will be larger. With an accurate synchronization system, synchronization is never lost and need not be reestablished. TDMA overhead losses are reduced dramatically.

Current terminal TDMA modem designs include sophisticated rapid carrier and clock acquisition circuits. Unique word detection hardware is provided to establish burst data epoch (time). Data pattern scramblers prevent long strings of data-ones or data-zeros which might interfere with the wideband data clock circuits needed for rapid acquisition. All of this hardware, which may represent most of a current-design TDMA modem, is unnecessary in a demod/remod satellite communication system which is designed to provide continuous, accurate synchronization.

A good, crystal oscillator provides the finest terminal time-frequency standard available with the current state of the art. The satellite downlink provides most of the time-frequency information needed by a satellite communication terminal. The station standard needs only short-term stability (<1 second) to "clean up" the high frequency downlink phase noise introduced by the terminal receiver. Crystal oscillators are superior to any other available technology for short-term stability including atomic time/frequency standards. Exotic frequency standards are not needed.

Careful digital synthesis techniques are required to avoid introducing time errors and phase noise, especially when synthesizing uplink frequency and timing from a reference crystal oscillator. The amount of hardware is small, however, and advanced digital synthesis techniques may be implemented with large-scale integrated circuits to produce time-frequency synthesis equipment with low unit cost.

The 30/20 GHz communication system baseline utilizes on-board digital data processing techniques with uplink demodulation and downlink remodulation to provide high communication efficiency. Downlink synchronization problems are essentially eliminated by this technique, since all downlink modulation is synchronized to a single satellite time/frequency reference. This reference is easily tracked by small user terminals using narrowband phase-locked loop techniques.

Uplink synchronization presents several problems, however. There are two major system synchronization error sources:

- System oscillator drifts
- Satellite position changes.

The user terminal gains information about system oscillator changes by tracking the downlink signal and comparing to the terminal time/frequency standard. The information gained can have high bandwidth and SNR, but is about 1/4 second old due to transmission time delay.

Satellite position changes cause doppler frequency errors and transmission delay timing errors. Downlink timing measurements cannot correct both system oscillators and satellite position errors, since corrections must be applied in opposite directions for the two error sources. Since system oscillator drifts are higher bandwidth and larger error sources, downlink signal tracking errors are usually applied as if they resulted entirely from oscillator drifts, and satellite position errors must be corrected by other means. These means may include an error feedback channel from the satellite, another information channel providing information about the satellite position, or another information channel providing oscillator drift information.

The baseline terminal synchronization approach selected for this study uses direct tracking of the downlink signal timing to correct system oscillator errors, and corrects satellite position change errors using satellite position information received over a system "order wire" information channel. The process is described in Figure 4-1. The satellite position is measured very accurately using the high rate data clocks of the large tracking terminals. This data is distributed to the small terminals by the system order wire. The small terminals make open-loop timing corrections to the required accuracy.

Example terminal receiver and transmitter block diagrams are illustrated in Figures 4-2 and 4-3. These block diagrams are compatible with the process described in Figure 4-1 and are based on comparison and trade-off of several potential approaches described below.



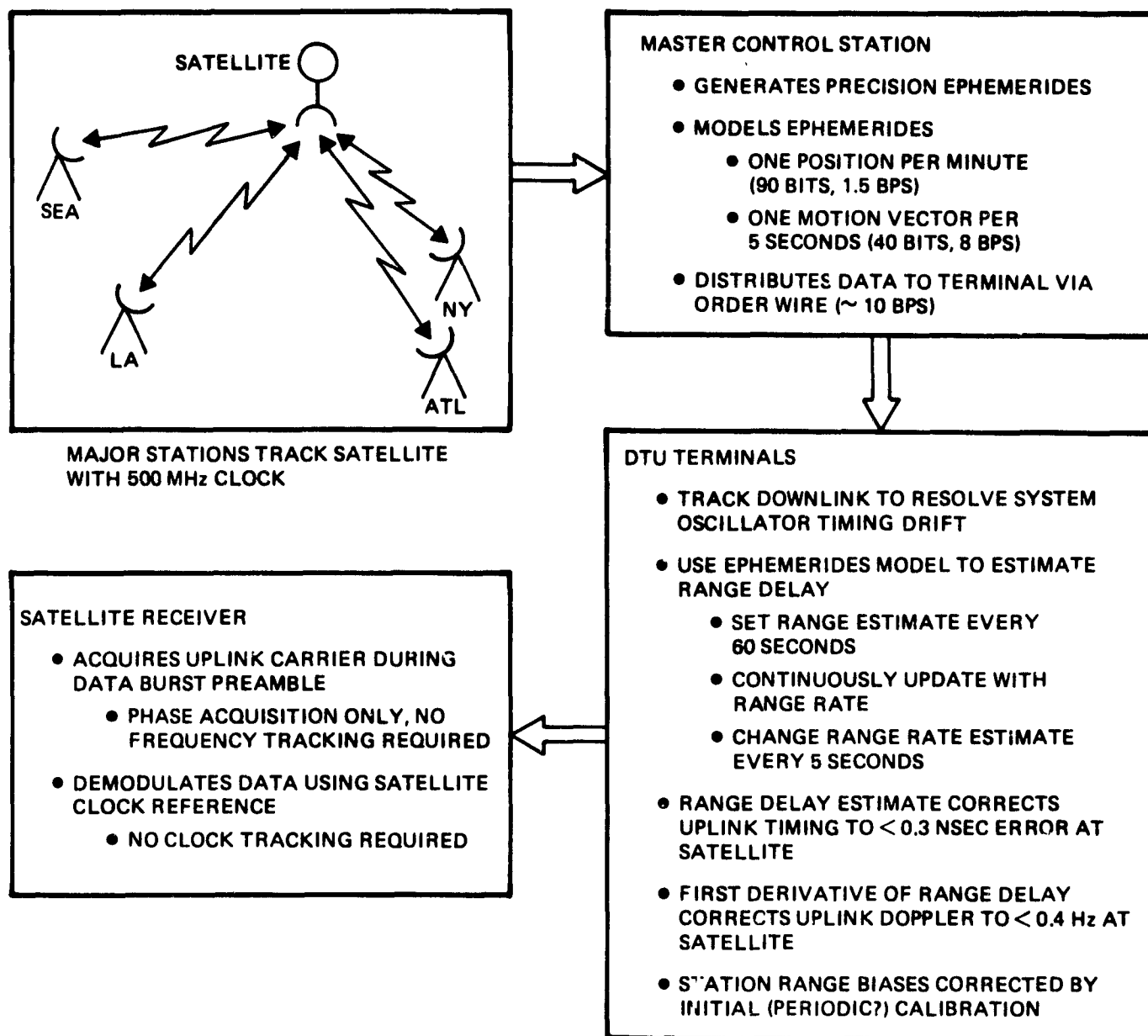


Figure 4-1. Terminal Timing Control

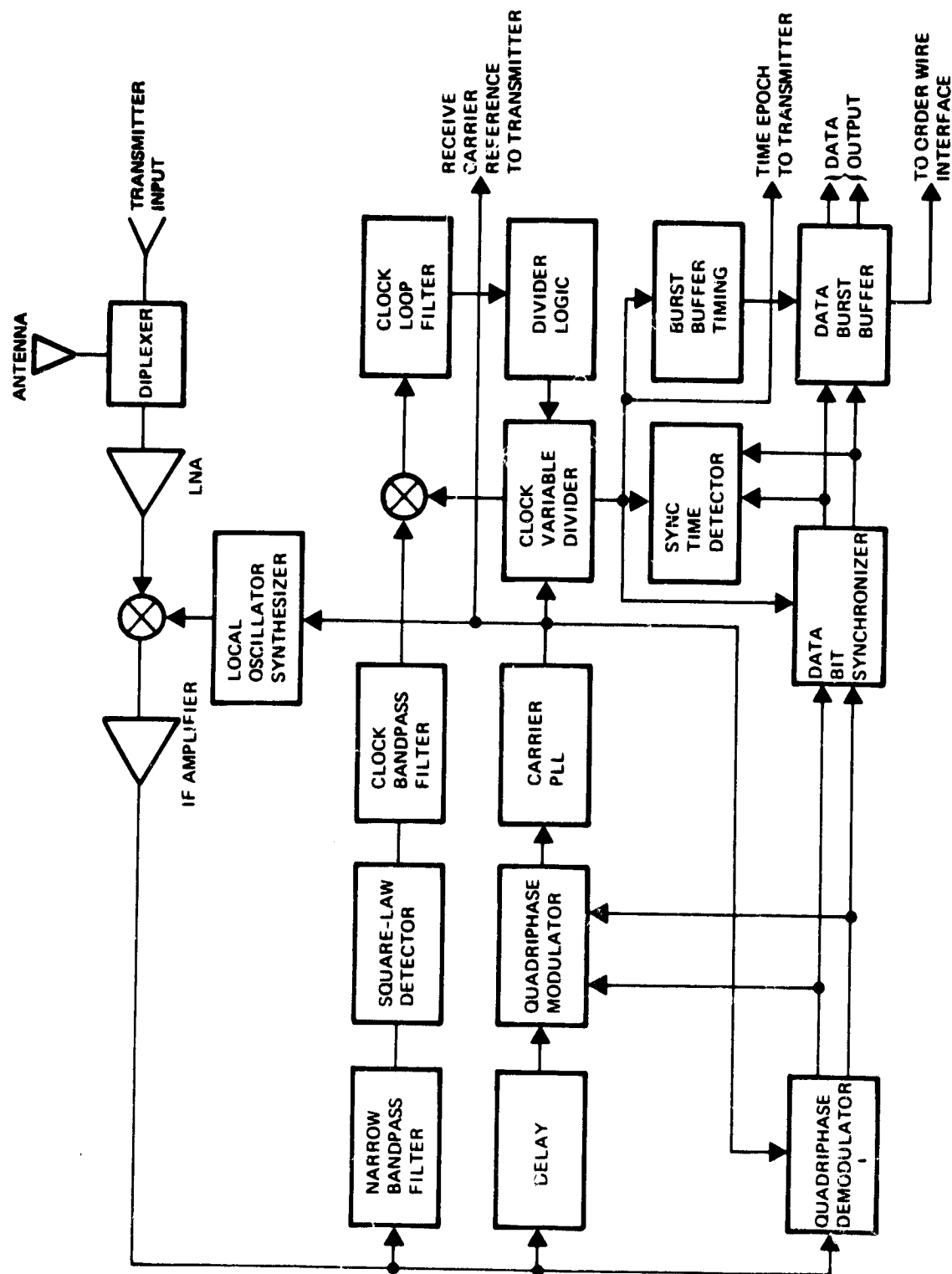


Figure 4-2. Terminal Receiver Block Diagram

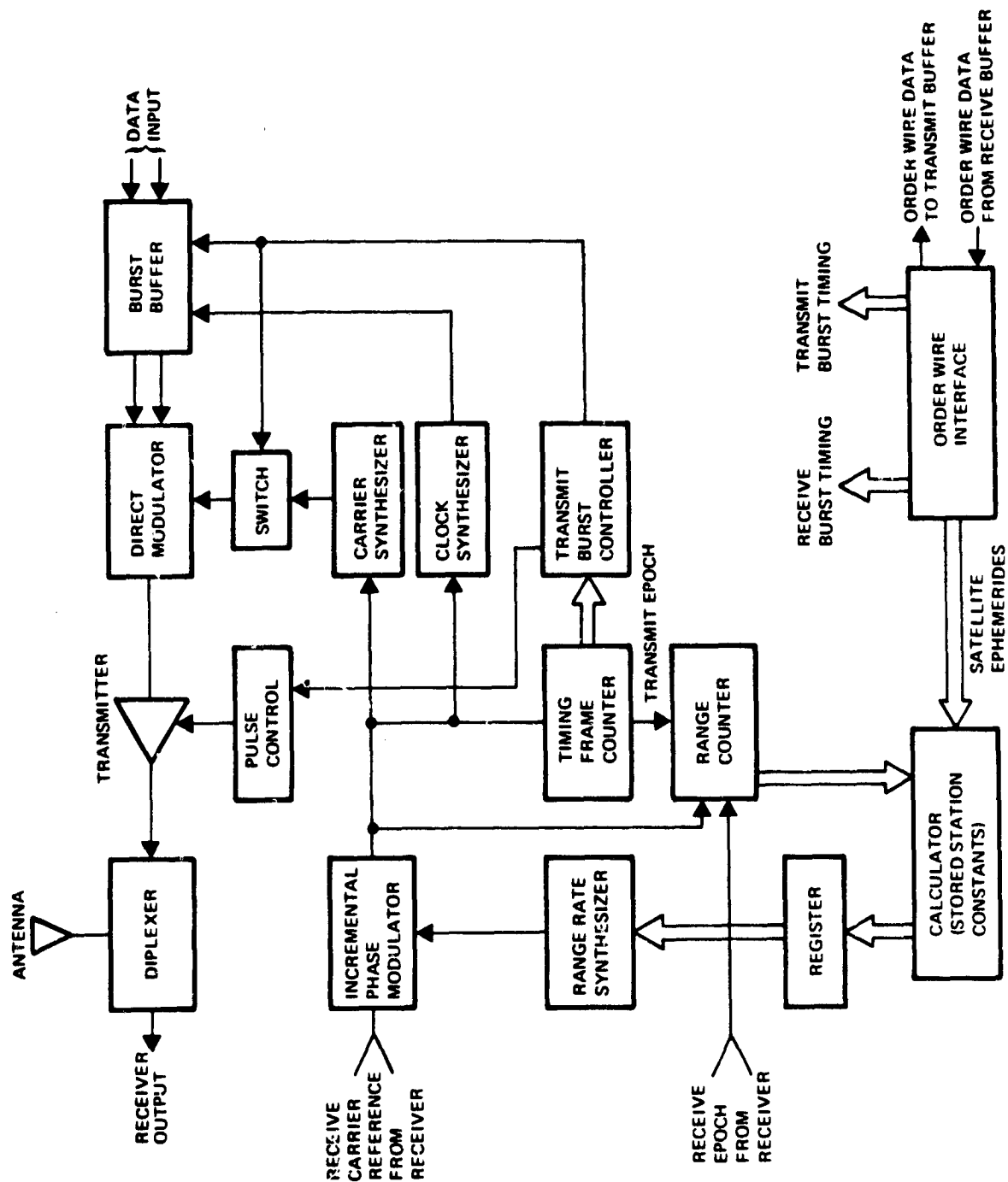


Figure 4-3. Terminal Transmitter Block Diagram

The receiver of Figure 4-2 uses remodulation of the incoming signal to generate a carrier component at the IF input frequency. By demodulating the I- and Q-channel modulation and remodulating on another copy of the input signal, the modulation is removed from this second copy. The reconstructed carrier is then tracked with conventional phase-locked loop (PLL) techniques. A similar approach is used in TRW fast-acquisition TDMA burst modems, but the PLL is replaced by a filter-limiter with quench circuits. The delay circuit prior to the remodulator compensates for the modulation delay through the demodulator and resynchronizes the two signal paths.

Data clock extraction is accomplished by filtering a third copy of the IF signal to a bandwidth somewhat less than the modulation bandwidth. This converts the modulation phase transients into amplitude modulation transients, which are then detected by a simple AM square-law detector. The clock component thus generated is used to synchronize a digital PLL which uses the received carrier frequency as its input frequency reference. This results in carrier-aided clock generation. Carrier aiding should remove most clock phase noise and allow a narrow clock loop bandwidth that will remain in synchronization at very low input SNR.

System frame synchronization is detected from the received burst-rate data stream after the demodulator output has been bit-synchronized using the regenerated data clock. The synchronization signal can be as little as one bit per data-frame and still provide excellent synchronization performance.

Received data is converted from an intermittent data stream at the TDMA burst rate to a continuous data stream at a lower data rate by the receive data burst buffer. The data is then output to the terminal interface hardware. Receive carrier reference and receive epoch-time reference signals are output to the terminal transmitter.

The terminal transmitter must generate signals at the proper transmit time. When this is properly done bursts arrive at the satellite when they are expected and can be demodulated without overlapping other uplink signals. Transmit timing is derived by tracking the received signal timing and advancing the transmit timing to compensate for transmission delays. The amount of timing advance depends primarily on the satellite range from the particular terminal, and can be calculated very accurately from the satellite position or ephemerides.

The transmit terminal of Figure 4-3 accepts receive carrier reference, receive timing epoch, and order-wire data from the terminal receiver. The order-wire data is processed by the order-wire interface to extract precision satellite ephemerides generated by the master control station. The ephemerides are used by a calculator circuit to determine precise range and range-rate values.

Terminal transmit timing advance is measured by a counter which starts on the transmit timing epoch pulse and stops on the receive timing epoch pulse. The timing advance is compared to satellite range, and transmit timing is varied by calculator control of the transmit timing phase through an incremental phase modulator.

Once the transmit timing advance is correct, the timing calculator calculates range rate values (about once every 5 seconds) and generates the transmit timing reference from the receive carrier reference using a range-rate digital synthesizer. Satellite range is calculated and compared to transmit timing advance about once per minute, but the range-rate correction process should make any further transmit range correction unnecessary by integrating the range-rate correction.

Other portions of the terminal transmitter block diagram require little comment. Transmit carrier and clock signals are synthesized from the range-rate-corrected transmit timing reference. Transmit signal bursts are generated at times assigned by the master control station, using the range-corrected timing epoch signal as a reference. Data is burst-buffered and modulated on the transmit signal by direct carrier modulation at the final transmit frequency.

The output signal burst is switched on and off by gating the carrier input to the direct modulator. The transmitter is shown to be modulated on and off also. This may be done to reduce transmitter dissipation if reduced dissipation reduces overall transmitter costs. A tradeoff of pulse control costs versus increased power supply, power, and transmitter cooling cost is required. If transmitter on-off modulation is used, the transmitter will be turned on prior to the data burst to allow phase stabilization prior to transmission.

### 4.3.3 Alternate Systems Studied But Not Selected

#### 4.3.3.1 Completely Coherent Systems

In a completely coherent system the satellite would not track either carrier or data-clock phase. It would measure the phase error terms and transmit them to the terminals. The terminals would use this data to estimate the optimum carrier and clock phase for the next burst. The number and complexity of tracking loops, and hence system cost, would be minimized.

The HP105 A/B specification for 10 MHz crystal oscillators specifies the time domain stability as

$$\sigma_{\Delta_t}(2, \tau) \text{ sec} \leq \begin{cases} 1.5 \times 10^{-12} & \text{for 0.1 second} \\ 5.0 \times 10^{-12} & \text{for 1.0 second} \end{cases}$$

Assuming the satellite and terminal oscillators can both meet the same specification, and assuming the 0.25-second stability to be at least as good as the 1.0-second stability, the one-sigma time error over the transmission delay period is

$$\sqrt{2} (0.25) (5 \times 10^{-12}) \approx 1.77 \times 10^{-12} \text{ seconds}$$

for the combined contribution of both oscillators.

At an uplink carrier frequency of 30 GHz this results in an irreducible phase error term of

$$360^\circ (1.77 \times 10^{-12}) (30 \times 10^9) = 19.1^\circ, 1\sigma$$

Thus, with perfect feedback of phase error measured at the satellite, it might just be theoretically possible to build a completely coherent communication system.

To the best of our knowledge, no one has ever tried to operate a carrier-synchronous communication system as described, even at lower frequencies. Extremely good oscillators (but apparently available technology) would be required. Great care would be necessary in design of the terminal

phase control, upconverters, and downconverters. Such an approach is probably too risky for a commercial system. It would be interesting to operate an experimental system this way, however, if it could be done without compromising a more conventional baseline approach.

#### 4.3.3.2 Completely Noncoherent Systems

Some coherence is required in TDMA systems to prevent burst overlaps at the satellite. Completely noncoherent systems are not attractive for highly efficient communications, although they do find use where communication and coordination between users is impractical.

#### 4.3.3.3 Downlink Tracking Systems

Tracking the downlink signal and estimating uplink transmit timing can provide cancellation of system oscillator drifts to the accuracy discussed. If the satellite is assumed stationary at a known location, errors result from a satellite stationkeeping errors. Satellite station accuracies of about 0.03 degree can be achieved, north/south and east/west. The position errors are  $\pm 22,000$  meters. Radial eccentricity errors will probably be less, but we will assume a 22,000 meter radial error from user terminal to satellite.

Timing errors will then be  $\pm 75 \mu s$ . Assuming diurnal satellite motion, frequency errors are caused by a 1.6 m/s peak velocity. The error is  $5.4 \times 10^{-9}$  times the carrier frequency or about 160 Hz at the 30 GHz uplink frequency. The data clock frequency errors are 2.7 Hz at 500 Mbps, 0.68 Hz at 125 Mbps, and 0.14 Hz at 25 Mbps.

A system could operate with downlink tracking only, provided that adequate TDMA guard times, carrier acquisition range, and data clock acquisition range are all provided. There are several techniques available to reduce the requirements placed on the satellite demodulators and to improve TDMA guard-time efficiency, however. Several that fall in the range between downlink tracking only and being completely coherent will be discussed. The objective is to define a level of system coherence which minimizes system cost.

C-2

#### 4.3.3.4 Downlink Tracking Plus Ephemerides Systems

A downlink tracking plus ephemerides system is summarized in Figure 4-3. By measuring the satellite position error, the time and frequency errors described above may be predicted and corrected. The significant questions show accurately how corrections can be made, what additional system hardware is required (especially in the smallest terminals), and what is the overall impact on system cost.

Satellite ephemerides will be determined using the high-rate 500-Mbps data clock to determine range from several large stations. Range accuracies of several millimeters should be achievable. A 1-degree phase measurement accuracy provides 3 mm range resolution. Since we are interested in variation rather than biases, 1 cm accuracy should be readily achievable.

Distribution of the satellite precision ephemerides to the small terminals allows them to calculate satellite range to an accuracy of 2 or 3 cm. With the same technology used in hand-held programmable calculators, complex but well-defined calculations may be carried out. This should not add significant cost to terminals, provided the calculation rate is low. Calculator hardware will be interfaced with the communications and control terminal hardware. Any requirement for human operators at small terminals is avoided.

Direct calculation of 0.01-meter resolution ranges with  $\pm 22,000$  meter diurnal variations imply a calculation rate of:

$$\frac{22,000}{0.01} \times \frac{2\pi}{(24)(3600)} = 160 \text{ per second}$$

This is clearly impractical for calculator technology and might push micro-computer technology.



The most trivial increase in sophistication, using line segments to model the range variation, requires distribution of both three dimensional position and velocity vectors, but drops the calculation rate to

$$\frac{2 (22,000)}{0.01} \times \left[ \frac{2 \pi}{(24)(3600)} \right]^2 = 0.023 \text{ per second}$$

or 43 seconds per calculation. This is a reasonable rate for calculator calculation using direct hardware interfaces to the calculator.

The line segment approach to range calculation requires 69 bits for position vectors and about 30 bits for velocity. The data rate is then about 16 bps. Data rate may be reduced to 8 bps by transmitting the range correction about once per minute, and increasing the accuracy of the derivatives by 6 bits. The individual terminal stores a nominal range number which is generated by a calibration process. The terminal receives complete satellite state vectors:  $(\Delta X, \Delta Y, \Delta Z, \dot{X}, \dot{Y}, \dot{Z})$  at 1-minute intervals. Each vector is 100 bits long. The terminal receives 30-bit velocity vectors  $(\dot{X}, \dot{Y}, \dot{Z})$  every 5 seconds. The hard-wire-interfaces terminal calculator uses a stored set of partial differentials (calculated by an off-line facility based on the terminals geographic location) to calculate a range correction and range correction derivative.

The stored nominal range and the calculated range correction are input to the transmit timing unit. The range correction derivative is input to the transmit doppler correction unit.

The transmit doppler correction unit derives a frequency reference signal from the terminal receiving equipment. This signal contains information on system oscillator drifts and phase noise. The correction unit generates a doppler-corrected transmit frequency reference, multiplying the receive frequency reference by:

$$1 + \frac{2\dot{R}}{C}$$

$\dot{R}$  = estimated satellite range derivative

C = speed of light

Multiplication is accomplished by using the receive frequency reference signal as the input reference to a coherent synthesizer, and using the correction factor to digitally define the synthesizer output frequency. The corrected reference thus generated is used to generate the terminal uplink carrier and data clock signals using fixed frequency generator techniques.

The transmit timing unit accepts a receive-time signal from the terminal receiving equipment and generates a transmit-timing signal which is advanced in time by

$$\frac{2R}{C} \text{ seconds}$$

R = estimated satellite range

The transmit timing unit also accepts the transmit frequency reference described above, and calculates new range estimates by integrating it in a transmit timing counter.

The result of the process described is correction of range timing errors to about 0.2 ns and doppler errors to about 0.35 Hz. Assuming that mechanization hardware errors can be held to similar values, prediction of uplink timing can make data clock tracking loops on the satellite unnecessary for 125 Mbps and lower uplink data rates.

Fast-acquisition carrier tracking loops on the satellite are still required to resolve carrier phase, but individual AFC tracking loops in the satellite are not necessary with the 0.35-Hz error.

The system described has the advantage of easy initial timing acquisition. Downlink or receive timing is achieved by searching for frame sync with the receiver. Uplink or transmit timing results from receiving the satellite position data and calculating the transmit correction. No low-level PN code or initial-acquisition TDMA-slot techniques are needed.

#### 4.3.3.5 Downlink Tracking with Satellite Timing Feedback Systems

The satellite can measure uplink timing errors by looking at the carrier and code tracking loop errors during or after receiving each uplink signal burst. By sending the timing error signal back to the terminal that originated the burst, timing errors can be nulled in a closed time-tracking loop.

The high bandwidth timing errors caused by system oscillator drifts are nulled by downlink tracking. Satellite range errors are due to phenomena that for the most part have periods of 24 hours or longer. The range variation may be large but it is a very "smooth" low-bandwidth function.

An adequate communication bandwidth would result from digitizing the tracking error of one user terminal each frame. The measurement rate is then one measurement per millisecond. With 10,000 users each user would get one measurement of his error each 10 seconds. A digital smoothing predictor/filter with a bandwidth on the order of 0.01 Hz could continuously update the uplink timing reference.

The satellite timing error would have to be derived from the data clock, since the carrier tracking ambiguity range is smaller than the errors we need to measure. The satellite would require a fast-acquisition carrier-tracking demodulators and data clock error measurement circuits on each demodulator.

A block diagram for clock timing error correction is shown in Figure 4-4. The hardware required can operate at very low speed and would not increase the hardware cost or power consumption significantly.

Initial acquisition with a feedback timing system will present some difficulties. When a terminal tries to join the system, downlink timing may be found by a simple search. Uplink timing must be predicted and the uncertainty searched until timing is within the clock-error circuit ambiguity range. For a 125 Mbps burst rate the ambiguity range is 4 ns. The ambiguity range can be extended, but only by adding more satellite hardware.

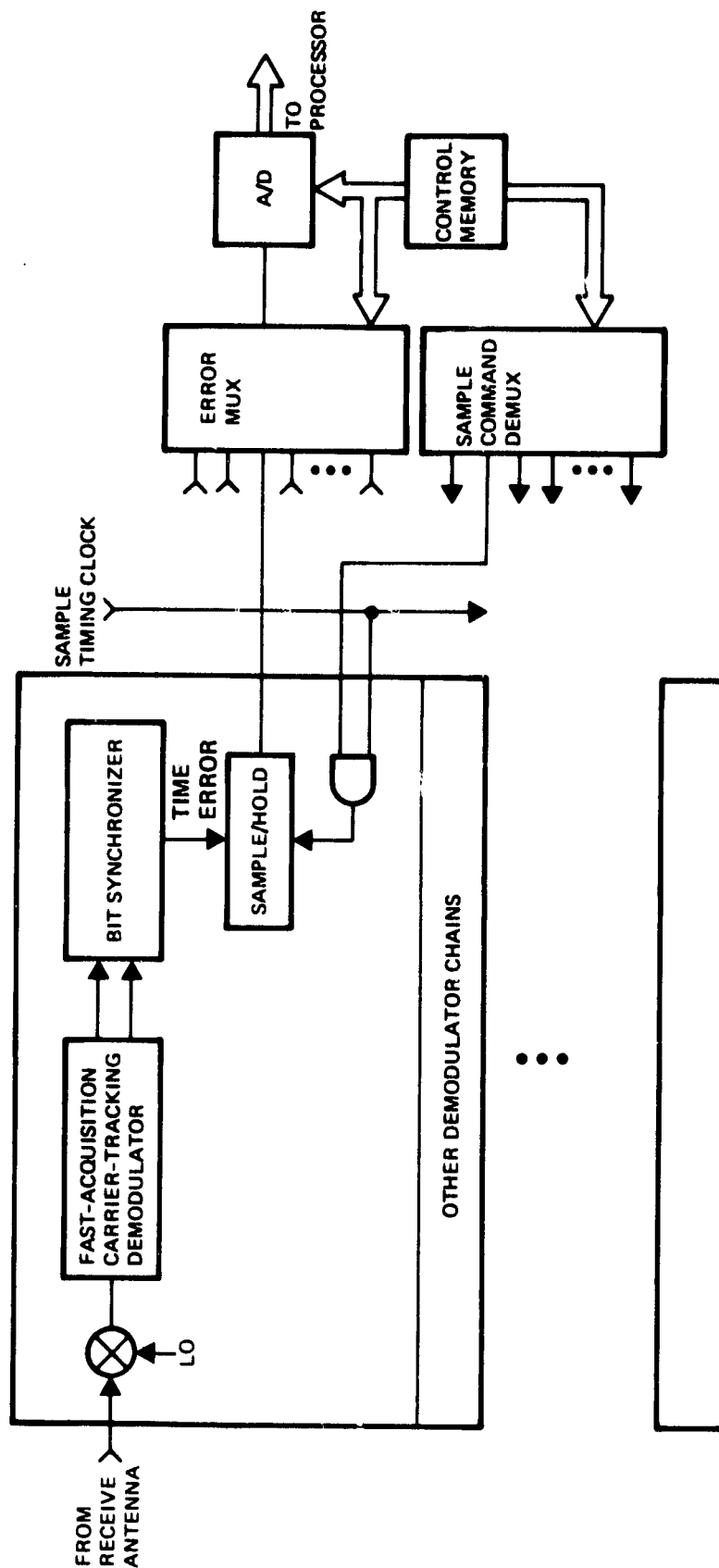


Figure 4-4. Satellite Hardware for Uplink Timing Error Feedback

#### 4.3.3.6 Downlink Tracking with Uplink Timing Monitor System

TDMA and SSTDMA systems in use or in the planning stages allow each terminal to monitor at least part of the uplink burst by routing the signal back to the originating area. When all stations are in the same satellite antenna pattern, as in the Canadian TDMA systems that utilize ANIK spacecraft, each station monitors uplink timing by observing his own burst placement in the downlink. Advanced WESTAR, which will be the first SSTDMA system, returns part of each station's signal to the originating area, allowing similar direct monitoring. Some point-to-point SSTDMA systems have been considered. Special switch modes are provided to connect stations to themselves, and again provide direct self-monitoring of the uplink burst timing.

Uplink timing cannot be monitored directly in a demodulation/remodulation system, since the timing error information is removed by the demodulation process. The "conventional" direct timing monitor technique is not available, unless we find some way to bypass the demodulation process for at least part of each terminal's burst signal. The hardware complication necessary to provide this in the satellite is shown in Figure 4-4. The extra hardware required both in the satellite and in the terminals make this approach unattractive.

#### 4.4 VOICE CHANNEL ROUTING PROCEDURE

The voice channel is the standard unit or basic quantization level of traffic for the processor system. Each voice channel is 64 kbps and interfaces with the individual terminal as part of a 24-channel DS1 signal. The DTU terminal strips out unassigned channels and transmits only active channel data from the DS1 signal. To establish a new voice channel routing through an operating terminal the following procedure (Figure 4-5) is followed.

When a previously inactive channel is activated on the terminal DS1 interface the terminal DS1 input buffer notes that the unassigned channel code (10011000 or 00011000) has changed. The terminal control hardware notifies the master control station (MCS) by order wire that it requires another voice channel TDMA uplink allocation.

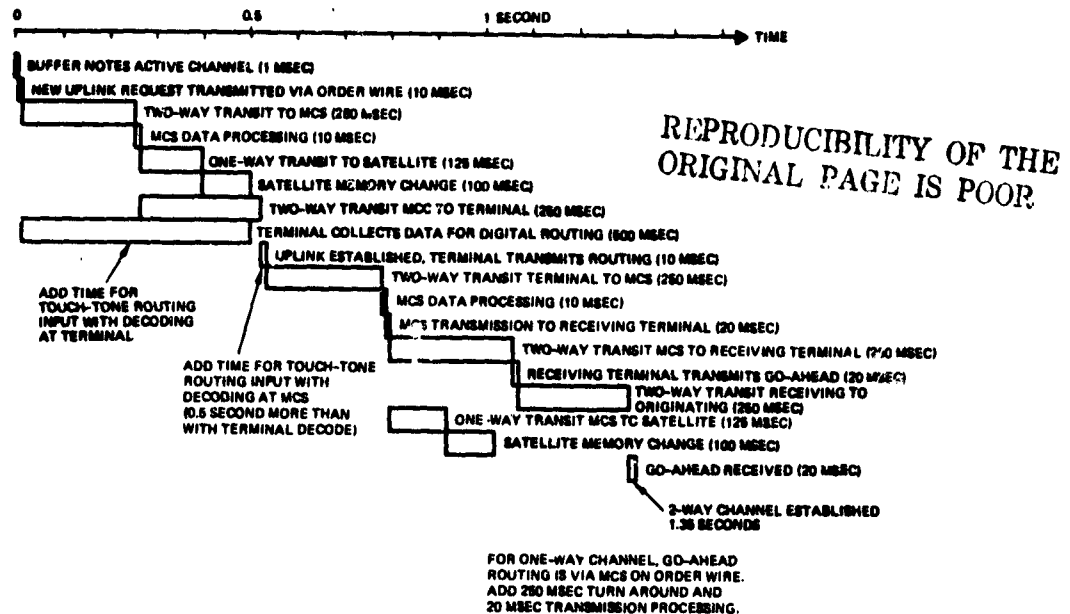


Figure 4-5. New Voice Channel Establishment Time Line

The MCS establishes the increased TDMA uplink allocation by exercising the TDMA assignment algorithm and, if necessary, the beam scan algorithm to make TDMA time available. The satellite processor routing is modified to route the new voice channel to the master control station. The originating terminal is then notified to begin transmitting the new voice channel.

The originating terminal transmits the incoming voice channel to the MCS in the newly assigned TDMA slot. This TDMA slot will be assigned adjacent to the existing TDMA slot, and will increase the TDMA burst duration.

The MCS receives the new voice channel and receives, via that channel, the desired routing. This may be in the form of touch-tone signals or a specialized digital header. The MCS uses the desired routing to change the satellite processor routing, and notifies the receiving terminal of its new downlink TDMA assignment via the order wire. If a duplex channel is being established, the return half-channel is simultaneously established.

The process described above must be accomplished rapidly. The speed required will set the command data rate required to modify the on-board processor and scanning-beam control memories.

Figure 4-5 is a time-line of the above process. With certain assumptions about MCS data processing time, satellite memory-change time, and terminal response time; circuit establishment can occur in about 1.35 seconds. This is dominated by two-way transit times (1.25 seconds), but most of the time lost to transit is being utilized by processes which occur in parallel. Satellite memory changes which require less than 125 ms have no impact. MCS data processing and order wire data transmitting are in-line and must be minimized.

REPRODUCIBILITY OF THE  
ORIGINAL PAGE IS POOR

## 5. ANTENNA REQUIREMENTS

General requirements for an antenna system for a 30/20 GHz satellite providing CONUS communications links are given in Table 5-1. The uplink and downlink frequency bands are those allocated for 30/20 GHz satellite use.

The 18 fixed-beam, high-density, traffic centers are shown in Table 5-2 and on the map in Figure 5-1. Each center will be supported by of 500 Mbps satellite capacity, except for New York which requires 1 Gbps capacity. A total of 8000 Mbps is needed for the conglomerate of 18 fixed-beam users. The scanned-beam users will require less than 2000 Mbps total capacity.

The design features having the heaviest impact on the 30/20 GHz satellite performance were found to be:

- a) Generating closely-spaced fixed beams, while simultaneously maintaining a high degree of sidelobe control
- b) Generating two or more scanned beams in a single phase array aperture
- c) Achieving high antenna gain at 30/20 GHz in complicated antenna assemblies
- d) Minimizing the number of large antenna assemblies needed on-board a single spacecraft.

The recommended baseline approach is a two-assembly approach. Each antenna assembly combines the generation of half the fixed and half the scanned beams on both transmit and and receive frequencies on a single assembly. The fixed beams are generated by feeds of a design previously developed for NASA by TRW at 12/14 GHz. The scanned beams are generated by space-fed arrays.

### 5.1 INTERFERENCE CONTROL

This traffic pattern and capacity requirements can be accommodated by the eighteen fixed beams and six scanned beams with the frequency plan shown in Figure 5-2. Only four scanned beams are required if the 2.0 GHz bandwidth can be used with very high efficiency, but more will be needed if operational requirements prevent that. Beam numbering is consistent throughout the traffic center list, coverage map, and frequency plan. Note that when



Table 5-1. 30/20 GHz Antenna System Requirements

Parameter	Requirements
Uplink frequency band	27.5 to 30.0 GHz
Downlink frequency band	17.7 to 20.2 GHz
Number of fixed beams dedicated to high density traffic centers	18
Number of scanned beams to serve low density traffic	6
Transmit beamwidth	0.35°
Receive beamwidth	0.25°
Transmit gain	52 to 54 dB
Receive gain	54 to 56 dB
Fixed beam sidelobe level	26 dB for beams 0.75° to 1.0° apart, 29 dB for beams 1.0° to 2.0° apart, 34.0 dB for beams more than 2.0° apart (for both transmit and receive)
Scanned beam sidelobe level	28 dB (required by both transmit and receive)
Isolation between fixed and scanned beams	By frequency
Antenna maximum diameter	12 feet
Time of implementation	Late 1980's

Table 5-2. High-Density Traffic Centers

1. New York	7. Pittsburgh	13. Denver
2. Washington, DC	8. St. Louis	14. Houston
3. Boston	9. Phoenix/Tucson	15. Minneapolis/St. Paul
4. Los Angeles	10. Seattle/Portland	16. San Francisco/Bay Area
5. Chicago	11. Atlanta	17. New Orleans
6. Detroit/Cleveland	12. Dallas/Ft. Worth	18. Miami

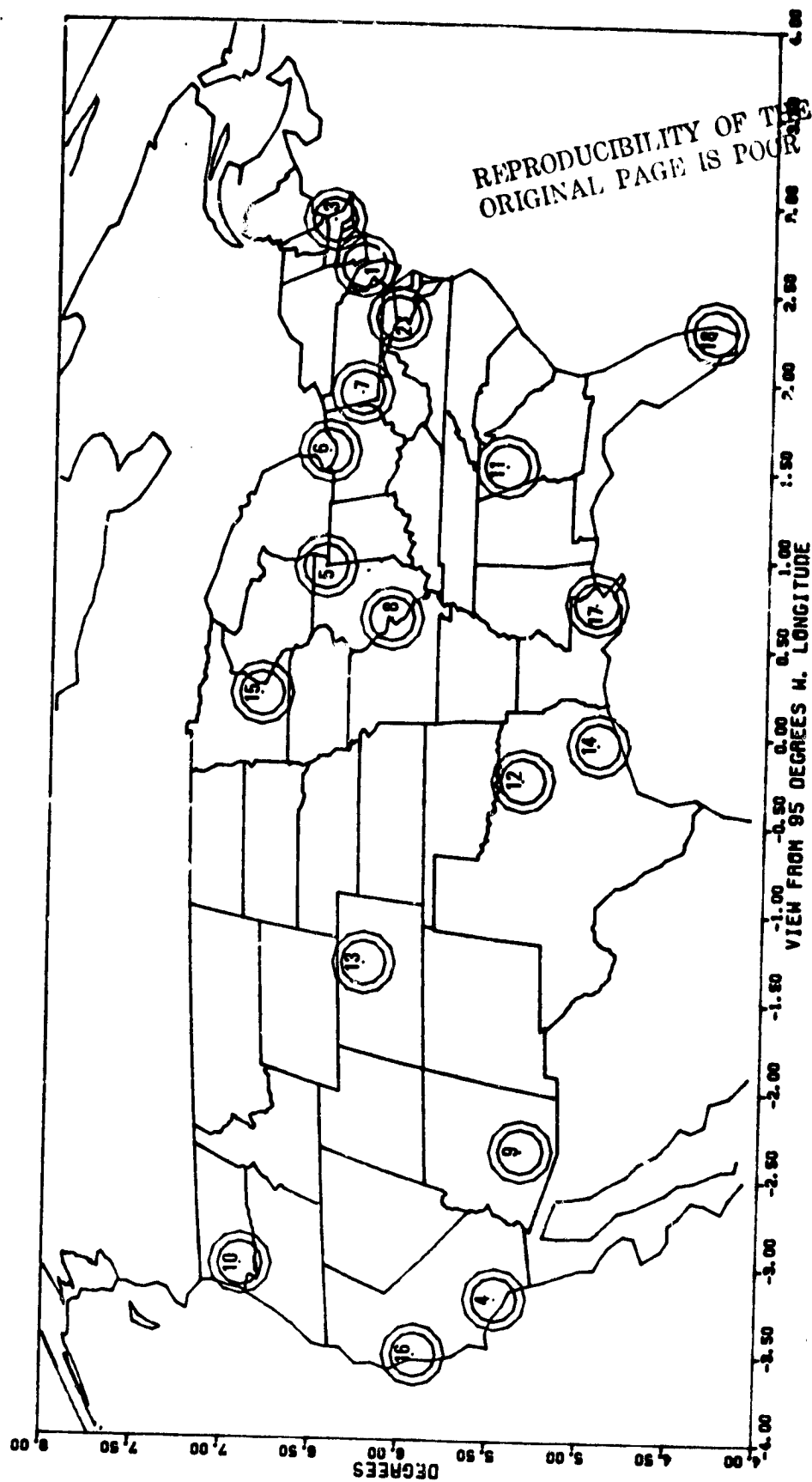


Figure 5-1. Fixed-Beam Coverage of CONUS (Small Circles for Uplink Beams, Large Circles for Downlink Beams)

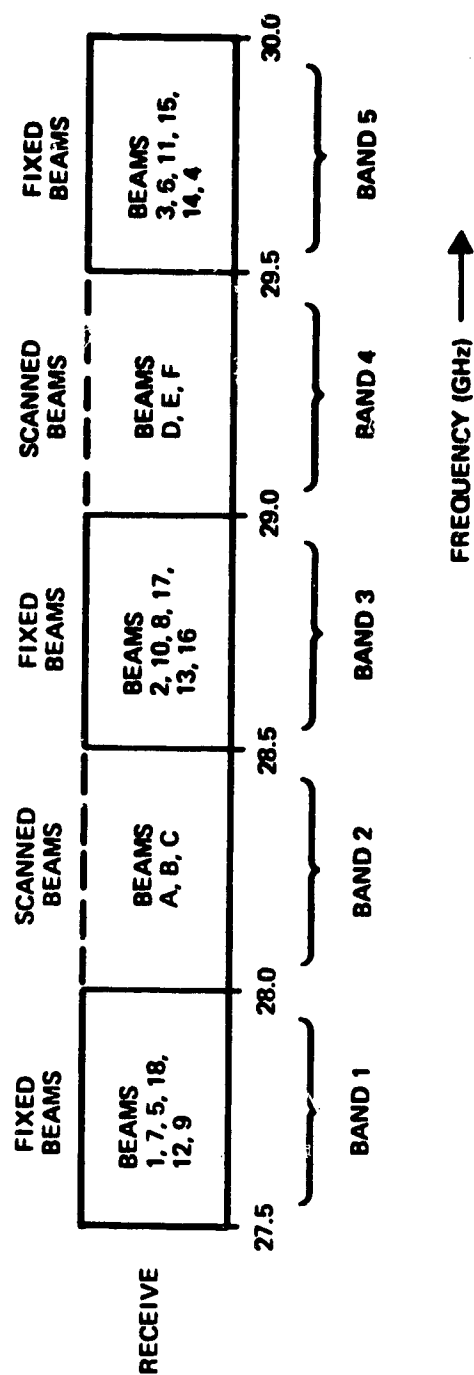
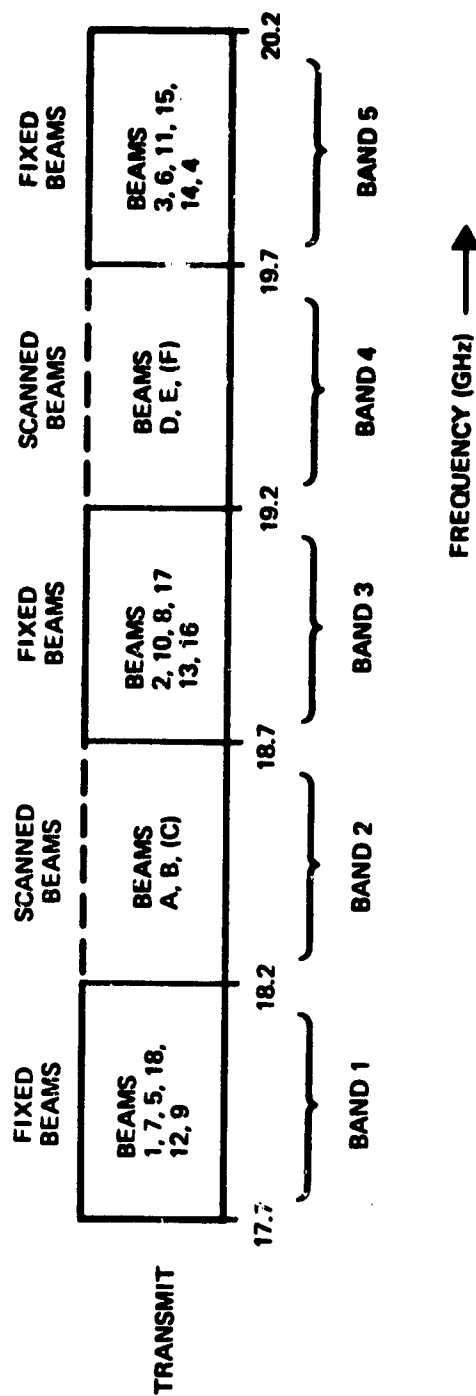


Figure 5-2. 30/20 GHz Fixed- and Scanned-Beam Frequency Plan

the frequency plan of Figure 5-2 is used for the beams on the map in Figure 5-1 neither sidelobe nor polarization isolation is needed between adjacent beams; these beams use separate frequencies.

The beamwidth, gain, and sidelobe requirements for the fixed beams were obtained from the power budgets of Tables 5-3 and 5-4, for the uplink and downlink, respectively.

Table 5-3 shows that in clear weather interference from other beams in the same frequency band, rather than noise, limits the uplink performance. Note that the isolation values used for interferors are 5 dB higher than the required sidelobe levels of Table 5-1. This is because a user in one beam may be on the 3-dB coverage edge of his beam and may slide down his beam edge another 2 dB with pointing error, while the sidelobe of the interferor may at the same time peak on him. The interferors are large users with 500-Mbps bandwidth.

In rainy weather, with transmitters turned up to combat rain attenuation, interference from other users in clear weather also limits the total uplink performance. Ground transmitters increase their power when they are in rain; large users also have diversity stations and small users employ rate to error correction coding and three times their normal length TDMA slots.

The Downlink is also seen to be interference limited in clear weather, as shown in Table 5-4. In fact, the downlink transmitter could be turned down 5 or 6 dB when all three ground stations are in clear weather. However, if one downlink beam is working at high power through a rainstorm, interference to the other beams is increased by the transmitter using high power. Interferors in the downlink budgets are large users in large user links and small users in small user links, so that the interference bandwidth is matched to the signal bandwidth. In the rain, the downlink performance is more limited by thermal noise than by interference.

Downlink pointing, coverage, and circuit losses are 2.0 dB lower than for the uplink. The beam was allowed to be larger ( $0.35^\circ$ ) on the downlink than on the uplink ( $0.25^\circ$ ) so that coverage and pointing losses are smaller. The gain requirements on the antennas are stringent, and there are difficult requirements to be met on the sidelobes of the transmit and

Table 5-3. Fixed Beam Power Budgets Uplink (No Rain)

Frequency	30 GHz
Ground Transmitter Power	
1) Small Direct User (50 watts)	17.0 dBW
2) Large Trunk User (100 watts)	20.0 dBW
Ground Antenna Gain	
1) Small direct user (3.0 meter, 50 percent efficiency)	56.6 dB
2) Large Trunk User (5.0 meter, 60 percent efficient)	61.8 dB
Path Loss	-213.7 dB
Satellite Antenna Gain (3.0 meter, 30 percent efficiency)	54.5 dB
Pointing, Coverage, and Circuit Losses	-9.0 dB
Received Signal Power	
1) Small, Direct User	-94.6 dBW
2) Large Trunk User	-86.4 dBW
Satellite Noise Temperature (580°K, 3 dB N. F.)	27.6 dBK
Boltzmann's K	-228.6 dBW/HzK
Data Rate	
1) Small Direct User (125 Mbps)	81.0 dB.Hz
2) Large Trunk User (500 Mbps)	-87.0 dB.Hz
Noise Power	
1) Small Direct User $E_b/N_o$	-120.0 dBW 25.4 dB
2) Large Trunk User $E_b/N_o$	-114.0 dBW 27.6 dB

Table 5-3. Fixed Beam Power Budgets Uplink (No Rain) (Continued)

Interference (Large Users)	
1) Small Direct User	-110.4 dBW
One interferor at 21.0 dB isolation	
One interferor at 24.0 dB isolation	
Three interferors at 29.0 dB isolation	
$E_b/N_o$	15.8 dB
2) Large Trunk User	-104.4 dBW
One interferor at 21.0 dB isolation	
One interferor at 24.0 dB isolation	
Three interferors at 29.0 dB isolation	
$E_b/I_o$	18.0 dB
Total $E_b/N_o$	
1) Small Direct User	15.4 dB
2) Large Trunk User	17.6 dB

(Rain in Link, Worst Case Gulf Area)

Increase in Power because of Rain	
1) Small Direct User	10.0 dB
2) Large Trunk User	13.0 dB
Coding (for small users only)	
Rain Loss	
1) Small Direct User	-17.0 dB
99.5 percent availability	
2) Large Trunk User	-17.0 dB
Two diversity stations, 99.5 percent availability each	
Total $E_b/N_o$	
1) Small Direct User	18.4 dB
2) Large Trunk User	13.6 dB

Table 5-4. Fixed Beam Power Budgets Downlink (No Rain)

Frequency	186 Hz
Satellite Transmit Power (30 watts, 30 percent efficiency)	14.8 dBW
Satellite Antenna Gain (3.0 meter, 40 percent efficiency)	52.6 dB
Path Loss	-209.3 dB
Ground Antenna Gain	
1) Small Direct User (3.0 meters, 70 percent efficiency)	53.5 dB
Pointing, Coverage, and Circuit Losses	-7.0 dB
Received Signal Power	
1) Small Direct User	-95.4 dB
2) Large Trunk User	-91.0 dBW
Ground Station Noise Temperature (580°K, NF = 3.0 dB)	27.6 dBK
Boltzmann's K	-228.6 dBW/HzK
Data Rate	
1) Small Direct User (125 Mbps)	81.0 dB.Hz
2) Large Trunk User (500 Mbps)	87.0 dB.Hz
Noise Power	
1) Small Direct User	-20.0 dBW
$E_b/N_o$	24.6 dB
2) Large Trunk User	-114.0 dBW
$E_b/N_o$	23.0 dB

Table 5-4. Fixed Beam Power Budgets Downlink (No Rain) (Continued)

Interference	
1) Small Direct User	113.4 dBW
One Interferor at 21.0 dB isolation	
One Interferor at 24.0 dB isolation	
Three Interferors at 29.0 dB isolation	
$E_b/N_0$	180.0 dB
2) Large Trunk User	-109.0 dBW
One Interferor at 21.0 dB isolation	
One Interferor at 24.0 dB isolation	
Three interferors at 29.0 dB isolation	
$E_b/I_0$	18.0 dB
Total $E_b/N_0$	
1) Small Direct User	17.1 dB
2) Large Trunk User	16.8 dB

(Rain in Link; Worst Case Gulf Area)

Rain Loss	
1) Small Direct Users	-7.0 dB
99.5 percent availability	
2) Large Trunk User	-7.0 dB
Two diversity stations, 99.5 percent availability each	
Increase in noise from rain	1.0 dB
Total $E_b/N_0$	
1) Small Direct User	14.2 dB
2) Large Trunk User	13.3 dB

receive beams. Sidelobe control combined with frequency plan management and time-slot interference-control techniques must all be used to prevent system self-interference.

The scanned-beam budgets are similar to the small user budgets for the fixed beams, except that the antennas are expected to be 1 or 2 dB more lossy and the interference is 1 or 2 dB less since it will only arise from two other interferors rather than five.



## 5.2 CANDIDATE ANTENNAS

The candidate antenna systems include separate fixed- and scanned-beam apertures and combined fixed- and scanned-beam apertures. Since each aperture is large (3.0 meters with approximately 3.0-meter focal length) a serious effort was made during the antenna study to minimize the total number of apertures required.

### 5.2.1 Fixed-Beam Assembly

An antenna assembly that generates the required 18 fixed beams for both transmit and receive is shown in Figure 5-3. A cluster of nine transmit and receive feeds is used to generate nine of the fixed beams on horizontal polarization, and a similar cluster is used to generate the other nine fixed beams on vertical polarization. The horizontal polarization grid allows the clusters of feeds to be separated physically. This is necessary because the required beams are so close together that the feeds cannot be fit into a single cluster, especially when the large feeds needed for a good sidelobe control are used.

The feed has been dimensioned for 24 GHz, halfway between the transmit and receive frequencies of 18 and 30 GHz. The sidelobe control will not be as good as it would be if separate feeds (and therefore separate apertures) were used for transmit and receive.

This feed design is based on a feed developed under a NASA LEWIS/TRW contract and has been built and tested at 12/14 GHz. A picture of the horn tested at 12/14 GHz is shown in Figure 5-4. Figure 5-5 shows a primary pattern of this feed. Figures 5-6 and 5-7 show the computed secondary pattern of this feed in a reflector where test data from the feed was used as input to the computer program. Figure 5-6 shows the pattern on the reflector axis and Figure 5-7 shows the pattern with the feed located so as to scan the 7.5 beamwidths. Note that the sidelobes levels are 40 dB or more down for the on-axis beam and 35 dB or more down for the scanned beam at a distance of two beamwidths or more from the beam peak. Sidelobe levels will be somewhat higher for the 30/20 GHz aperture, but the levels required in Table 5-1 are achievable.

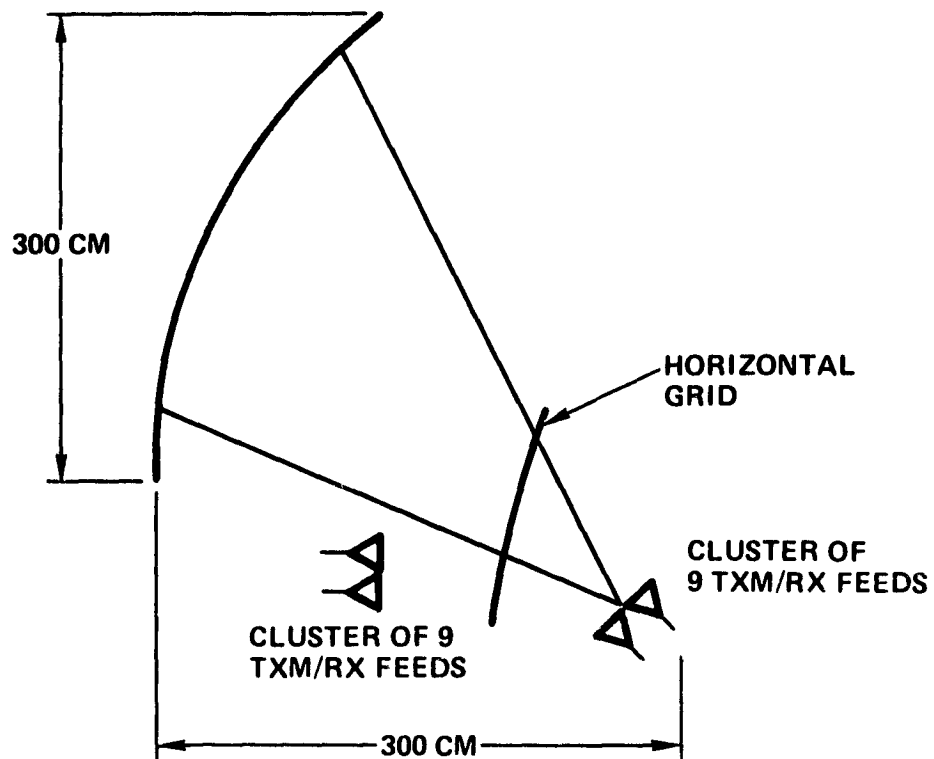


Figure 5-3. Fixed Beam Assembly

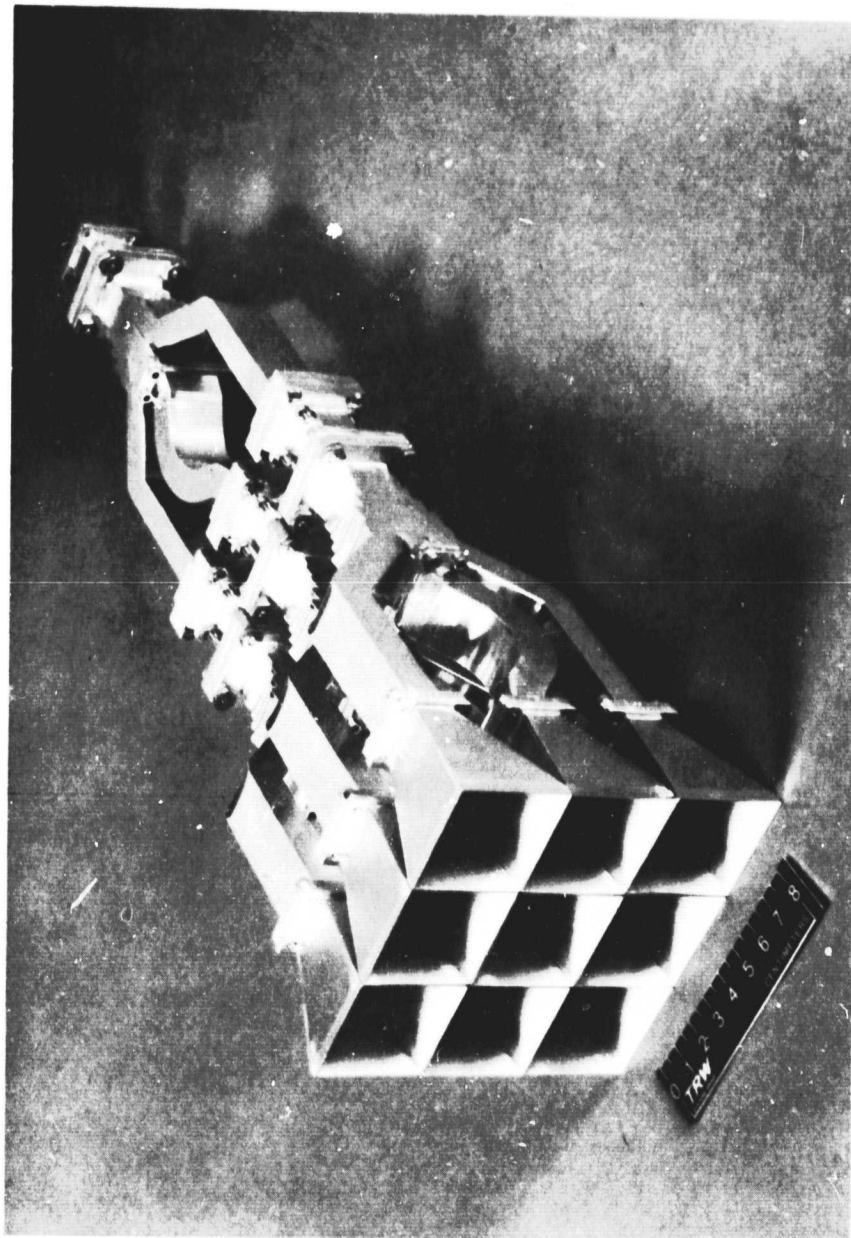


Figure 5-4. Breadboard Feed Cluster

REPRODUCIBILITY OF THE  
ORIGINAL PAGE IS POOR

5-12

R5-042-79

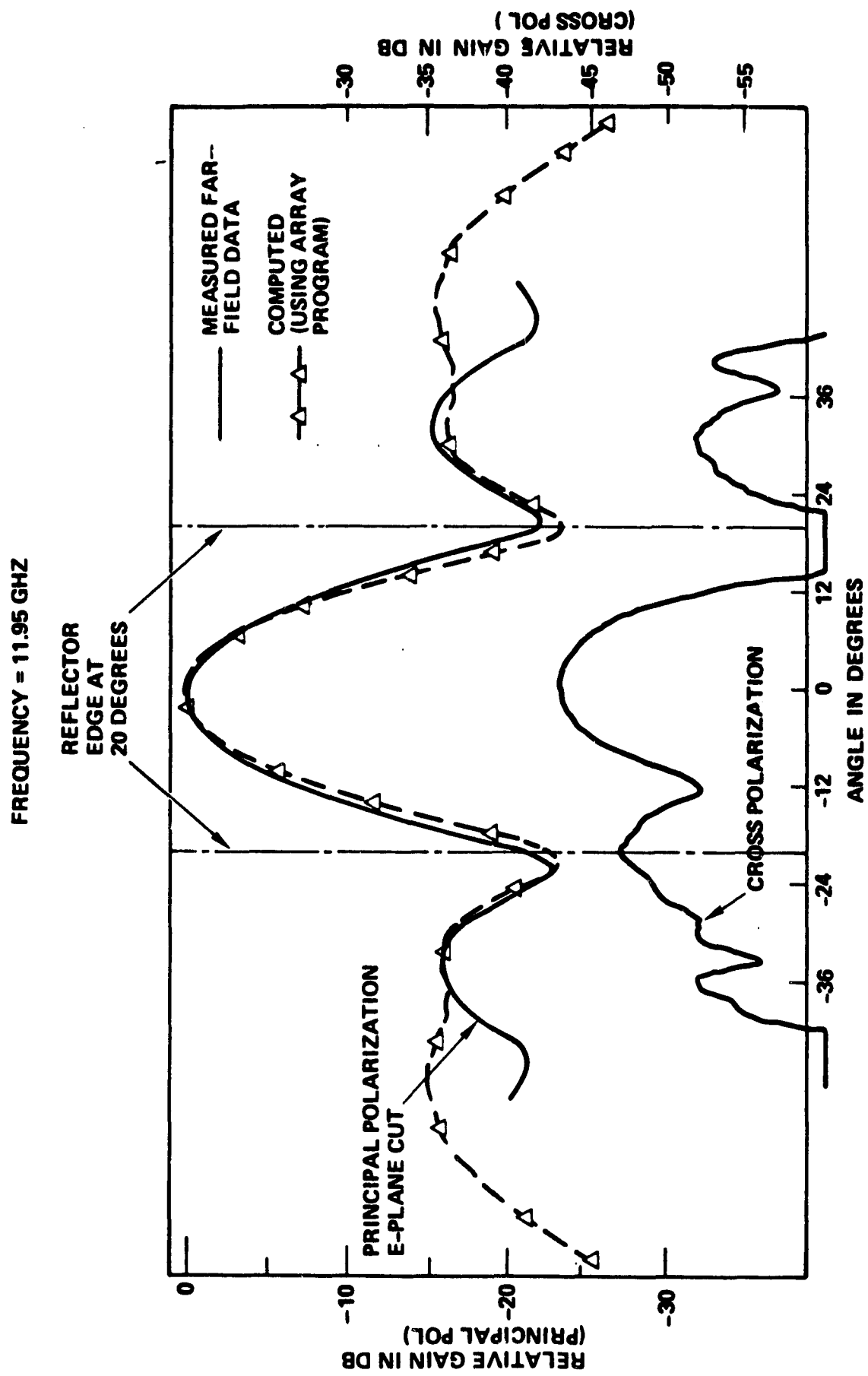
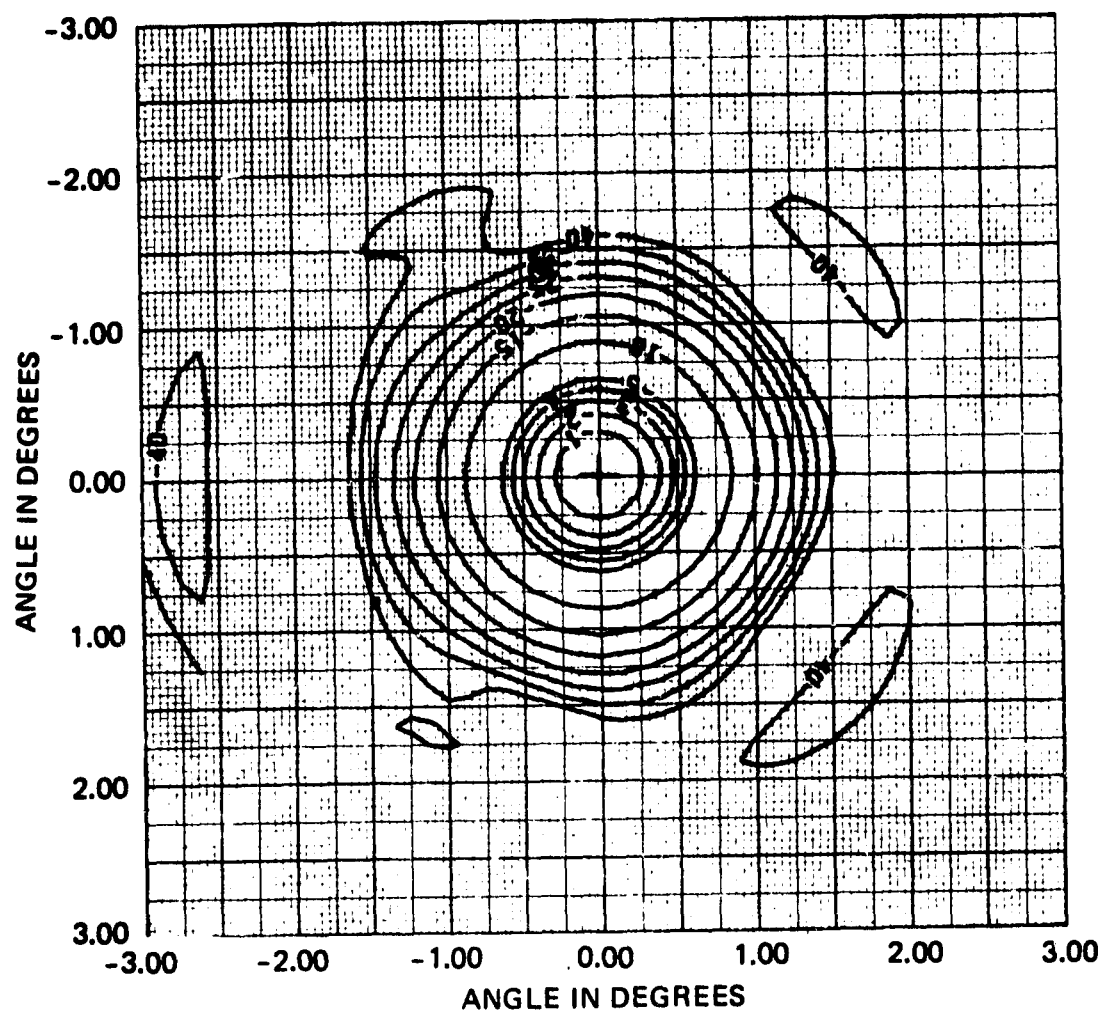


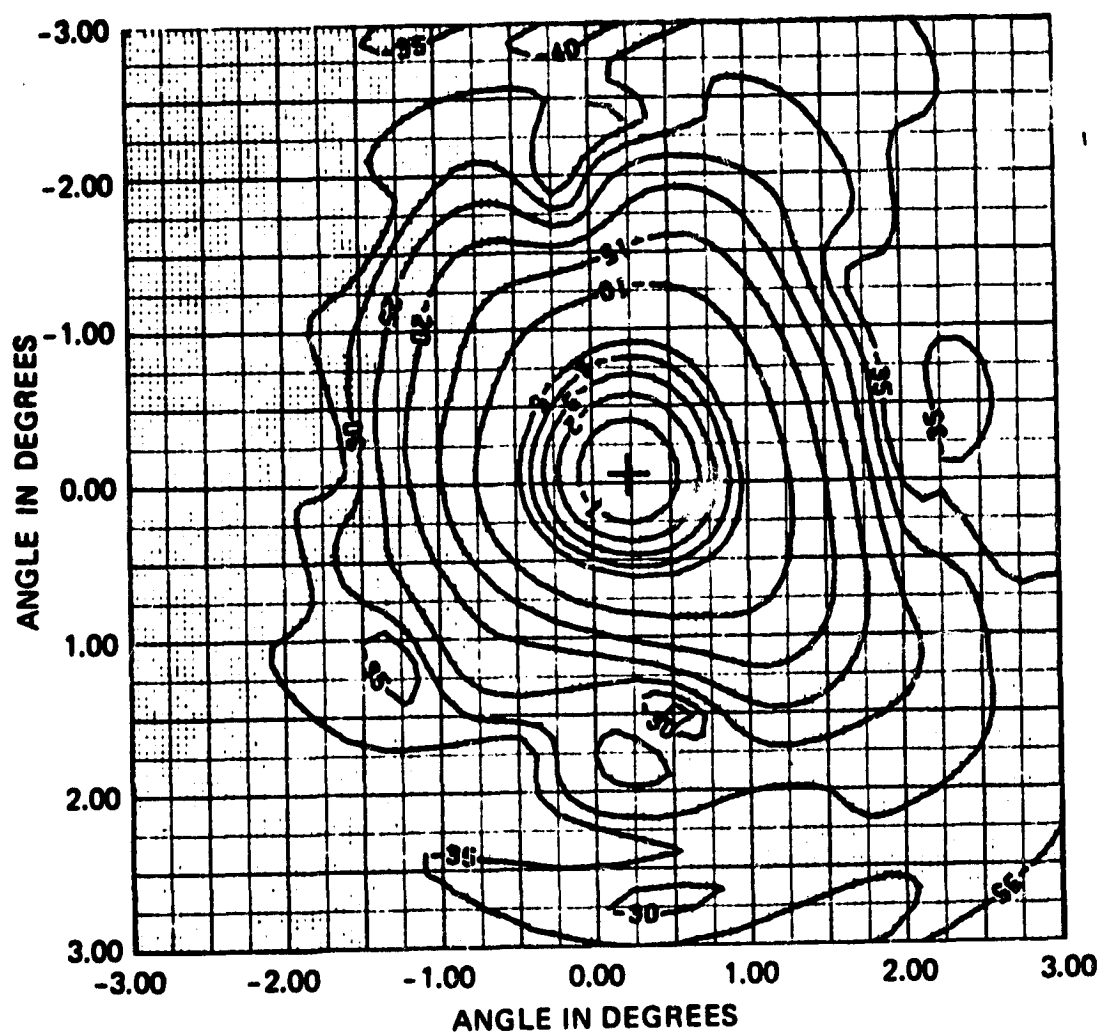
Figure 5-5. Measured and Computed Primary Patterns of Breadboard 9-Horn Cluster Feed



FREQUENCY = 11.95 GHZ  
 PHI = 0 DEGREES  
 TH = 0 DEGREES

REPRODUCIBILITY OF THE  
 ORIGINAL PAGE IS POOR

Figure 5-6. Computed On-Axis Secondary Contour Using Measured Near-Field Data of Breadboard 9-Horn Cluster



**FREQUENCY = 11.95 GHZ**

**PHI = 248.5 DEGREES**

**TH = 7.5 DEGREES**

REPRODUCIBILITY OF THE  
ORIGINAL PAGE IS POOR

Figure 5-7. Computed Hawaii Secondary Contour Using Measured Near-Field Data of Breadboard 9-Horn Cluster Feed

Beamwidths generated with this aperture are 0.25 degree on receive (30 GHz) and 0.35 degree on transmit (18 GHz). The beam spacing on one polarization is 1.05 degree on the reflector boresight and less for beams located off boresight. A few closely spaced beams may need to be generated with smaller feeds, and hence less sidelobe control.

Isolation between beams in the same 500-MHz frequency band (see Figure 5-2 for frequency plan) and on the same polarization is through sidelobe control. Isolation between beams in the same frequency band and on different polarizations is through combined sidelobe control and polarization isolation. Adjacent beams always use separate frequency bands. To show how this is arranged, a frequency and polarization plan for each feed is shown in Table 5-5. Polarization can be used to enhance isolation achieved by sidelobe control.

Table 5-5. Frequency and Polarization Plan for Fixed Feeds

Beam	Frequency Band	Polarization
1	1	H
5	1	H
7	1	H
9	1	V
12	1	V
18	1	V
2	3	V
8	3	V
10	3	H
13	3	H
16	3	V
17	3	H
3	5	V
4	5	H
6	5	V
11	5	H
14	5	H
15	5	V

Two or three of these nine-aperture feeds can be adapted for monopulse tracking to aid in satellite pointing control. RF attitude error sensing is needed to accurately correct satellite motion and attitude changes. Since these particular feeds have not been used for this purpose in the past, this feature requires development. Pointing compensation will be accomplished by either moving the large reflector or controlling the satellite. Since the satellite will carry at least two large antennas, it is probably more economical and better technically to control the satellite rather than the reflector.

#### 5.2.2 Fixed-Beam Assembly with Monopulse Feeds and Subreflectors

An antenna assembly that generates some (perhaps as many as nine) of the fixed beams for both transmit and receive is shown in Figure 5-8. The feeds are wideband dual mode horns that generate both sum and difference monopulse beams. The monopulse tracking feature aids in maintaining beam pointing in orbit. Because the feeds are so large, a subreflector is employed to increase the focal length. This allows the larger feeds to be spaced far apart, while retaining close beam spacing. Even with the increased focal length, the fixed beam spacing is approximately 1.26 degrees so that two or possibly three such antennas are required to generate the fixed beams. This may be acceptable for a satellite generating fixed beams only, but if scanned beams must also be generated the number of apertures required becomes three or four.

Isolation between beams on one such assembly is through frequency separation for some feed pairs and sidelobe control for other feed pairs. The two reflectors would use orthogonal linear polarizations. Beam isolation between reflectors is by means of either frequency or a combination of sidelobe control and polarization isolation. The beam polarization and frequency schedule is as shown in Table 5-5.

#### 5.2.3 Scanned-Beam Apertures

The required scanned beams can be generated by phased arrays. Because of the large aperture size (3.0 meters) needed for the 30/20 GHz beams, generation of the beams directly by a small-element phase array would result in a very heavy antenna. Therefore, a cassegrain antenna arrangement, such as shown in Figure 5-9, was studied. Four to six transmit and



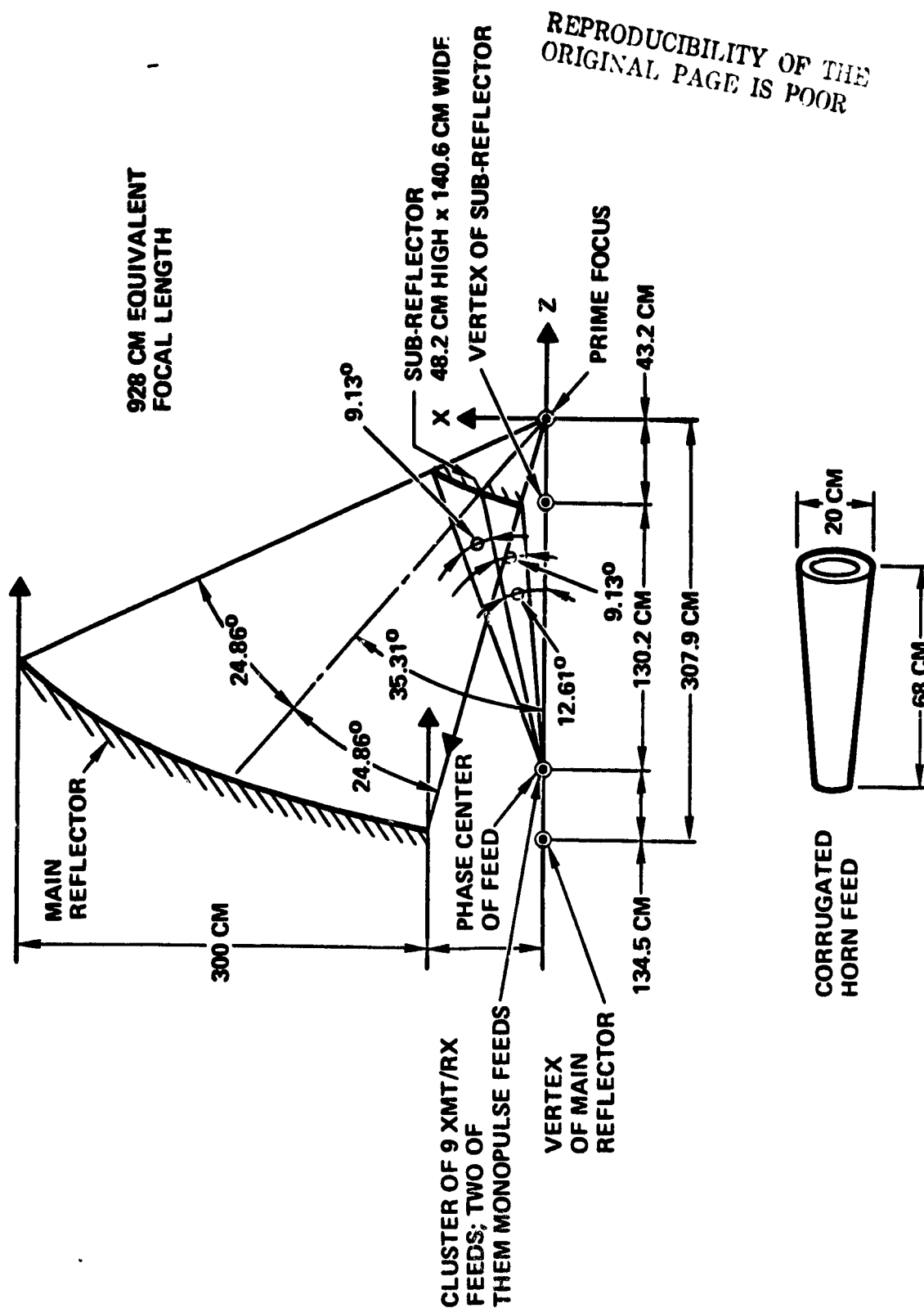


Figure 5-8. Fixed-Beam Assembly with Monopulse Feeds

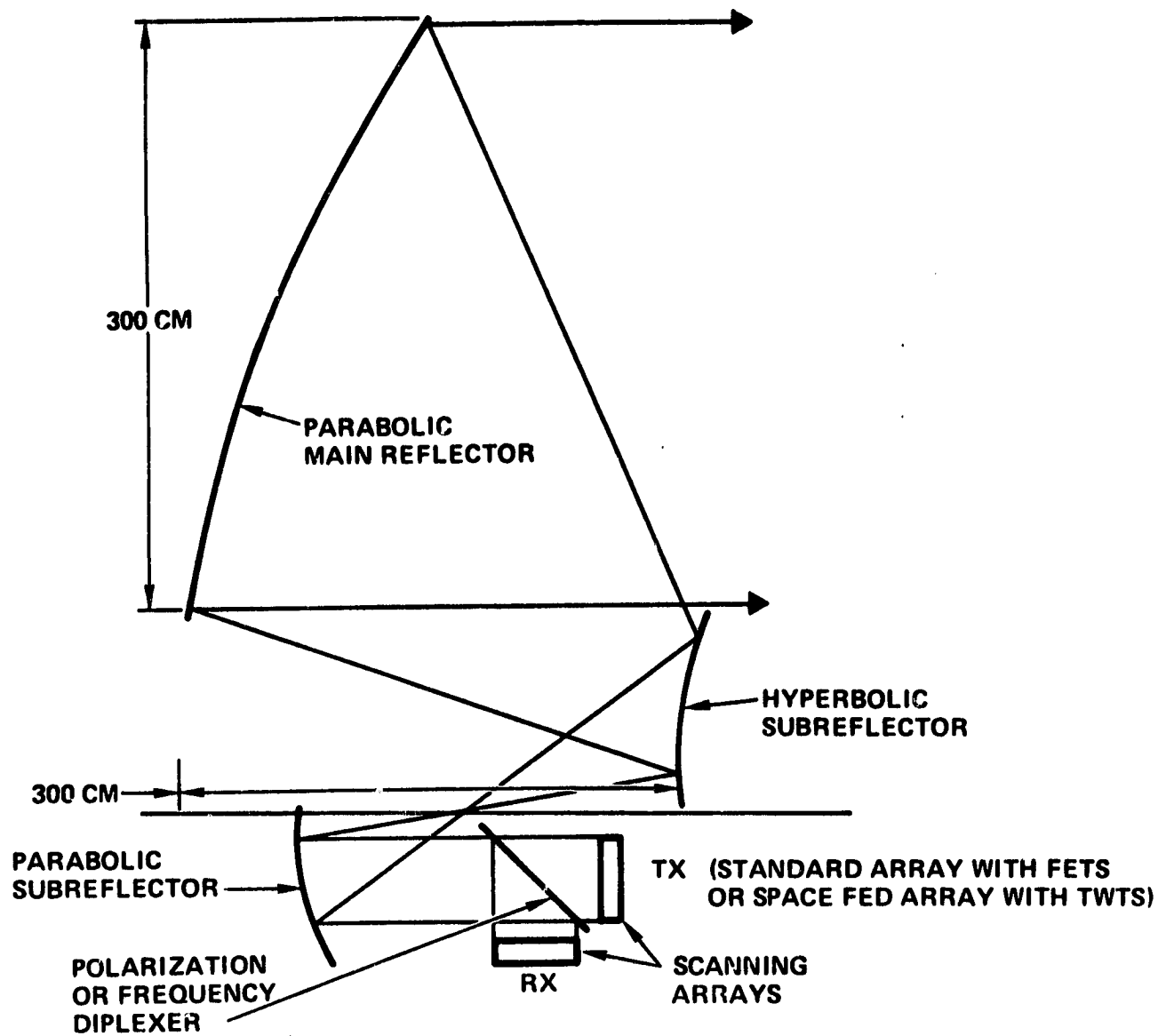


Figure 5-9. Multiple Reflector Scanned-Array System with Hyperbolic Subreflector

four to six receive scanned beams are required. Isolation between beams is by frequency (two or three beams in frequency band two and two or three in frequency band four, as shown in the frequency plan of Figure 5-2) and by spacing and sidelobe control for scanned beams on the same frequency.

Two types of phased arrays can be considered as candidates: arrays of feeds with a solid state transmitter for each feed or space fed arrays with a TWT transmitter for each beam. The solid state array approach would permit only two beams to be formed in one aperture: one in frequency band two and one in band four. Or, all the beams could be generated in one aperture if the array were really composed of two or three separate arrays with elements of any one of the arrays interspersed with elements of the other arrays, resulting in thinned arrays for all scanned beams. The total complement of four to six scanned beams would then require two or three such apertures for the simple arrays or one aperture if the interspersed array approach were used. Additionally, each FET would be required to handle two carriers at a time (one in frequency band two and one in band four).

The best candidate for generation of all the scanning beams in one aperture appears to be the space fed array shown in Figure 5-10. Here, generation of four scanned beams is shown, and the same approach can be used for six beams. A TWT is used to power each beam on transmit. Each TWT need accommodate a carrier in only one of the frequency bands: one, three or five. The four to six feeds are then positioned with respect to the array of dishes so that the beams are always separate. For example, the four feeds might be positioned so as to divide CONUS in east-west manner into four quarters; each beam assigned to scan one quarter. The first array of dishes is used to receive these feed horn outputs. Phase shifters are then used to position the wavefront at the output of the second array of dishes. The phase shifts are varied to accomplish the scanings, and the beams are simultaneously scanned in the same directions.

On receive, a space fed array can again be used with receivers appearing in the diagram of Figure 5-10 instead of TWTs.

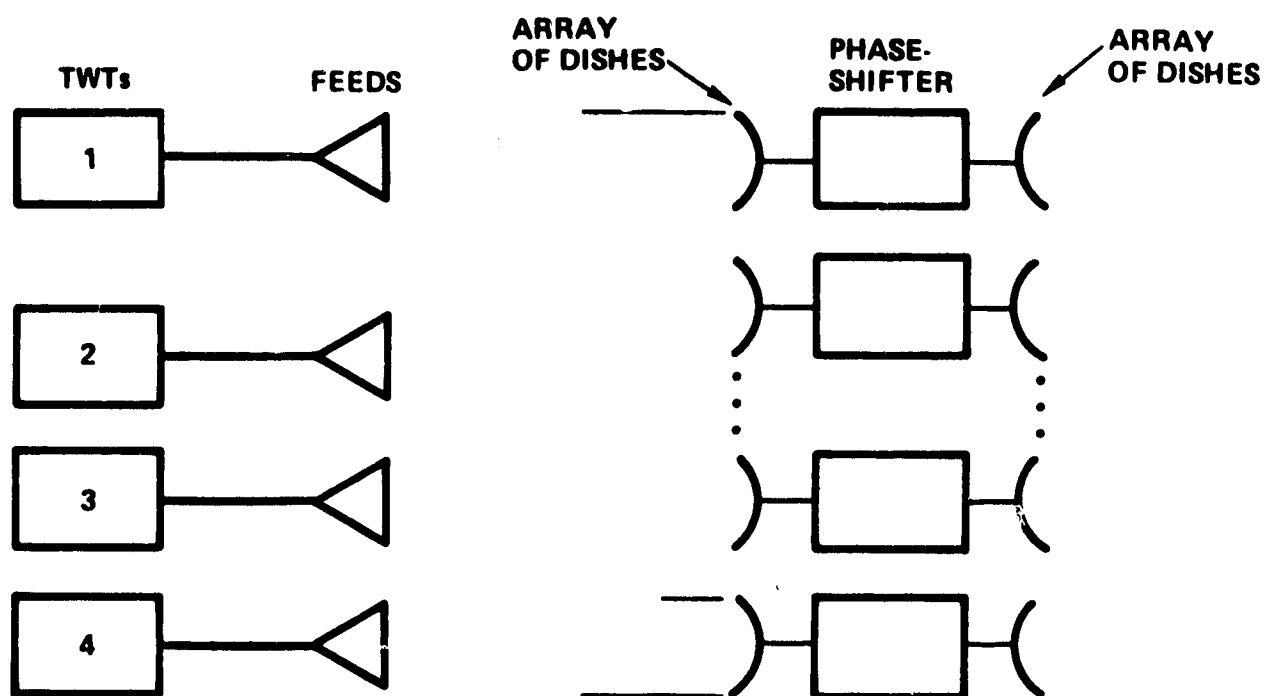


Figure 5-10. Space-Fed Array Scanning (Transmit)

#### 5.2.4 Combined Fixed- and Scanned-Beam Apertures

An antenna assembly that generates half the fixed and half the scanned beams in a single aperture is shown in Figure 5-11. A cluster of nine transmit and receive feeds is used to generate nine of the fixed beams on one polarization in one aperture, and a similar cluster is used to generate the other nine fixed beams on a second polarization in a second aperture. The polarization diplexer is a horizontal grid in one of the apertures and a vertical grid in the second required aperture. With the two clusters of feeds separated physically by placing them in different apertures, the closely spaced beams can be generated. This is necessary because the required beams are so close together that the feeds cannot fit into a single cluster, especially when the large feeds needed for good sidelobe control are used.

The fixed beam feeds are of the same design as that described in Section 5.2.1, "Fixed Beam Assembly." Figures 5-12 and 5-13 show some candidate layouts of feeds for the 18 fixed beams. One of the feed

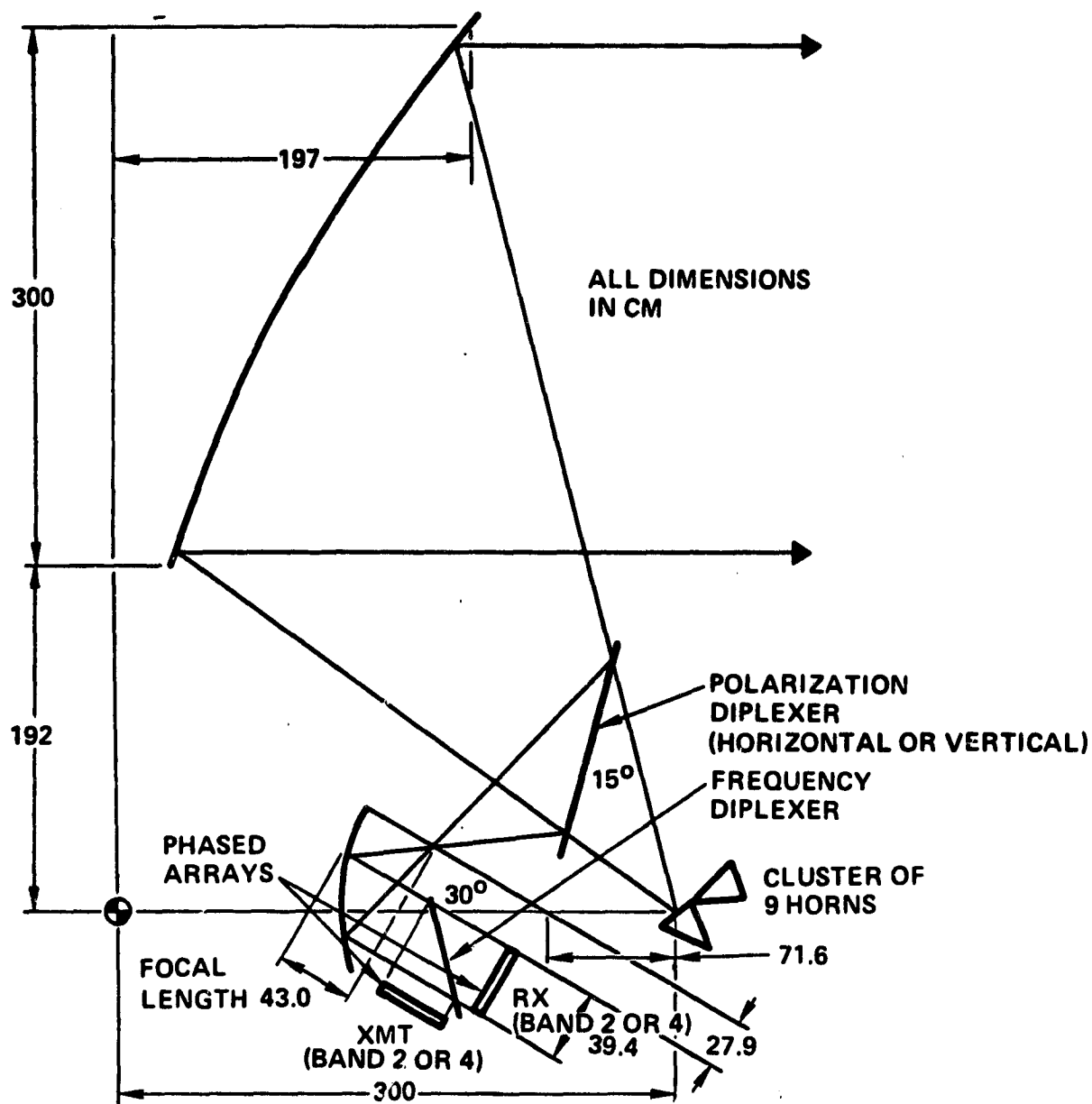


Figure 5-11. Combined Fixed- and Scanned-Beam Reflector Assembly

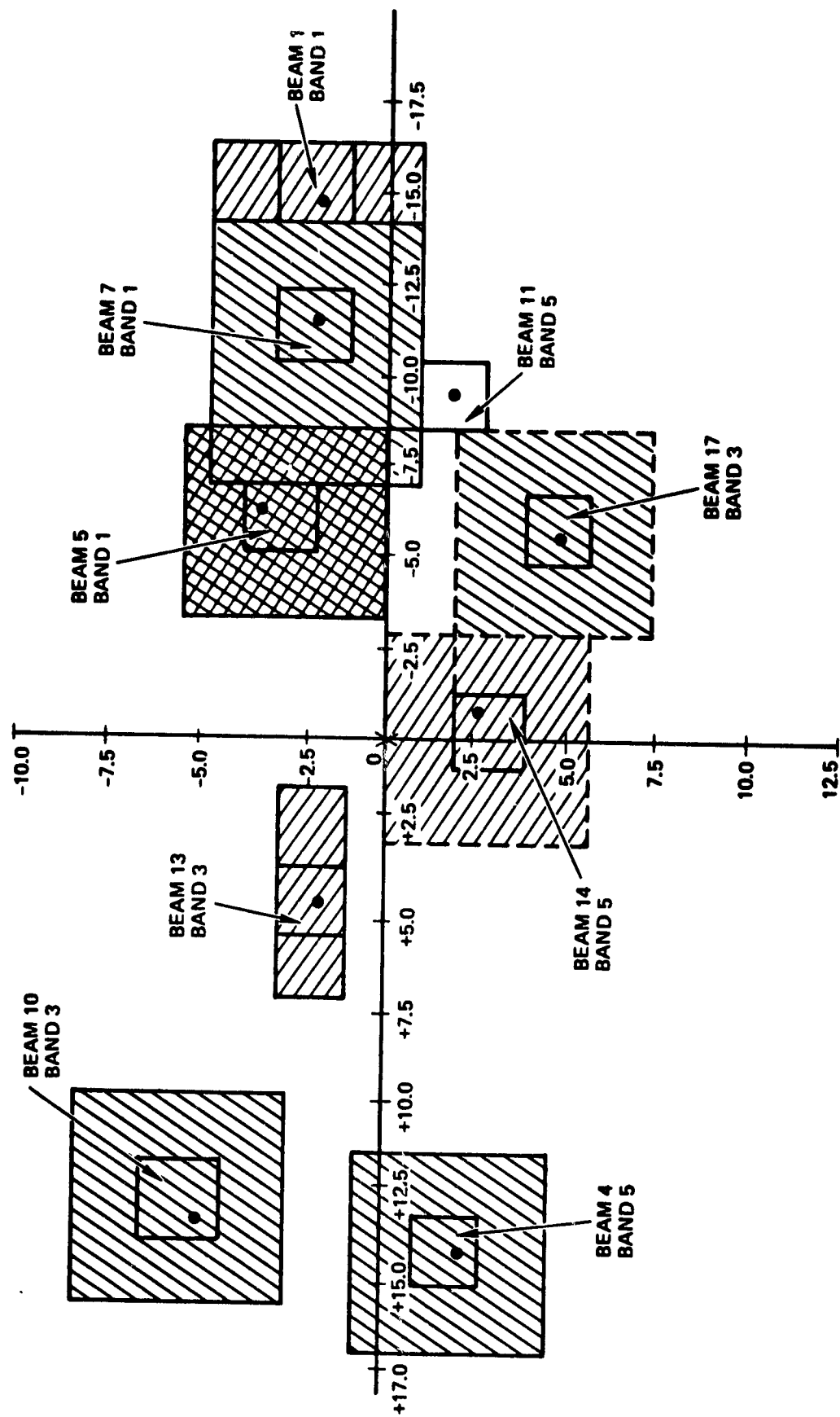


Figure 5-12. Fixed-Beam Assembly, Horizontal Polarization

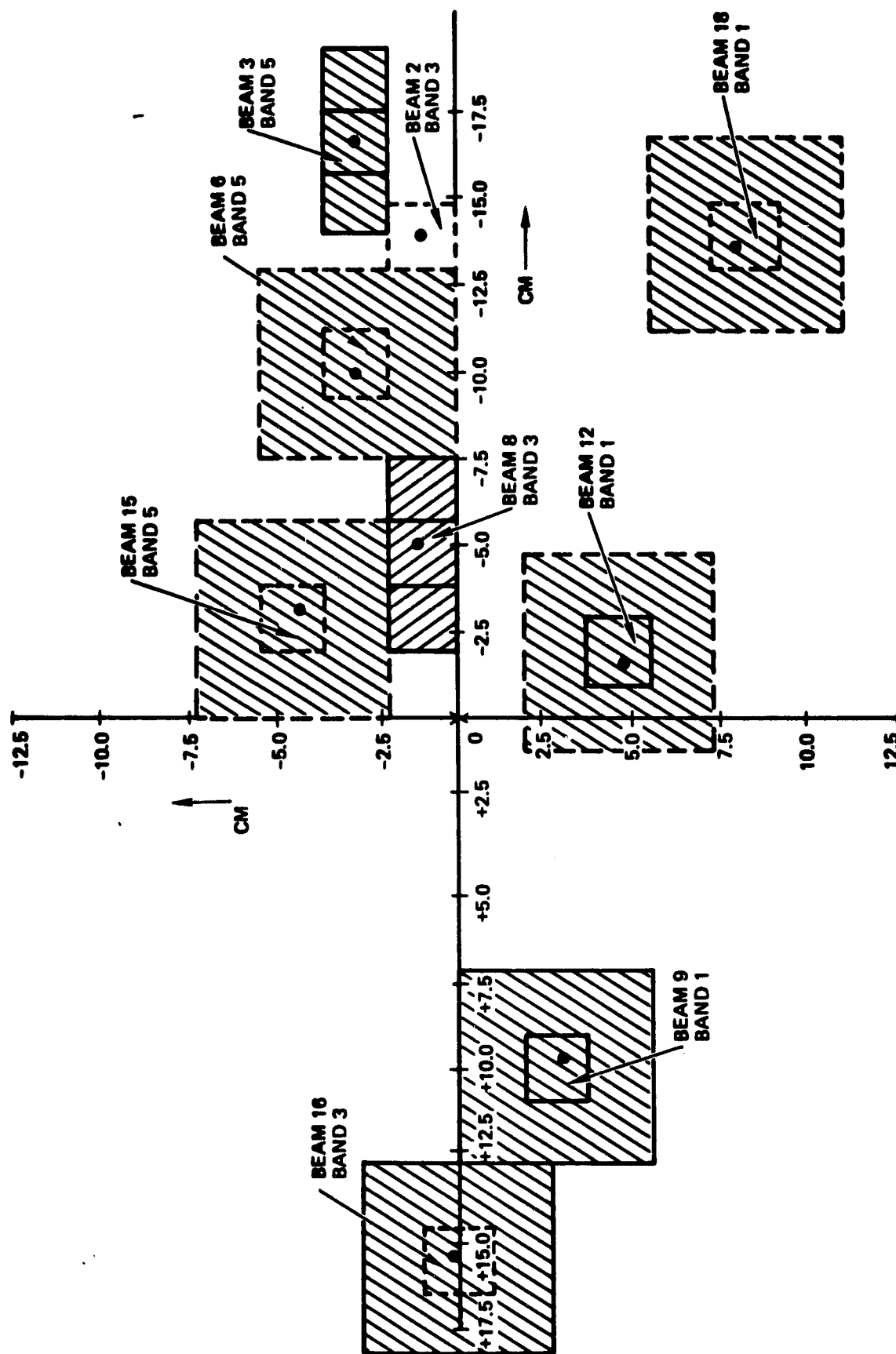


Figure 5-13. Fixed-Beam Assembly, Vertical Polarization

clusters consists of horizontally polarized feeds and one consists of vertically polarized feeds. The beam numbers and frequency bands of each element are also marked. Note that there is room for most, but not all, of the beams to have complete sidelobe control. All but beams 2 and 11 have at least partial sidelobe control. Beam 2 does not interfere with any beam in its band and on its polarization that is closer than 2 degrees away. Beam 11 does not interfere with any beam in its band and on its polarization that is closer than 1.75 degrees away. Some relief from the feed crowding will be obtained because the beam deviation factor is less than unity, but we do not know at this time if it will be sufficient to permit full sidelobe control on all beams.

The isolation between fixed beams is the same type and quality as that described above where complete sidelobe control can be used and of lesser effectiveness with partial control. The frequency and polarization plan for each of the beams is also the same as that shown in Table 5-5.

The scanned beams can be generated as shown in Figure 5-11 in a nearly identical configuration to that of the scanned array in Figure 5-9. This time, however, each scanned array need produce beams in one frequency band only: one aperture contains transmit and receive arrays for band two and one for band four. Therefore, if the arrays are to be solid-state arrays, each transmitter (or receiver) need handle only one carrier at a time.

Each transmit (or receive) phased array must, then, generate two or three beams on the same frequency. If the phase array is a space-fed array this is accomplished by using a separate TWT and feed for each of the two or three beams. If the phased array is made up of a number of solid state transmitters and feed horns, the elements providing each of the beams must be interspersed with the elements providing the other beams. This is illustrated in Figure 5-14. Each of the two or three arrays is then a thinned array with potential feed crowding and/or grating lobe problems.

Because of the reasons discussed, the space fed array seems the best choice at the moment. The interspersed phased array design can be carried as a backup in case the space-fed array potential cannot be realized.



1	2	3	1	2	3	1	2	3	1	2	3
2	3	1	2	3	1	2	3	1	2	3	1
3	1	2	3	1	2	3	1	2	3	1	2
1	2	3	1	2	3	1	2	3	1	2	3
2	3	1	2	3	1	2	3	1	2	3	1
3	1	2	3	1	2	3	1	2	3	1	2

#### ARRAYS 1, 2 AND 3 HAVE SEPARATE INPUTS

Figure 5-14. Three Separately-Fed Arrays with Interspersed Elements

Since all these designs use very large apertures and focal lengths, the comparison of prime importance to be made is which configuration can minimize the number of antenna assemblies. Two candidates using only two such assemblies are:

- a) One combining an all fixed beam assembly, such as described in Figure 5-3, with an all scanned beam assembly, such as described in Figure 5-9.
- b) Two assemblies, each of which combines both fixed and scanned beam generation in the same assembly, as described in Figure 5-11. All other candidate designs, used three or more antenna assemblies to generate the complement of fixed and scanned beams.

The combined problem of obtaining close beam spacing simultaneously with a high degree of sidelobe control is a problem for the fixed beam design. There is no clear advantage of either one of the two designs described above over the other in this respect: both use identical feed clusters and make identical use of polarization grids.

For the scanned arrays, the biggest design issue is how to create four to six scanned beams in one or two apertures. The second design described above, namely the one that combines fixed- and scanned-beam generation in a single assembly, has a clear advantage in this respect. It must generate only two or three beams per aperture, while an all scanning assembly would be required to generate four to six scanned beams in a single aperture.

Either of the two assemblies described above presents many opportunities for interference through scattering and reflections. The isolation between scanned beams in the same frequency band is the same for both assemblies, because both generate two or three beams in the same band in the same aperture. However, the fixed beam isolation of the combined fixed-card scanned-beams assembly is clearly superior. In this case only three fixed beams are generated in each frequency band in each aperture; while in all the fixed beam assembly, six such beams must be generated in a single aperture.

The stage of technology development is another important consideration. Either space fed or interspersed solid state phased arrays would be used in either of the assemblies described above. Neither technology is well developed, and both candidates require about the same development effort. Similarly, the cassegrain used with the phased array requires development and is used in both designs. No clear superiority of either candidate is evident.

The clear choice for the fixed feed assembly is the feed design previously developed at 12/14 GHz. It is small enough to generate closely spaced beams while providing good sidelobe control.

### 5.3 POINTING CONSIDERATIONS

Stationkeeping and attitude error typical of the TDRSS bus are taken to be representative of current satellite attitude control capability. The bounding envelopes for the pitch/roll errors and the yaw errors are shown in Figure 5-15. Table 5-6 provides roll, pitch and yaw error magnitudes corresponding to the different operating modes. In addition to these attitude errors, stationkeeping errors result in departure from nominal station by  $\pm 0.1$  degree in latitude and  $\pm 0.1$  degree in longitude. Attitude errors are corrected once per month using four burn periods for a total of

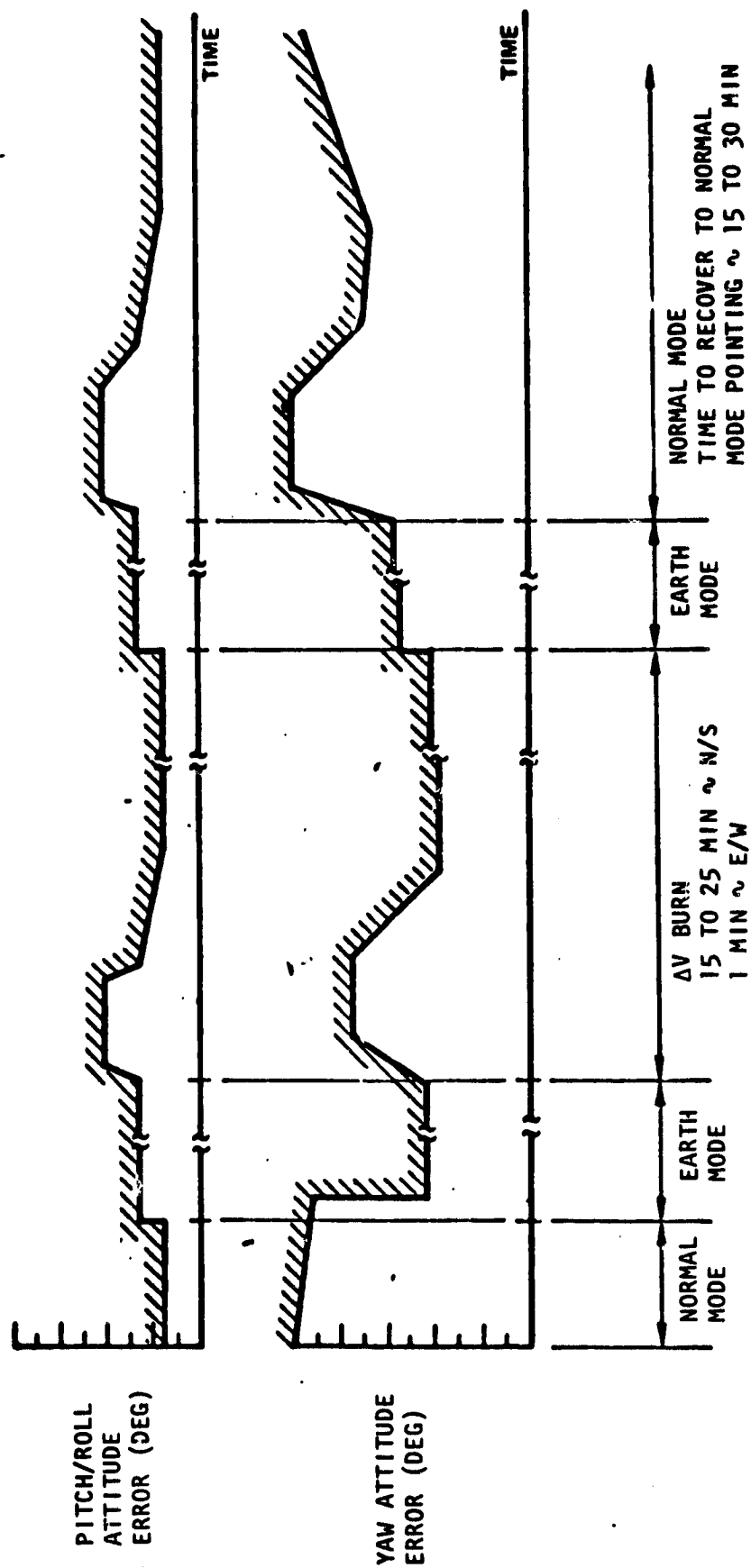


Figure 5-15. Bounding Envelopes for Attitude Control Response for ΔV Operation

Table 5-6. Attitude Performance Capabilities During Stationkeeping Sequence

CONDITION	ATTITUDE (DEG)	
	ROLL/PITCH (CEP = 0.99)	YAW ( $3\sigma$ )
NORMAL MODE	0.10/0.15	1.00/1.00
EARTH MODE (PRE- $\Delta V$ )	0.25/0.30	0.50/0.75
$\Delta V$ - PEAK TRANSIENT ERROR - ERROR AFTER TWO MINUTES	0.36/0.40 0.20/0.20	0.70/1.25 0.60/0.75
EARTH MODE (POST- $\Delta V$ )	0.30/0.35	0.60/0.80
- PEAK TRANSIENT ERROR - TIME TO REACH STEADY-STATE	0.61/— ROLL - 800 SEC/1800 PITCH - 400 SEC/1800	1.27/— 800 SEC/1800

.10/.15 ——— CAPABILITY/REQUIREMENT

about 25 minutes. One-pound thrusters are fired first to the north and 12 hours later to the south. Each thruster is fired for one-half the total estimated correction required. Twelve hours later east or west corrections are made. Stationkeeping errors affect the pointing accuracy of the ground terminals. If 3-meter antennas are used at the ground terminals, a 0.1 degree stationkeeping error causes a loss of 0.54 dB.

Attitude errors as well as stationkeeping errors affect pointing accuracy of the spacecraft antennas. Figure 5-17 summarizes pointing losses that can be experienced at the trunk terminals for the assumed combinations of attitude and stationkeeping errors. In calculating these errors, the satellite assumed to be at its nominal location and body coordinates equal orbit coordinates. The direction to the target is calculated based on these assumptions. The direction actually pointing because of the roll, pitch and yaw errors is calculated. Then the direction to the target from the actual orbit position including position errors is calculated. The direction actually pointing is compared to this latter direction to get the pointing error.

Different combinations of the errors produce different pointing errors, but the selected error values typically produced the greatest pointing errors.

Pointing loss in dB is shown in Table 5-7 for users at the nominal beam center and for users at the nominal - 3 dB contour. As would be expected, the users located on the beam contours experience the greatest degradation.

These calculations indicate the desirability of providing error compensation. The most promising candidate approach is to replace two or of the spot beam feeds by autotrack feeds and use the autotrack information to upgrade the attitude control of the spacecraft. A single autotrack feed can provide roll and pitch correction. Two autotrack feeds pointing at separated trunk terminals in the CONUS can provide all of the required pointing corrections, including yaw. Four autotrack feeds should probably be provided to increase system reliability.

Table 5-7. Pointing Losses Caused by Spacecraft Attitude and Stationkeeping Errors

TERMINAL NAME	LOCATION	DISTANCE FROM S/C NM	SPACE LOSS--AT 30GHZ,db	POINTING ERROR DEG.	P O I N T I N G	
					USER AT NOMINAL BEAM CENTER	L O S S, db USER AT NOMINAL 3db CONTOUR
NEW YORK	40.67N73.83W	20504	-213.7	.228	-1.00	-7.48
WASHINGTON/PHILADELPHIA	38.92N77.00W	20379	-213.6	.225	-0.98	-7.41
BOSTON/HARTFORD	42.33N71.08W	20626	-213.7	.229	-1.01	-7.51
LOS ANGELES	34.00N118.25W	20295	-213.6	.259	-1.29	-8.25
CHICAGO	41.83N87.75W	20382	-213.6	.240	-1.11	-7.74
DETROIT/CLEVELAND	41.93N82.38W	20432	-213.7	.236	-1.07	-7.68
BUFFALO/PITTSBURGH	40.43N80.00W	20397	-213.6	.232	-1.04	-7.58
ST. LOUIS/MEMPHIS	38.67N9025W	20231	-213.6	.237	-1.08	-7.70
PHOENIX/TUCSON	32.87N111.50W	20125	-213.5	.250	-1.21	-8.02
SEATTLE/PORTLAND	46.55N122.50W	20873	-213.8	.275	-1.46	-8.66
ATLANTA	33.75N84.38W	20079	-213.5	.222	-0.95	-7.34
DALLAS/FT. WORTH	32.77N97.07W	19988	-213.5	.233	-1.05	-7.60
DENVER/COL. SPRINGS	39.30N104.75W	20291	-213.6	.252	-1.22	-8.07
HOUSTON	29.75N95.42W	19879	-213.4	.225	-0.98	-7.41
MINNEAPOLIS/ST. PAUL	45.00N93.20W	20506	-213.7	.249	01.20	-8.00
SAN FRANCISCO BAY	37.75N122.45W	20526	-213.7	.268	-1.38	-8.48
NEW ORLEANS	30.00N90.05W	19900	-213.4	.220	-0.93	-7.29
MIAMI	25.75N80.25W	19867	-213.4	.200	-0.77	-6.83

ASSUMPTIONS: STATION KEEPING ERROR -.1° LONG

ATTITUDE ERRORS

YAW 1.0°, 35  
PITCH 0.10° } .99 CEP  
ROLL 0.10° }  
S/C LOCATION 00°N95°W19351 N.M.ALT.

### 5.3.1 Scanning Beam with Phased Arrays

Figure 5-16 is a sketch of a multiple reflector antenna having spot beam coverage provided by phased arrays. The energy from the main reflector is split by a polarization diplexer. The energy of one polarization proceeds to the cluster of horns which provide spot beam coverage. The energy of the other polarization is reflected from the surface of the polarization diplexer and directed to the focal plane of the parabolic secondary reflector shown in the figure. This energy then proceeds as a plane wave to the frequency diplexing reflector where it is reflected to the receiving phased array. The transmitting phased array transmits directly through the frequency diplexing reflector to the parabolic secondary reflector.

A principal advantage of the use of multiple reflectors in the phased array antenna system is reduction by the factor  $(f_o/f_e)^2$  in the size of the individual radiating elements required in the array.  $f_o$  and  $f_e$  are the focal lengths of the secondary and main reflectors, respectively. In the design discussed here, this ratio is equal to 1/7 and this allows a 49 times reduction in the size of the array elements.

The field of view required of the main reflector approximately 3 degrees in elevation by 6 degrees in azimuth for CONUS coverage by a spacecraft stationed at 0°N 95°W. This field of view is magnified by  $f_e/f_o = 7$  by the two reflectors to become 21 degrees x 42 degrees insofar as the phased arrays are concerned, and this angular coverage determines the beamwidth and aperture size required of the array elements. Table 5-8, which lists features of the scanning beam system, shows that 132 elements are required in the transmit array and 380 elements are required in the receive array, assuming the arrays are filled. Filled arrays having tapered amplitude distribution are desirable for good sidelobe control. It may be feasible to thin the arrays to a useful extent and also maintain adequate sidelobe control without introducing grating lobes by pseudo randomly removing some of the array elements. This capability should probably be reserved to allow operation with randomly failed elements as a graceful degradation or redundancy technique, however.

Table 5-8. Phased Arrays for Scanning Beams

Item		Frequency, GHz	
<u>Main Reflector Parameters</u>			
Wavelength, $\lambda$	$\lambda$	0.01667 m	0.01 m
Main reflector diameter	D	3 m	3 m
Dia in monelengths	$D/\lambda$	180	300
Half power beamwidth	$71\lambda/D$	0.39°	0.24°
Gain, maxtheoretical	$(\pi b/\lambda)^2$	55 dB	59.5 dB
Gain, 50 percent efficiency		52 dB	56.5 dB
<u>Telescope Parameters</u>			
Magnification Power = $n = f_o/f_e$		7 x	7 x
Entronic pupil dia, D		3 m	3 m
Exit pupil dia, $d = D/M$		0.429 m	0.429 m
Exit pupil dia/ $\lambda = d/\lambda$		25.73	42.9
Exit pupil area - $\pi d^2/4$		$520 \lambda^2$	$1445 \lambda^2$
Brightness ratio $(\Delta/d)^2 = 7^2 =$		49	49
Entronic pupil FOV		3° x 6°	3° x 6°
Exit pupil apponent FOV $M \times FOV =$		21° x 42°	21° x 42°
<u>Array Parameters</u>			
Dia (less than exit pupil)		0.400 m	0.400 m
Area (less than exit pupil)		$452 \lambda^2$	$1256 \lambda^2$
Beamwidth $71\lambda M/D$		2.73°	1.68°
Gain, max theoritical		38.2 dB	42.6 dB
FOV coverage		21° x 42°	21° x 42°
Number of elements		132 (11 x 12)	380 (19 x 20)
Array dimensions L x W		50.6 cm x 27.6 cm	53.2 cm x 28 cm
<u>Feed Horn Parameters</u>			
Horn L x W		4.6 cm x 2.3 cm	2.8 cm x 1.4 cm
Effective area/horn		$4.52 \lambda^2$	$12.56 \lambda^2$
Gain/horn = $4\pi LW/\lambda^2$		16.8 dB	16.8 dB
Horn coverage angles $\frac{\lambda}{L} \times \frac{\lambda}{W}$		21° x 42°	21° x 42°



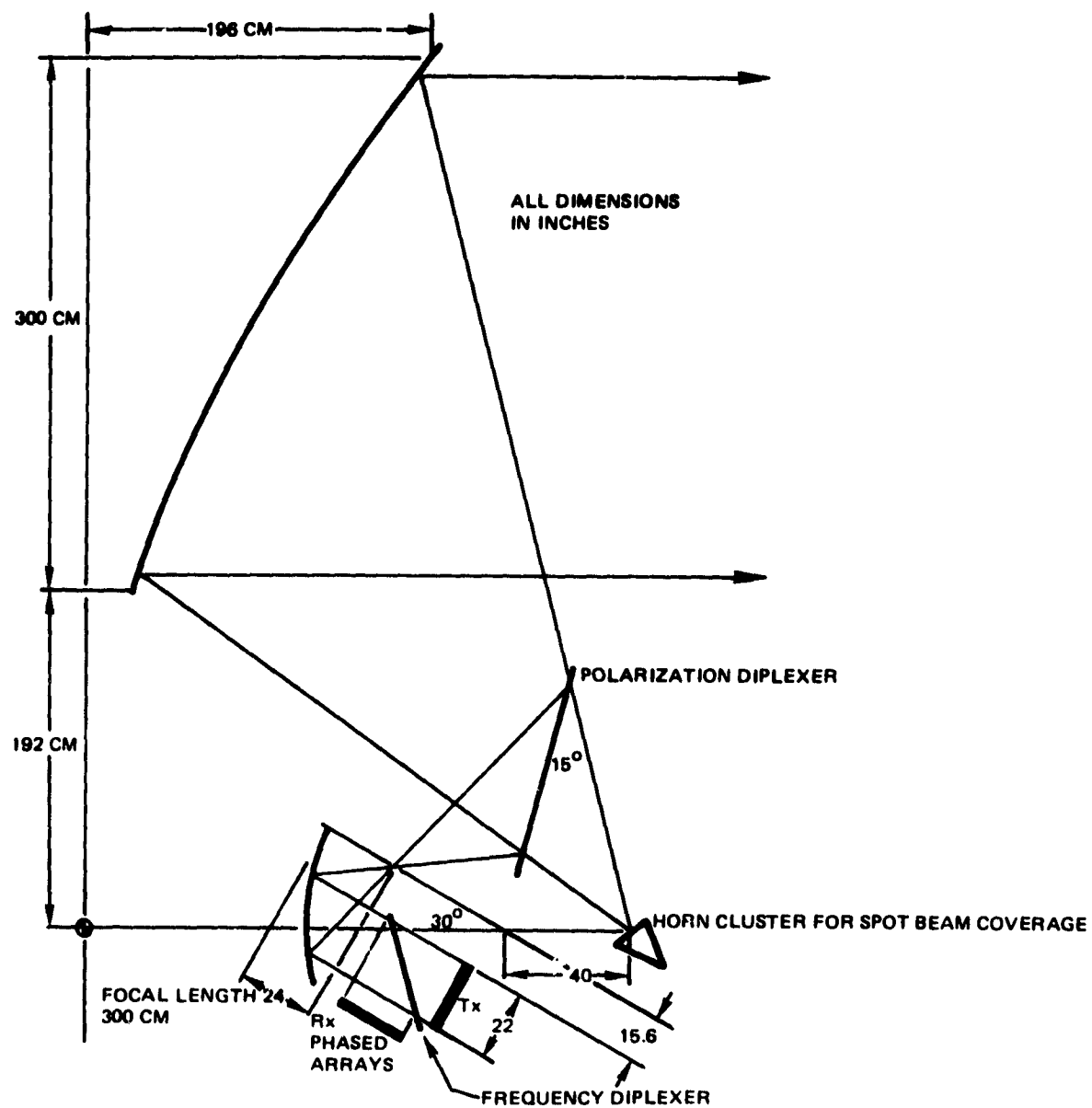


Figure 5-16. Multiple Reflector System with Tilted Subreflector

There is a possibility that the secondary reflector in this system could be eliminated by placing a phased array beyond the focal point of the main reflector. The weights of this array would be set up to focus the array in the main reflector focal plane. This is similar to the use of a focusing transmission lens, and approach would eliminate a source of loss; energy spillover at the secondary reflector. This could be accomplished without complicating the array itself in any way.

#### 5.4 RECOMMENDATIONS

The recommended baseline candidate for continued satellite configuration studies is the use of two combined fixed and scanning assemblies. The fixed beams are generated using scaled versions of the horns developed at 12/14 GHz. The scanned beams are generated using space fed-arrays. An interspersed solid state design should be concurrently considered as a backup phased-array design.

Incorporating both fixed and scanned beams generated at both transmit and receive frequencies is a challenge for the broad frequency range required (18 to 30 MHz). A four-assembly design should also be considered as a backup using two apertures for transmit and two apertures for receive.

## 6. DTU TERMINAL COST CONSIDERATIONS

The 30/20 GHz satellite communications network must economically accommodate a large number of small earth terminals. In order to accomplish this, the terminal's physical characteristics must allow deployment in heavily populated areas. In many places they will be rooftop mounted on existing buildings. With the large number of terminals anticipated, the cost per terminal must be very small. A cost/size balance must be achieved between the hardware modules required to process the transmit/ receiver signals and the "link dependent" hardware which is dictated by performance required to interface with the spacecraft. Estimation of 30/20 GHz communications terminal costs will initially consider optimizing terminal cost/size variables. The other terminal cost elements will then be added to determine an overall terminal cost estimate.

### 6.1 GENERAL DTU TERMINAL REQUIREMENTS

The uplink interface with the satellite at 30 GHz consists of transmitting a burst communications mode signal at 125 Mbps. The uplink EIRP required is 71 dBW to achieve uncoded performance with 15-dB weather margin and a 3-dB satellite demodulator efficiency. The 18-GHz received signal level at the antenna input has a nominal level of -146.2 dBW. This incident power level provides a weather margin of 10 dB with a terminal demodulator efficiency of -3 dB. The worst case thermal noise level at the antenna input is less than 280°K with the projected FET receiver capability.

The terminal hardware variables required to accommodate these basic satellite interface characteristics are the antenna aperture size, pointing accuracy, and power amplifier output and the losses associated with generating the required uplink EIRP. These variables must be balanced against receiver front-end noise characteristics.

The data port interface characteristics are established by the multiplexer/demultiplexer hardware employed at the user end. We assume a standard T1 (or DS1 signal) multiplexer/demultiplexer interface of 1.544 Mbps. This interface is comprised of NRZ binary data with a frame of 193 bits. There are 24 8-bit data words followed by a sync bit. Each data word corresponds to a 64 kbps data or voice channel. The frame rate is 8K

frames per record. A 12-bit sync word is employed, one bit of each word contained in each frame. The resulting sync word rate is 667 sync words per second. The absence of information in any channel at this interface is designated by employing one of two unique binary 8-bit sequences designated as either 10011000 or 00011000. Multiple TI multiplexer/demultiplexer interface ports can be accommodated at this baseband interface.

The terminal hardware at the TI external interface port will detect and remove the idle channel sequence prior to transmission on the uplink. Correspondingly, an idle channel sequence must be inserted in data stream when information is not being received on the downlink. The hardware required to process baseband signals for receive and transmit in the burst 125 Mbps mode is considered basic fixed-plant terminal hardware. Auxiliary hardware required for operation and test of the terminal is also in this fixed-plant hardware category.

## 6.2 VARIABLE TERMINAL HARDWARE ELEMENTS

The antenna pedestal pointing capability and the antenna size are key factors in establishing a practical terminal configuration. Here a balance is required between antenna gain (larger aperture size) and deployment constraints (smaller apertures). The analysis of this balance is begun by determining the transmit and receiver gain and beamwidth as a function of antenna diameter (see Figure 6-1). The aperture sizes of interest range from 1 meter (3.28 feet) to 10 meters (32.81 feet) covering a 20-dB peak gain variation.

The transmit and receive beamwidths (1, 3 and 6 dB) are superimposed on the gain plots to bound the loss in peak gain as a function of antenna pointing accuracy. With a step track system, the antenna can be pointed to with an accuracy of 1/10 of the beamwidth. This implies a loss in gain less than 0.5 dB. For this application, with satellite inclination held to much less than 0.1 degree, one can easily position the antenna manually to within  $\pm 0.25$  degree of the peak gain. The transmit antenna gain exhibits large excursions from the peak gain above 3 meters and the gain falls off radically above about 3-1/2 meters. For receive gain, the fall-off occurs above 5 meters. One cannot expect to achieve a pointing error much less than  $\pm 0.25$  degree when one considers worst-case environmental factors such as wind loading thermal variations and building sway.

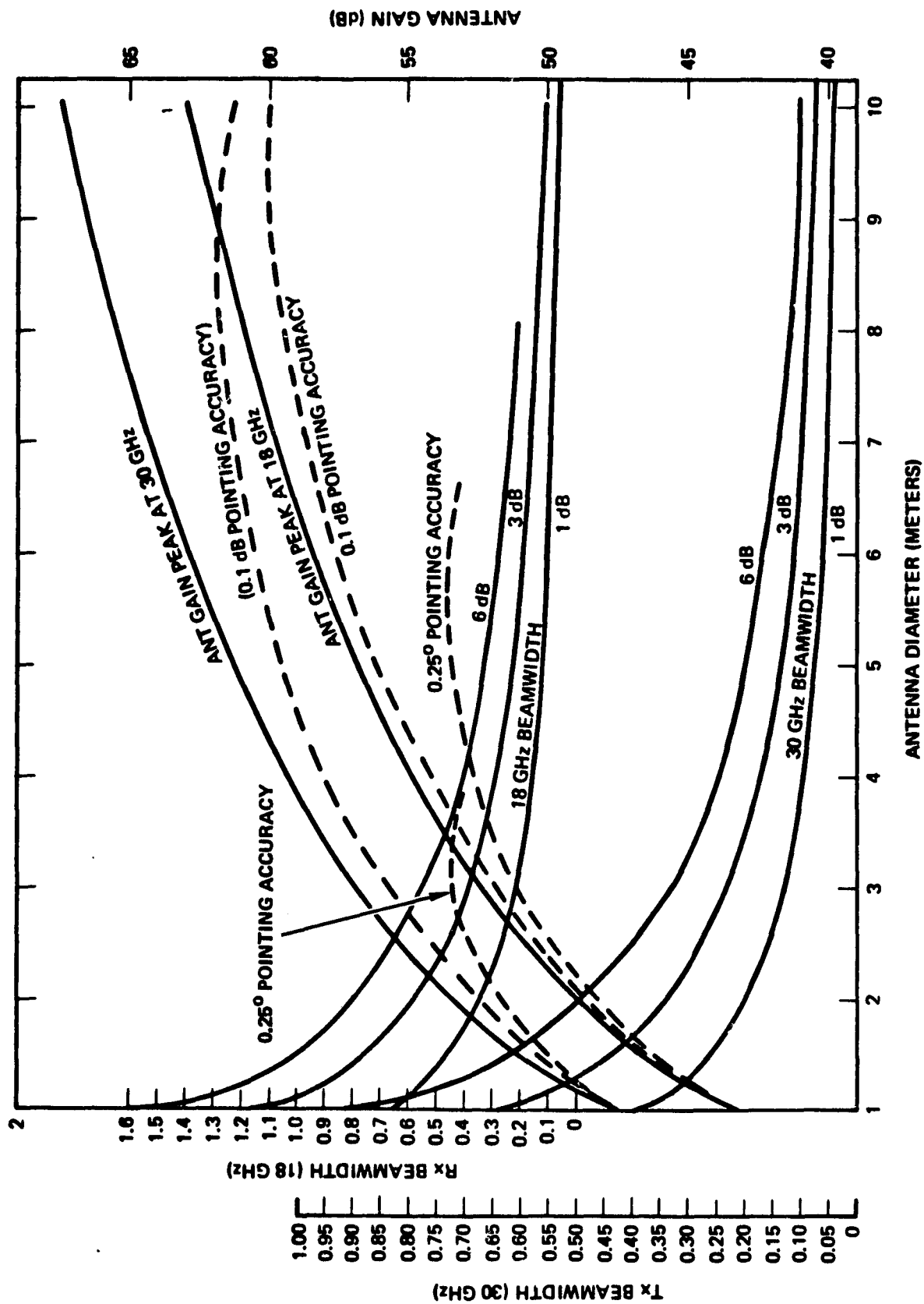


Figure 6-1. Antenna Gain and Beamwidth as a Function of Antenna Diameter

For more benign locations, however, we can expect to achieve a manual pointing accuracy of within  $\pm 0.1$  degree. Here the gain falls off with aperture size and is extended to above 7 meters on transmit and 10 meters on receive. Thus, the advantage of employing a larger aperture to maximize the link gain must take into consideration the degree of mechanization required to effectively point the antenna in the direction of the satellite to minimize the loss factors encountered therein.

#### 6.2.1 Uplink Performance and Cost Variables

To further expand on the aperture variables for operation at 18/30 GHz we next consider cost and efficiency factors. Because of the large transmit-to-receive frequency separation, the feed structure for transmit/receive operations is an important factor. Optimizing their feed for transmit (30 GHz) one can expect to achieve a maximum efficiency for Transmit of 68 percent with receiver efficiency on the order of 45 percent.

Maximizing efficiency for receive (18 GHz) one can expect a receive efficiency greater than 55 percent with a corresponding transmit efficiency on the order of 50 percent.

A survey of pedestal costs variations with size and pointing mechanization was conducted. To provide a consistent base, this cost survey was done for small quantity buys of terminals currently being produced for operations at C- and X-band. The median cost values established by this survey (conducted in 1978) were then projected to K-band and plotted to establish trends rather than absolute cost factors.

The results of the cost survey are shown parametrically with the uplink gain in Figure 6-2. The peak transmit gain at 68 percent efficiency is first plotted as a function of antenna size. The cost trend is superimposed. The gain plot includes 2.5-dB fixed losses. Pedestal cost excludes the pointing mechanization. It was estimated from this cost survey that the electronics and motor drive for autotrack would add \$60K to the overall terminal cost. It was also estimated that step tracking with slow level sensing of the received signal level (closed loop) would add one-half the auto-track costs (\$30K).

From Figure 6-2, one can project the cost/performance trends for transmit operation. The most economic transmit pedestal would use manual

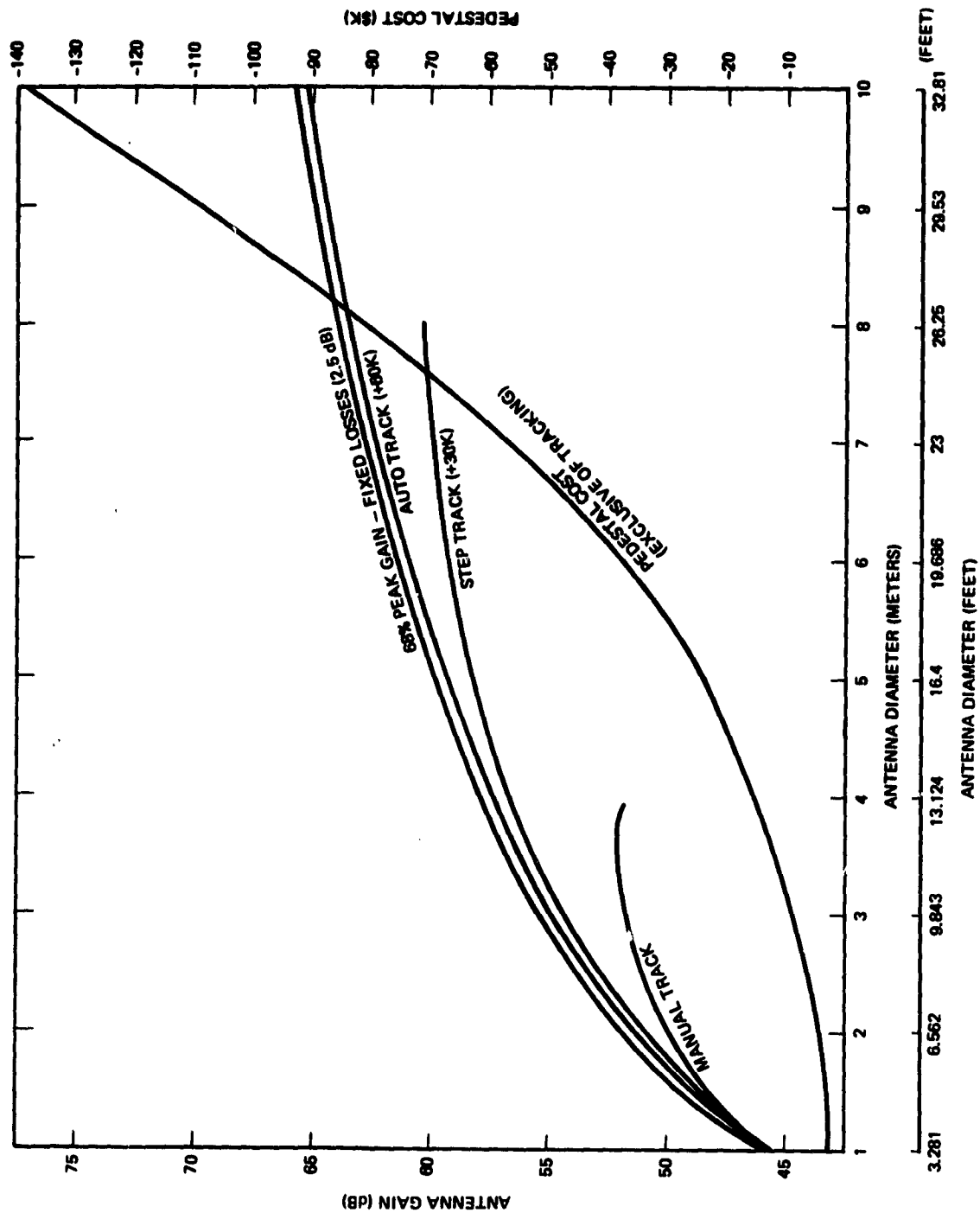


Figure 6-2. Pedestal Tx Gain and Cost for Aperture Size and Tracking

pointing and support a 3- to 4-meter antenna. The transmitter power required is large, on the order of 700 to 800 watts. Step tracking operation extends the antenna size capability beyond 5 meters with reduction in transmit power required to the order of 20 watts. Tracking cost and increased antenna size cause substantial increase in overall terminal cost.

To further illustrate the uplink cost variables, one needs to add transmitter cost factors. In Figure 6-3 the surveyed Transmit costs (median cost projections) were shown as functions of power output. TWT costs were projected over the range from 50 watts to 1 Kw for a redundant PA configuration with an automatic switchover to minimize link outage.

Projecting solid-state power amplifier costs at 30 GHz is much more difficult than projecting TWT cost factors. Projecting costs is even more difficult when one extends this projection beyond 30 watts. By surveying the solid-state advances made over the last several years at X-band where one can effectively project 20-watt operation, and considering the 2- to 4-watt amplifiers currently in development at V-band, one can project solid-state operation in the tens of watts operation at 30 GHz by 1985. The resultant cost/power output projections are displayed in Figure 6-3 on an expanded scale covering the 10 to 90-watt range. Operation above 30 watts is shown dotted to emphasize the uncertainty.

These pedestal and transmitter performances cost variables are integrated to portray overall cost factors.

#### 6.2.2 Downlink Performance/Cost Variables

Reception of a nominal -146.2 dBW signal level with the specified margins and loss factors requires one to establish the effective terminal receiver noise temperature that can be economically provided. Terminal G/T can then be parametrically portrayed by analyzing the antenna gain and overall noise level in consort with the cost factors.

The LNA cost survey resulted in projected cost ranging from \$2K with a 480°K noise temperature to \$45K for a 60°K amplifier noise temperature as shown in Table 6-1. The receiver noise temperature includes antenna noise temperature during rain.



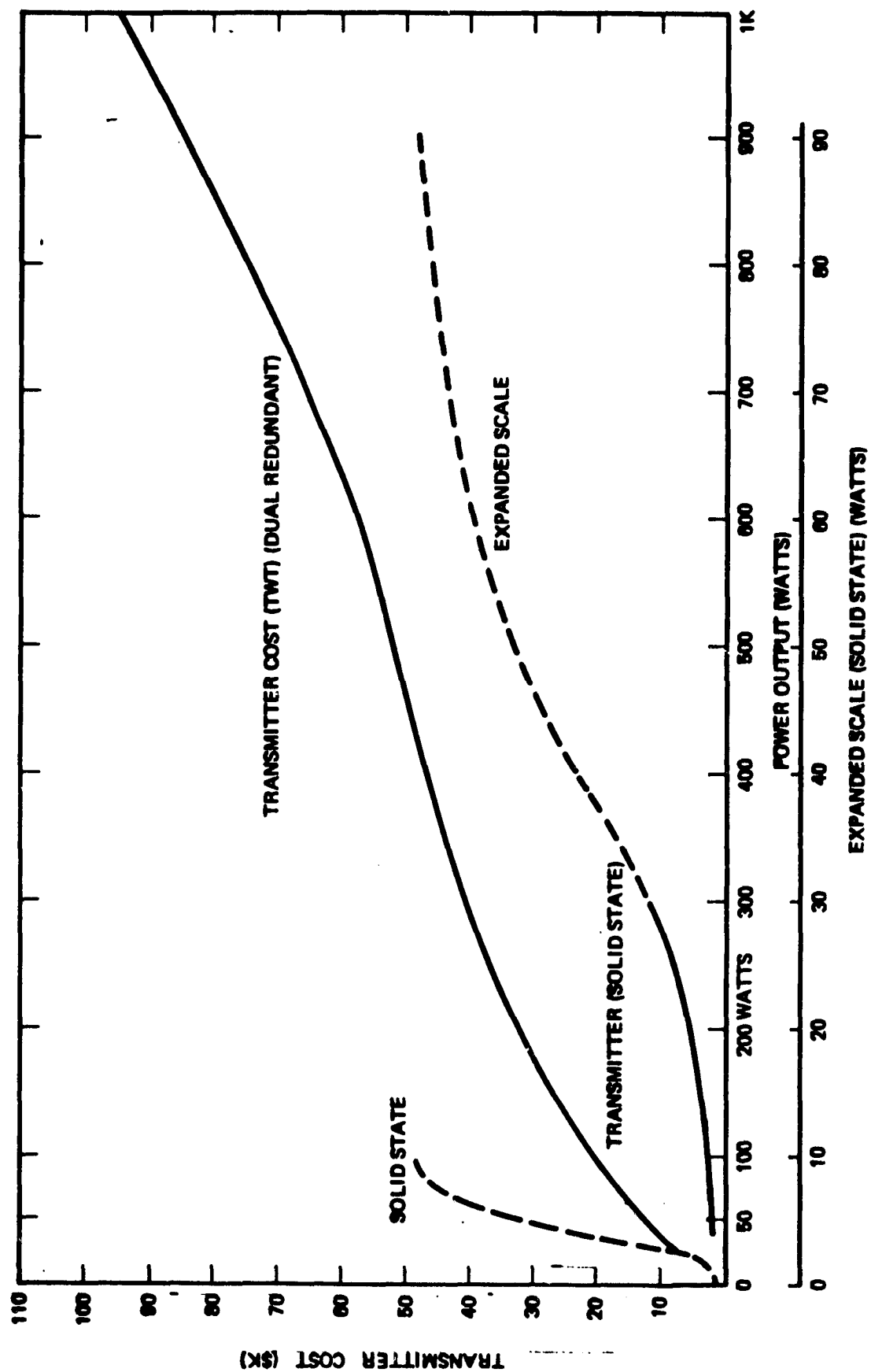


Figure 6-3. Transmitter Cost for Output Power

Table 6-1. Receiver Performance/Cost Variables

LNA		Receiver Performance	
Noise Temperature (°K)	Cost (\$K)	Noise Temperature (°K)	(dB)
480	2	760	28.8
320	4	600	27.8
220	27	500	27.0
150	35	430	26.3
60	45	340	25.3

The breakpoint in cost occurs below 320°K for an LNA, or at an overall terminal noise temperature of 600°K. This crossover in cost reflects the point at which cooling is required for technology in the 1985 time frame. This table portrays that an 8 to 1 variation in LNA noise temperature will result in only a 2 to 1 variation noise temperature.

Antenna gain at 18 GHz is plotted for 45 percent receive efficiency (see Figure 6-4). Included in this plot are 1-dB ohm losses and a 1-dB overall receive degradation allowance. The overall gain as a function of the type of tracking employed illustrates the effect of pointing losses. A G/T of 22.2 dB is required to achieve the specified margins.

Superimposed on the receive gain plot is the overall noise temperature, expressed in decibels, to reflect the front end cost factors. Receive performance (G/T) characteristics and LNA cost factors can thus be integrated into the overall terminal cost variables.

### 6.2.3 Terminal Cost Variables

With cost trend/performance characteristics projected for transmit and receive operation, one can integrate the results to optimize overall terminal characteristics. The integrated transmitter and pedestal cost are developed in Figure 6-5 for three antenna pointing modes to achieve a 71-dBW EIRP. Terminal transmit costs exhibit broad minima in the 2-1/2 to 3-1/2 meter antenna size range. When one integrates LNA cost factors with the transmit cost curves, cost becomes prohibitive below 3 meters. The optimal performance/cost range is shifted to the 3-1/2 meter (11.5 feet) to 4-1/2 meter (14.7 feet) range. The pedestal weight will vary from 1200 to

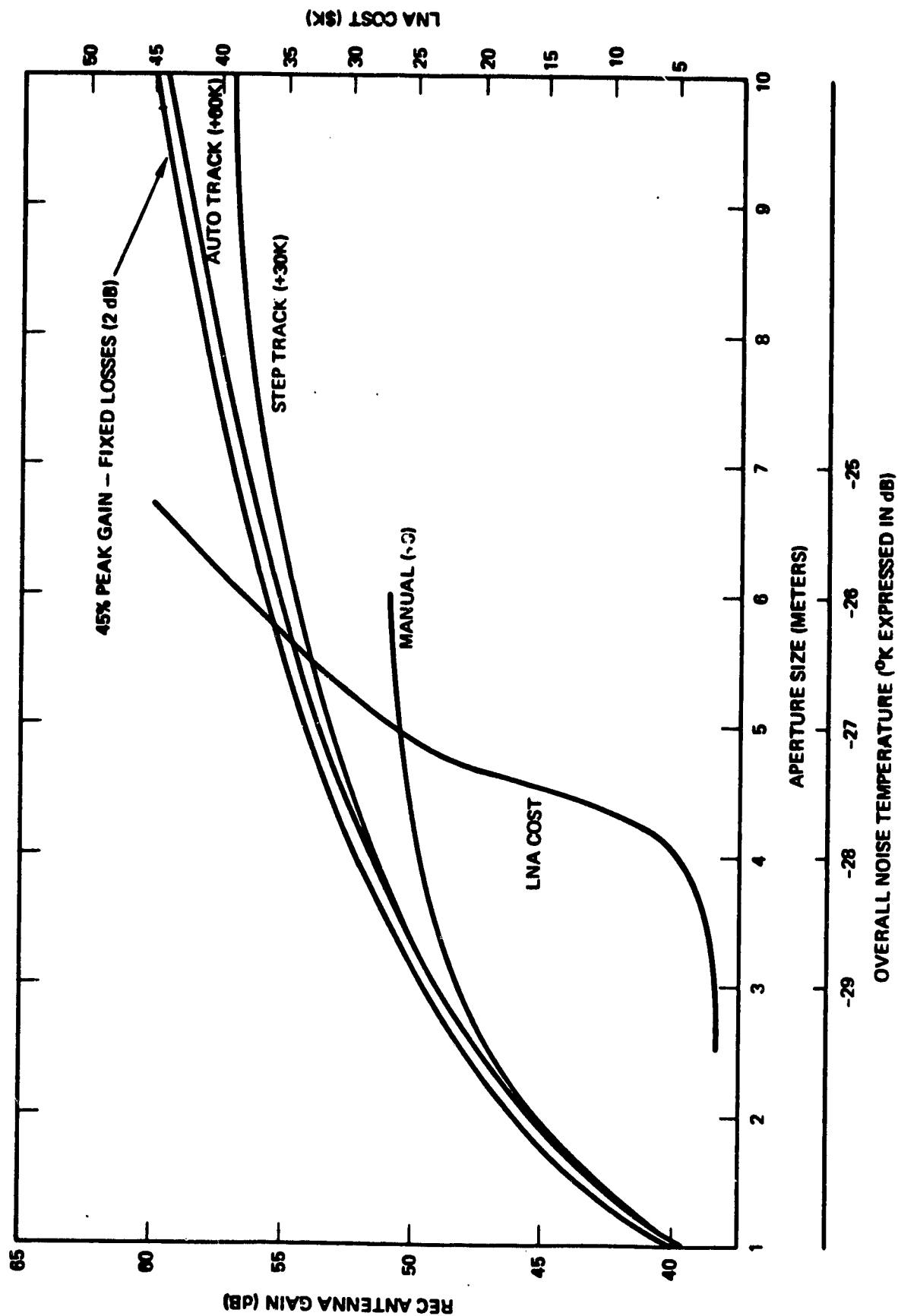


Figure 6-4. Pedestal Receive Gain as a Function of Aperture Size, LNA Cost, and as a Function of Noise Temperature

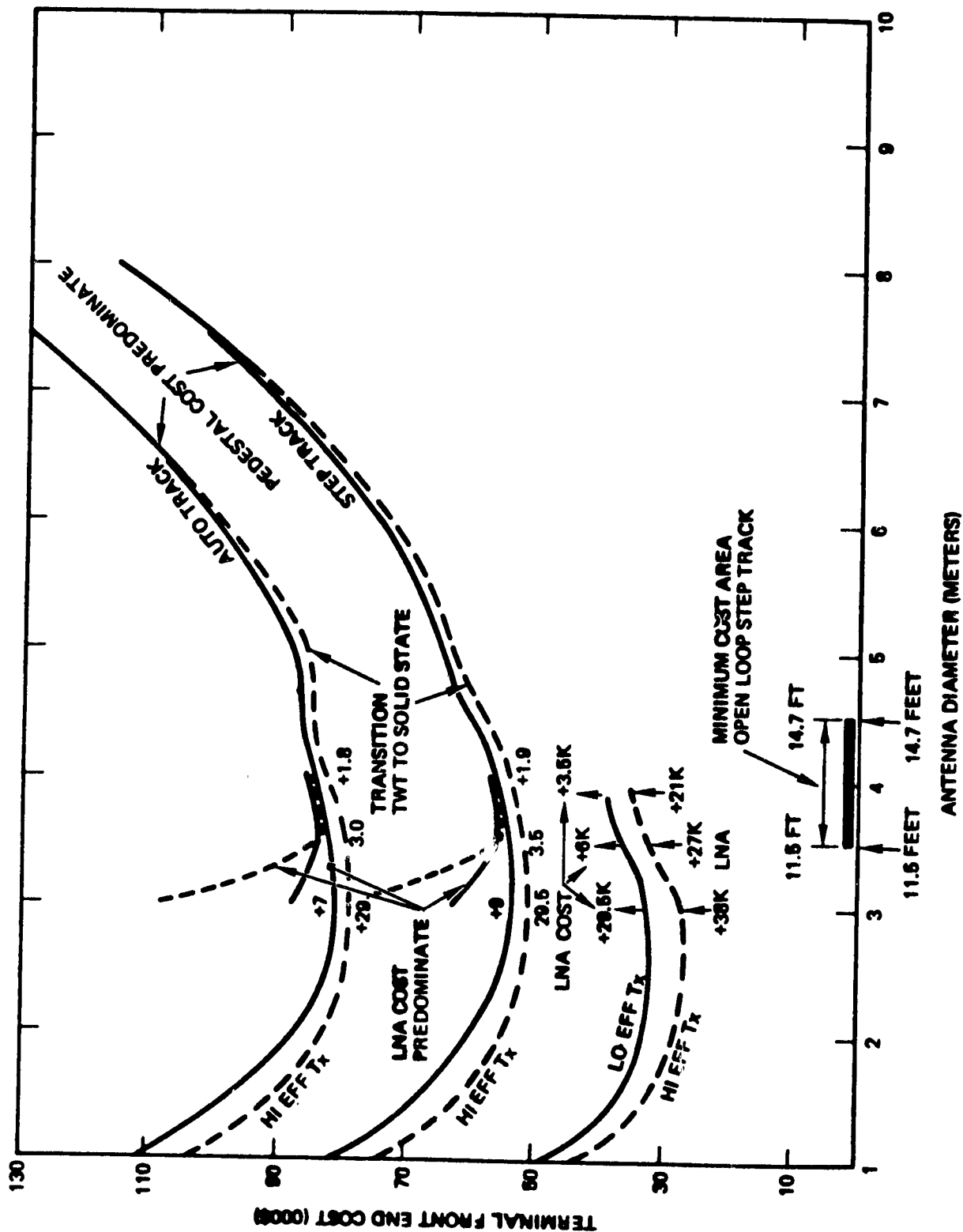


Figure 6-5. Terminal Front-End Cost as a Function of Aperture Size (LNA and Transmitter and Pedestal)

1600 pounds. This weight range should not place excessive constraints on site selection.

Transmitter costs predominate with small antenna sizes (1 to 2 meters) whereas antenna costs predominate at the large antenna sizes (above 5 meters). LNA cost factors for the main pointing mode (bottom curve) tend to merge costs with the step track operations. By maximizing the receive aperture efficiency one can show potential advantage for manual operation over step track in the 3-1/2 meter antenna size range.

To further expand on the 3-1/2 to 4-1/2 meter pedestal-size cost analysis, performance and cost characteristics are tabulated (see Table 6-2). With smaller apertures (3-1/2 meters) the LNA amplifier without cooling and the solid state transmitter power output are pushing the state of the art projected for the 1985 time frame. At the other extreme (4-1/2 meter aperture) both these modules can be more comfortably projected for this time frame. Cost values displayed in this table were the projected median values resulting from the cost survey for the procurement of small quantities (up to 10) of modules from the various specialty houses. Cost factors for modules in the mid range (4 meter) will be employed in establishing the overall terminal cost factors.

### 6.3 SMALL TERMINAL COST PROJECTIONS

The functional and physical configuration for a 18/30 GHz terminal is portrayed in Figure 6-6. The fixed hardware modules are shown in solid lines while the variable modules are shown in dashed lines. This hardware configuration consists of those modules necessary to interface at baseband with TI of modulator/demodulator.

The encoder/decoder module contains buffers to convert from a DS1 format to a burst formatted data structure. The FEC coding algorithm assumed for costing this module is rate 1/2 Verterbi with  $K = 7$  constraint length. It is anticipated that the coding/decoding functions would be bypassed except during severe rain conditions. During adverse weather conditions, when the link characteristics are marginal, this module would be employed to establish an additional 10 dB margin in the overall link performance. It is estimated that this encoder/decoder module will cost \$3K and take up 3 inches of rack space.

Table 6-2. Terminal Cost Variables

	71 dBw EIRP Min 15 dB Margin in Uplink (30 GHz)		-146.2 dBW Incident Power Level 10 dB Margin in Downlink (18 GHz)
	3-1/2 Meters 11.5 ft	4 Meters 13.1 ft	4-1/2 Meters 14.7 ft
LNA			
Temperature (°K)	380°K	550°K	720°K
Cost (\$)		\$2K	\$1.9K
Power Amp			
Power (dBW)	15.5 dBW	14.5 dBW	13.6 dBW
Cost (\$)	(36 watts) \$18K	(28 watts) \$10K	(23 watts) \$7K
Pedestal			
Tx Gain Peak	59.2 dB	60.3 dB	61.4 dB
Pointing Loss	1.2 dB	1.3 dB	1.5 dB
Receive Gain Peak	53 dB	54.1 dB	55.3 dB
Pointing Loss	0.6 dB	0.7 dB	0.9 dB
Cost		\$15.5K	19.5K
Open Loop Step Track		30K	30K
Pedestal Cost Total		\$57.5K	\$58.4K

Fixed Losses

Tx (-2.5 dB) 1.5 dB line loss 1.0 dB degradation  
 Rx (-2 dB) 1.0 dB line loss 1.0 dB degradation  
 Demod eff -3 dB over theoretical  
 Input noise temperature (aperture) = 280°K

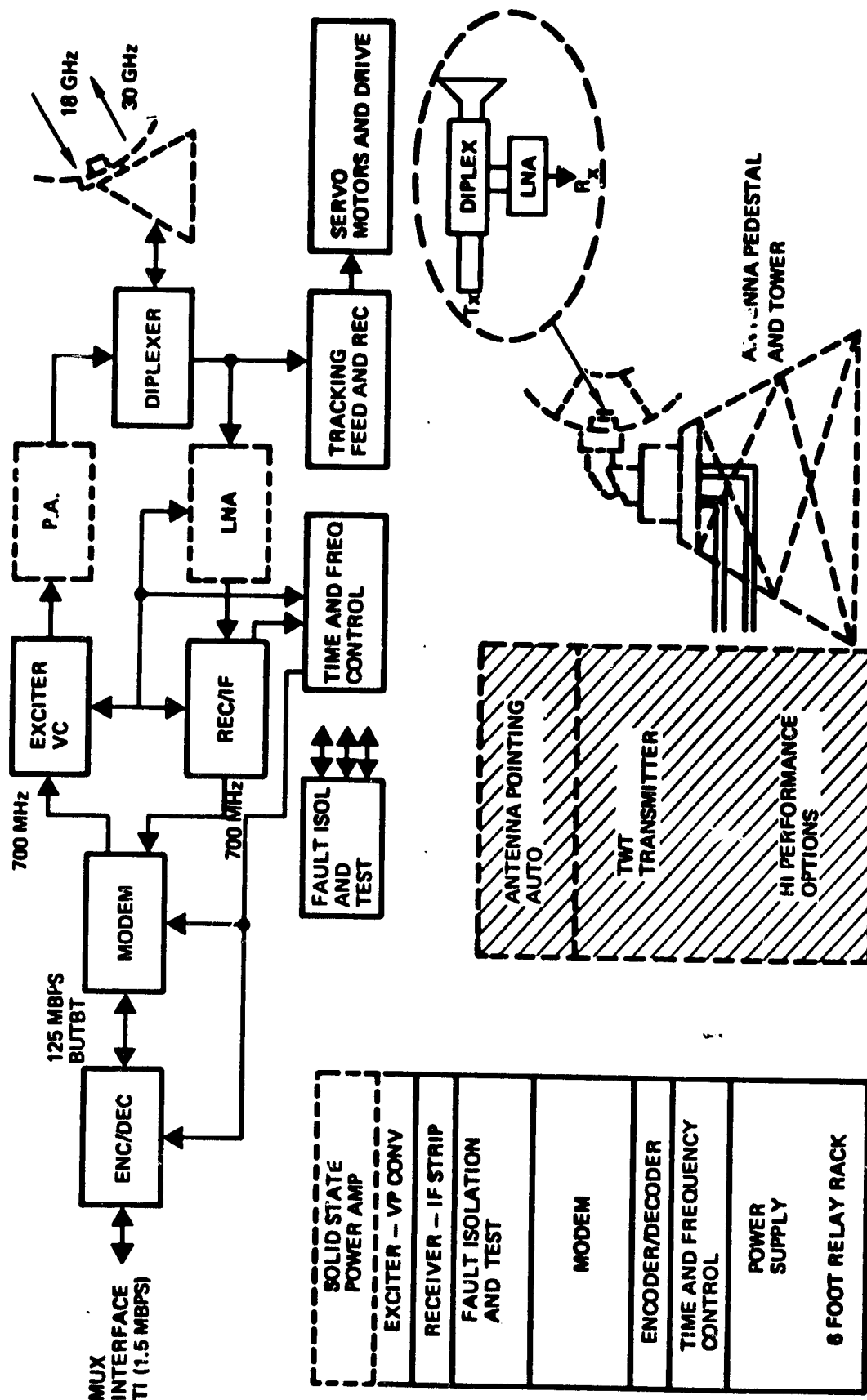


Figure 6-6. Small Earth Terminal Hardware (Functional and Physical Configuration)

The modem, which inserts the necessary preamble and formats the signal for transmission, modulates a 700 MHz IF frequency with a PSK modulation structure. This module acquires and tracks the input IF frequency, previously downconverted from the 18 GHz received satellite signal. Here the signal is PSK burst demodulated at the interface with the decoder module. This module is estimated to cost \$125K after development in small production quantities. It is projected to take up 10 inches of rack space in a 19-inch relay rack housing.

The 700 MHz burst modulated signal is amplified, filtered and upconverted to interface with the power amplifier. The upconverter/exciter module outputs at 30 GHz with 10 dBm output. It is expected to cost \$12K and be housed in a 6-inch rack configuration.

The power amplifier, LNA and pedestal design and associated cost factors were established for the 4-meter terminal configuration defined previously. The 28-watt power amplifier is expected to take up 6 to 8 inches of rack space. The LNA, with a 550°K noise temperature, is mounted in the antenna aperture in consort with the transmit receive diplexer. The diplexer for 18 GHz receive with a 2.5 GHz bandwidth and a 30 GHz transmit frequency is expected to cost \$2.5K. Step track antenna positioning was employed as a cost-effective compromise between manual and auto/track operation.

A dual conversion receiver/IF module interfaces with the LNA and provides filtered 700 MHz output to the modem (demodulator). This receiver will take up 6 inches of rack space and is estimated to cost \$16K for small quantity buys.

A time and frequency control module consists of a frequency standard and frequency generation equipment which synthesizes frequencies for the up and down conversion processes. In addition, the clock rates are derived for operating the encoder/decoder and modem modules. The time and frequency references shall be slaved to the downlink signal and will correct for doppler and transmit timing variations. This module is expected to take up 8 inches of rack space and cost \$25K.

The fault isolation and test hardware module will contain basic diagnostic equipment to establish the overall status of the terminal.



Performance monitoring processes will provide data on overall terminal condition and on individual drawer or module performance. This module, being terminal unique, is expected to cost \$30K after development and require at least 10 inches of rack space in the terminal.

#### 6.3.1 Cost Summary

The small terminal complement for 18/30 GHz operation is comprised of a single relay rack (less than 6 feet) of drawer-mounted hardware modules and a 4-meter antenna and pedestal. The diplexer and uncooled front end amplifier, located in antenna subassembly, interface through a transmit waveguide routed to rack mounted power amplifier, and coaxial cable to the receiver IF module. Other pedestal interfaces include antenna positioning control and power to the motor drive elements. Rack mounted hardware includes power supplies interfacing to 220 Vac three-phase commercial power.

The cost estimates of the hardware complement are tabulated in Table 6-3. The small quantity cost factors associated with each element assume reasonable development activities supporting this new frequency band of operation. It is expected that development funds would be required in two areas. The first development area is the solid state power amplifier. One can readily expect low-power TWT technology to achieve the projected cost targets. In fact, the price will probably be substantially less than for a solid-state transmitter. Overall reliability will be increased and the associated terminal downtime will be considerably reduced with solid state operation.

The second development area is the terminal modem. The modem is considered here as a "system peculiar" hardware module. As such, one would not expect the commercial electronic hardware suppliers to commit a sizeable investment to development of a cost effective hardware package.

The small quantity (up to 10) cost projections, tabulated in Table 6-3, when integrated, results in a \$293,000 terminal cost. This cost is further categorized as 73 percent for the electronic rack complement, including cables and 17 percent for the pedestal hardware complement. In assessing small quantity cost factors, the modem (43 percent) stands out as the single largest contributor to overall terminal costs. This cost element can be

Table 6-3. Cost Projections Summary

	Rack Space (inches)	Small Quantity Cost (\$)	Total (%)	Development Cost (\$)	Large Quantity Estimate (\$)	(%)
<u>Rack Mounted Modules</u>						
Power Supply	12	7K	2.4		5K	3.9
Time and Freq Control	8	25K	8.5		15K	11.7
Encoder Decoder	3	3K	1.0		2K	1.6
Modem	12	125K	42.7	2000K	35K	27.3
Fault Iso and Test	10	30K	10.2		20K	15.6
Receiver - IF	6	16K	5.5		10K	7.8
Exciter-up Conv	6	12K	4.1		8K	6.3
Power Amp (Solid Sta)	6	10K	3.4	1000K	5K	3.9
Other (Rack, Cables)	-	15K	5.1		5K	3.9
Subtotal	5'3"	\$243K	72.9		\$105K	72.0
<u>Pedestal Mounted</u>						
Diplexer		2.5K	0.9		1.5K	1.2
LNA		2.0K	0.7		1.5K	1.2
Antenna and Pedestal		15.5K	5.3		10.0K	7.8
Step Track		30.0K	10.2	200K	10.0K	7.8
Subtotal		\$50K	17.1		\$23K	18.0
Total		\$293K			\$128K	

REPRODUCIBILITY OF THE  
ORIGINAL PAGE IS POOR

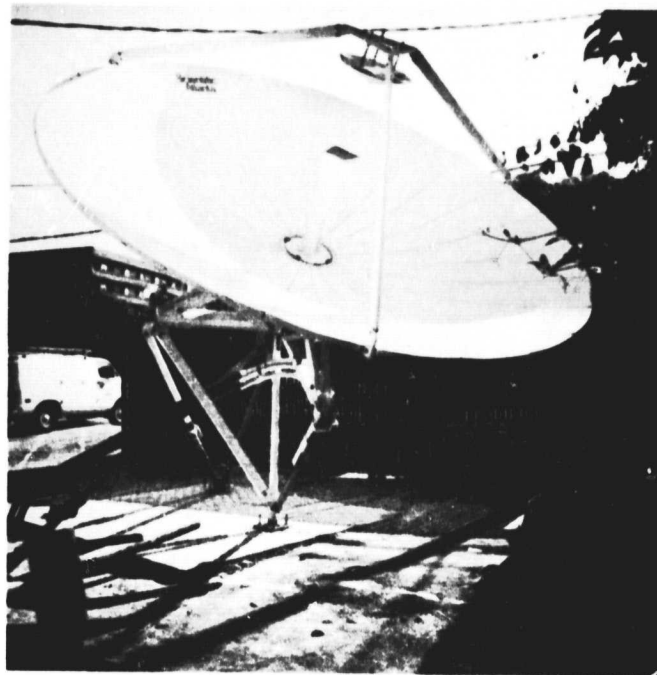


Figure 6-7. C-Band TVRO Antenna, Front View

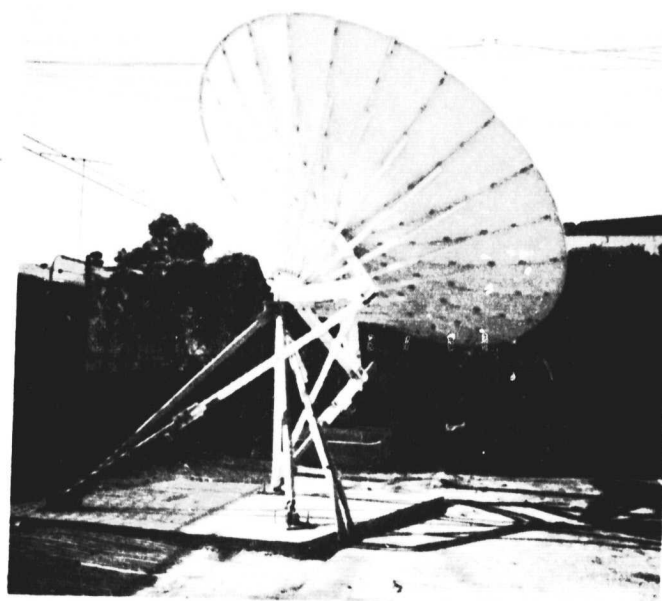


Figure 6-8. C-Band TVRO Antenna, Rear View



Figure 6-9. C-Band TVRO Equipment Reciver and Monitor

REPRODUCIBILITY OF THE  
ORIGINAL PAGE IS POOR



Figure 6-10. C-Band TVRO Equipment Installation

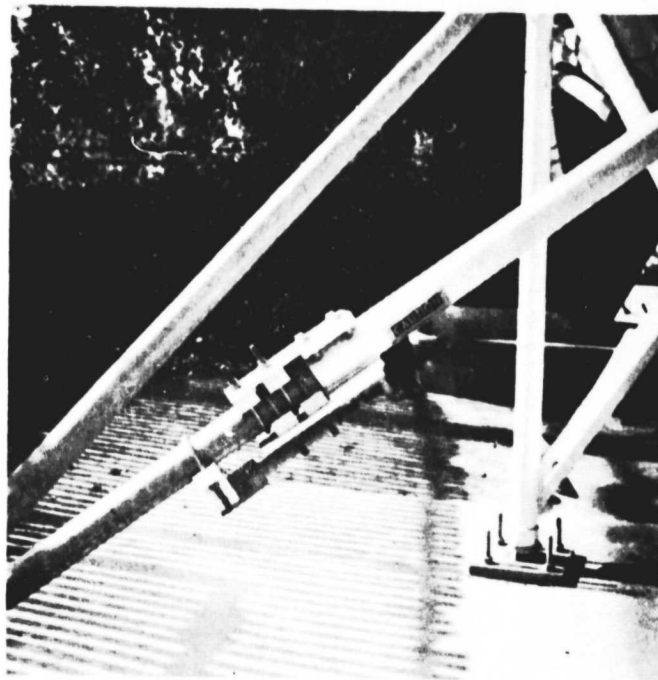


Figure 6-11. C-Band TVRO Antenna Azimuth Drive

REPRODUCIBILITY OF THE  
ORIGINAL PAGE IS POOR



Figure 6-12. C-Band TVRO Antenna Elevation Drive

## 7. IDENTIFICATION OF CRITICAL TECHNOLOGY

Critical technology may be identified from several points of view. Critical technologies will be concentrated on to support an efficient 30/20 GHz communication satellite that will benefit significantly from demonstration in an experimental satellite flight test. These critical technologies will be categorized as being communications or noncommunications technologies, and as being flight experiment candidates or not.

New noncommunications spacecraft technologies in areas such as shuttle-orbit to final-orbit propulsion, north/south stationkeeping propulsion, power and attitude control subsystems may be as important to communications satellite economics as the communications technologies. Inclusion of such technologies in an experimental satellite development effort should be considered. Use of experimental subsystems that are critical to mission success must be backed up with more conventional subsystems, where possible. Failure of an experimental technology item should not be allowed to prevent communication system testing.

Use of different technologies to provide functional redundancy, and integration of new state-of-the-art components for, in some cases, the first time on a spacecraft, leads to the conclusion that an experimental satellite should be relatively large. Growth margins for undeveloped hardware should be generous to prevent the cost escalation that results when weight reduction programs are required.

### 7.1 COMMUNICATIONS CRITICAL TECHNOLOGIES

The communications critical technologies that have been identified as being required for an efficient and economically viable 30/20 GHz communications system are:

- On-board satellite TDMA burst demodulators using RF LSI techniques.
- Low noise FET preamplifiers, uncooled and with passive radiation or other long-life reliable cooling techniques.
- Low noise mixers, either diode or FET, either cooled or uncooled.

- FET transmitters with efficiencies approaching 25 percent dc to RF conversion, including single-carrier and multiple-carrier designs.
- TWTA's with high efficiency, 10 to 100 watts power outputs, and extremely high reliability. Both dual-mode and single-mode designs may be required.
- Multibeam scanning antennas that can efficiently radiate several 20 to 100 watt signals with independent beam pointing and acceptable long-life and reliability characteristics.
- Multibeam scanning transmit antennas with solid-state multi-carrier element transmitters (if we are unable to develop TWT-compatible multiple beam scanning antennas).
- Multibeam scanning receive antenna/receivers with excellent efficiency and low noise temperature.
- SSTDMA IF switch matrices with approximately 20/20 interconnectivity, excellent linearity, isolation, and with reliability and redundancy compatible with 10 years operating life.
- On-board digital processors providing routing interconnection, burst buffering, data rate change, single-burst-per-station for both uplinks and downlinks, and adaptive error correction coding independently on individual uplink and downlink bursts.
- Microwave LSI 20-GHz direct modulators for satellite on-board use.
- Improved packaging techniques to reduce the electronic box housing weight. Electronic component weight is usually negligible compared to the housings, cables, and connectors.
- Uplink error correction codes, algorithms, and decoders compatible with TDMA burst operation.

One of the most important, if not the most important, communication technology for the 30/20 GHz Mixed User Architecture System is the on-board satellite TDMA burst demodulator. As many as 100 demodulator units, including redundancy, may be required. These can be fabricated in RF LSI at very low size, weight, and power levels, but the technology development time is relatively long. Using discrete components will make the number of demodulators needed impractical for an economic satellite design. This would, in turn, result in losing most of the system advantages (DTU terminal cost advantages) of digital on-board routing and processing.

## 7.2 NONCOMMUNICATIONS CRITICAL TECHNOLOGIES

### 7.2.1 North/South Stationkeeping

Several spacecraft technologies that are not communications technologies strongly affect the cost effectiveness of communication satellites. The most readily available example is propulsion for north/south stationkeeping. Extension of satellite lifetimes to 10 years and more greatly increases the percentage of satellite weight devoted to propulsion, if traditional stationkeeping propulsion systems are used.

Other noncommunications technologies can have significant impact on system economics and should be considered for development as part of a communications satellite technology development program.

#### Fuel Required - Percent of S/C Weight versus Specific Thrust

- As much as 20 percent of a 10-year Comsat total weight must be devoted to stationkeeping fuel. Heated hydrazine or bipropellant thrusters reduce this to 15 percent. This is still a huge penalty. North/south stationkeeping will usually be provided in keeping with the trend of making user terminals less complex and placing the complexity burden in the satellite.
- Ion propulsion is especially attractive since the fuel requirement becomes very small, the thrust level is very low and thus does not disturb attitude control. By providing vectored thrust with a bias momentum system other thrusters are not required.

### 7.2.2 Attitude Control

There are several attitude control concepts that could be developed to reduce the spacecraft weight allocation to this function. In particular the following items should be investigated:

- Magnetic suspension momentum wheels with limited range two-axis gimbal capability. Such a capability should extend system life by removing bearing wearout as a failure mechanism. The limited range two-axis gimbal capability allows fine satellite antenna pointing without additional gimbals and antenna system complication.
- Integrated momentum wheel and earth sensors. Techniques have been suggested, but not developed, to integrate earth sensors with momentum wheels; taking advantage of wheel rotation to achieve earth-scan and reducing the number of units to be integrated in the satellite design process.



### 7.2.3 Integrated Satellite Propulsion Systems

No efficient means of moving a communication satellite from shuttle parking orbit to final synchronous orbit now exist. An integrated satellite propulsion system, utilizing much of the satellite on-orbit attitude control system and perhaps with an integrated structural approach, should be much more effective than IUS or PAM/SSUS systems. IUS does place a large spacecraft weight (5000 pounds) in final orbit, but utilizes almost an entire shuttle payload and is very expensive itself. The PAM/SSUS vehicles provide perigee burn only, requiring a significant integrated satellite propulsion system or a separate AKM to provide apogee propulsion. If an integrated satellite propulsion system must be provided it seems logical to have it accomplish all high-thrust propulsion.

The propulsion system used for satellite apogee (and perhaps perigee) propulsion will not, in general, be applicable for north/south station-keeping. Very low thrust levels are strongly preferred during actual communication operation to prevent degradation of attitude control with consequent disruption of communication service.

## 8. SSTDMA ARCHITECTURE STUDIES

This section contains documentation of several SSTDMA architectural study efforts that are not necessarily consistent with the 30/20 GHz baseline system architecture presented elsewhere in this report. They are presented here to demonstrate some of the breadth involved in the system architecture design effort, and because some of the approaches described and evaluated herein may later prove attractive for incorporation into the 30/20 baseline system architecture.

Study efforts described herein include a system synthesis using space-fed array techniques, a survey of synchronization methods for SSTDMA systems, short-frame versus long-frame mechanization comparison for TDMA systems, a description of the "Greedy Algorithm" for SSTDMA mode design/selection, and documentation of a literature search on different techniques for efficient bandwidth-conservative digital modulation.

### 8.1 A SPACE-FED-SCANNING-BEAM DIRECT-TO-USER SATELLITE COMMUNICATION SYSTEM

Two fairly obvious techniques for mechanizing a scanning-beam DTU communication system are: phased arrays with element transmitters and receivers, and switched fixed-beam antennas with diplexed transmitters and receivers. This section will describe a third system approach using a multiple scanning-beam, space-fed-phase array antenna (Figure 8-1).

The advantages of this approach are:

- a) High power TWTAs transmitters may be used with high efficiencies.
- b) Redundancy techniques are available to provide adequate reliability without high-power RF switching.
- c) Cooled parametric amplifiers may be used since few receivers are required.

The disadvantages of this approach are:

- a) The multiple beams may not be scanned independently. This reduces the effective capacity.
- b) Phase shifter losses may reduce transmitter efficiencies and increase receiver noise temperatures.

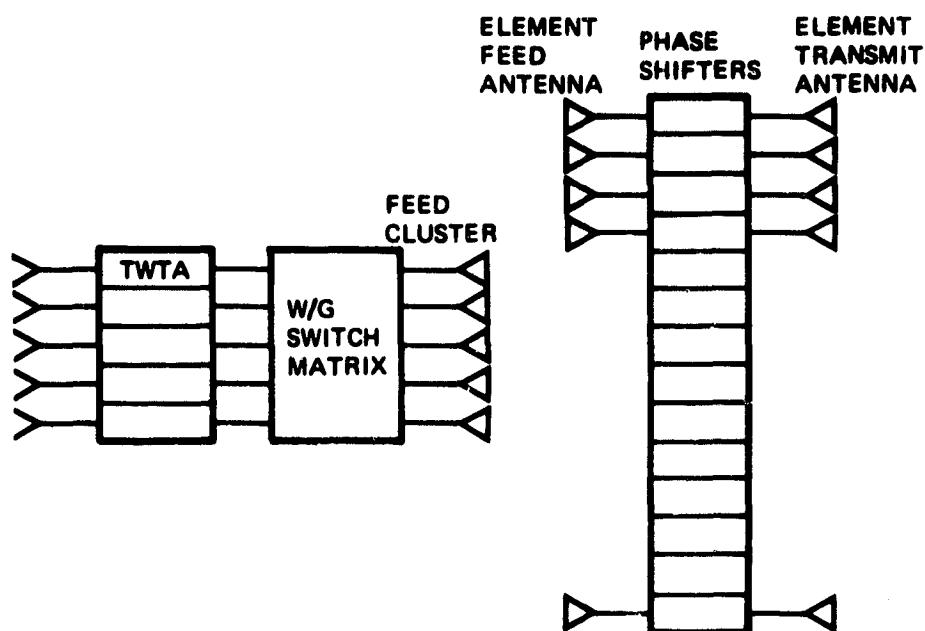
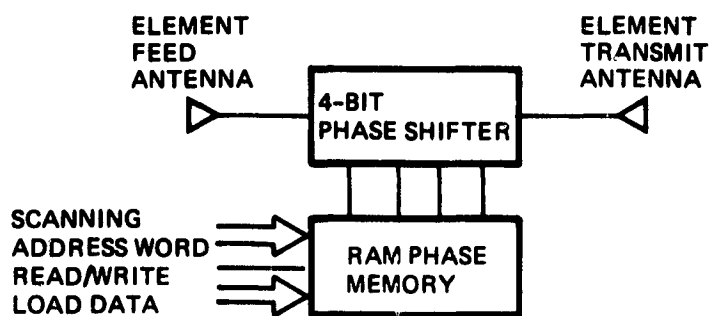


Figure 8-1a. Multiple-Beam Space-Fed Phase Array



- RAM PHASE MEMORY RETAINS ALL PHASES REQUIRED DURING FRAME PERIOD
- ADDRESS IS DISTRIBUTED TO ALL ELEMENTS IN PARALLEL FOR TIMING/CONTROL

Figure 8-1b. Space-Fed Array

A space-fed array may be mechanized as either a transmission array (lens) or reflection array (as in a parabolic reflector). Reflection arrays with large elements were investigated but proved difficult to illuminate properly. We will assume a transmission array mechanization herein. Each of the 100 to 300 elements making up the array consist of a transmission array antenna, a three- or four-bit phase shifter, a feed antenna, and phase shifter control electronics (including digital storage for control data) necessary for the phased array pointing control.

A single space-fed array could possibly be made broadband enough for simultaneous 18 and 30 GHz use. Physical shaping of the array to parabolic form might be required to prevent phase dispersion over this large bandwidth.

As shown in Figure 8-1, a waveguide switch matrix may be placed between the TWTAs and the feeds. The primary purpose of this matrix is to provide TWTA redundancy switching. A secondary purpose is to provide configuration flexibility for the multiple beam pattern. If more downlink feeds are provided than normally are needed, the downlink multiple beam pattern can be modified to better match downlink data requirements as part of the overall MBA scan pattern selection process. Since mechanical waveguide switches are required for low loss, modification of the downlink multiple beam pattern will be done occasionally. Pattern modification as part of the beam scanning process is probably impractical using the switch matrix technique, due to the slow switching time and potential wearout characteristics of mechanical waveguide switches.

If active downlink multiple beam pattern reconfiguration is needed, a technique to accomplish this is illustrated in Figure 8-2. Several TWTAs operate into FDM demultiplexers. The demultiplexers have two outputs, each connected to a different feed in the multiple-beam pattern. Rapid switching between the two resulting beam positions is accomplished by switching the TWTA input frequency. This is easily accomplished in the IF-to-Ka-band upconverter which provides the TWTA input signal.

Another way to increase the flexibility of the space-fed downlink scanning MBA is illustrated in Figure 8-3. In this approach we again provide more TWTAs and feeds than are required, and simply turn off the TWTA output when that particular beam is not required. This technique

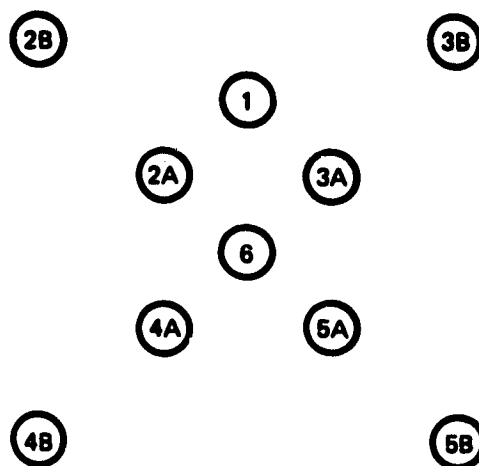


Figure 8-2a. Possible Downlink Scanning-Beam pattern with Some Two-Position Beams

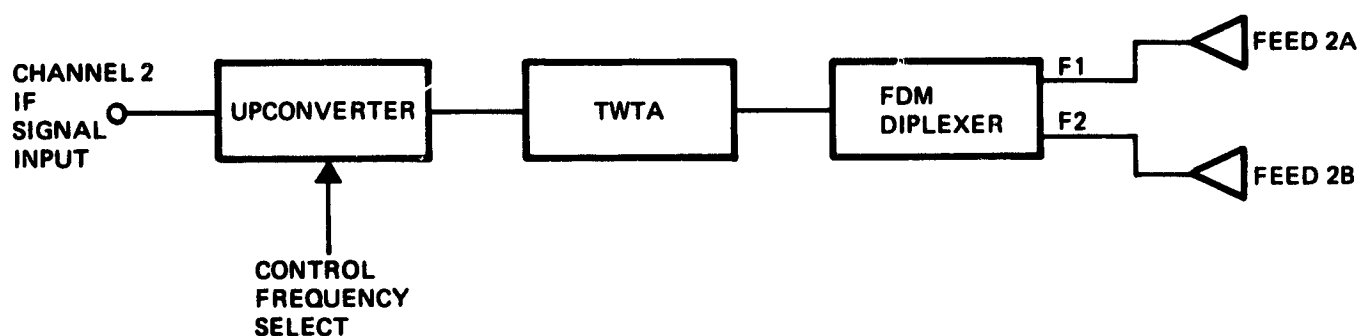
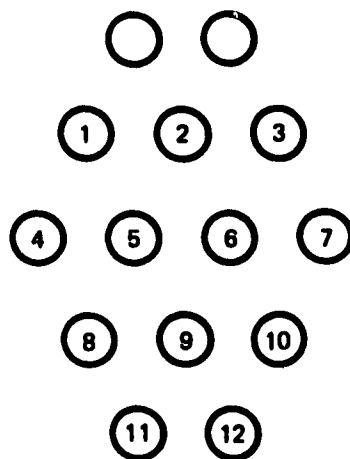


Figure 8-2b. Mechanization of High-Speed, High-Power, Low-Loss Beam Switching by Frequency Selection



- ANY PATTERN OF ANY NUMBER OF BEAMS MAY BE SELECTED AT ANY TIME
- AVERAGE NUMBER OF BEAMS ENERGIZED IS SIX TO EIGHT

Figure 8-3a. Possible Downlink Scanning-Beam Pattern with Rapid TWTA ON/OFF Beam Pattern Control

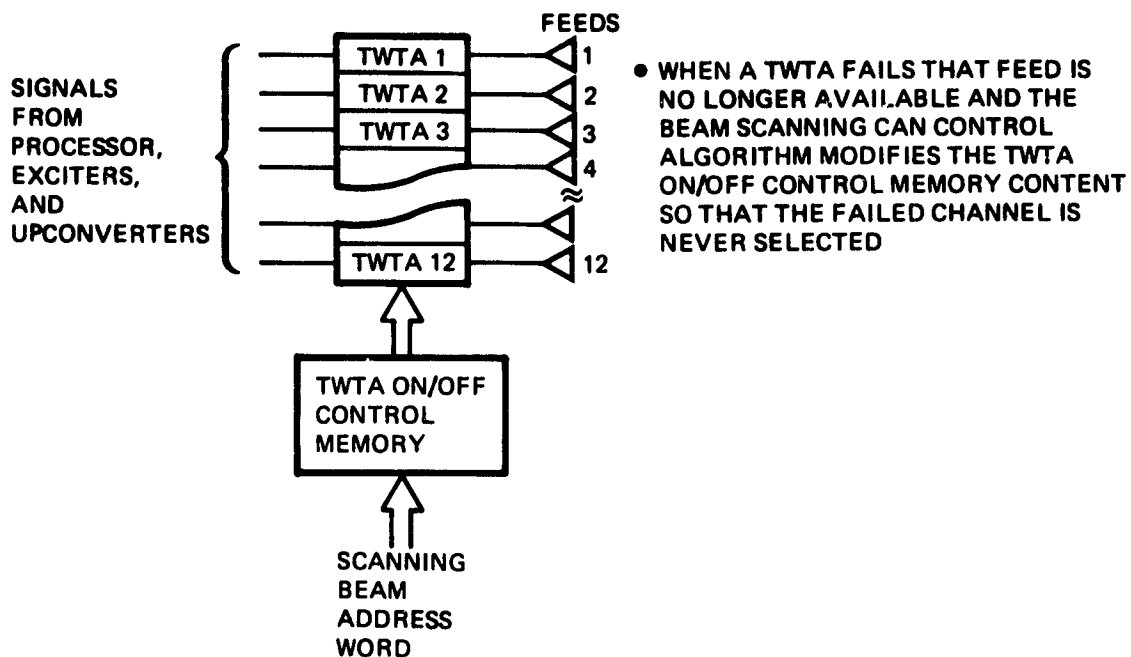


Figure 8-3b. Mechanization of High-Speed, High-Power, Low-Loss Beam Pattern Reconfiguration by TWTA ON/OFF Control

requires special TWTAs designs in which the TWT beam current can be turned on and off rapidly, since high overall power efficiency is needed. If TWT beam current gating is used to achieve space-fed MBA flexibility, a large reliability advantage also becomes available. No switches are required between the TWT outputs and the antenna feeds. TWT failures simply place constraints on the available beam patterns. Providing more downlink beams than required achieves a very high level redundancy. As TWTA's fail the system impact is on the scan pattern optimization computer program in the system master control station. As long as there are enough remaining TWT units to achieve the current required downlink capacity, there is no loss of system capability.

## 8.2 DOWNLINK SIGNAL DESIGN

Orthogonal linear polarizations for transmit allow two TWTA's to transmit simultaneously on a single downlink beam. Polarization would not be used for signal isolation but merely for transmitter power combining. The two TWTAs would use different frequencies in the 20 GHz downlink band. Signal isolation results from this frequency separation.

The scanning array must provide the entire direct-to-user (DTU) and small trunking user capacity outside those areas with fixed-beam coverage. As many FDM uplinks as desired may be used to achieve capacity. However, the entire downlink capacity must be provided through a relatively small number of TWT transmitters.

The traffic demand model calls for 2 Gbps of DTU and small trunking traffic in the low density regions. With four downlink beams, the downlink data rate is required to be 500 Mbps for each beam. Assuming quadriphase modulation, the I- and Q-channel data rates are 250 Mbps. This is a high but not unreasonable data rate. An RF integrated circuit receiver demodulator using batch fabrication techniques for its construction should result in a reasonable receiver cost. This data rate is very high, however, and the area coverage requirement should be examined to verify that it is really this high. Also, fixed-beam coverage could be added in some areas where DTU density is high, even if no trunking users are present.

Since all data is demodulated, buffered, reformatted, and remodulated on the satellite, the TDMA switching losses consist of the beam switching time and the carrier acquisition time for each beam position. All data downlinked to a particular area will be modulated on a single satellite-generated carrier, so there is only a single carrier acquisition time per beam position. All users in that area acquire carrier simultaneously. Furthermore, by placing the highest data-rate, more sophisticated users first in the downlink burst; less sophisticated and perhaps lower-data-rate users can utilize earlier parts of the burst as their carrier and clock acquisition preambles.

Carrier and clock acquisition time at 500 Mbps should be less than 0.4 microsecond. One to 2.0 microseconds will be required for both beam switching and first-user carrier acquisition. With 100 beam positions, the total time loss is 100 to 200 microseconds per frame. The frame period is 1 ms. The TDMA efficiency is then 80 to 90 percent.

Since only two TWTAs are used for each downlink beam, they should be relatively high power. It is perhaps not unreasonable to hypothesize powers in the 50- to 100-watt range. Nonetheless, a 30-watt single TWT power level was used in the first-cut power budget. This results in a 7.2 dB rain margin which is very nearly adequate for 99.9 percent availability over more than half of the area of the United States. This probably represents a good, clear-weather design point. Higher downlink margins should be achieved by coding or data repeats when and where needed. Another possibility is to allow users to vary antenna size upward or downward and to match their availability needs, considering their local climate.

### 8.3 UPLINK SIGNAL DESIGN COMMENTS

Uplink FDM may be used to reduce terminal peak data rate requirements. Total uplink capacity should be 2 Gbps, or slightly higher due to traffic imbalance considerations. Consider using a single beam over 100 positions, and assume that the minimum dwell period is 1/200 of a frame period. This allows some flexibility in assigning dwell periods. The minimum peak data rate for any single user is then 200 times his average data rate. If equal dwell times are required for all locations this drops to 100 times. But



since traffic is not uniformly distributed and some concentrations require 100 Mbps traffic, the peak receive capability in the satellite would have to be 10 Gbps. This is unattractive, and variable dwell periods will be assumed for the scanning beams.

Sizing for a 1 Mbps, low-capacity user, a 6 Mbps medium capacity user, and a 35 Mbps high capacity DTU terminal; we require peak data rates of 200, 1200, and 2100 Mbps, respectively. The data indicate that single-beam uplinks are inadequate. The total capacity problem can be handled for a limited number of users. The peak-to-peak average factor for medium- and high-capacity users cannot be achieved.

A space-fed downlink phased array may be used. If so, a separate multibeam uplink antenna should be considered. This may be a reasonable combination, since the efficiency and reliability problems on the uplink and downlink are sufficiently different to justify independent solutions. Uplink and downlink data rates and formats may be selected independently with the on-board processor correcting any incompatibilities.

#### 8.4 TDMA FRAME PERIOD SELECTION

The frame period is the amount of time between data bursts to and from a particular user. Frame period selection is driven by several factors:

- a) TDMA losses
- b) On-board and terminal data buffer size
- c) Data time delay.

TDMA loss considerations lead to long frame periods. Buffer size considerations lead to short periods. Time delay considerations favor short periods, but are not usually significant when compared to the 260 ms turn-around propagation delay.

With 100 to 200  $\mu$ s lost to TDMA switching and acquisitions, frame periods on the order of several milliseconds are attractive. Ten millisecond periods give 98 to 99 percent TDMA efficiency. With a 3 Gbps throughput the satellite buffer size is about 60 Mbits. If 64 kbit chips are available and space qualified, 900 chips are required.

This is clearly a subject for a fairly detailed tradeoff. For the purpose of defining a system baseline, a 1-ms frame period has been selected. TDMA efficiency is then 80 to 90 percent and burst buffer size is 6 Mbits (92 each 64 kbit chips). Buffer time delay through the entire system is less than 5 ms and is negligible compared to propagation delay.

#### 8.5 SYNCHRONIZATION METHODS FOR SSTDMA

The baseline approach for the 30/20 GHz Mixed User Architecture Study is to implement an SSTDMA/SDMA (Spacecraft Switched Time Division Multiple Access/Space Division Multiple Access) system. The general idea is to employ multiple beam antennas pointed at different areas (spot or area-coverage beams) within the U.S. Use of space division allows high EIRP and frequency reuse. The number of beams available are shared on a time division basis as described below.

With the exception of certain fixed beams, it is assumed that a switch matrix exists in the satellite to cyclically provide interconnections between all transmitters and receivers in the system. The switch is most likely controlled by an on-board oscillator, but may be controlled from the ground. In any case, the satellite switch presents a timing reference that is not present in conventional TDMA systems. It is assumed that the switch is programmed by a master station and that, at any given time, every terminal knows when its transmissions should arrive at the satellite so as to be received correctly. The problem considered here involves determining the satellite time at the ground station and to compensate for other errors such as propagation delays due to satellite motion.

It should be pointed out that while some authors in the literature never mention the words "initial acquisition," their "synchronization" papers invariably include it. Thus, techniques from initial acquisition papers are first mentioned but there is inevitable overlap with the synchronization section. Essentially, initial acquisition is the process whereby a station is brought into synchronization with an operating TDMA network from a cold start. The primary objective is to not interfere with existing communications in the network.

### 8.5.1 Initial Acquisition

The task of initial acquisition can be briefly defined as the process of placing a burst within a TDMA frame when a station has been inactive long enough so as to have no a priori information as to where its burst should rightfully go. Two fundamental issues are then:

- a) Where should a given burst be properly placed within a frame?
- b) At what time should a station transmit so as to attain the above location for its burst?

The latter is determined by knowledge of the round trip propagation time (approximately 270 ms) between the earth station and a satellite. The former question is answered upon reception of a reference burst back at the station attempting acquisition. A third problem present in SSTDMA burst communication is:

- c) How does a station achieve initial acquisition without interfering with the data transmission of other stations within its beam?

If a station is the first in its beam to use the system, this is obviously no problem. The solution for the second station (and subsequently all the rest) entering the system is to transmit at a relatively lower power level, e.g. 20 dB down from the normal power level. Since the typical satellite transponder will be operated near saturation, the nonlinear effect will be such that acquisition information exists "virtually" only where it is supposed to be. That is, the contribution of the initial acquisition signals will be noticeable only when no data bursts exist (e.g., the acquisition window). The degradation due to noise during this low level period will be discussed later.

A useful approach previously proposed for identifying the acquisition "aperture gate" is to transmit a pulse of width  $\Delta$  once per frame, each time advancing the pulse by  $\Delta$  seconds from the beginning of the frame. Thus, the frame length is swept until the aperture gate is reached (see Figure 8-4).

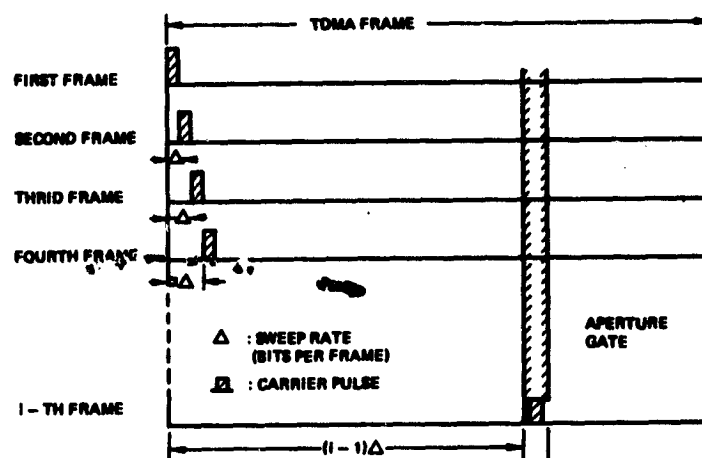


Figure 8-4. Acquisition Signal In The Simple Approach

After counting the number of TDMA frame periods between transmission and reception due to the aperture gate, subtraction of the number of frame periods for round trip propagation yields the correct time for that station to transmit the burst. This method is quite simple, but it has the disadvantage of requiring range prediction to determine the time to transmit the burst.

Two cases need to be considered relative to the above scheme:

- 1) Spot beams
- 2) Area-coverage beams.

For the purposes of this discussion only, a spot beam is defined as one being solely occupied by a single (probably trunking) terminal. It is thus assumed there may be no loop-back aperture. For area-coverage beams the above procedure would be useful since a TDMA terminal will directly view its own acquisition signal. However, a "spot-beam" needs the assistance of some other TDMA terminal which will detect the swept carrier pulse and then inform the acquiring terminal. Since the assisting terminal cannot know the initial transmission of the swept carrier pulse, it must also send back its received time and own estimated propagation delay. The additional error in the round trip delay time to and from the assisting terminal will tend to render the final result too inaccurate.

The need for range prediction above arises since the initial transmit time of the swept carrier cannot be known at the receiving side. However, a simple modification can alleviate this problem. Prior to the procedure in Figure \_\_\_\_, a wide carrier pulse (an integer multiple of frame lengths) is transmitted. The receiver eventually detects the wide pulse and, using that time as a reference, starts counting the number of frame lengths until the above swept narrow pulse is received. Since this count represents the total number of frames needed for the swept pulse to reach the aperture, multiplication by delta (the sweep-width) yields the correct burst transmission time.

#### 8.5.1.1 Carrier-Pulse Detection

The situation above lends itself to the usual envelope threshold detection (after narrowband filtering) to decide whether or not a pulse exists. This is essentially the classical radar detection problem where two types of errors can occur, a "miss" and a "false alarm." The former type of error only delays the time to achieve initial acquisition. Since this procedure, hopefully, will not be required very often, a "miss" is not considered too serious an error. Conversely, a false alarm misleads a station into sending (at a high-power level) data bursts at the wrong times. This interferes with system communication and must be considered very serious.

During acquisition, as previously noted, the carrier-to-noise ratio is very low. To raise the probability of correct detection and lower the probability of errors, integration over several frames is employed. For the first wide carrier pulse, the aperture window is completely filled with signal; thus, the noise bandwidth of the filter can be made relatively narrow (proportional to the duration of the thin aperture window). Therefore, the wide carrier detection should be adequate; still, integration could be used for further improvement. For the narrow pulse, the energy per bit will not guarantee sufficient reliability; thus, digital integration counting the number of detections  $N$  within  $M$  frames is necessary before comparing to a threshold. This procedure can be used in conjunction with PN sequences.

### 8.5.2 Synchronization Schemes

Initial Acquisition is essentially the process whereby a station is brought into synchronization with an operating TDMA network. Hopefully, this will seldom be needed excepting cold start-up and major equipment failures. The purpose of the synchronization function is for a terminal to arrive and stay in its preassigned time slot for transmission. The achievable accuracy of synchronization will have implications on the amount of guard time per frame. This in turn is a major factor in determining the frame efficiency.

What is presented below is a three step synchronization scheme. Specifically, it consists of a coarse search mode, a fine search mode, and a tracking mode. From here on in, it will be assumed that each station does have a sync window once per TDMA frame where its own transmission is looped back to itself. The time between two successive windows is the frame length. A ground station achieves synchronization when its sync burst signal falls in the sync window causing it to be modulated by the window. By comparing the modulation to the known burst, the timing base can be adjusted.

Basically, the coarse-search mode attempts to at least partially hit the sync window with a sync burst. Since the sync window width is relatively narrow, this will take too much time if a small increment is used. Once the window has been hit, a smaller step size (fine search mode) can be successfully employed.

Two types of coarse search signals are described:

- a) PSK Sync Bursts
- b) PSK Coded Search Signals.

#### PSK Sync Burst

A PSK sync burst consists of two pulses of the same carrier, but with opposite polarities, 0 and 180 degrees. Stations achieve synchronization by transmitting a train of such bursts at its own unique frequency. The width is slightly larger than the sync window. The relative transmission time is incremented until the window is hit, in which case (depending on the relative widths of the 0 degrees and 180 degrees modulated pulses)

the timing need only be slightly advanced or retarded. Assuming nominal ratio of sync window to frame length of 1/125 this process will take anywhere from 270 ms to 40 s (20 s is about average). Unfortunately one has to wait one round-trip time before sequentially incrementing the next burst time. The bandwidth for such a PSK sync burst of 6  $\mu$ s width (750  $\mu$ s frame) is obtained from the bit rate requirement which would be 0.33 Mbps. Finally, we note that this approach will initially create interference to other bursts.

### PSK Coded Search Signals

By using a PSK Coded Search Signal, coarse search synchronization is always achieved within 270 ms, independent of the ratio of frame length to sync window duration. At that point fine search can begin using PSK sync bursts. Two types of coded search signals are:

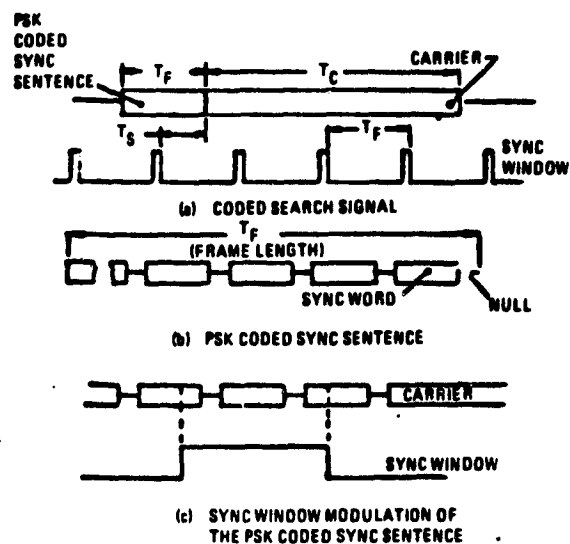
- a) Single-frame Coded Sync Sentence
- b) Multi-frame Coded Sync Sentence

#### Single-frame Coded Sync Sentence

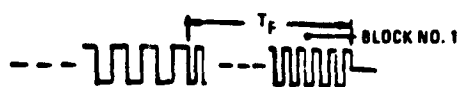
In this case the coarse signal consists of both a carrier part and a PSK coded sync sentence. The former can be several frame lengths while the latter portion is one frame length. After a one-way delay, carrier pulses are generated at the satellite and the earth station uses them for carrier lock. The sync window is wide enough to  $T_s$  seconds later pass at least one sync word back down to the station. By identifying this word (unique in the sync sentence) the station calculates  $T_s$  by identifying the code word following the first null (see Figure 8-5) below. Thus coarse search synchronization is essentially achieved in one round trip time.

#### Multi-frame Coded Sync Sentence

This signal is identical to the one above except that many frames of sync sentences appear after the carrier portion. Each succeeding block in the sentence has a bit rate reduced by a factor of two. The signal duration is longer and so the interference is 50% higher but the bandwidth is a factor of 10 less than the single-frame version. Considering fast acquisition, narrow bandwidth and short interference time, the coded search signal using a PSK multi-frame sync sentence appears to be best.



PSK Single - frame Coded Sync Sentence



(a) SETUP OF THE PSK MULTI-FRAME SYNC SENTENCE

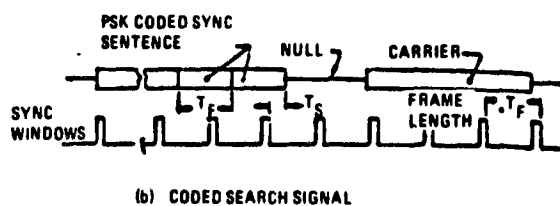


Figure 8-5. Codea Sync Sentences



### Fine Search Mode Using PSK Sync Bursts

The remaining problem is to reduce the initial timing inaccuracy left after coarse synchronization. By comparing the sync window modulation to a known burst sequence, timing is adjusted on a finer scale. Two methods are described:

- a) Digital control
- b) Analog control.

#### Digital Control

PSK sync bursts are looped back after sync window modulation. The bursts are coherently detected producing a waveform with positive and negative parts. The video burst is used to gate clock pulses into a counter. The counter counts up or down corresponding to the sign of the burst sample. The time based is sequentially adjusted to half the error. Precision is restricted to the width of a clock pulse (30 ns) with such a digital approach.

#### Analog Control

In this case the coherently detector video wave form is integrated pulse by pulse to produce an error voltage: This voltage drives a VCO slightly changing the frequency over a short period, in effect producing a phase shift. Another train of pulses is sent and the procedure eventually converges to a zero VCO input voltage (zero timing error). The limits of accuracy depend on the number of pulses integrated and the SNR. Thus, precision can be essentially reduced to zero with an analog control. As in the digital case, satellite motion is still the main source of error.

### Tracking Mode Using PSK Sync Bursts

Since the VCO in Analog Control above has two adjustable parameters, i.e., phase and frequency, the latter can be used to reduce the timing error due to satellite motion. A tracking network inputs a small correction voltage to the VCO, so as to produce a small frequency offset. In this way, it is anticipated the timing error can be reduced to several nanoseconds.

### 8.5.3 Synchronization with Three Control Stations

In a recent paper, a technique is described that requires only three master control stations to transmit synchronization signals. From its received signal each of the three stations calculates space delay. If not all of the stations are located colinearly (ideally they should form an equilateral triangle to the satellite), the satellite coordinates can be calculated. The three stations can achieve this measurement using sync techniques. Next; it only remains for these control stations to broadcast their space delays to the rest of the system. Since every station knows where the three stations are located, it can find its own propagation delay by simple geometric calculations. All that remains for any other station acquire synchronization is for some kind of time reference signal to be received. There are two possibilities described below:

#### Modified Sync Window

This "modified" sync window is suggested as a possible connection where all satellite transmitters are connected to all satellite receivers. All diode switches in the matrix must be closed simultaneously for the sync window duration. This may be achieved by applying a strobe to all the buffer decoders for the sync window duration. This degrades the uplink SNR for any one spot beam due to the number of receivers but the more limiting downlink performance is unaffected. This the detection of downlink signals is essentially unchanged by this modification.

The three control stations independently lock on to the modified sync window using techniques discussed earlier in this section. The one-way propagation delays are then easily calculated. What remains is to suitably encode this information to the other stations. One simple way is to use a PSK range signal where the propagation is expressed as a binary number and a 0 degrees phase shift represents a binary 0 and a 180 degrees phase shift represents a binary 1. Similarly, an FSK signal could also be used.

The earth station desiring synchronization then needs only to receive the three propagation delays from the control station and lock onto the time base of any one of the three signals for a reference. In this manner all the rest of the stations passively acquire synchronization.

### Transmission Through Data Windows

An alternative plan is for the satellite to send a reference sync burst to all beam zones at the beginning of the frame. The sync window is not needed since the master stations can lock onto the data windows for their areas. This is done with conventional techniques. Thus, they can measure the propagation delays and transmit them to the other stations using ordinary data windows. The other stations acquire sync passively by using this data (to calculate its own space delay) in conjunction with the satellite reference burst.

#### 8.6 SHORT-FRAME TDMA VERSUS LONG-FRAME TDMA

One of the critical issues to be resolved in a phase modulated system is the method of acquisition at the earth terminals of carrier and data clock phase-information. Two basic approaches warrant consideration. The first is to use carrier and data clock tracking loops in the earth station receivers. Since data arrives from many different stations in a time-division multiplexed format, the earth stations receive data from any one given station only once per TDMA frame. If there are many users in the system, there will be long delays between subsequent burst arrivals from any given station. Thus the tracking loop must attempt to remember the previous phase (called "flywheeling") from frame to frame. Typically, if the loop is designed to optimize memory length, its ability to follow any sudden phase changes will be unacceptable. It is thus wise to select a reasonably short frame length (short-frame TDMA).

An alternative approach is termed long-frame TDMA. In this case the receiver performs independent acquisitions at the beginning of each data burst. Since no attempt is made to remember the phase from burst to burst, more overhead time will be required. The best way to combat this efficiency problem is to make the frame length longer.

TRW has had practical experience in building and testing both long-frame and short-frame SSTDMA systems through prior contracts. The short-frame TDMA scheme was used in a contract report in 1976. Some results from that report are reported in the following pages. Some fundamental issues are:

- o Private-line earth terminals must be very inexpensive possibly at the cost and inconvenience of the richer trunking users.
- o Short-frame TDMA tends to be more efficient since phase information from frame to frame is remembered.
- o However, short-frame TDMA may require a single earth station to have a separate PLL for each of all earth stations with which it will communicate.

Critical tradeoff factors then become efficiency, cost of additional tracking loops in short-frame, and cost of memory required in long-frame TDMA. Since the cost of the DTU terminal must be kept low and since memory becomes increasingly less expensive, the long-frame TDMA approach will be the baseline choice in the study.

The key features of TRW SSTDMA analysis and laboratory demonstration are listed below:

- o Uses QPSK mod, demod, and bit sync to achieve a 800 Mbps rate
- o Free running 4 x 4 microwave spacecraft switch matrix used
- o Filter with loop transfer function with -3 dB point at 5 kHz and damping = 0.707 optimum for class considered
- o Later found loop gain compensation necessary to counteract performance impairment caused by reduction of signal power due to burst mode operation
- o  $B_cR$  versus  $E_b/N_o$  and time into the burst plotted for several combinations of frame and subframe lengths
- o Phase noise added to simulate expected range of values generated by oscillators in ground and satellite stations
- o Measured performance degraded by 2.5 to 4 dB relative to ideal PSK - similar to long-frame TDMA.

## 8.6.1 Summary of Short-Frame SSTDMA Results

### 8.6.1.1 Phase Noise

Various levels of phase noise were added into the test setup, as shown in Figure 8-6. In reality this noise would be a result of oscillators in all of the ground/space-ground links. This phase noise would enhance the degradation caused by the finite time required for the satellite-switched signal to reach full power. Since the data is increased due to the additional uncertainty in determining phase locations the phase noise was then measured just prior to the input to the demodulator for data detection. It was found that sometimes more phase noise was present in the output data channel than appeared at the input to the tracking loop.

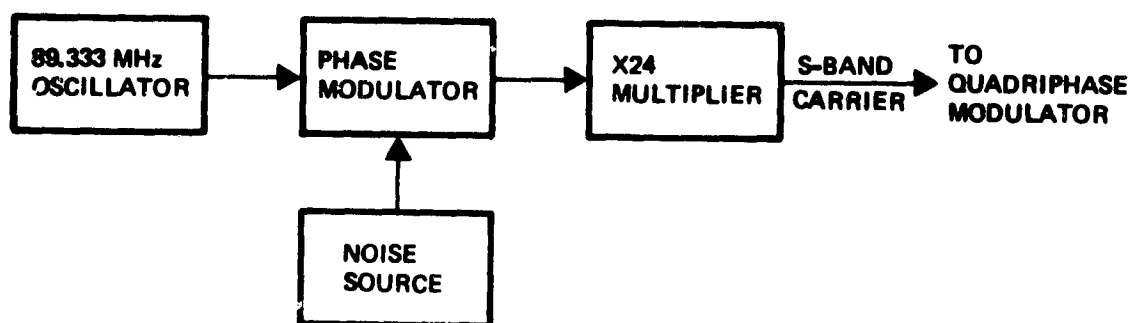


Figure 8-6. Phase Noise Versus Data Detection

### 8.6.1.2 Filter Loop

Filters were considered of the form of

$$|H(f)|^2 = \frac{1 + (2\zeta f/f_n)^2}{\left[1 - \left(\frac{f}{f_n}\right)^2\right]^2 + \left(\frac{2\zeta f}{f_n}\right)^2}$$

where

$$\begin{aligned}\zeta &= \zeta_0 \sqrt{d} \\ f_n &= f_{n_0} \sqrt{d}\end{aligned}$$

and

$\zeta$  = the loop damping factor for the SSTDMA mode

$\zeta_0$  = the loop damping factor for the continuous mode

$d$  = the duty factor (burst length/frame length)

$f_n$  = the loop natural frequency (Hz) for the SSTDMA mode

$f_{n_0}$  = the loop natural frequency (Hz) for the continuous mode

Within this class, simulation showed that a 3 dB frequency of 5 kHz and a damping of 0.707 resulted in the best BER performance. Due to the effect of the duty factor  $d$ , and AGC was later required to provide constant average power as  $d$  is varied. The results of the simulation verified the notion that a narrow loop bandwidth provides the best phase memory characteristic, possibly at the expense of initial acquisition time.

#### 8.6.1.3 Probability Distribution of Steady-State BER

Figures 8-7a and 8-7b show the measured distribution of the time required to reach steady-state BER. For example, by 8 bits into the burst, 75 percent of the cases reached steady-state BER. By 16 bits into the burst, over 90 percent had reached steady-state BER. These graphs represent an accumulation of data taken for various expected frame lengths, subframe lengths, phase noise values, and SNR. The SNR ranged from 11 to 17 dB (high values only). The frame lengths ranged from 2.56 to 328  $\mu$ s. Similarly, the subframe lengths were programmable from 0.08 to 7.92  $\mu$ s. The phase noise values measured were from 0.5 degree to approximately 10 degrees. While the degradation from ideal QPSK varied greatly with the above parameters, the time to reach steady-state BER was reasonably constant. Figures 8-8a and 8-8b constitute such a representative sample.

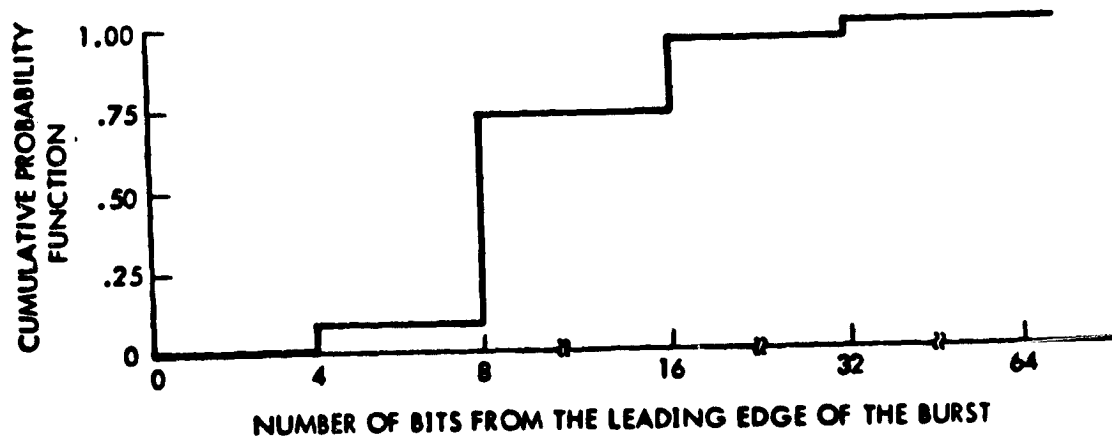


Figure 8-7a. Distribution of Occurrence of Steady-State BER as a Function of Position Within a Data Burst

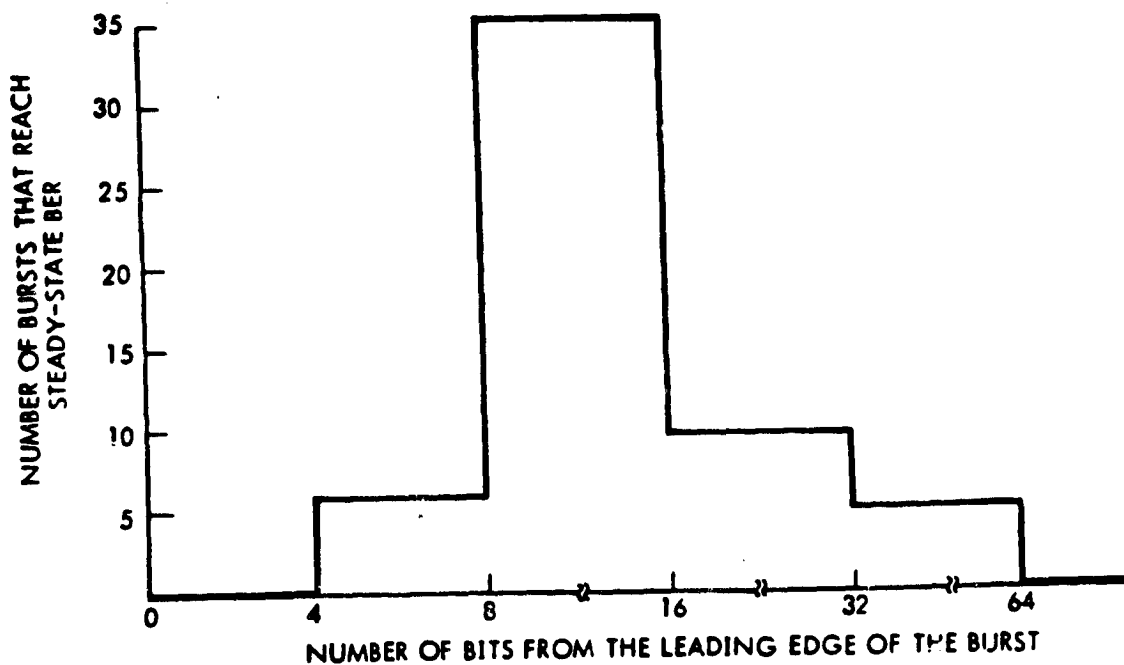


Figure 8-7b. Cumulative Probability of Bursts to Reach Steady-State BER as a Function of Position Within a Data Burst

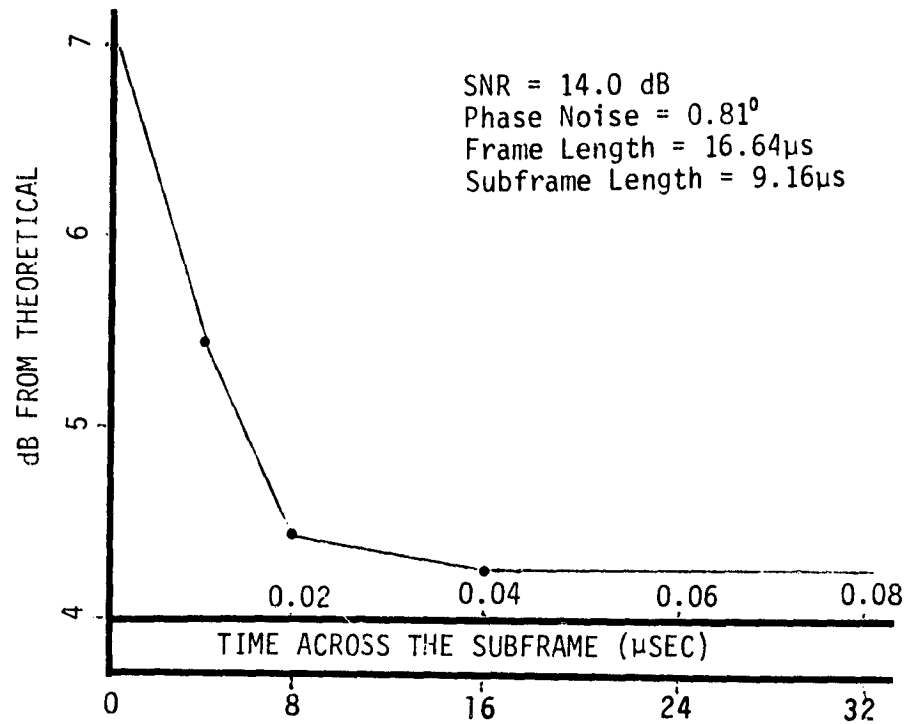


Figure 8-8a. BER versus Position

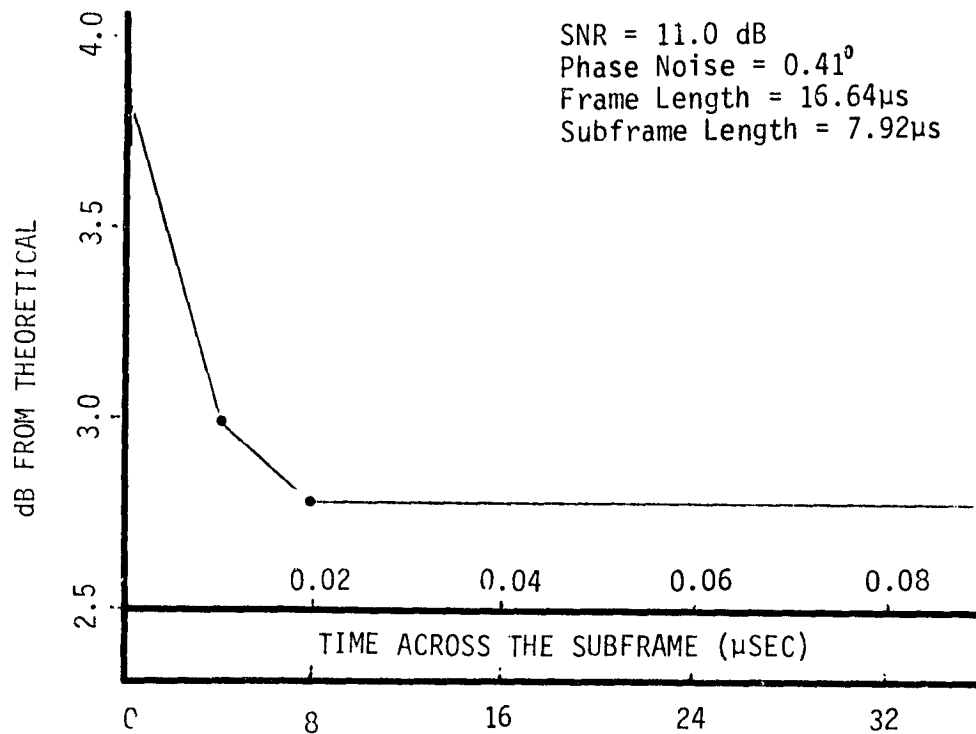


Figure 8-8b. BER versus Position



#### 8.6.1.4 Loop Memory

Initially, it was planned to fix the subframe length and sequentially increase the frame length until the PLL lost lock. This value was recorded. Unfortunately, drifting problems arose and all that was shown was for a frame length of up to 128  $\mu$ s; the loop did not lose lock. This was true for burst lengths as short as 0.160  $\mu$ s.

#### 8.6.1.5 BER versus $E_b/N_0$ Performance Curves

Several weeks of tests were performed to measure steady-state BER versus  $E_b/N_0$ . As expected, as the duty factor increases, the performance approaches that of continuous transmission. Figure 8-9 shows a representative sample of 14 cases considered corresponding to different frame lengths, subframe lengths, and phase noise values. The results seem comparable but slightly worse than the long-frame TDMA curves in an earlier study. However, as will soon be noted, the guard time of short-frame TDMA is shorter (the efficiency is greater).

#### 8.6.1.6 Guard Interval Budget

Table 8-1 illustrates the guard interval budget for the short-frame TDMA study. As was discussed previously, the subframes occur for only a short portion of each frame. Thus, the phase-locked loop must flywheel through the time when no signal is present. Any drift in the VCO during this time must be taken into account in the guard interval budget. The budget is self-explanatory, but the following comments should be made.

- a) The first entry is due to the "turn-on" time of the SSTDMA switch.
- b) The second entry is actually almost totally due to bit synchronization assuming the flywheeling capability is good.

In summary, the guard interval budget appears to be about half to two thirds of that for burst-to-burst acquisition. However, in light of the ever-decreasing cost of memory, if inexpensive receivers are the goal, the long-frame TDMA approach would be more desirable.

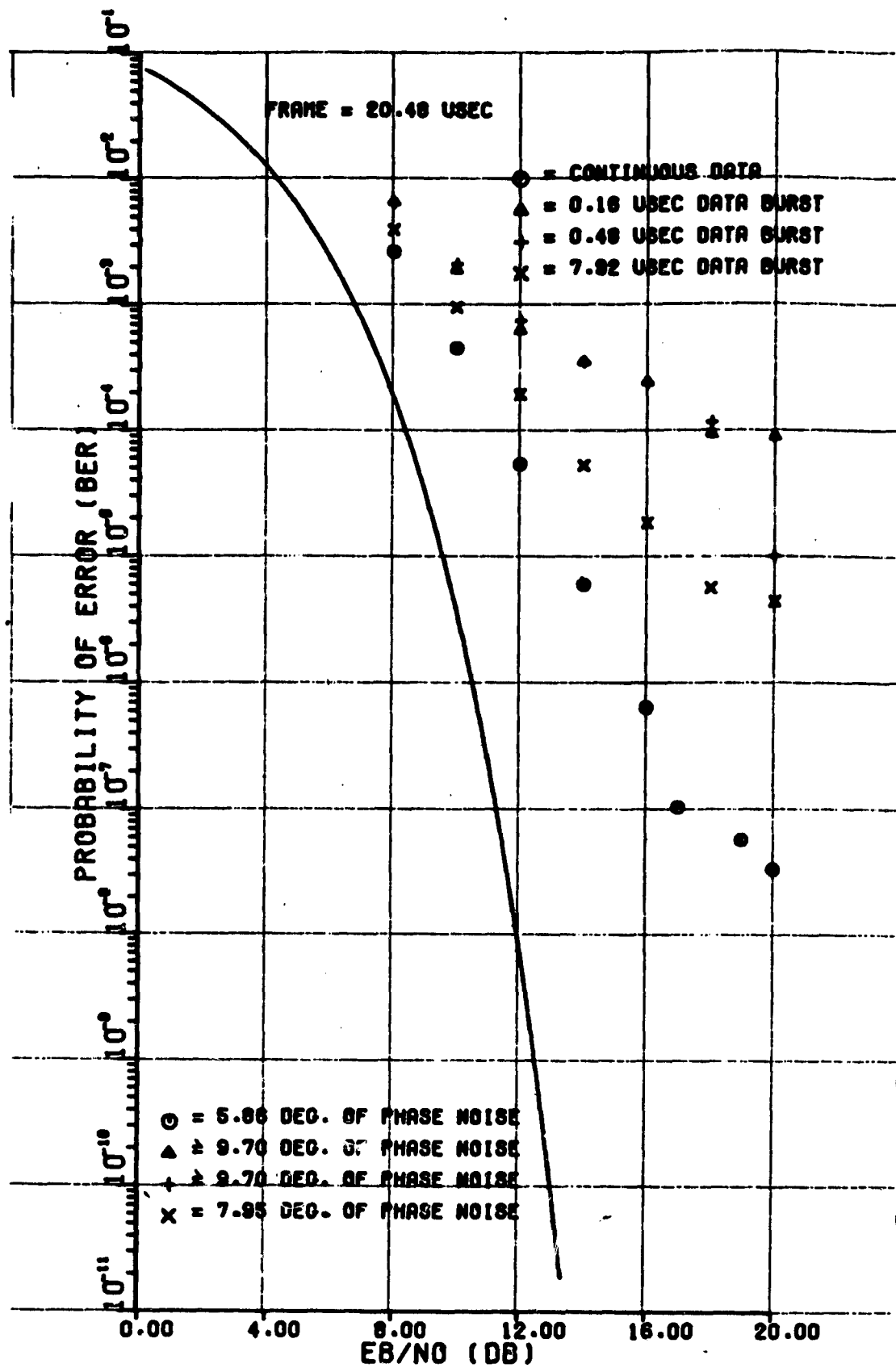


Figure 8-9. BER vs  $E_b/N_0$

Table 8-1. Guard Interval Budget

Parameter	Value (nsec)	Comment
Switching Time of SSTDMA Switch	20.0	Data from SSTDMA experiment
Acquisition Time of Phaselock Demodulator	20.0	Measured data
Acquisition Time of Bit Synchronizer		
Measurement Error of Time Delay in Ground Terminal	5.0	The applicability of this entry depends on the synchronization technique used
Measurement Error of Spacecraft Processing Time	5.0	The applicability of this entry depends on the synchronization technique used
Range Uncertainty due to Synchronization Limitations	7.0	3 bits x 2.22 nsec/bit
Range Uncertainty due to Spacecraft Motion	3.1	8.8 ft/sec x 0.35 sec (round trip) x $1.018 \times 10^{-10}$ sec/ft
Oscillator Short-Term Stability	0.1	$10^{-10}$ sec/sec
Logic Jitter	0.2	10% of bit time for jitter due to noise on data causing early or later triggering of logic circuits
Total	60.4	

#### 8.7 EFFICIENT TRAFFIC SCHEDULING FOR THE SSTDMA SWITCH

The problems of synchronization and acquisition to the TDMA frame via the SSTDMA switch have been addressed. It is critical to minimize the amount of overhead time necessary per frame to prepare the system for effective communication. It is equally important to use the available "communication data time"  $T_D$  efficiently by programming the  $n \times n$  switch matrix intelligently. What appears to be a simple procedure when  $n$  is small, becomes increasingly tedious as the number of transmitters (and the

number of subsequent options) grows. Thus, as the distribution of traffic demands changes, it is important to have a relatively fast and simple computer algorithm to calculate an "efficient" frame setup. This is then accomplished through a switch controller in the satellite. The switch sequence is used to cyclically interconnect system transmitters to receivers. In this way the transponders appear to have beam-hopping capability.

The question arises as to what is an efficient scheme. In general, there may be other factors to consider. For example, if overlapping (in space) beams are used, it may be important for them not to be transmitting ever at the same time using the same frequency. Such considerations are intimately involved with beam deployment and types of orthogonality employed. In this section, a general approach is given regardless of such conditions. It is assumed that an  $n \times n$  traffic matrix is given and the scheduling will be efficient in the sense that the traffic is most densely packed. Since it turns out there are many such efficient schedules, a further restriction is imposed. This restriction is to minimize the number of satellite switching events. As has been seen earlier, these switching events can cost 20 to 30 nanoseconds additional guard time. In what follows, an approach called the "Greedy Algorithm"<sup>1\*</sup> is presented. An example is given, but due to some errors appearing in Reference 1, the correct solution is supplemented.

#### Key Features

- A lower bound on the time to communicate all the traffic in a given matrix is the time represented by its busiest row or column.
  - The algorithm proposed always achieves this lower bound.
- Finding such a scheme that also minimizes the number of switching events is mathematically untractable. The minimum number would be  $n$  (uniform traffic matrix).
  - The algorithm proposed always guarantees no more than  $n^2 - n$  number of switchings.
  - Simulations indicate this upper bound is pessimistic in practice, i.e., the number of switchings<sub>2</sub> proposed by the algorithm is virtually always less than  $n^2 - n$ .

The proposed algorithm is shown in Figure 8-10.

\* See references in Section 8.8.

### C. "Greedy Algorithm"

"Greedy Algorithm" consists of the following steps.

**Step 1:** Find a row (or column) that has maximum traffic in a given matrix  $D^{(i)}$ . This row (or column), say the  $i_0$ th row (or column), is called a "critical" row (or column).

**Step 2:** Find a maximum element ("critical" element) in the critical row (or column).

**Step 3:** Disregarding the row and column which contain the "critical" element, find the maximum element in the residual elements.

**Step 4:** Repeat the same procedure as Step 3 (by  $N$  times), again eliminating the rows and columns which contain(s) the elements selected in the previous steps.

**Step 5:** Extract  $N$  elements found in the former steps, thereby dividing the given matrix  $D^{(i)}$  into two parts,  $D_1^{(i)}$  and  $D_2^{(i)}$ .

**Step 6:** If the  $i_0$ th row (or column) of the matrices  $D_1^{(i)}$  and  $D_2^{(i)}$  are also critical row (or column), go to Step 10. Otherwise, go to Step 7.

**Step 7:** When there exists an element larger than the "critical" element in the first matrix  $D_1^{(i)}$ , put back excess amount of traffic to the second matrix  $D_2^{(i)}$  so that the "critical" element is maximum in  $D_1^{(i)}$ .

**Step 8:** If the  $i_0$ th row (or column) of  $D_2^{(i)}$  is not critical, put back the same amount of traffic from  $D_2^{(i)}$  to  $D_1^{(i)}$  within the limit of Step 7, so as to maintain the  $i_0$ th row (or column) critical.

**Step 9:** If  $D_1^{(i)}$  is zero, select the second largest element as "critical" and repeat the same procedure.

**Step 10:** Repeat those from Step 1 as to the second matrix  $D_2^{(i)}$  by setting  $D_2^{(i)} = D^{(i+1)}$ . This process is repeated  $l$  times until  $D_2^{(i)} = 0$ , and finally  $D$  is expanded as follows:  $D = D_1^{(1)} + D_1^{(2)} + \dots + D_1^{(l)}$ .

**Step 11:** Compose transmit-frame format by arranging the nonzero elements of  $\{D_1^{(i)}\}$ .

The procedure is illustrated with the following example.

#### Example

An example traffic matrix is given as follows:

$$D = \begin{bmatrix} 1 & 1 & 1 & 7 \\ 3 & 2 & 4 & 2 \\ 1 & 3 & 2 & 1 \\ 5 & 4 & 2 & 1 \end{bmatrix}$$

#### 1) The 1st Iteration:

**Steps 1-2:** The 4th row is critical. Element  $d_{41}$  is the critical element.

**Steps 3-5:**  $D = D_1^{(1)} + D_2^{(1)}$

$$= \begin{bmatrix} & & & 7 \\ & & 4 & \\ & 3 & & \\ 5 & & & \end{bmatrix} + \begin{bmatrix} 1 & 1 & 1 & \\ 3 & 2 & & 2 \\ 1 & & 2 & 1 \\ & 4 & 2 & 1 \end{bmatrix}$$

**Step 6:** The 4th row of  $D_1^{(1)}$  is not critical.

**Step 7:** Excess traffic of  $d_{14}$   $2 = d_{14} - d_{41}$  should be put back to  $D_2^{(1)}$  and finally

$D = D_1^{(1)} + D_2^{(1)}$

$$= \begin{bmatrix} & & & 5 \\ & & 4 & \\ & 3 & & \\ 5 & & & \end{bmatrix} + \begin{bmatrix} 1 & 1 & 1 & 2 \\ 3 & 2 & & 2 \\ 1 & & 2 & 1 \\ & 4 & 2 & 1 \end{bmatrix}$$

#### 2) The 2nd Iteration:

**Steps 1-5:**

$$D_2^{(1)} = D_1^{(2)} + D_2^{(2)} = \begin{bmatrix} & & & 2 \\ 3 & & & \\ & & 2 & \\ & 4 & & \end{bmatrix} + \begin{bmatrix} 1 & 1 & 1 & \\ & 2 & & 2 \\ 1 & & & 1 \\ & & 2 & 1 \end{bmatrix}$$

**Steps 6-8:** The 4th row of  $D_2^{(2)}$  is not critical. To maintain the critical condition in  $D_2^{(2)}$  the traffic in  $D_1^{(2)}$  under the condition of Step 7 should be put back to  $D_2^{(2)}$ . Then

$$D_2^{(2)} = D_1^{(2)} + D_2^{(2)} = \begin{bmatrix} & & & 2 \\ 3 & & & \\ & & 2 & \\ & 3 & & \end{bmatrix} + \begin{bmatrix} 1 & 1 & 1 & \\ & 2 & & 2 \\ 1 & & & 1 \\ & 1 & 2 & 1 \end{bmatrix}$$

REPRODUCIBILITY OF THE  
ORIGINAL PAGE IS POOR

Figure 8-10. The "Greedy Algorithm"

Upon repeating the same procedure, the frame breakdown is expressed as

$$D + D_1^{(1)} + D_1^{(2)} + D_1^{(3)} + D_1^{(4)} + D_1^{(5)} + D_1^{(6)}$$

and the frame structure is as shown in Figure 8-11.

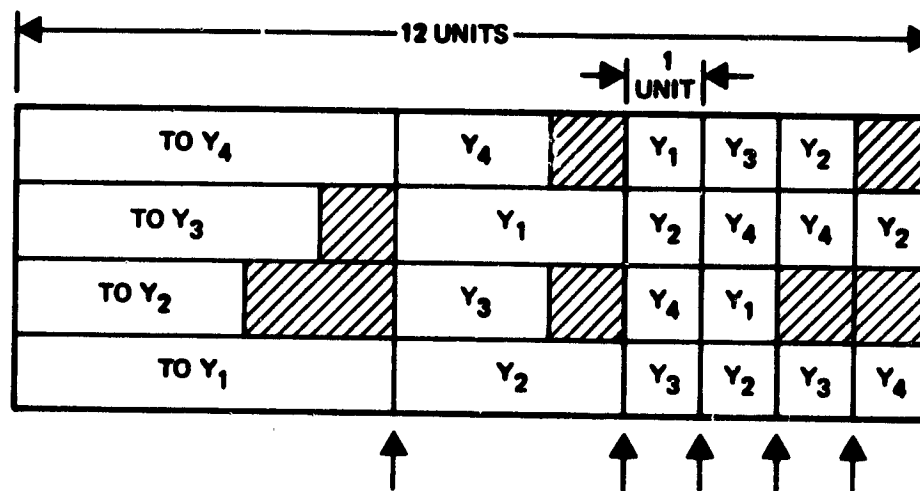


Figure 8-11. Frame Format for D

Using a random number generator to create traffic matrices, the simulated graph of Figure 8-12 was obtained.

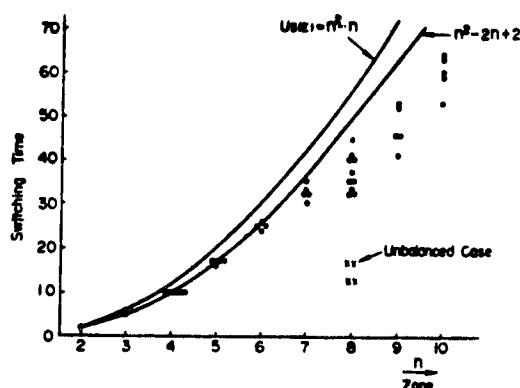


Figure 8-12. Simulation of "Greedy Algorithm"

In summary, an algorithm that is easily implemented by computer has been given. It transmits the required traffic in the minimum amount of time with a nearly minimal number of switching events.

## 8.7 COMPARISON OF MODULATION FORMATS

The two major signalling techniques for satellite communication applications are frequency-shift keying (FSK) and phase-shift keying (PSK). Both methods exhibit constant envelope. This feature is highly desirable for nonlinear satellite channels since the modulation is impervious to such impairments. Within the PSK class, there exist several modified methods of modulation such as simple biphase PSK (BPSK), quaternary PSK (QPSK), and offset QPSK (OQPSK). Minimum-shift keying (MSK) is a relatively recent discovery which can be considered either as a variant of OQPSK or as a continuous-phase FSK (CPFSK) signal. In what follows, a detailed comparison is made. The major features of this comparison, which promotes the relative superiority of MSK and OQPSK, are:

- a) PSK tends to provide superior (ideal) performance (+3 dB) to FSK and thus is generally favored for high data rate efficient satellite communication link applications.
- b) BPSK, QPSK, and OQPSK all perform optimally when used over ideal (linear all-pass with additive WGN) channels. Since the latter two QPSK schemes have twice the bandwidth efficiency of BPSK, they are better choices. Let  $T$  be the bit period, then MSK also is optimal if the receiver bases its decision on observations over two bit periods.
- c) In the presence of appreciable phase jitter, the co-channel orthogonality of QPSK experiences cross-channel interference, resulting in significant detection loss relative to BPSK. The use of OQPSK will yield detection loss equal to the average of BPSK and QPSK, while still retaining the latter (double) bandwidth efficiency of QPSK.
- d) Since MSK is a type of FSK, it can be noncoherently detected (by a discriminator) whereas QPSK systems require a fully coherent or differentially coherent detection scheme. This provides for an inexpensive, flexible demodulation alternative when the received  $E_b/N_0$  is sufficiently high.
- e) MSK is a form of OQPSK where half-cycle sinusoidal pulse weightings, as opposed to rectangular, are used. It can also be expressed as a continuous-phase FSK signal.
- f) Both OQPSK and MSK are superior to QPSK under bandlimiting or hardlimiting operations as are routinely encountered in satellite communications.



- g) Generally speaking, for system bandwidths exceeding  $2R$ , where  $R$  is the binary data rate, MSK will provide lower BER than OQPSK for equal transmitted power. For  $B < 1.1R$ , OQPSK will exhibit a lower BER. For values of  $B$  inbetween, the difference is not felt to be significant enough ( $< 1$  dB) to be a determining factor.
- h) Comparison of power spectral densities reveals that MSK has a wider main lobe but much smaller sidelobes when compared to OQPSK (same spectrum as QPSK). Thus OQPSK is most advantageous in bandwidth-limited systems whereas MSK would be preferred in power-limited systems with adequate bandwidth to accommodate its wider main spectral lobe.

As increasing digital communication traffic competes for frequency allocation in RF band, the need for efficient use of the available spectrum becomes obvious. Such methods as frequency-reuse through multiple beam antennas and dual polarization are beneficial in this regard. Source encoding techniques are employed frequently to compress redundant data. Last, it is important to choose a spectrally efficient modulation technique, that is, one that maximizes the bandwidth efficiency. The bandwidth efficiency is the ratio of data rate to channel bandwidth measured in bits/sec/Hz.

In general, there may be restrictions and limitations in any given communications scenario. An intelligent decision is based on the details of channel nonlinearities and passband characteristics that directly determine system performance. One such restriction is that of constant envelope. This is a critical feature since memoryless nonlinearities will produce extraneous sidelobes when passing signals that have amplitude fluctuations. This, in turn, can cause spillover into adjacent channels. A typical example is in a TDMA environment where TWT amplifiers are operated near saturation or in FDMA where ground terminal power amplifiers are in the nonlinear operating region. Thus, the use of constant envelope, bandwidth efficient digital modulation schemes is necessary.

#### 8.7.1 Comparison of PSK and FSK

Both PSK and FSK have the desirable constant envelope feature. While binary FSK uses two distinct frequencies to represent to binary levels, binary PSK uses two antipodal or opposite phases of a single carrier. The common measure of comparison is the required  $E_b/N_0$  to achieve a given BER. This comparison is for an ideal channel, which is a linear, all-pass



channel, corrupted only by WGN of single-sided power spectral density  $N_0$  watts/Hz. Optimal receivers for binary signals over an ideal channel are matched filters. PSK is among a class of schemes (observing a signal for  $T$  seconds) that is optimal in that minimum  $E_b/N_0$  is required to achieve a given BER. This optimal class is termed the class of antipodal or orthogonal signals. Such signals are in simple terms mutually independent. It can easily be shown that coherent FSK will suffer 3 dB performance degradation over an ideal channel relative to PSK.

#### 8.7.2 Advantages of Offset QPSK as Compared to Conventional QPSK or Bi-Phase PSK

While BPSK is also optimum in the sense noted above, due to the orthogonality of the sine and cosine functions, QPSK can also be optimally detected with the accompanying advantage of twice the bandwidth efficiency of BPSK. Conveniently, a modulated QPSK signal is given by the sum of two separate binary PSK signals as

$$s(t) = \frac{1}{\sqrt{2}} a_I(t) \cos(2\pi f_c t + \frac{\pi}{4}) + \frac{1}{\sqrt{2}} a_Q(t) \sin(2\pi f_c t + \frac{\pi}{4}) \quad (1)$$

where  $a_I$  and  $a_Q$  are the I- and Q-channel data streams. Equivalently, using trigonometric identities, it can be expressed more simply as

$$s(t) = \cos[2\pi f_c t + \theta(t)] \quad (2)$$

where  $\theta = 0$  degrees,  $\pm 90$  degrees, and 180 degrees, depending on the four possible combinations of  $a_I(t)$  and  $a_Q(t)$ .

As can be seen in Figure 8-13, offset QPSK (sometimes called staggered QPSK) differs from conventional QPSK only in that the relative starting times of the two bit streams are staggered by  $T$  seconds. This phase change does not change the power spectrum at all and as mentioned previously, both schemes are optimal for an ideal linear all-pass channel. However, as it turns out, OQPSK is superior when bandlimiting and hardlimiting operations, such as encountered in satellite communications, are involved. Essentially, the poorer performance of QPSK is due to the fact that the phase can change  $180^\circ$  instantaneously if both bits  $a_I$  and  $a_Q$  change. Since OQPSK uses staggered starting times, no more than an absolute instantaneous phase

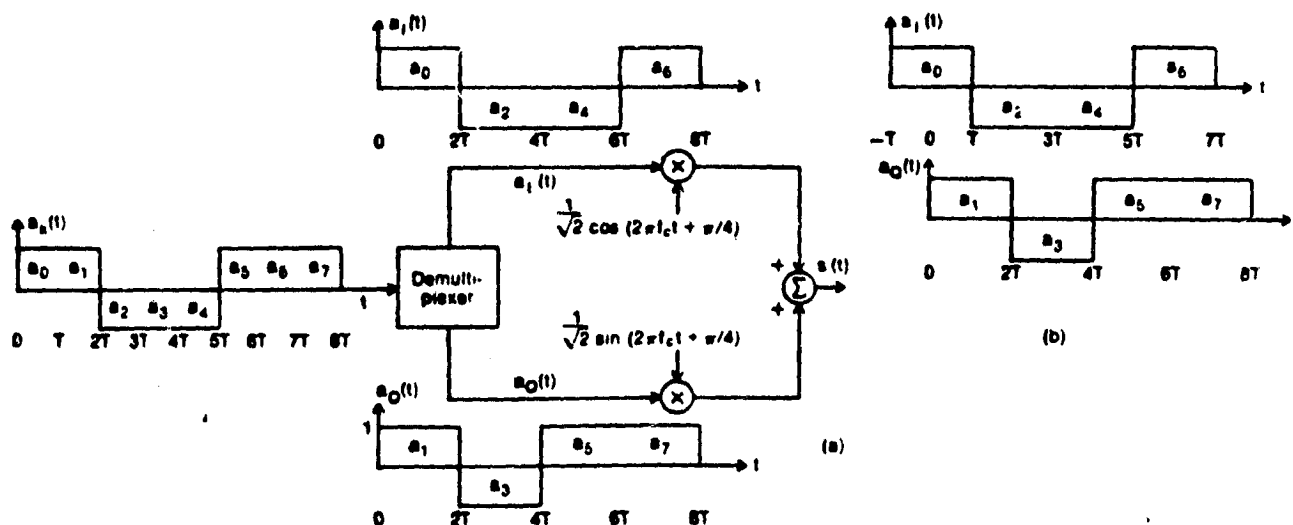


Figure 8-13. (a) QPSK Modulator; (b) Staggering of Data Streams in OQPSK

change of 90 degrees can occur. A phase shift of 180 degrees can cause the envelope of a bandlimited signal to go to zero. Hardlimiting will then restore some of the original (undesirable) frequency sidelobes that the bandlimiting removed. This may interfere with other existing communications on the satellite downlink. Thus, it is the presence of the 180-degree phase shift that degrades the performance of conventional QPSK. As can be shown, the T-second offset of OQPSK is also the optimum offset time in terms of phase jitter immunity in the presence of additive WGN.

Although simple binary PSK has only half the bandwidth efficiency of QPSK or OQPSK, it is the least of all degraded by carrier phase jitter in the coherent detector. Since QPSK employs two channels, under nonideal conditions, interchannel interference (cross coupling) results in deteriorated performance relative to single channel BPSK. It has been proven that OQPSK has a detection loss that is the average of the lower BPSK loss and the higher QPSK loss. Here detection loss represents required increase in the SNR of the coherent carrier phase reference (from a noisy unmodulated auxiliary carrier) to achieve a given BER. Typically, the use of OQPSK allows +3 dB relaxation relative to QPSK on the requirement of SNR of the phase reference. Figures 8-14 through 8-16 illustrate the BER performance versus SNR of the phase reference for BPSK, QPSK, and OQPSK.

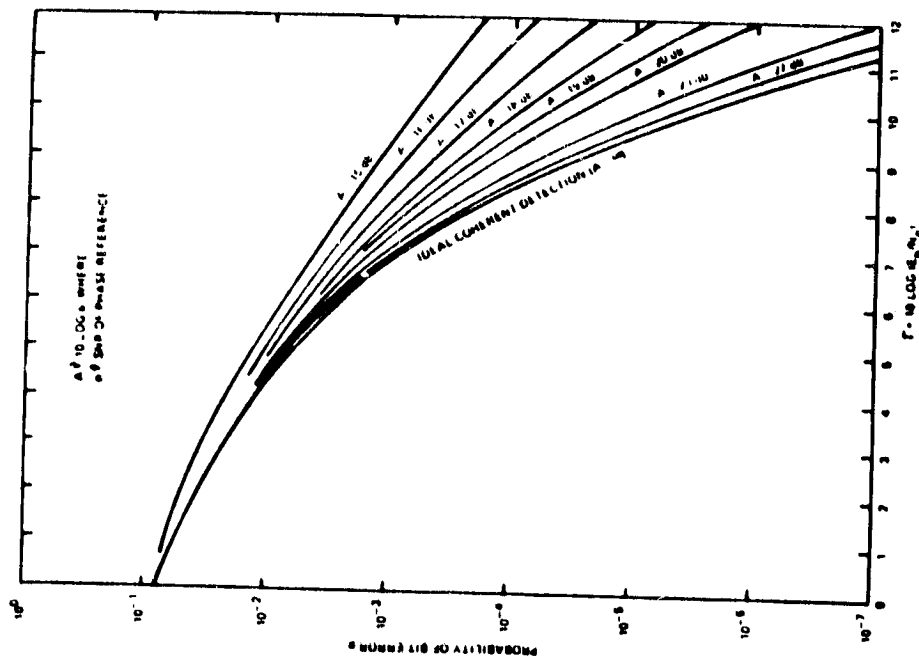


Figure 8-15. Coherent Detection Performance for Conventional QPSK

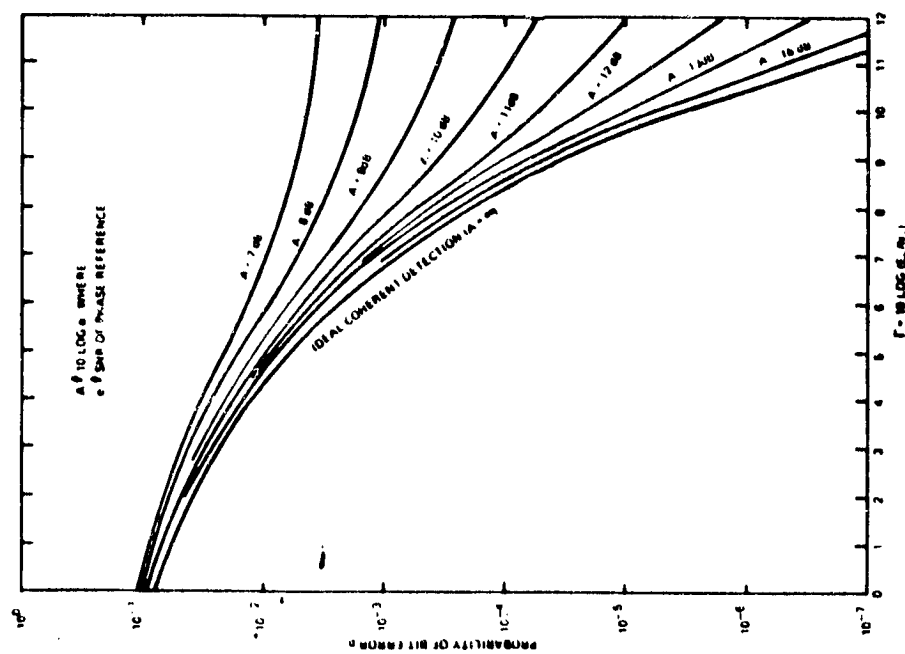


Figure 8-14. Coherent Detection Performance for BPSK

REPRODUCIBILITY OF THE  
ORIGINAL PAGE IS  
POOR

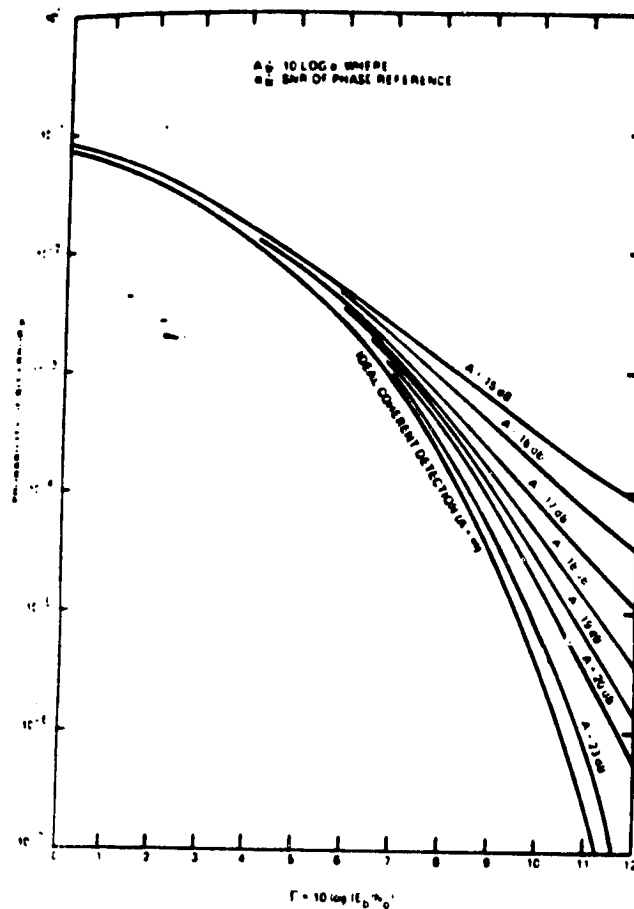


Figure 8-16. Coherent Detection Performance for Offset QPSK

REPRODUCIBILITY OF THE  
ORIGINAL PAGE IS GOOD

### 8.7.3 Minimum Shift Keying (MSK)

In the previous section, it has been shown that OQPSK is superior to QPSK for typical bandlimited, nonlinear (in general, nonideal) channels. A description of MSK will now be given and it will be seen that MSK also has superior performance relative to QPSK and in some cases should even be favored over OQPSK.

As noted earlier, MSK can be viewed as a form of OQPSK with half-sinusoidal rather than rectangular pulse weighting. Equation (1) is thus modified for MSK as

$$s(t) = a_I(t) \cos\left(\frac{\pi t}{2T}\right) \cos(2\pi f_c t) + a_Q(t) \sin\left(\frac{\pi t}{2T}\right) \sin(2\pi f_c t) \quad (3)$$

Figure 8-17 illustrates the various components involved in the MSK waveform of Equation (3). Similarly, as with QPSK in Equation (2), a trigonometric identity can cast (3) in the form

$$s(t) = \cos\left[2\pi f_c t + b_k(t) \frac{\pi t}{2T} + \phi_k\right] \quad (4)$$

where  $b_k = +1$  when  $a_I$  and  $a_Q$  have the same sign and  $b_k = -1$  when they have opposite signs. The phase term  $\phi_k$  is 0 or  $\pi$  corresponding to  $a_I = 1$  or  $-1$ . From Figure 8-17 and Equation (4) it can be deduced that

- 1) MSK has constant envelope
- 2) MSK does not contain any phase discontinuities
- 3) MSK represents also an RSK signal with  $f_+ = f_c + 1/4T$  and  $f_- = f_c - 1/4T$ . Thus the frequency deviation is half the bit rate, i.e.,  $f_+ - f_- = 1/2T$ .

This is the minimum frequency separation (usually it is  $1/T$ ) which allows two FSK signals to be orthogonal and so, the name minimum-shift keying is used. Note from Figure 8-17 (f) that the phase increases linearly and so MSK can also be viewed as continuous-phase FSK signal.

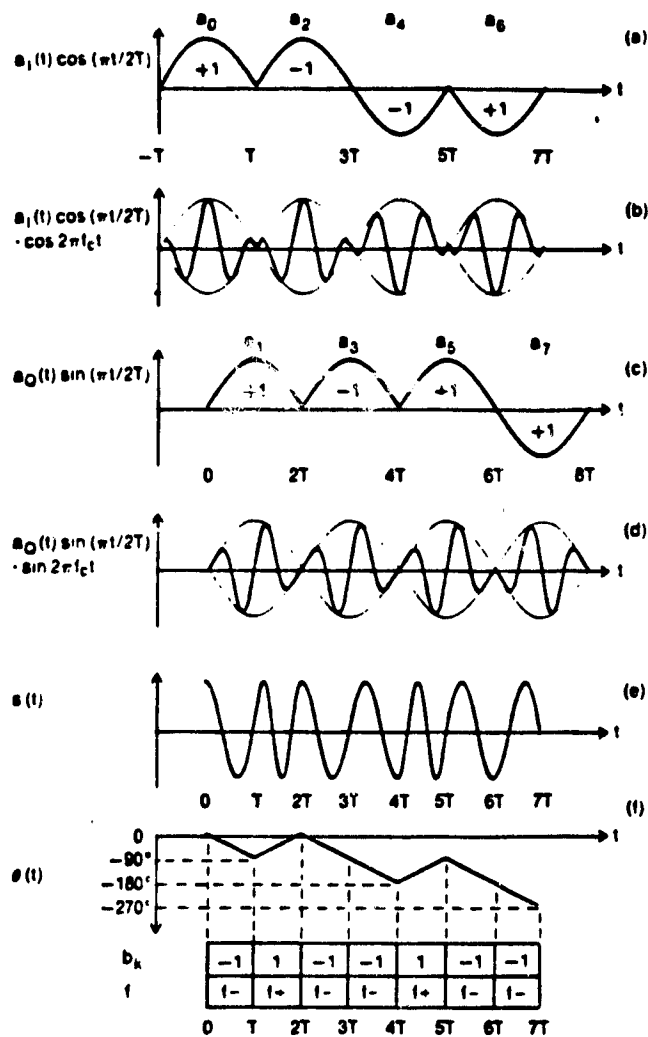


Figure 8-17. MSK Waveforms

REPRODUCIBILITY OF THE  
ORIGINAL DOCUMENT

Figure 8-18 shows a comparison of power spectral densities for QPSK, OQPSK, and MSK. As previously pointed out, MSK does have a wider main lobe but its sidelobes contain much less energy than either form of QPSK. Thus, in relatively wideband satellite links MSK would be more spectrally efficient than QPSK or OQPSK. However, in very narrowband links, OQPSK will be preferred.

When bandwidth efficiencies below 1 bit/sec/Hz are required, MSK has excellent special properties as an alternative to QPSK. The fact that it has continuous phase has advantages in a variety of applications. Also it has simple transmit, receive, and synchronization circuits, as will now be discussed.

Figures 8-19 through 8-21 illustrate the modulator, receiver, and synchronization circuits for MSK. The modulator consists mainly of two bandpass filters and subsequent multipliers to form the in-phase and quadrature-phase components. The demodulator essentially consists of integrate and dump match filtering over twice the symbol period.

The self-synchronization circuit is really the most interesting. While  $s(t)$  has no discrete components that can be used for synchronization, it does have strong components at  $2f_+$  and  $2f_-$  when passed through a (non-linear) squaring device. The squarer doubles the modulation index resulting in the conventional  $1/T$  frequency separation (known as Sunde's FSK). After the multiplications and additions indicated, a lowpass filter recovers the needed timing signal. Thus, MSK has a simple self-synchronization circuit.

#### 8.7.4 BER Performance of MSK

Both BPSK and QPSK have optimal performance over an ideal channel. It can also be shown that MSK will be optimal if a longer bit memory ( $2T$ ) is used before a decision has to be made. This is a crucial point and in fact, if only  $T$  seconds were allowed, MSK would be 3 dB worse than QPSK.

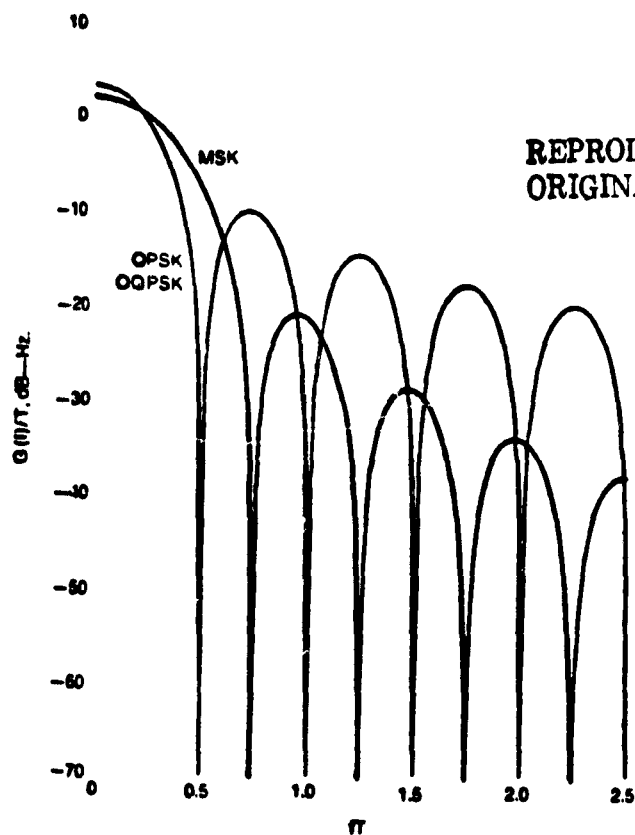
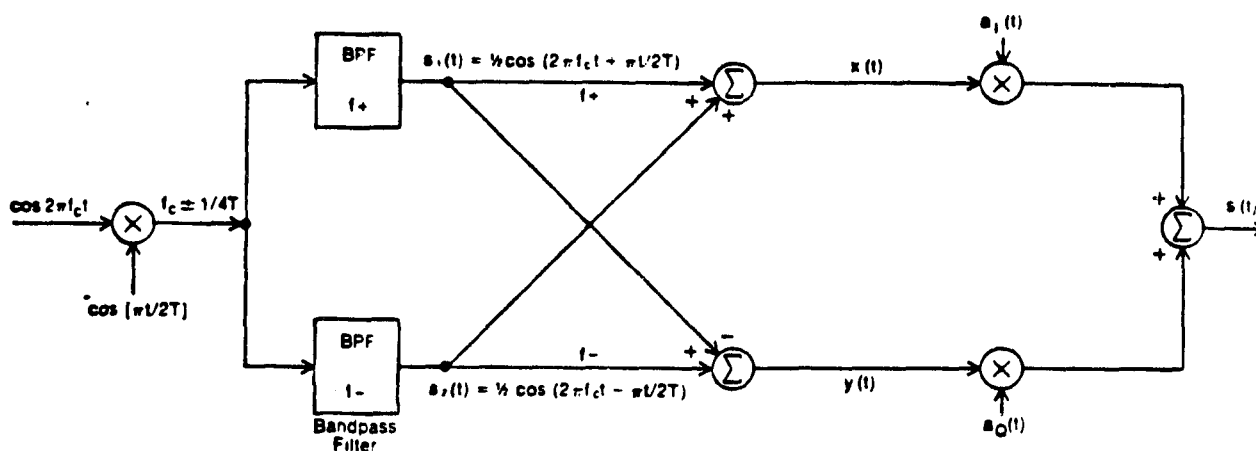


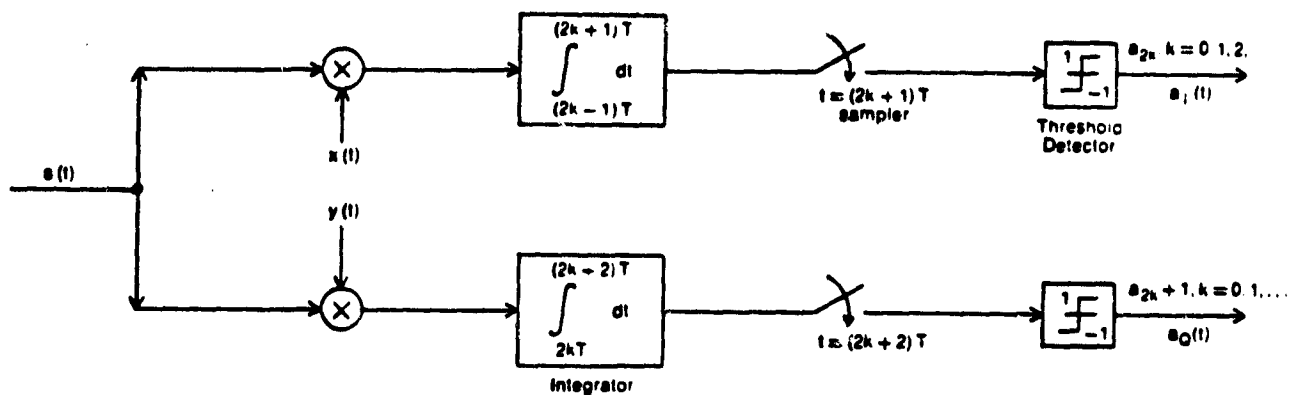
Figure 8-18. Spectral Density of QPSK, OPQSK, and MSK



$$x(f) = \cos(\pi/2T) \cos 2\pi f_c t; \quad y(t) = \sin(\pi/2T) \sin 2\pi f_c t$$

Figure 8-19. MSK Modulator

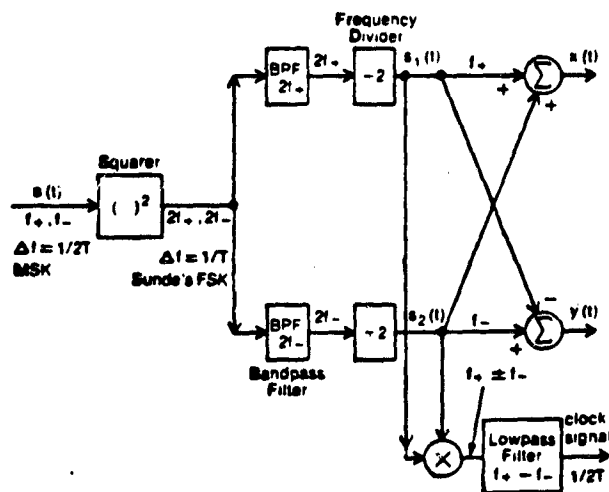




$$x(t) = \cos(\pi t/2T)\cos 2\pi f_c t; \quad y(t) = \sin(\pi t/2T)\sin 2\pi f_c t$$

Figure 8-20. MSK Receiver

REPRODUCIBILITY OF THE  
ORIGINAL PAGE IS POOR



$$f_+ = f_c + 1/4T; \quad f_- = f_c - 1/4T$$

Figure 8-21. Synchronization Circuits for MSK

A further advantage of MSK, since it is an FSK signal variation, is that it can be noncoherently detected by a discriminator, as opposed to QPSK which must use a fully coherent or differentially coherent detector. This allows for an option that can be used for inexpensive demodulation when the received SNR is adequate. Coherent detection can still be used to achieve performance commensurate with that of QPSK. Computer simulations have verified the notion that MSK and OQPSK have their relative advantages when the ratio of channel bandwidth to binary data rate is large and small, respectively. A definitive comparison of the two, in general, is detailed and highly dependent on the type of channel nonlinearities and passband characteristics involved. For ratios  $1 \leq B/R \leq 2$ , typically the choice between the two will not be significant.

#### 8.7.5 Conclusions

It has been shown that PSK is favored over FSK, in general, for high data-rate applications. Among PSK approaches, both QPSK and OQPSK would be favored over BPSK since they have twice the bandwidth efficiency. The only exception is when the coherent carrier phase reference is extremely noisy. Since biphase has no cochannel interference problems with which to be concerned, its immunity to phase jitter is reduced from dual channel QPSK schemes. In most situations, the detection loss will be small and so biphase would not be used.

There is virtually no argument to favor QPSK over OQPSK. The latter has the same ideal channel performance, but in applications with noisy carrier phase reference, it has far better (nonideal) performance. This should not be particularly surprising since OQPSK is essentially a special case of QPSK.

The overall decision in most cases, reduces to a choice between MSK and QPSK. Both have robust behavior with respect to nonregeneration of undesirable sidelobes (after bandlimiting and hardlimiting). MSK does have additional features of noncoherent detection ability and invulnerability to additional filtering sidelobe regeneration.

The choice between the two modulation schemes usually comes down to the extent to which bandwidth limitations exceed power considerations. For minimum bandwidth, OQPSK is the better choice. However, if a larger channel bandwidth can be tolerated, MSK will be the more efficient format.

It should be noted that other closely related formats have been tested. Certain "MSK-type" modulation methods have been studied recently. Rather than half-sinusoidal MSK pulses, some use a sinc pulse with a larger slope. In general, the noise protection of these modified schemes has not been tremendously significant relative to the increased complexity involved.

Last, as an example, with a system noise bandwidth of 5 MHz, for data rates even up to 2.5 Mbps MSK would seem to be the better alternative.

#### 8.8 REFERENCES

- 1) Yasuhiho Ito, Yoshiyori Urano, Tahuro Muratani, and Masahisa Yamaguchi, "Analysis of a Switch Matrix for an SS/TDMA System," Proceedings of the IEEE, Vol 65, No. 3, March 1977.
- 2) H. Kurihara, A. Ogawa, and Y. Hirata, "A New Initial Acquisition Technique for FDM-TDMA Satellite Communications System," Proceedings of the Third Digital Conference, 1975.
- 3) C.R. Carter and S.S. Hayken, "Precision Synchronization to a Switching Satellite Using PSK Signals," ICC, 1974.
- 4) C.R. Carter, R. DeBuda, and S.S. Hayken, "A New System Synchronization Technique for the Switching Satellite," IEEE Transactions on Communications, April 1977.
- 5) C.R. Carter and S.S. Hayken, "A New Synchronization Technique for Switched TDMA Satellite Systems," IEEE Transactions on Communications, May 1974.
- 6) M. Asakira, Y. Tsuji, M. Fukui, Y. Sohma, T. Hara, "Synchronization and Acquisition in SDMA Satellite Communication Systems," ICC, 1974.
- 7) H. Ganssmantel and B. Ekstrom, "TDMA Synchronization for Future Multitransponder Satellite Communication," ICC, 1974.
- 8) P.P. Nuspl, K.E. Brown, W. Steenaart, and B. Gicopoulos, "Synchronization Methods for TDMA," Proceedings of the IEEE, Vol. 65, No. 3, March 1977.
- 9) W.C. Lindsey and M.K. Simon, Telecommunication Systems Engineering, Prentice-Hall, New Jersey, 1973.
- 10) "Effect of noisy phase reference on coherent detection of offset PQSK signals," IEEE Transactions on Communications, Vol. COM-22, pp. 1046-1055, August 1974.

- 11) R.D. Gitlin and E.H. Ho, "The Performance of Staggered Quadrature Amplitude Modulation in the Presence of Phase Jitter," IEEE Transaction Communication, Vol. COM-24, pp. 809-820, August 1976.
- 12) S.A. Gronemeyer and A.L. McBride, "MSK and Offset QPSK Modulation," IEEE Transactions Communications, Vol. COM-24 pp. 809-820, August 1976.
- 13) S. Pasupathy, "Minimum Shift Keying: a Spectrally Efficient Modulation," IEEE Communication, Mag., Vol 17, No. 4, pp. 14-20, July 1979.
- 14) W.B. Osborne and M.B. Luntz, "Coherent and Noncoherent Detection of CPFSK," IEEE Transaction Communication, Vol. C0, pp. 1023-1036, August 1974.
- 15) M.K. Simon, "A Generalization of Minimum Shift-Keying (MSK) Type Signaling based upon Input Data Symbol Pulse Shaping," IEEE Transaction Communication, Vo. COM-24, pp. 845-856, August 1976
- 16) M. Rabzel and S. Pasupathy, "Spectral Shaping in MSK-type Signals," IEEE Transaction Communication, Vol COM-26 pp 189-195, January 1978.